# INTERNATIONAL INDIAN OCEAN EXPEDITION

# USC&GS SHIP PIONEER - 1964

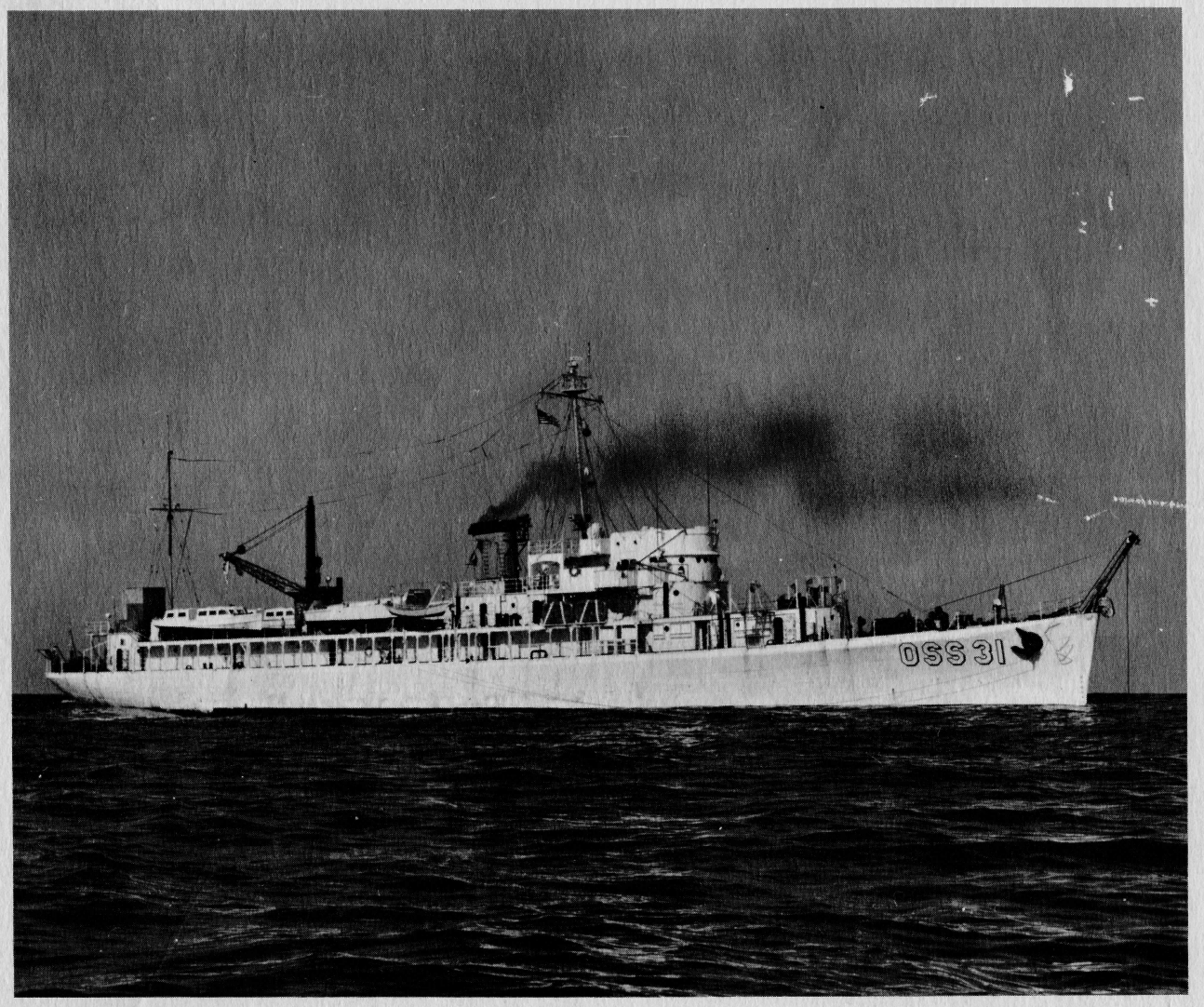


VOLUME 1

## Cruise Narrative and Scientific Results

U.S. DEPARTMENT OF COMMERCE
ENVIRONMENTAL SCIENCE SERVICES ADMINISTRATION

# INTERNATIONAL INDIAN OCEAN EXPEDITION

# USC&GS SHIP PIONEER - 1964

## VOLUME I

### Cruise Narrative and Scientific Results

11 February to 11 August, 1964

**U.S. DEPARTMENT OF COMMERCE**
John T. Connor, Secretary

ENVIRONMENTAL SCIENCE SERVICES ADMINISTRATION
Robert M. White, Administrator

COAST AND GEODETIC SURVEY
James C. Tison, Jr., Director


UNITED STATES GOVERNMENT PRINTING OFFICE, WASHINGTON : 1965

For sale by the Superintendent of Documents, U.S. Government Printing Office
Washington, D.C., 20402 - Price $1.25

# Contents

# Illustrations

# Tables

# Introduction

The USC&GS ship *Pioneer* returned to San Francisco, Calif., on August 11, 1964 after completing a 6-month, 31,507-nautical mile voyage to the Indian Ocean. The cruise began on February 11, 1964 and extended farther from the United States than any previous cruise by a Coast and Geodetic Survey vessel. The period March 23 to June 23 was devoted to special survey work in the northeast Indian Ocean as part of the United States Government's official participation in the International Indian Ocean Expedition. Among the many scientific accomplishments of the cruise were measurements of water properties along three north-south lines across the Equator in the Indian Ocean, special geophysical investigations in the Andaman Sea and Bay of Bengal, detailed exploration of the Ganges Submarine Canyon in the Bay of Bengal and the Trincomalee Submarine Canyon off Ceylon, and brief investigations of the Java, Mindanao, Palau, Yap, and Mariana Trenches en route.

The generalized trackline of the *Pioneer* during the 1964 cruise is shown on chart 1 (facing page 140). This chart also shows the location of the bathythermograph profile sections. The trackline and types of data collected are shown in greater detail on figure 1 for the Strait of Malacca and Andaman Sea, figure 2 for the Bay of Bengal and northeast Indian Ocean, and figure 3 for the South China, Java, Celebes, and Philippine Seas.

During the trip the *Pioneer* made port stops at Honolulu, Hawaii; Manila, Republic of the Philippines; Jesselton, Singapore, and Penang, Malaysia; Calcutta, India; Colombo, Ceylon; Ko Phuket, Thailand; Djakarta, Republic of Indonesia; and the islands of Palau and Guam in the western North Pacific. Dates of arrival and departure from these ports are given in table 1. At each port visited, a special effort was made to welcome aboard all those interested, to give local scientists an opportunity to see the *Pioneer*'s facilities, and to benefit from the mutual exchange of ideas (figs. 4 and 5).

TABLE 1.—*Chronology of events, USC&GS ship* Pioneer *Indian Ocean Expedition*

| *Date (1964)* | *Event* |
|---|---|
| February 11 | Departed San Francisco, Calif. |
| February 22 | Arrived Honolulu, Hawaii |
| February 25 | Departed Honolulu |
| March 10 | Arrived Manila, Philippines |
| March 16 | Departed Manila |
| March 19 | Arrived Jesselton (Island of Borneo), Malaysia |
| March 19 | Departed Jesselton |
| March 23 | Arrived Singapore, Malaysia |
| March 27 | Departed Singapore |
| April 7 | Arrived Penang, west coast Malay peninsula, Malaysia |
| April 9 | Departed Penang |
| April 25 | Arrived Calcutta, India |
| May 2 | Departed Calcutta |
| May 19 | Arrived Colombo, Ceylon |
| May 25 | Departed Colombo |
| June 9 | Arrived Penang, Malaysia |
| June 11 | Departed Penang |
| June 11 | Arrived Ko Phuket, Thailand |
| June 11 | Departed Ko Phuket |
| June 23 | Arrived Djakarta (Java), Indonesia |
| June 28 | Departed Djakarta |
| July 9 | Arrived Palau, western North Pacific |
| July 11 | Departed Palau |
| July 17 | Arrived Guam, western North Pacific |
| July 19 | Departed Guam |
| July 30 | Arrived Honolulu, Hawaii |
| August 4 | Departed Honolulu |
| August 11 | Arrived San Francisco, Calif. |

## International Indian Ocean Expedition

The International Indian Ocean Expedition (IIOE) was the first major cooperative effort on the part of many nations to study one of the scientifically least-known areas of the world, the Indian Ocean and adjacent seas. Some 20 nations and more than 40 ships participated in this international-scale investigation from 1962 through 1965—the period of greatest activity being the

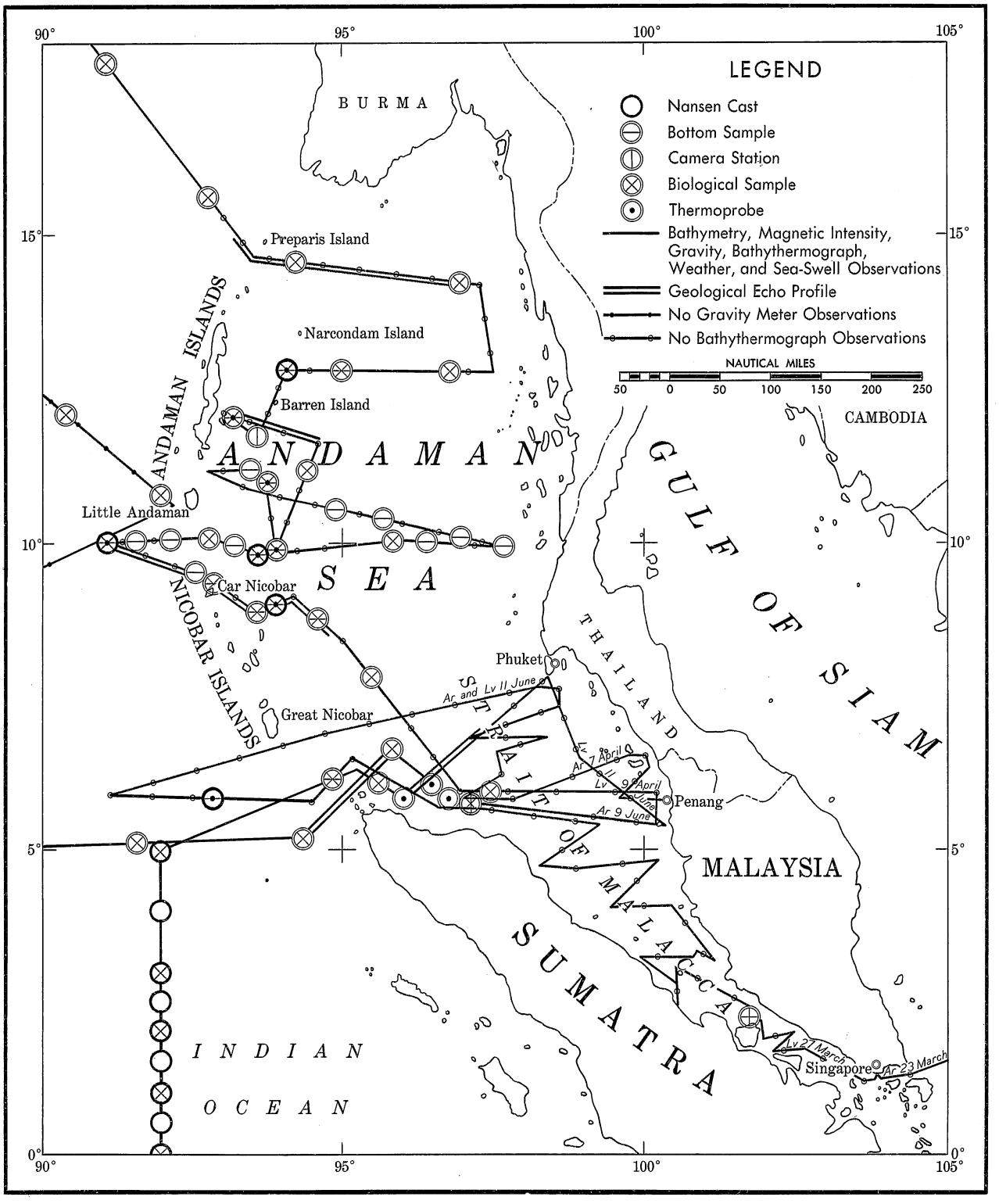


FIGURE 1.—USC&GS ship *Pioneer* observations in Andaman Sea and Strait of Malacca, March—June 1964.

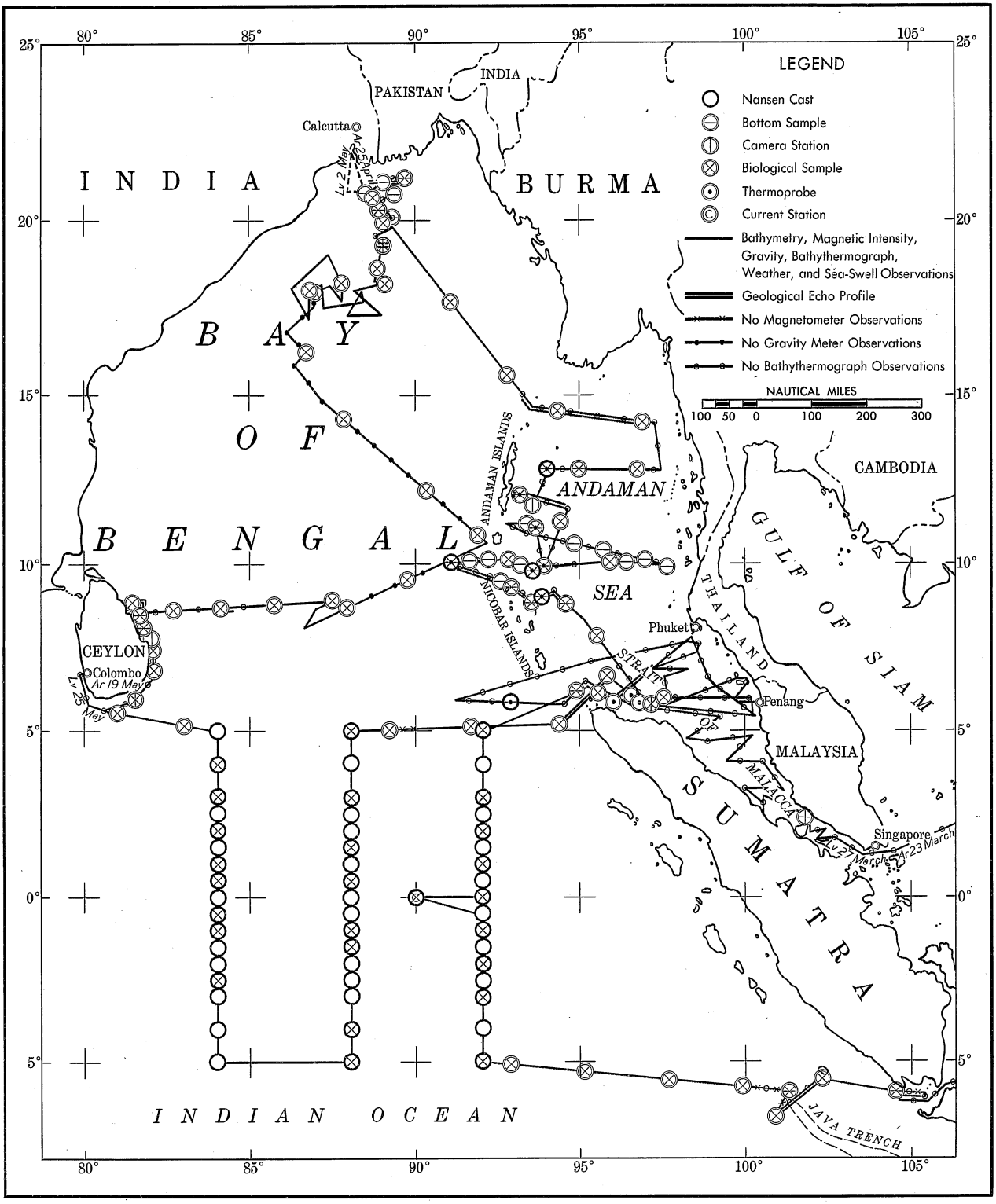


FIGURE 2.—USC&GS ship *Pioneer* observations in Bay of Bengal and northeast Indian Ocean, May–June 1964.

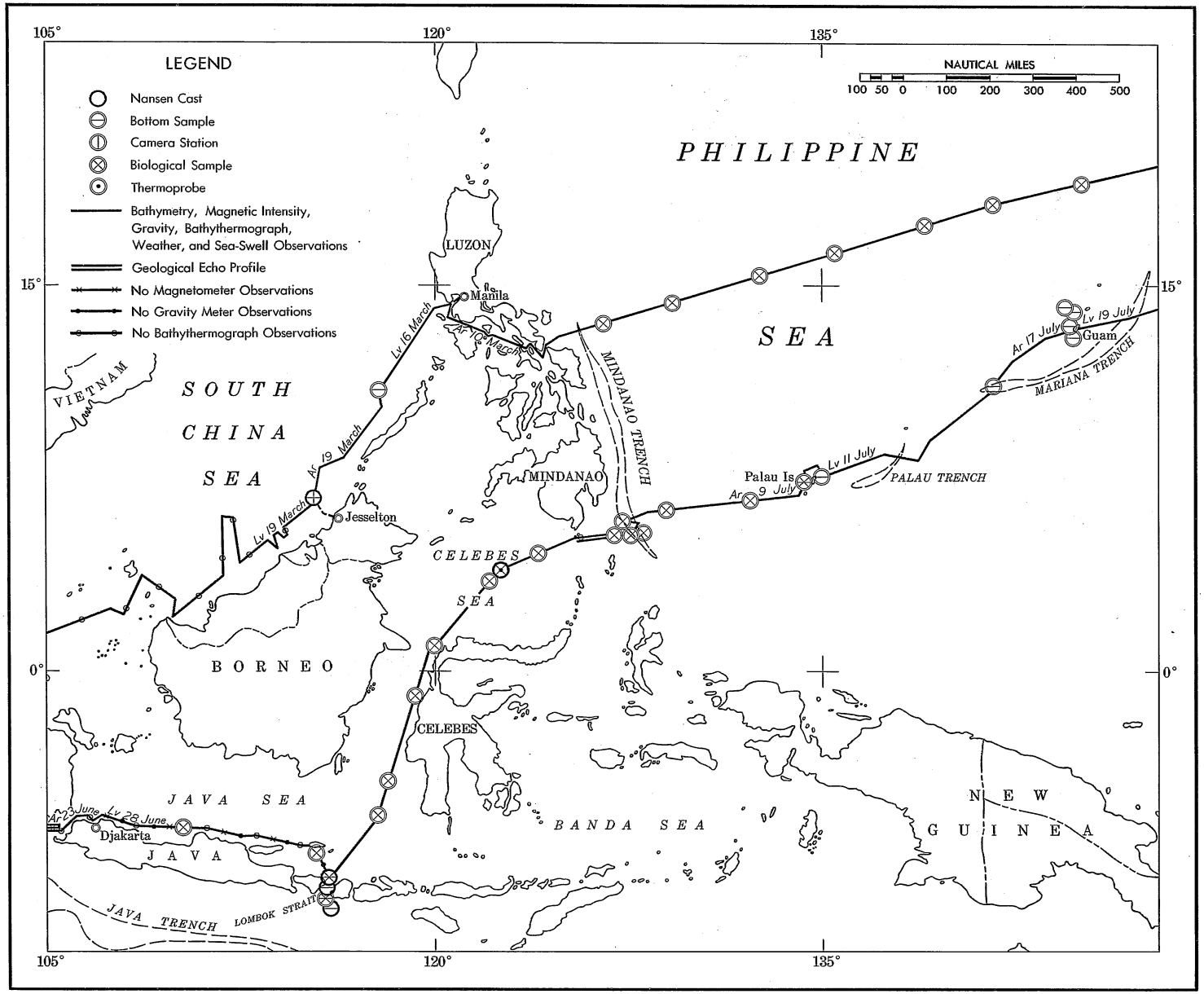


FIGURE 3.—USC&GS ship *Pioneer* observations in South China, Java, Celebes, and Philippine Seas, March, June–July 1964.

years 1963 and 1964. General supervision and coordination of the total program was the responsibility of the Intergovernmental Oceanographic Commission (IOC) of the United Nations Educational, Scientific, and Cultural Organization (UNESCO). The other principal sponsor was the International Council of Scientific Unions (ICSU) through its Scientific Committee of Oceanic Research (SCOR). In the United States, the National Academy of Sciences-National Research Council (NAS-NRC) was given the responsibility for determining scientific objectives and the National Science Foundation (NSF) for planning the Federal Government participation and general fiscal support of the various individual programs.

Basic scientific objectives of the IIOE as defined by the IOC included: Delineation of the features of the ocean-basin topography and the underlying crustal structure; determination of water characteristics and circulation; study of large- and small-scale ocean-meteorological relationships; and, evaluation of the abundance and distributions of living organisms in the sea and the nutrients contributing to their productivity. Answers were sought to many problems having a bearing upon the economic development and well-being of the Asian countries bordering the Indian Ocean. The overall scientific effort was expedited by special disciplinary and interdisciplinary programs in biology, meteorology, physical oceanography, geology, and geophysics.

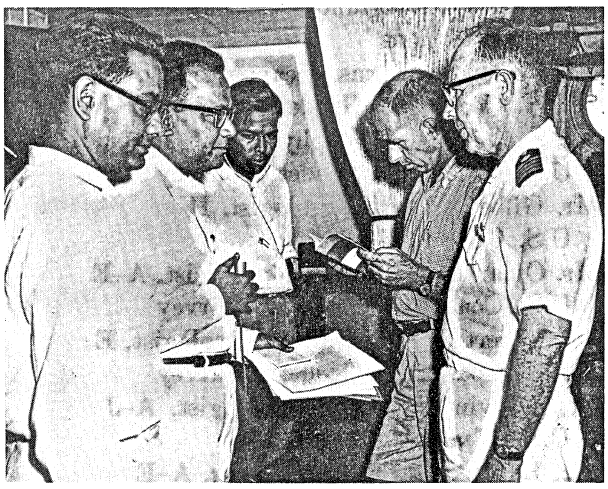

FIGURE 4.—Captain E. B. Brown, commander of the *Pioneer* (on the right), and Dr. H. B. Stewart, Jr., chief scientist (second from right), discuss cruise during taped interview for Calcutta radio.

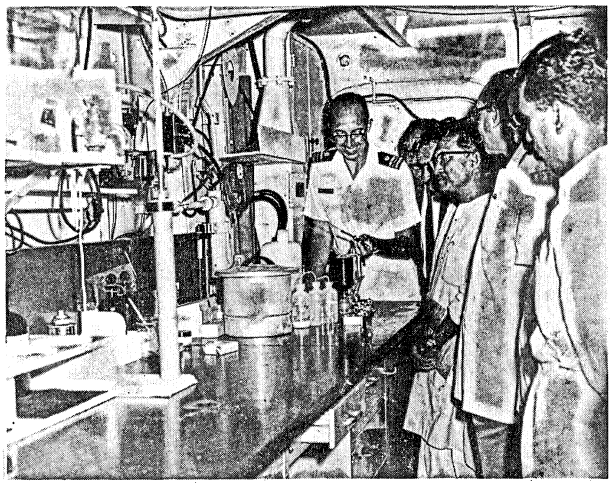

FIGURE 5.—Scientists at Calcutta inspect *Pioneer*'s laboratory facilities.

A documentary sound-motion picture of the International Indian Ocean Expedition was produced aboard the *Pioneer* by a United Nations motion picture team. This team—which included Mr. Ramakantha Sarma, director, and Mr. William Borglund, cameraman—boarded the *Pioneer* at Manila, and departed the ship at Calcutta, India. During the period March 16 to April 25, 1964 the team filmed the activities of the scientists and crew as they conducted investigations in the South China Sea, Strait of Malacca, Andaman Sea, and Bay of Bengal (fig. 6). The many kinds of investigations that were conducted and the wide variety of sampling, measuring, and observing techniques that were employed provided the basis for a one-hour educational film on modern oceanographic exploration. The film, which was released in early 1965 by National Educational Television, is entitled "The Count Down Under."

## Participating Personnel

The *Pioneer* was under the command of Captain Edward B. Brown, USC&GS, during the entire expedition. Dr. Harris B. Stewart, Jr., Deputy Assistant Director, Office of Oceanography, USC&GS, was chief scientist during the Manila-Singapore-Calcutta-Colombo legs of the expedition. To accomplish the varied programs scheduled aboard the *Pioneer*, Coast and Geodetic Survey personnel were accompanied by scientists and technicians from other U.S. Government agencies, educational institutions, industrial organizations, and by scientists from foreign

FIGURE 6.—United Nations motion picture team aboard *Pioneer*.

governments and agencies. Many scientists participated only during certain parts of the cruise. U.S. agencies having personnel aboard the *Pioneer* were the Naval Oceanographic Office, Weather Bureau, Bureau of Commercial Fisheries, National Oceanographic Data Center, Geological Survey, and Public Health Service. Civilian organizations represented during the cruise included the University of Hawaii, Scripps Institution of Oceanography, University of Southern California, University of Michigan, and Rayflex Corporation. Foreign governments represented were the Republic of the Philippines, Malaysia, India, and Republic of Indonesia. The United Nations was represented by the motion picture team. A list of the ship's commissioned officers and participating scientists and technicians follows.

### SHIP'S OFFICERS

Capt. Edward B. Brown
Commanding Officer
Cdr. Howard S. Cole
Executive Officer
Cdr. Ralph E. Ulrich
Chief Engineer
Lcdr. William D. Barbee
Operations & Navigation Officer
(First part of cruise)
Lt. Ray E. Moses
Operations & Navigation Officer
(Last part of cruise)
Lt. Edward L. Spencer
Medical Officer, U.S. Public Health Service
Lt. Seymour R. Kotler
Lt. (jg) Stephen Z. Bezuk
Lt. (jg) Edward R. Dohrman
Lt. (jg) Gerald R. Schimke
Ens. Paul W. Larsen
Ens. John B. Jones
Ens. Joseph M. Lushene
Ens. Danford A. Moore
Ens. Woodrow E. Bliss, Jr.
Ens. David L. Hough

### SCIENTISTS AND TECHNICIANS

[Listed alphabetically; letters indicate leg of cruise according to key at end of listing.]

Dr. J. B. Alexander, geologist, D
Director, Geological Survey of the Federation of Malaysia,
Ipoh, Perak, Malaysia
Mr. Vicente B. Alvarez, biologist, B–H
University of Hawaii,
Honolulu, Hawaii
Mr. William Borglund, camerman, C, D
United Nations
Dr. Robert E. Burns, oceanographer, D
U.S. Coast and Geodetic Survey
Mr. Sam A. Bush, geophysicist, E–J
U.S. Coast and Geodetic Survey
Mr. Gilbert Corwin, geologist, H
U.S. Geological Survey
Mr. Omar E. DeWald, geophysicist, A–E
U.S. Coast and Geodetic Survey
Dr. Robert S. Dietz, marine geologist, E
U.S. Coast and Geodetic Survey
Mr. Melvin Fields, meteorologist, A–J
U.S. Weather Bureau
Mr. Byron Hale, photographer, A–E
U.S. Coast and Geodetic Survey
Mr. Reginald N. Harbison, geophysicist, A, D–H
U.S. Coast and Geodetic Survey

Mr. A. C. Hill, company representative, A
Rayflex Corporation,
Dallas, Tex.

Mr. Joseph Jadamec, oceanographer, A, B
U.S. National Oceanographic Data Center

Mr. Everett C. Jones, biologist, A
U.S. Bureau of Commercial Fisheries

Mr. Reginald B. Jones, oceanographer, F
U.S. Coast and Geodetic Survey

Mr. George Keller, marine geologist, D
U.S. Naval Oceanographic Office

Col. K. L. Khosla, geodesist, E
Head, Geodetic Branch,
Survey of India,
Dehra, Dun, India

Mr. John W. Kofoed, geological oceanographer, G, H
U.S. Coast and Geodetic Survey

Mr. John Linberg, company representative, D
Rayflex Corporation,
Dallas, Tex.

Mr. Manuel Llorca, fisheries biologist, C
Philippine Fisheries Commission,
Manila, Philippines

Mr. Richard Malloy, geophysicist, A
U.S. Coast and Geodetic Survey

Mr. Mario Manansala, oceanographer, C
Philippine Bureau of Coast and Geodetic Survey,
Manila, Philippines

Mr. Aubrey B. McCollum, geophysicist, A
U.S. Coast and Geodetic Survey

Mr. Anugerah Nontiji, F
Institute of Marine Research,
Pasar Ikan, Djakarta, Indonesia

Mr. ONG Koh Sin, fisheries biologist, D
Fisheries Research Laboratory,
Penang, Malaysia

Mr. Richard B. Perry, geological oceanographer, F, G, H
U.S. Coast and Geodetic Survey

Mr. George Peter, geophysicist, C, D
U.S. Coast and Geodetic Survey

Mr. Ronald K. Reed, physical oceanographer, F, G, H
U.S. Coast and Geodetic Survey

Mr. Kelvin S. Rodolfo, marine geologist, C–H
University of Southern California,
Los Angeles, Calif.

Mr. Ramakantha Sarma, film director, C, D
United Nations

Dr. Francis P. Shepard, marine geologist, E
Scripps Institution of Oceanography,
La Jolla, Calif.

Mr. James B. Soileau, meteorologist, A–J
U.S. Weather Bureau

Mr. Quintin Dick Stephen-Hassard, biologist, B–I
University of Hawaii,
Honolulu, Hawaii

Dr. Harris B. Stewart, Jr., chief scientist, C, D, E
U.S. Coast and Geodetic Survey

Dr. Joshua I. Tracey, Jr., geologist, H
U.S. Geological Survey

Mr. Austin Weeks, geophysicist, D–H
U.S. Coast and Geodetic Survey

KEY TO LEG OF CRUISE

Leg A. San Francisco to Honolulu, February 11 to 22.

Leg B. Honolulu to Manila, February 25 to March 10.

Leg C. Manila to Singapore, March 16 to 23.
Stop at Jesselton, March 19.

Leg D. Singapore to Calcutta, March 27 to April 25.
Stop at Penang, April 7 to 9.

Leg E. Calcutta to Colombo, May 2 to 19.

Leg F. Colombo to Djakarta, May 25 to June 23.
Stop at Penang, June 9 to 11.
Stop at Ko Phuket, June 11.

Leg G. Djakarta to Palau, June 28 to July 9.

Leg H. Palau to Guam, July 11 to 17.

Leg I. Guam to Honolulu, July 19 to 30.

Leg J. Honolulu to San Francisco, August 4 to 11.

## The Ship and Equipment

The *Pioneer* initially was designed for use by the U.S. Navy as a Seaplane tender (AVP Class) but was modified while under construction and completed in 1943 as a Patrol Torpedo Boat tender (AGF Class). The Coast and Geodetic Survey obtained the vessel after World War II. Since then the *Pioneer* has been used by the Coast and Geodetic Survey as a hydrographic survey ship and, since 1961, for broad research and survey

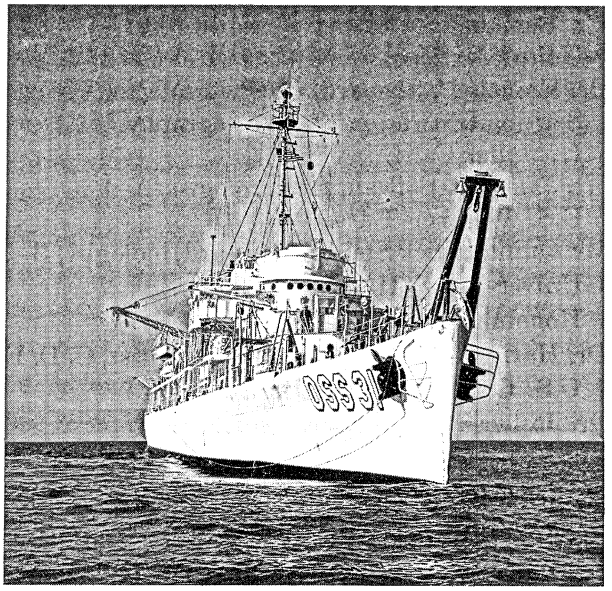

FIGURE 7.—View of *Pioneer* showing gallows frame on bow and ship's crane amidship.

activities in oceanography. The major features and operational characteristics of the *Pioneer* are as follows:

| | | |
|---|---|---|
| Overall length | 311.0 feet | 94.8 meters |
| Beam | 41.0 feet | 12.5 meters |
| Draft | 13.8 feet | 4.2 meters |
| Laden displacement (tons) | | 2,600 |
| Cruising speed (knots) | | 13 |
| Operational range (nautical miles) | | 10,000 |
| Ship accommodations: | | |
| Officers and scientists | | 20 |
| Technical party and crew | | 92 |

Additional personnel can be accommodated by making minor modifications in the space arrangement. The ship is propelled by two fixed-blade screws each driven by twin, opposed-piston diesel engines. Four generators provide the primary power supply—a 440-volt, 60-cycle, 3-phase, alternating-current system. The voltage can be stepped down to 115 v by regulated transformers.

The communications equipment includes two 1,000-watt transmitters that are capable of transmitting over a wide range of kilocycle frequencies. A new Northern 180-watt radio transmits on 2182–8364 kc and receives up to 12 megacycles. Other receivers on board are capable of receiving in the frequency range from 85 kc to 30 mc. Equipment used for navigational control and position fixing and that used in depth sounding and recording is described on pages 53 and 54.

The *Pioneer* is equipped with a heavy-duty, deep-sea anchoring and coring winch that carries 45,000 ft of 3/8- to 3/4-inch tapered wire rope. A "gallows frame" on the bow of the ship (fig. 7) facilitates the lowering and retrieving of heavy equipment. One oceanographic winch carries 30,000 ft of 5/32-inch wire for Nansen casts and other deep-water sampling work. There are two bathythermograph hoists. The ship's crane also can be used to handle heavy equipment over the side of the ship. Two 36-ft hydrographic launches and two LCVP-type landing craft are carried aboard the *Pioneer* (fig. 8).

The ship's evaporators can produce 10,000 gallons of fresh water per day. A wet laboratory for reading thermometers, drawing off water samples, and for the examination and preparation of bottom samples is located forward on the main deck level. A dry laboratory for the analysis of water samples is located amidships. This space also accommodates the magnetic and gravity recording instrumentation.

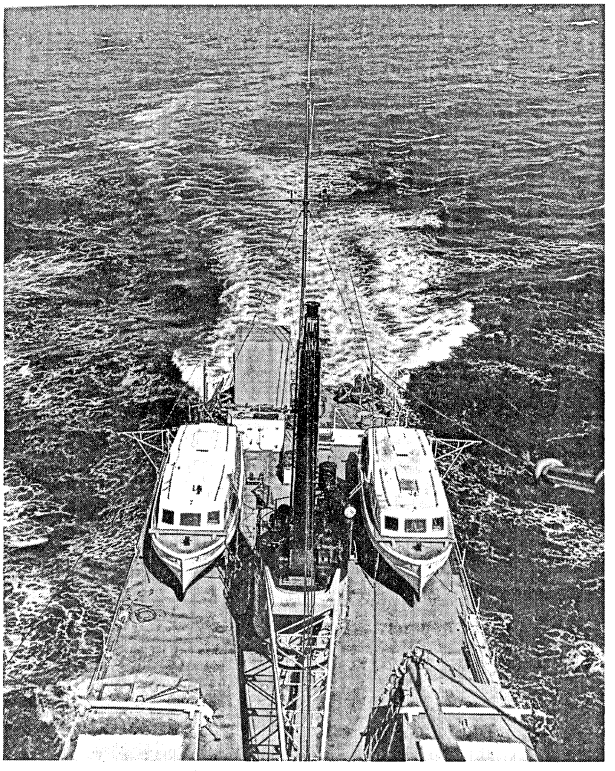

FIGURE 8.—Hydrographic launches and meteorological-balloon inflation shelter on aft portion of *Pioneer's* boat deck.

## Scientific Results

This volume describes the 1964 field operations of the *Pioneer* during the International Indian Ocean Expedition, summarizes the data obtained, and presents the preliminary scientific results of the cruise. Investigations conducted in the Pacific Ocean, en route to and returning from the Indian Ocean, are included. Table 2 gives the statistical summary of the accomplishments. Some of the results have appeared in scientific journals. They are brought together with other specially prepared papers at the end of those sections to which they apply. These contributions have been adapted for use in this volume with only slight changes in format, including the renumbering of figures and tables to provide consecutive numbering in this publication. The original figure or table number is shown within brackets in the figure captions and table titles, thusly: Figure 104[1] or Table 19[2]. Original sources of published articles are acknowledged in footnotes.

Volume 2 in this series of IIOE *Pioneer* cruise reports presents the oceanographic station data, bathythermograph data, and field descriptions of bottom samples. Other scientific findings and data tabulations will be published in this series as processing and analysis of the data are completed.

TABLE 2.—*Summary of accomplishments*

| | |
|---|---|
| Trackline soundings (nm) | 31,507 |
| Trackline magnetics (nm) | 29,112 |
| Trackline gravity (nm) | 25,982 |
| Geological echo profiling (nm) | 1,007 |
| Nansen stations | 63 |
| Water samples | 1,786 |
| Bottom samples | 104 |
| Biological net tows | 263 |
| Biological productivity samples | 4,688 |
| Camera lowerings | 9 |
| Bottom photographs | 4,000+ |
| Bathythermograph lowerings (with surface temperature and salinity) | 885 |
| Weather balloons | 302 |

790-089 O—66——2

# Physical Oceanography

The program in physical oceanography had as its principal objective the sampling of the water column along three north-south sections across the Equator in the northeast Indian Ocean. This phase of the *Pioneer*'s work was planned as part of the overall IIOE investigation to gain a better understanding of this vast oceanic area, its heat budget, patterns of flow and water transport, distribution of physical and chemical properties, and seasonal and geographical variation of observed distributions, particularly as influenced by the monsoonal atmospheric circulation over much of the region. In addition to this special emphasis, the temperature distribution within the 250-meter surface-water layer was measured throughout the cruise at regular intervals by bathythermograph lowerings.

## Oceanographic Stations

During the 1964 *Pioneer* expedition, 63 oceanographic stations were occupied—57 in the Indian Ocean; 3 in the vicinity of Lombok Strait; 2 in the Celebes Sea, at the same position; and, 1 in the South China Sea. Station positions were determined by astronomical sightings and dead reckoning. Figures 1 to 3 show the general locations of the stations. Table 3 gives their geographic positions, as taken from the corrected and adjusted plot of the ship's track.

*Station procedure.* Oceanographic casts usually were made to depths of 2,000 m or deeper. A standard bottle spacing of 18 Nansen bottles was used between the surface and 1,200 m on all stations except those taken near the Equator. Between 2°N and 2°S, 36 bottles were used between the surface and 1,200 m. A bathythermograph lowering was made before each shallow cast and the BT trace was referred to in determining the bottle spacing relative to the depth of the mixed layer and thermocline. On the deep stations, a sonar pinger was used at the end of the line to position the bottom bottle about 50 m above the bottom at the time of sampling (fig. 9). Temperature measurements and salinity and oxygen determinations were made for all oceanographic stations. Silicate determinations were made only for selected samples from stations 0009 to 0057.

Sea-water temperature measurements were made with deep-sea reversing thermometers attached to the Nansen bottles. Two protected thermometers were used on each bottle. In addition, unprotected thermometers—in direct contact with the water and subject to hydrostatic pressure—were used on most bottles below 100 m. Upon retrieving the cast, racking the bottles, and allowing sufficient time for the auxiliary thermometers to reach the temperature of the deck laboratory, the thermometers were read. A magnifying viewer was used

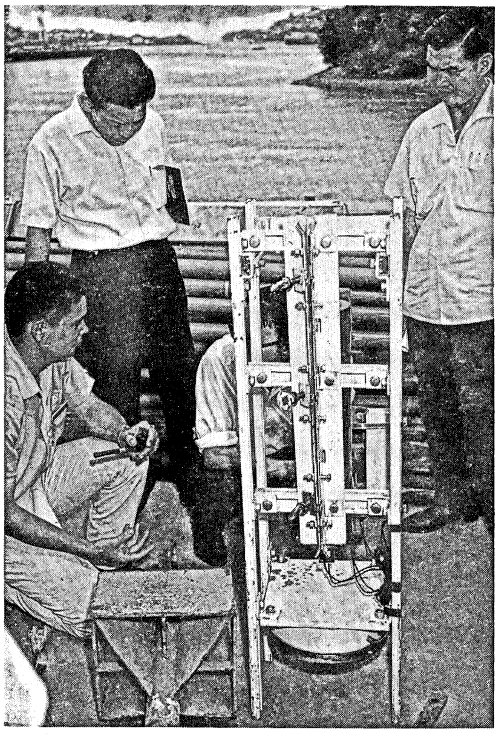

FIGURE 9.—Sonar pinger used to determine distance between end of hydrographic wire and sea floor.

TABLE 3.—*Oceanographic station positions*

| Station number | Date | Time | Latitude ° ′ | Longitude ° ′ |
|---|---|---|---|---|
| 1 | Mar. 18 | 0722 | 07 00. 2 N | 115 21. 2 E |
| 2 | Apr. 2 | 1921 | 05 51. 3 N | 92 32. 6 E |
| 3 | Apr. 11 | 0736 | 09 16. 0 N | 93 57. 7 E |
| 4 | Apr. 13 | 2046 | 10 06. 0 N | 91 08. 9 E |
| 5 | Apr. 15 | 0349 | 09 56. 3 N | 93 44. 8 E |
| 6 | Apr. 20 | 0540 | 12 49. 1 N | 93 58. 3 E |
| 7 | May 26 | 0944 | 04 57. 8 N | 84 12. 5 E |
| 8 | May 26 | 1545 | 04 00. 9 N | 84 14. 8 E |
| 9 | May 27 | 0430 | 02 53. 0 N | 84 14. 4 E |
| 10 | May 27 | 0741 | 02 26. 2 N | 84 06. 0 E |
| 11 | May 27 | 1246 | 01 55. 8 N | 84 15. 1 E |
| 12 | May 27 | 1903 | 01 25. 7 N | 84 09. 2 E |
| 13 | May 28 | 0939 | 00 58. 9 N | 84 29. 1 E |
| 14 | May 28 | 1939 | 00 29. 0 N | 84 06. 2 E |
| 15 | May 29 | 0914 | 00 00. 4 N | 84 09. 5 E |
| 16 | May 29 | 1510 | 00 28. 0 S | 84 07. 1 E |
| 17 | May 29 | 2210 | 01 03. 8 S | 84 00. 0 E |
| 18 | May 30 | 0342 | 01 29. 2 S | 83 59. 6 E |
| 19 | May 30 | 0833 | 01 56. 9 S | 84 01. 2 E |
| 20 | May 30 | 1305 | 02 28. 3 S | 84 03. 8 E |
| 21 | May 30 | 2113 | 03 00. 8 S | 83 55. 2 E |
| 22 | May 31 | 0211 | 03 59. 7 S | 83 58. 9 E |
| 23 | May 31 | 0830 | 04 58. 9 S | 84 07. 9 E |
| 24 | June 1 | 0626 | 05 03. 9 S | 88 16. 5 E |
| 25 | June 1 | 1412 | 04 03. 2 S | 88 03. 1 E |
| 26 | June 1 | 2355 | 03 00. 3 S | 87 55. 5 E |
| 27 | June 2 | 0533 | 02 31. 2 S | 87 57. 2 E |
| 28 | June 2 | 0959 | 01 59. 8 S | 88 00. 6 E |
| 29 | June 2 | 1443 | 01 29. 5 S | 87 57. 4 E |
| 30 | June 2 | 2054 | 01 00. 7 S | 87 56. 5 E |
| 31 | June 3 | 0641 | 00 30. 1 S | 88 04. 4 E |
| 32 | June 3 | 0935 | 00 01. 8 S | 88 07. 0 E |
| 33 | June 3 | 1509 | 00 25. 8 N | 88 06. 3 E |
| 34 | June 3 | 2044 | 00 58. 8 N | 87 54. 3 E |
| 35 | June 4 | 0310 | 01 30. 8 N | 87 54. 8 E |
| 36 | June 4 | 0908 | 02 00. 2 N | 87 51. 7 E |
| 37 | June 4 | 1156 | 02 29. 1 N | 87 52. 8 E |
| 38 | June 4 | 1720 | 03 01. 2 N | 87 53. 2 E |
| 39 | June 5 | 0043 | 04 00. 0 N | 87 50. 4 E |
| 40 | June 5 | 0655 | 05 00. 2 N | 87 51. 7 E |
| 41 | June 13 | 1420 | 04 59. 5 N | 92 00. 6 E |
| 42 | June 13 | 2239 | 03 46. 7 N | 92 00. 5 E |
| 43 | June 14 | 0509 | 02 46. 0 N | 92 00. 1 E |
| 44 | June 14 | 1043 | 02 14. 8 N | 92 00. 9 E |
| 45 | June 14 | 1421 | 01 51. 0 N | 91 59. 9 E |
| 46 | June 14 | 1821 | 01 27. 1 N | 91 58. 2 E |
| 47 | June 14 | 2330 | 00 54. 1 N | 91 55. 7 E |
| 48 | June 15 | 0540 | 00 28. 8 N | 91 57. 6 E |
| 49 | June 15 | 0949 | 00 03. 2 N | 91 55. 8 E |
| 50 | June 15 | 2100 | 00 04. 2 N | 89 55. 2 E |
| 51 | June 16 | 0934 | 00 19. 6 S | 91 51. 4 E |
| 52 | June 16 | 1410 | 00 44. 3 S | 91 49. 9 E |
| 53 | June 16 | 2212 | 01 16. 3 S | 91 58. 7 E |
| 54 | June 17 | 0332 | 01 50. 7 S | 92 01. 0 E |
| 55 | June 17 | 1009 | 02 27. 2 S | 91 59. 6 E |
| 56 | June 17 | 1438 | 02 58. 3 S | 92 00. 9 E |
| 57 | June 17 | 2307 | 04 04. 1 S | 92 06. 5 E |
| 58 | June 18 | 0543 | 05 05. 2 S | 92 08. 4 E |
| 59 | June 30 | 1155 | 09 03. 3 S | 115 39. 5 E |
| 60 | June 30 | 1814 | 08 41. 3 S | 115 41. 0 E |
| 61 | June 30 | 2121 | 08 30. 9 S | 115 44. 5 E |
| 62 | July 3 | 2049 | 04 00. 4 N | 122 36. 0 E |
| 63 | July 3 | 2238 | 04 00. 4 N | 122 36. 0 E |

TABLE 3.—*Oceanographic station positions*—Continued

and each thermometer was reread to avoid any error in the readings. If two readings did not agree within 0.02°C, both the main and auxiliary thermometers were read again and checked before the values were used. Immediately after each station, thermometer corrections were computed with a special oceanographic slide rule and depths of the bottles were determined by the thermometric and L–Z graphical methods.

Water samples were drawn from the Nansen bottles and salinity determinations were made using the inductive salinometer (fig. 10). Instrumental drift was determined at least every two hours. Oxygen samples were drawn and determinations were made by the modified Winkler method. Silicate samples were drawn into polyethylene bottles and quick-frozen. The frozen samples were shipped to Dr. D. P. Kharkar, Tata Institute of Fundamental Research, Colaba, Bombay, India. The silicate analysis was accom-

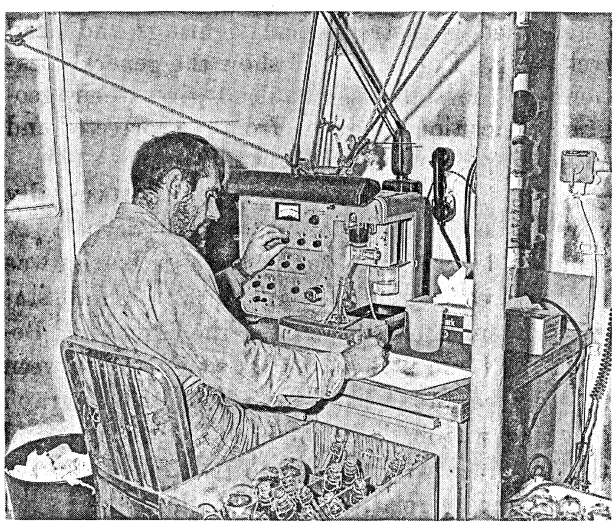

FIGURE 10.—Inductive salinometer used to determine salinity of water samples.

plished at the Institute by the molybdenum blue method at an 825-mu wavelength on a Beckman DU spectrophotometer. The silicate values were plotted and profiled by personnel of the Marine Data Division of the U.S. Coast and Geodetic Survey.

*IIOE standard station.* A special IIOE standard station at the Equator and 90°E was designated as a repeat station for all IIOE survey vessels operating in the area. This station (NODC number 0050) was occupied by the *Pioneer* at 00°04.2′N,89°55.2′E. A copy of the oceanographic data printout for station 0050 is shown in figure 11.

*Equatorial sections.* The greater portion of the oceanographic station program aboard the *Pioneer* was devoted to obtaining three north-south profiles of water properties across the Equator, south of the Bay of Bengal, to tie-in with the overall physical oceanographic investigations of the IIOE. These north-south profiles extended from 5°N to 5°S along meridians 84°E,

| REFERENCE | | SHIP | LATITUDE | LONGITUDE | DUPE INDICATOR | MARSDEN SQUARE | STATION TIME (GMT) | | | | YEAR | ORIGINATOR'S | | DEPTH TO BOTTOM | MAX. DEPTH OF SAMPLES | WAVE OBSERVATIONS | | | | WEATHER CODE | CLOUD CODES | | | NODC STATION NUMBER |
|---|---|---|---|---|---|---|---|---|---|---|---|---|---|---|---|---|---|---|---|---|---|---|---|---|
| COUNTRY CODE | IDENTITY NUMBER | CODE | ° ′ 1/10 | ° ′ 1/10 | | 10° 1° | MONTH | DAY | HR. 1/10 | | | CRUISE NUMBER | STATION NUMBER | | | DIR. | HGT. | PER. | SEA AMT. | | TYPE | AMT. | | |
| 31 | 201 | PI | 00042N | 089552E | | 028 | 09 | 06 | 15 | 210 | 1964 | 442 | 050 | 4371 | 39 | 18 | | | 3 | X5 | X | 9 | | 0050 |

| WATER | | WIND | | BAROMETER (mbs) | AIR TEMP. °C | | VIS. CODE | NO. OBS. DEPTHS | SPECIAL OBSERVATIONS |
|---|---|---|---|---|---|---|---|---|---|
| COLOR CODE | TRANS. (m) | DIR. | SPEED OR FORCE | | DRY BULB | WET BULB | | | |
| | | 22 | S09 | 071 | 256 | 250 | 6 | | |

| MESSENGER TIME HR. 1/10 | CAST NO. | CARD TYPE | DEPTH (m) | T °C | S °/₀₀ | SIGMA–T | SPECIFIC VOLUME ANOMALY–X10⁷ | ≅ ΔD DYN. M. X 10³ | SOUND VELOCITY | $O_2$ ml/l | $PO_4$–P µg-at/l | TOTAL–P µg-at/l | $NO_2$–N µg-at/l | $NO_3$–N µg-at/l | $SiO_3$–Si µg-at/l | pH µg-at/l | SCC |
|---|---|---|---|---|---|---|---|---|---|---|---|---|---|---|---|---|---|
| | | STD | 0000 | 2892 | 3414 | 2147 | 0063415 | 0000 | 15427 | 442 | | | | | | | |
| 210 | | OBS | 0000 | 2892 | 3414 | 2147 | | | 15427 | 442 | | | | | 001 | | |
| | | STD | 0010 | 2894 | 3413 | 2145 | 0063591 | 0064 | 15428 | 452 | | | | | | | |
| 210 | | OBS | 0010 | 2894 | 3413 | 2145 | | | 15428 | 452 | | | | | | | |
| | | STD | 0020 | 2900 | 3420 | 2148 | 0063321 | 0127 | 15432 | 448 | | | | | | | |
| 210 | | OBS | 0020 | 2900 | 3420 | 2148 | | | 15432 | 448 | | | | | | | |
| 210 | | OBS | 0029 | 2919 | 3443 | 2159 | | | 15440 | 450 | | | | | | | |
| | | STD | 0030 | 2918 | 3444 | 2160 | 0062216 | 0190 | 15440 | 450 | | | | | | | |
| 210 | | OBS | T0049 | 2904 | 3455 | 2173 | | | 15442 | 450 | | | | | | | |
| | | STD | 0050 | 2904 | 3455 | 2173 | 0061059 | 0313 | 15442 | 450 | | | | | | | |
| 210 | | OBS | 0074 | 2905 | 3458 | 2175 | | | 15446 | 445 | | | | | | | |
| | | STD | 0075 | 2905 | 3458 | 2175 | 0060979 | 0466 | 15446 | 445 | | | | | | | |
| 210 | | OBS | T0098 | 2902 | 3462 | 2179 | | | 15450 | 442 | | | | | 002 | | |
| | | STD | 0100 | 2897 | 3462 | 2181 | 0060539 | 0617 | 15449 | 440 | | | | | | | |
| | | *STD | 0125 | 2855 | 3462 | 2195 | 0059301 | 0767 | 15444 | 418 | | | | | | | |
| 210 | | OBS | 0132 | 2822 | 3462 | 2206 | | | 15438 | 412 | | | | | | | |
| 210 | | OBS | 0147 | 2152 | 3501 | 2438 | | | 15286 | 210 | | | | | | | |
| | | STD | 0150 | 2088 | 3502 | 2456 | 0034387 | 0884 | 15270 | 203 | | | | | | | |
| 210 | | OBS | T0196 | 1387 | 3510 | 2631 | | | 15071 | 150 | | | | | | | |
| | | STD | 0200 | 1368 | 3510 | 2635 | 0017396 | 1014 | 15065 | 154 | | | | | | | |
| 210 | | OBS | T0246 | 1206 | 3507 | 2665 | | | 15018 | 193 | | | | | | | |
| | | STD | 0250 | 1203 | 3507 | 2666 | 0014561 | 1094 | 15017 | 195 | | | | | | | |
| 210 | | OBS | T0295 | 1160 | 3504 | 2671 | | | 15009 | 210 | | | | | | | |
| | | STD | 0300 | 1154 | 3504 | 2673 | 0014001 | 1165 | 15008 | 210 | | | | | | | |
| 210 | | OBS | T0394 | 1042 | 3498 | 2688 | | | 14983 | 196 | | | | | | | |
| | | STD | 0400 | 1033 | 3498 | 2690 | 0012524 | 1298 | 14981 | 193 | | | | | | | |
| 210 | | OBS | T0494 | 0926 | 3497 | 2707 | | | 14957 | 151 | | | | | 035 | | |
| | | STD | 0500 | 0924 | 3497 | 2708 | 0010971 | 1415 | 14957 | 150 | | | | | | | |
| 210 | | OBS | T0594 | 0888 | 3499 | 2715 | | | 14960 | | | | | | | | |
| | | *STD | 0600 | 0885 | 3499 | 2715 | 0010384 | 1522 | 14960 | 127 | | | | | | | |
| | | STD | 0700 | 0838 | 3499 | 2723 | 0009815 | 1623 | 14958 | 121 | | | | | | | |
| 222 | | OBS | T0704 | 0836 | 3499 | 2723 | | | 14958 | 120 | | | | | | | |
| | | STD | 0800 | 0781 | 3497 | 2730 | 0009239 | 1718 | 14953 | 116 | | | | | | | |
| 222 | | OBS | T0882 | 0736 | 3496 | 2736 | | | 14949 | 112 | | | | | 048 | | |
| | | STD | 0900 | 0727 | 3496 | 2737 | 0008645 | 1808 | 14948 | 114 | | | | | | | |
| | | STD | 1000 | 0674 | 3494 | 2743 | 0008146 | 1892 | 14944 | 123 | | | | | | | |
| 222 | | OBS | 1062 | 0642 | 3493 | 2746 | | | 14942 | 130 | | | | | | | |
| | | STD | 1100 | 0621 | 3492 | 2748 | 0007652 | 1971 | 14939 | 138 | | | | | | | |
| | | STD | 1200 | 0566 | 3490 | 2754 | 0007136 | 2045 | 14934 | 159 | | | | | | | |
| | | STD | 1300 | 0516 | 3488 | 2758 | 0006697 | 2114 | 14930 | 178 | | | | | | | |
| 222 | | OBS | T1335 | 0499 | 3487 | 2759 | | | 14929 | | | | | | 062 | | |
| | | STD | 1400 | 0467 | 3486 | 2762 | 0006276 | 2179 | 14926 | 197 | | | | | | | |
| | | STD | 1500 | 0422 | 3484 | 2766 | 0005911 | 2240 | 14924 | 214 | | | | | | | |
| | | *STD | 1750 | 0330 | 3481 | 2773 | 0005121 | 2377 | 14927 | 260 | | | | | | | |
| 222 | | OBS | 1792 | 0318 | 3480 | 2773 | | | 14929 | 127Q | | | | | 072 | | |
| | | *STD | 2000 | 0277 | 3478 | 2775 | 0004815 | 2502 | 14946 | 293 | | | | | | | |
| 222 | | OBS | 2251 | 0237 | 3476 | 2777 | | | 14972 | 317 | | | | | | | |
| | | STD | 2500 | 0210 | 3475 | 2779 | 0004404 | 2732 | 15003 | 339 | | | | | | | |
| 222 | | OBS | 2715 | 0190 | 3474 | 2779 | | | 15031 | 354 | | | | | 082 | | |
| | | STD | 3000 | 0168 | 3473 | 2780 | 0004161 | 2946 | 15070 | 365 | | | | | | | |
| 222 | | OBS | T3182 | 0156 | 3473 | 2781 | | | 15097 | 375 | | | | | 076 | | |
| 222 | | OBS | T3660 | 0129 | 3472 | 2782 | | | 15168 | 414 | | | | | | | |
| 222 | | OBS | T3949 | 0116 | 3472 | 2783 | | | 15213 | 438 | | | | | | | |

FIGURE 11.—IIOE standard station, data printout.

88°E, and 92°E. The 17 stations along each profile section were located at 5°, 4°, and 3° both north and south of the Equator and at ½-degree intervals between 3°N and 3°S. The temperature, salinity, oxygen, silicate, and density distributions along the three north-south equatorial sections are shown in figures 12 to 26.

Temperature: The distribution of temperature along the three north-south sections is shown by figures 12, 13, and 14. Near the Equator, isothermal water of about 29°C was found from the surface to a depth of approximately 100 m. Between 100 and 200 m, the temperature decreased rapidly from 28°C to 14°C. Away from the Equator, toward the northern and southern ends of the sections, the isotherms of 28°C to 14°C are evenly spaced from 50 to 250 m. Beneath 250 m, the isotherms of 12°C to 2°C are evenly spaced along the entire length of the three sections.

Salinity: The salinity sections (figs. 15, 16, and 17) do not show the compaction of isopleths near the Equator as seen in the temperature sections. The salinity of the surface water increases from 34.20°/₀₀ (parts per thousand) in the north to nearly 35.00°/₀₀ in the south. Between 100 and 200 m, tongues of higher-salinity water (35.00°/₀₀ or greater) extend toward the Equator from both north and south. Beneath 200 m, the salinity decreases to 35.00°/₀₀, but the decrease is more rapid south of the Equator where the layer of water with salinities greater than 35.00°/₀₀ is less thick. Between 300 and approximately 800 m, the water south of the Equator is less saline than the water to the north. In the vicinity of the Equator, there is an interfingering effect of tongues of higher- and lower-salinity water. This feature of the subsurface salinity distribution is present on each north-south section observed by the *Pioneer*. The distribution of salinity at greater depths is marked by the rise of the 34.80°/₀₀ isohaline from 2,000 to 1,000 m in the southern part of the section along 92°E. This trend is less evident in the sections at 88°E and 84°E to the west.

Dissolved oxygen: The distribution of dissolved oxygen along the three sections is shown in figures 18, 19, and 20. Several localized pockets of water with relatively high dissolved oxygen content are present in the surface layer. These pockets have oxygen contents of 4.50 ml/L (milliliters per liter) and occur within a surface layer approximately 150 m thick which has an oxygen content of 4.00 ml/L or greater. Beneath this layer there is a pronounced decrease in the oxygen content of the water to a depth of 1,000 m. Within this subsurface zone of low oxygen content, a tongue of water with very low oxygen content extends southward from 5°N toward the Equator. Within the same zone south of the Equator, a tongue of water with slightly higher oxygen content, 2.00–2.50 ml/L, gently ascends northward over the water of very low oxygen content. Oxygen contents of 1.50 ml/L at the 1,000–m level and 3.00 ml/L at the 2,000–m level appear to be uniformly distributed throughout the region sampled by the three sections.

Dissolved silicate: The silicate distribution is shown in figures 21, 22, and 23 as determined from samples obtained on stations 0009 through 0057. The silicate content is less than 10 μg-at/L (microgram-atoms per liter) in the surface water and increases at a fairly uniform rate with increasing depth to concentrations in the range of 40–50 μg-at/L at a depth of approximately 800 m. Below this average depth, the silicate contents ranged from 40–100 μg-at/L, varied greatly in both lateral and vertical distribution, and did not exceed 110 μg-at/L.

Density: Figures 24, 25, and 26 show the distribution of density (sigma-*t* values) as computed from the temperature and salinity observations. Density values in the surface layer are less than 21.00 at only four stations, numbers 0043 through 0046, and reflect the distribution of temperature in the 200–m surface layer. Below 200 m, density increases at a more uniform and gradual rate throughout the area.

*Celebes Sea stations.* In the central portion of the Celebes Sea the *Pioneer* occupied two oceanographic stations, 0062 and 0063, at the site of a station occupied by the *Snellius* in 1929. Both *Pioneer* stations were at the same location. The first station, when completed, was followed immediately by the second station to sample the identical water column as nearly as possible. The results obtained and a comparison of the 1964 data with the *Snellius* station data of 1929 are presented in a paper by Dr. Robert E. Burns on pages 39 to 46.

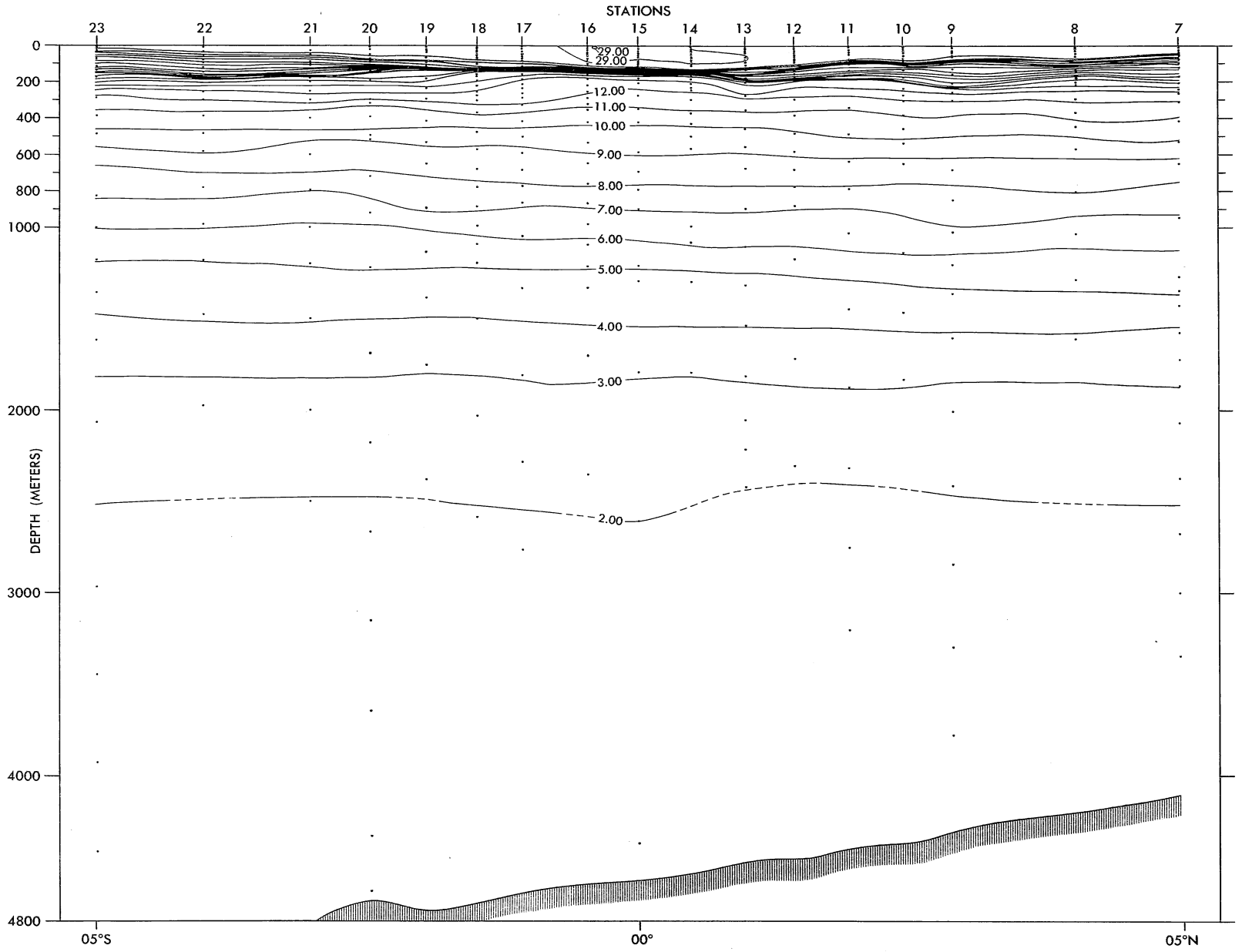


FIGURE 12.—Temperature distribution in °C along 84°E from 5°S to 5°N, May 1964.

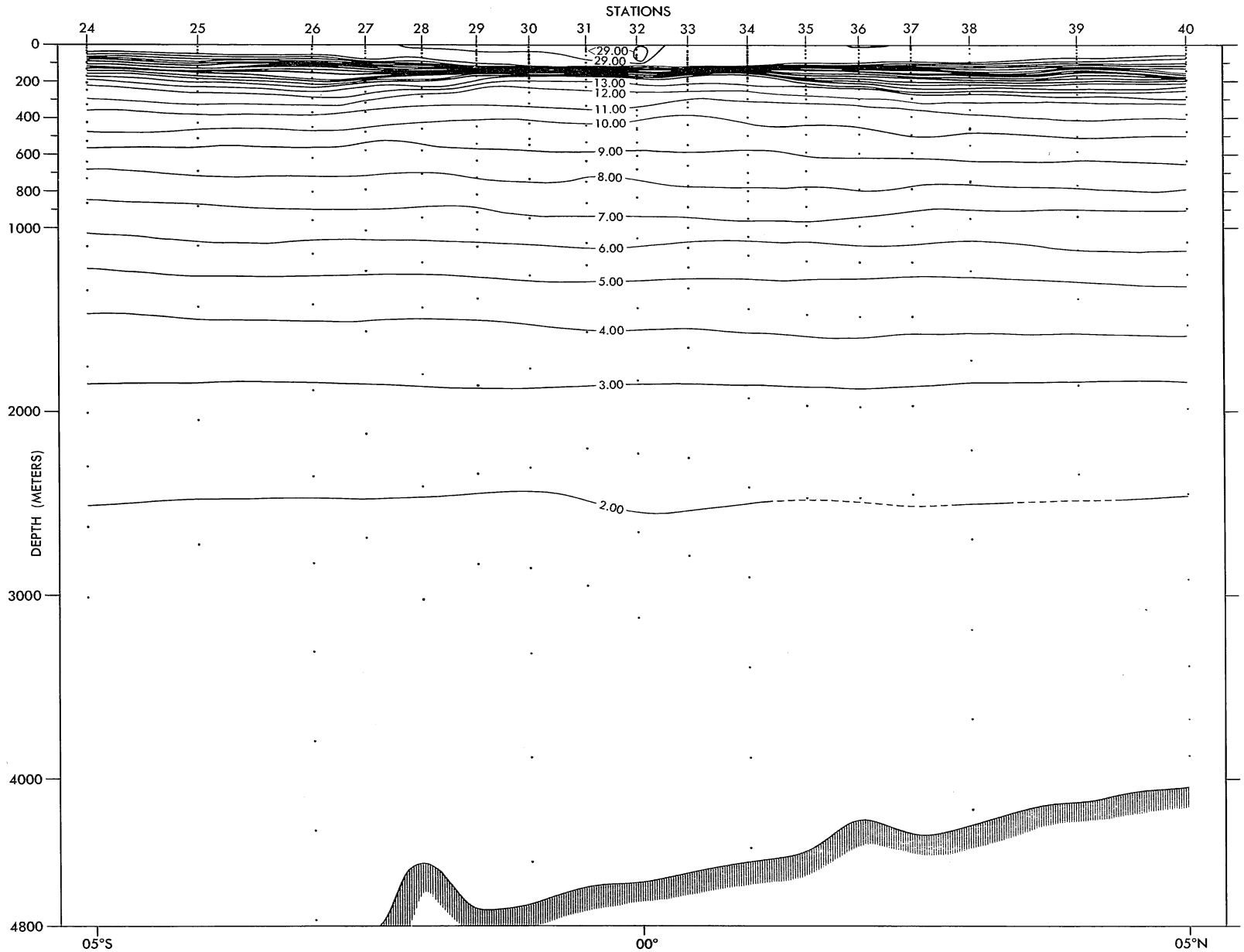


FIGURE 13.—Temperature distribution in °C along 88°E from 5°S to 5°N, June 1964.

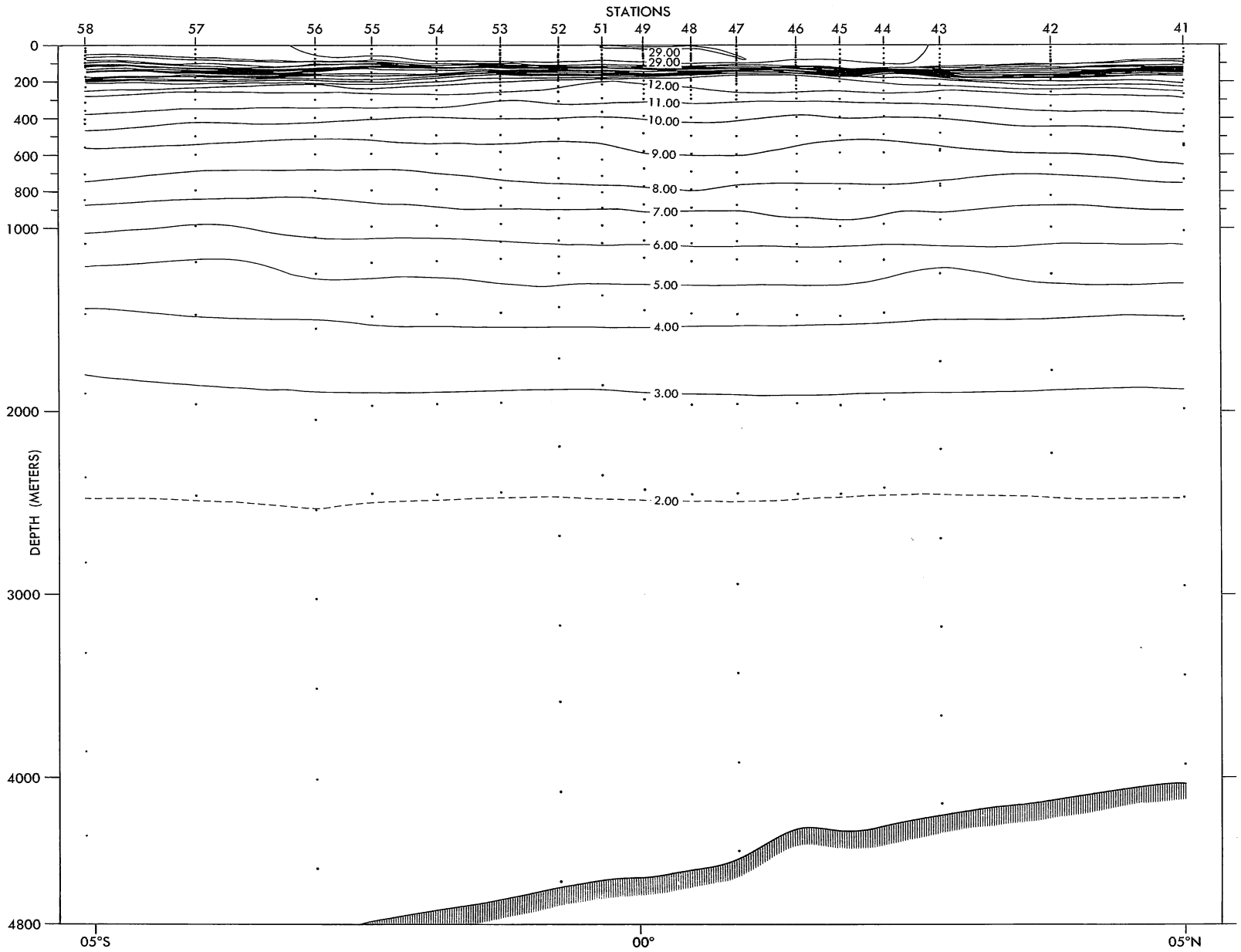


FIGURE 14.—Temperature distribution in °C along 92°E from 5°S to 5°N, June 1964.

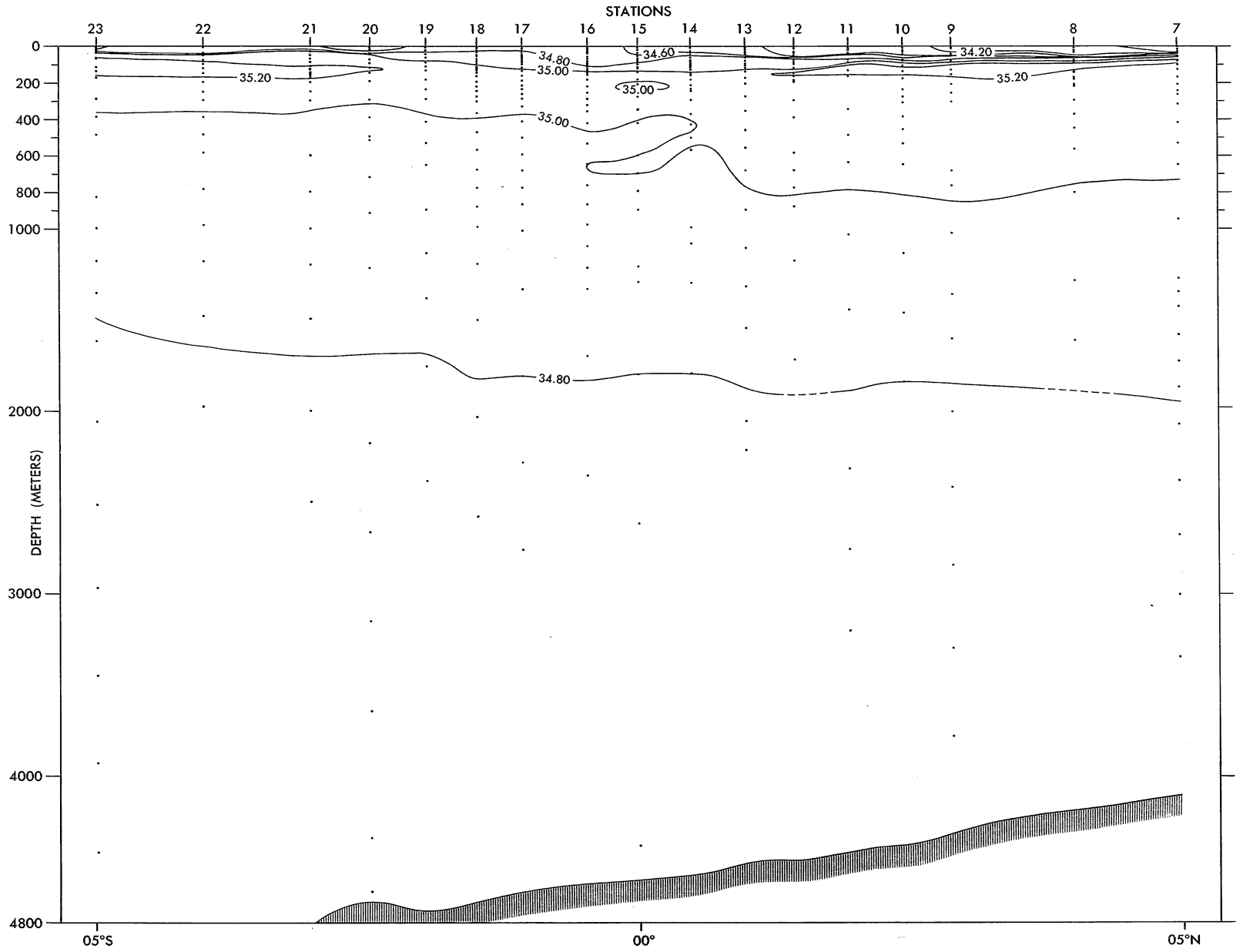


FIGURE 15.—Salinity distribution in °/oo along 84°E from 5°S to 5°N, May 1964.

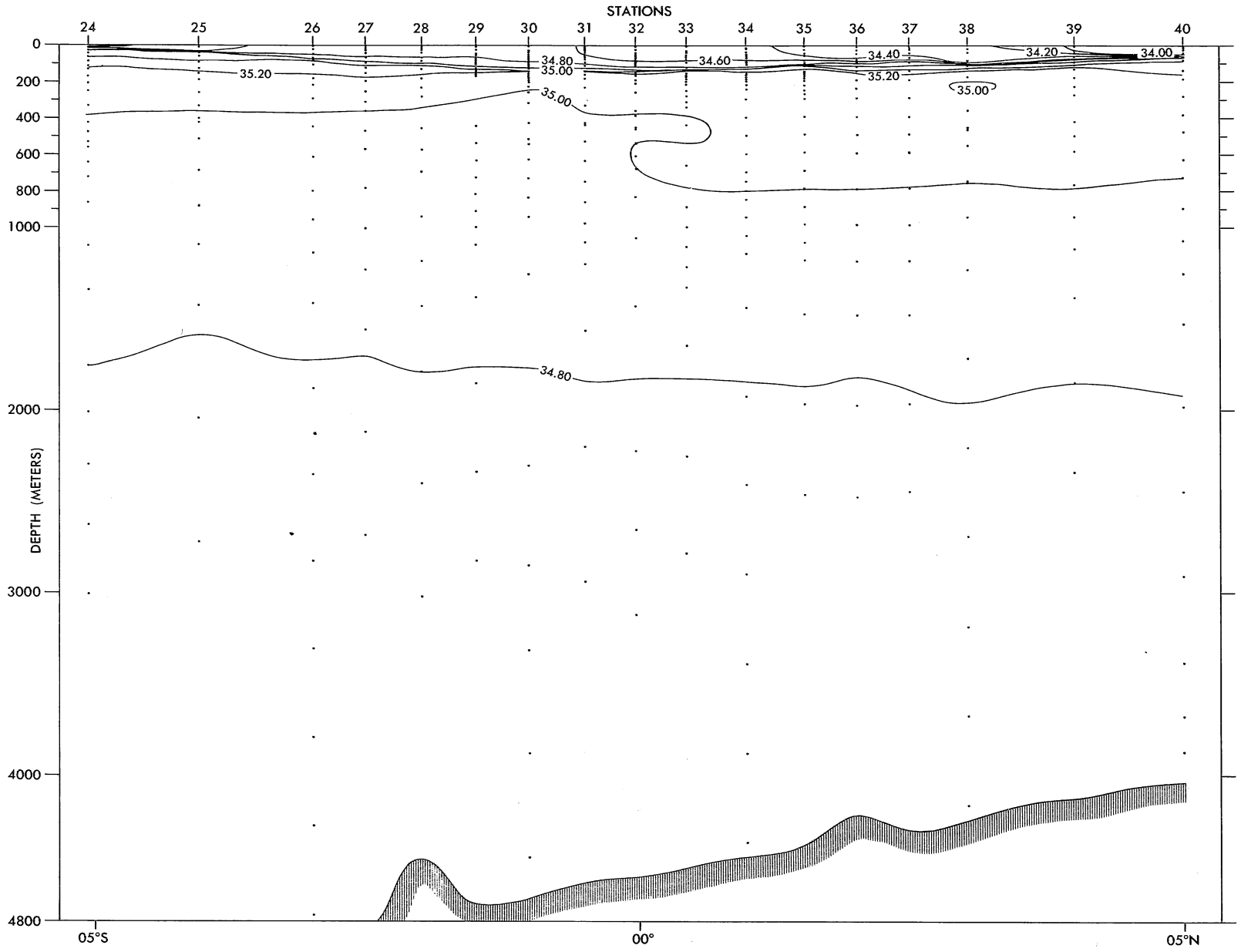


FIGURE 16.—Salinity distribution in °/oo along 88°E from 5°S to 5°N, June 1964.

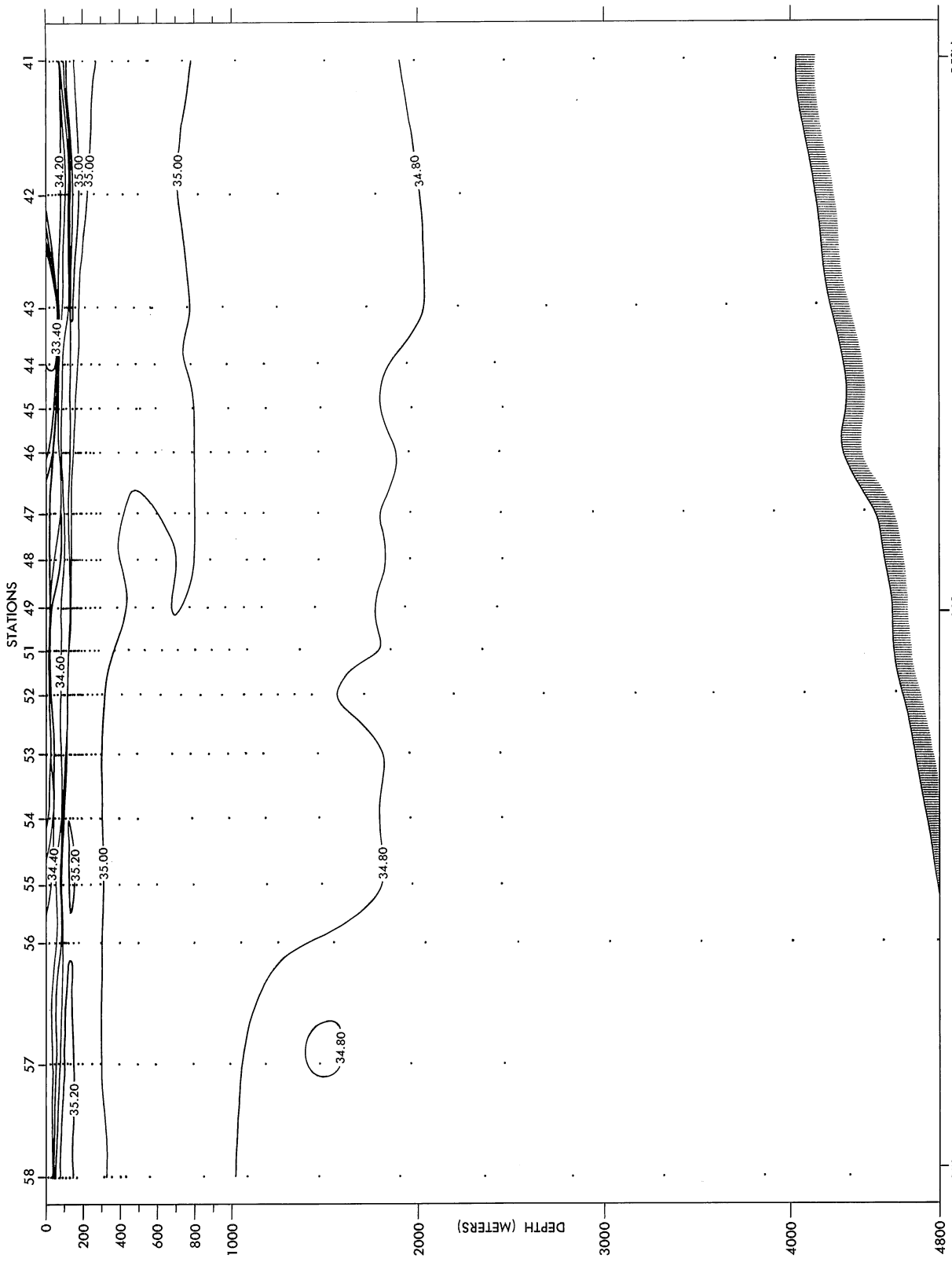


FIGURE 17.—Salinity distribution in °/oo along 92°E from 5°S to 5°N, June 1964.

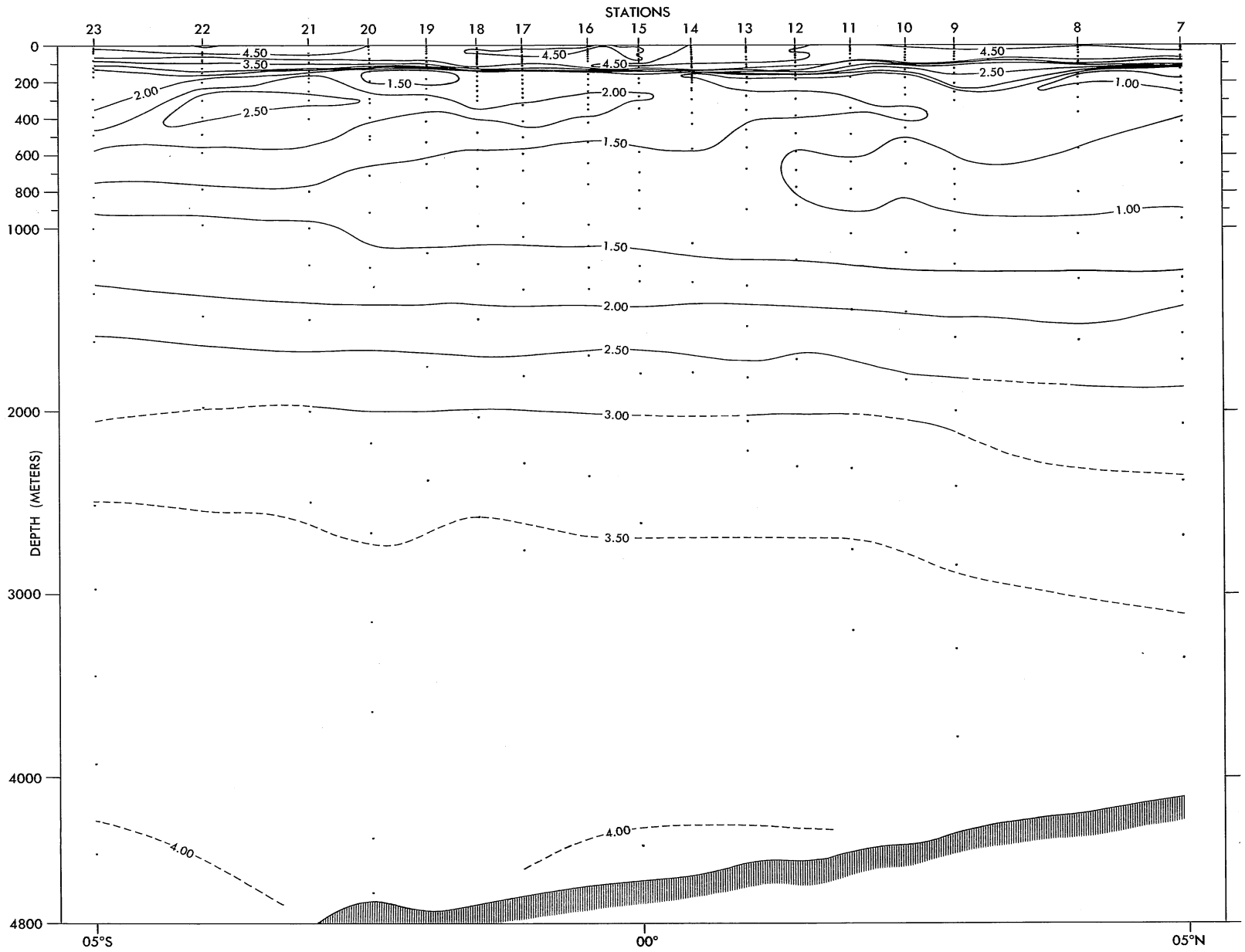


FIGURE 18.—Dissolved oxygen distribution in ml/L along 84°E from 5°S to 5°N, May 1964.

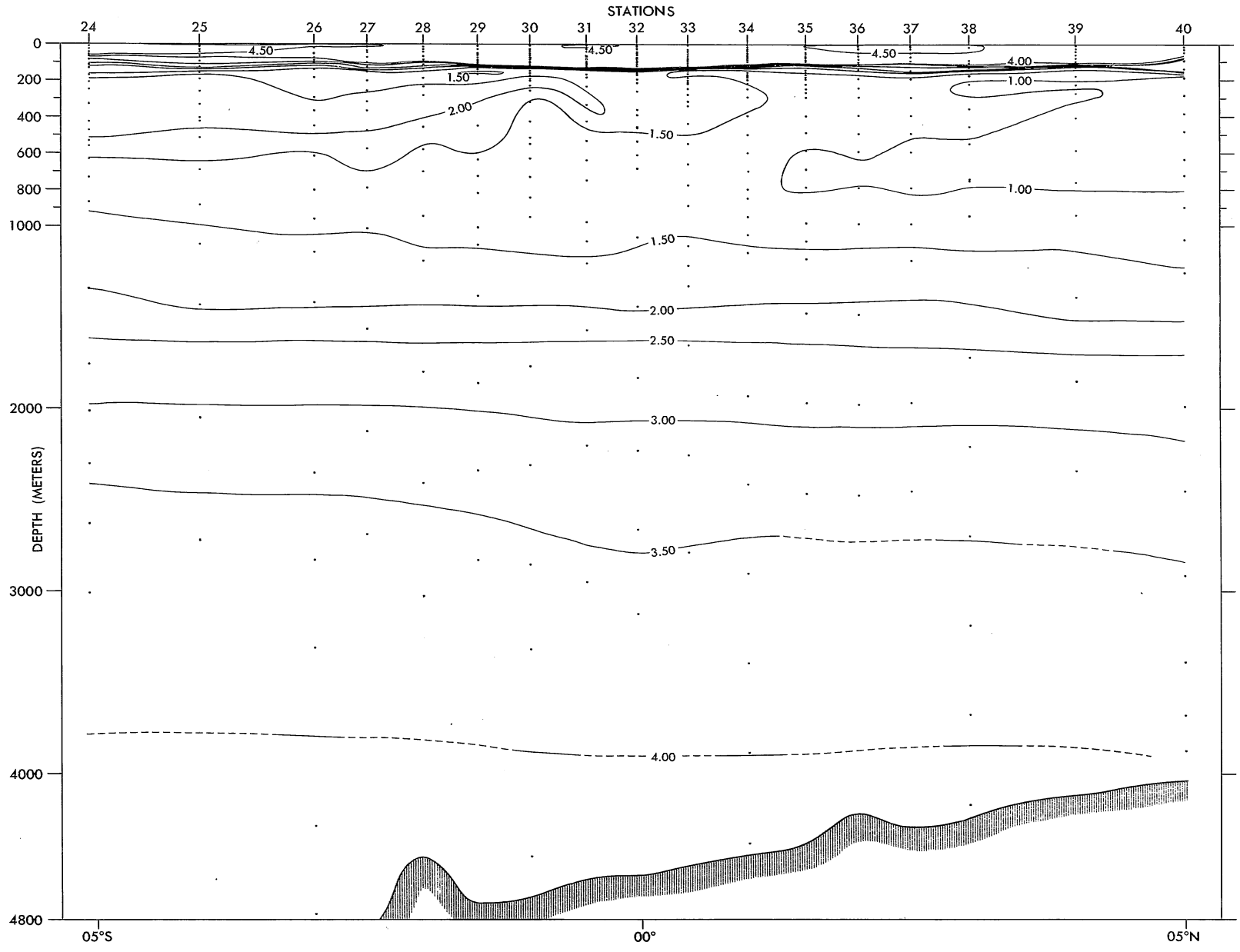


FIGURE 19.—Dissolved oxygen distribution in ml/L along 88°E from 5°S to 5°N, June 1964.

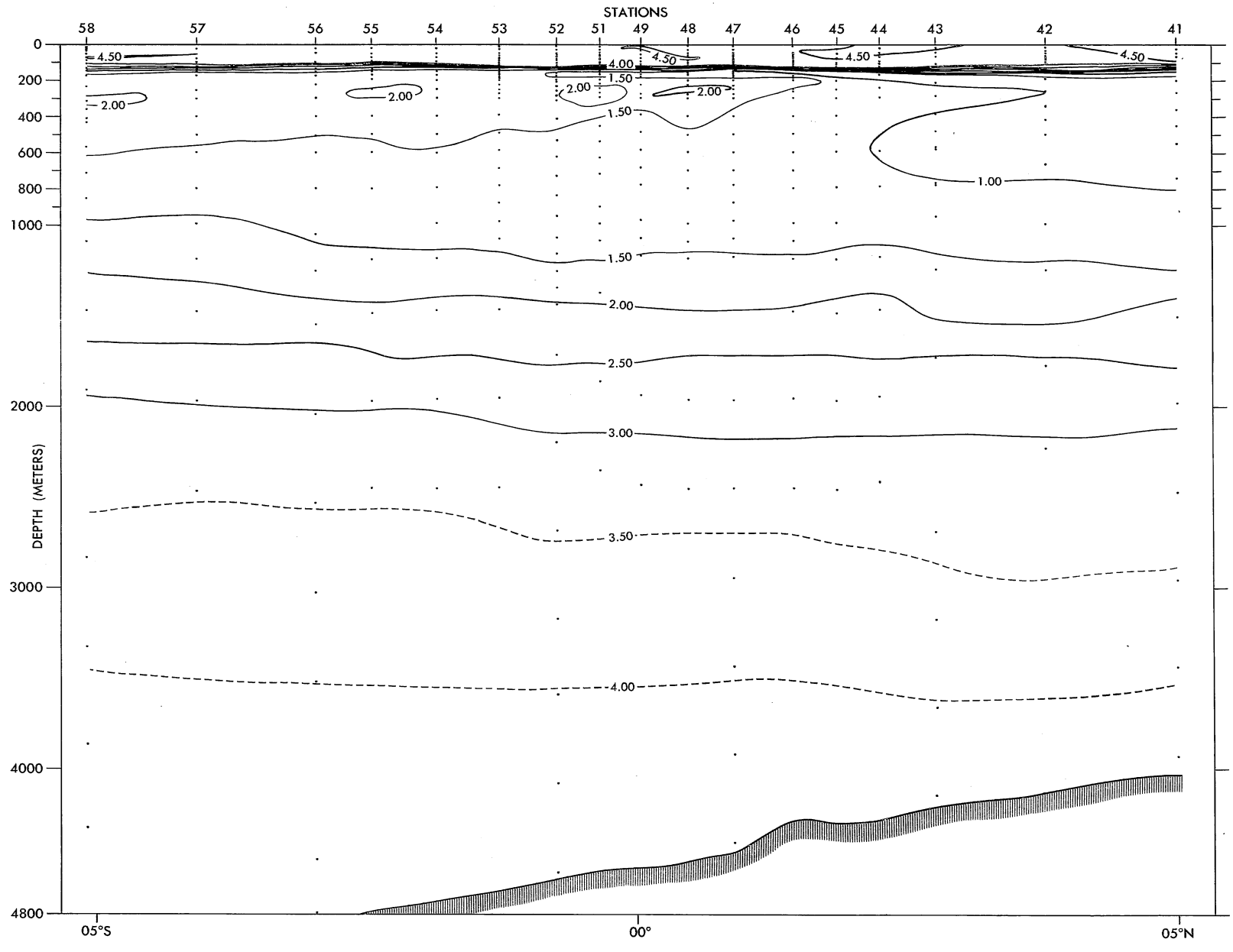


FIGURE 20.—Dissolved oxygen distribution in ml/L along 92°E from 5°S to 5°N, June 1964.

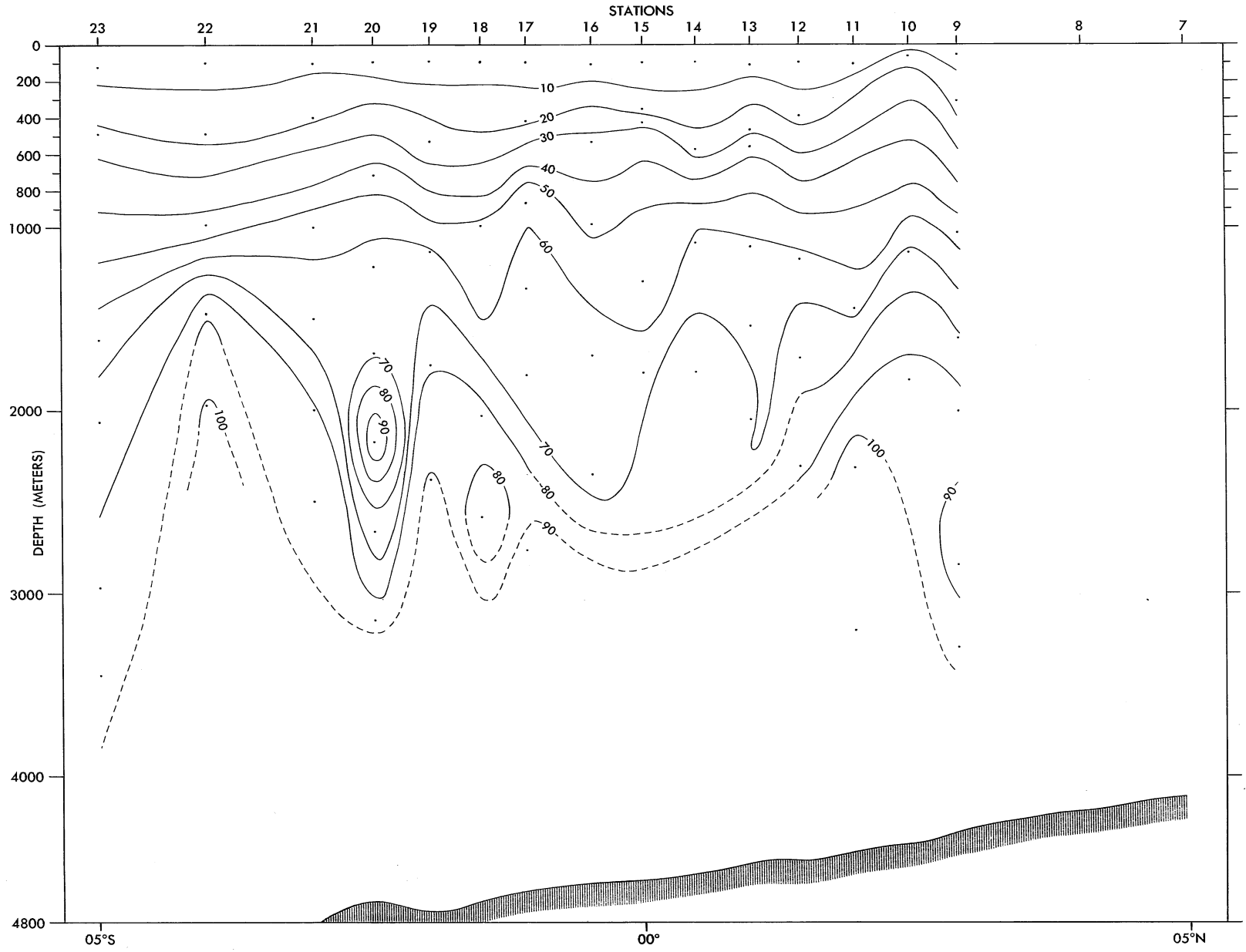


FIGURE 21.—Dissolved silicate distribution in μg-at/L along 84°E from 5°S to 5°N, May 1964.

790-089 O—66——3

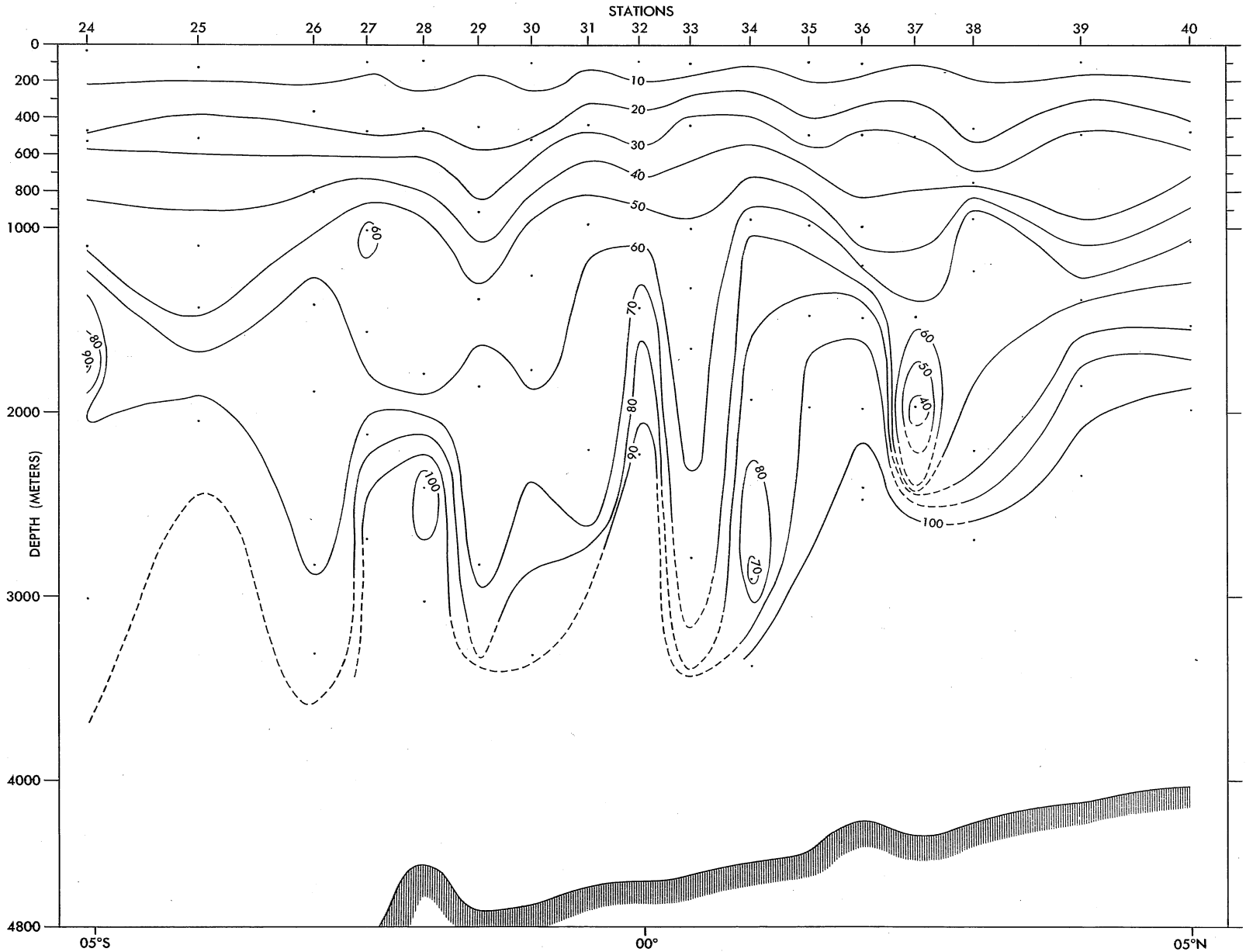


FIGURE 22.—Dissolved silicate distribution in μg-at/L along 88°E from 5°S to 5°N, June 1964.

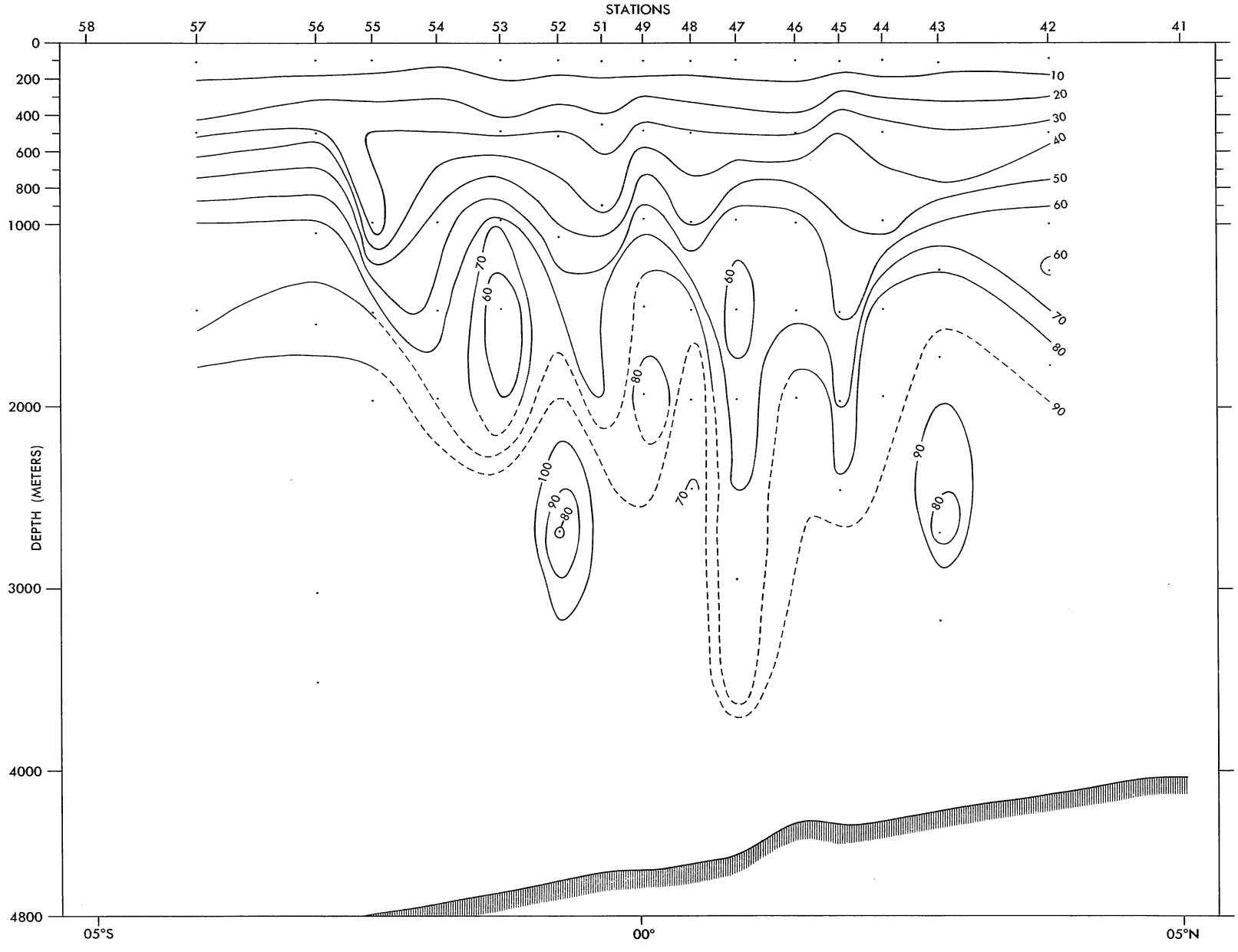


FIGURE 23.—Dissolved silicate distribution in μg-at/L along 92°E from 5°S to 5°N, June 1964.

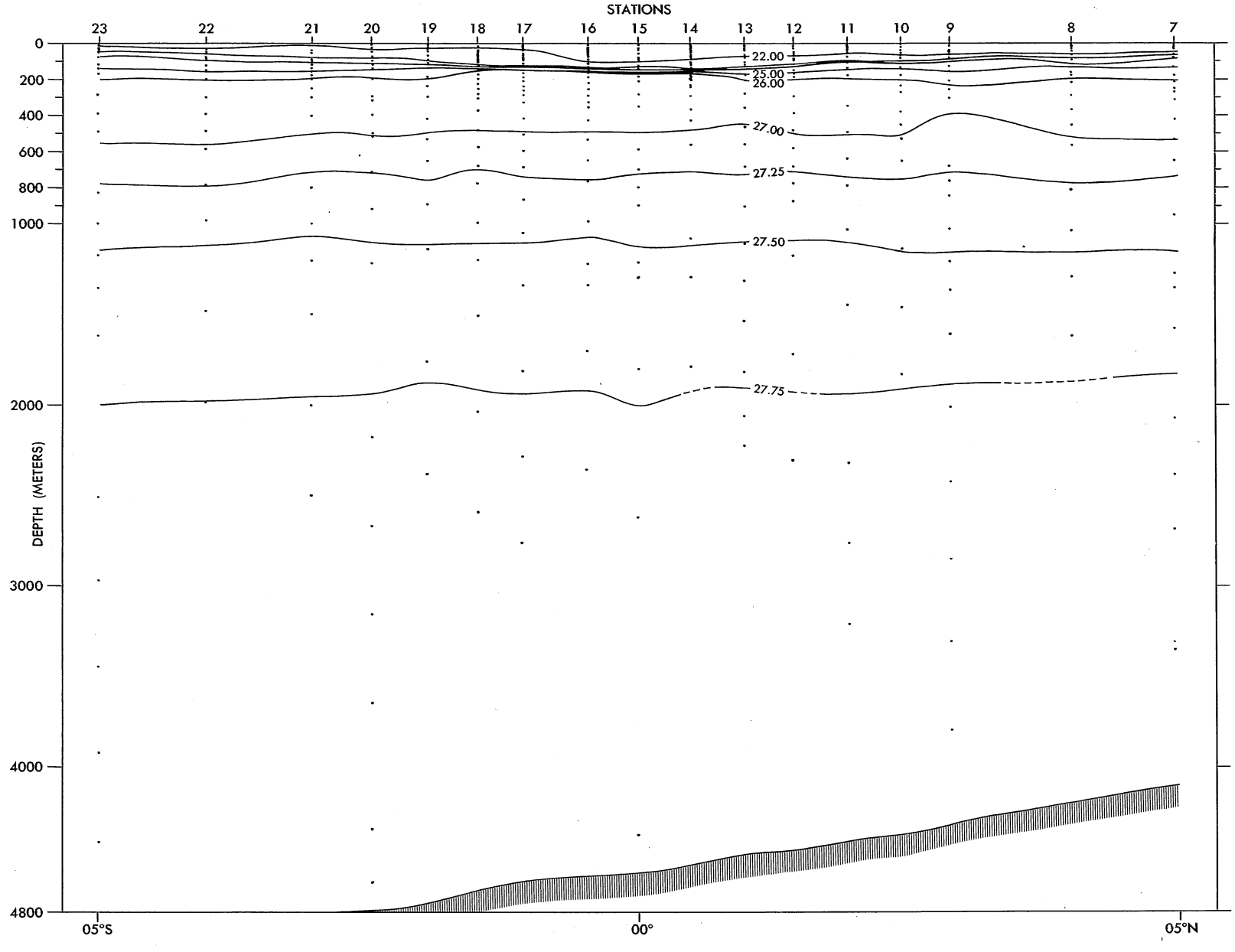


FIGURE 24.—Density distribution in $\sigma_t$ along 84°E from 5°S to 5°N, May 1964.

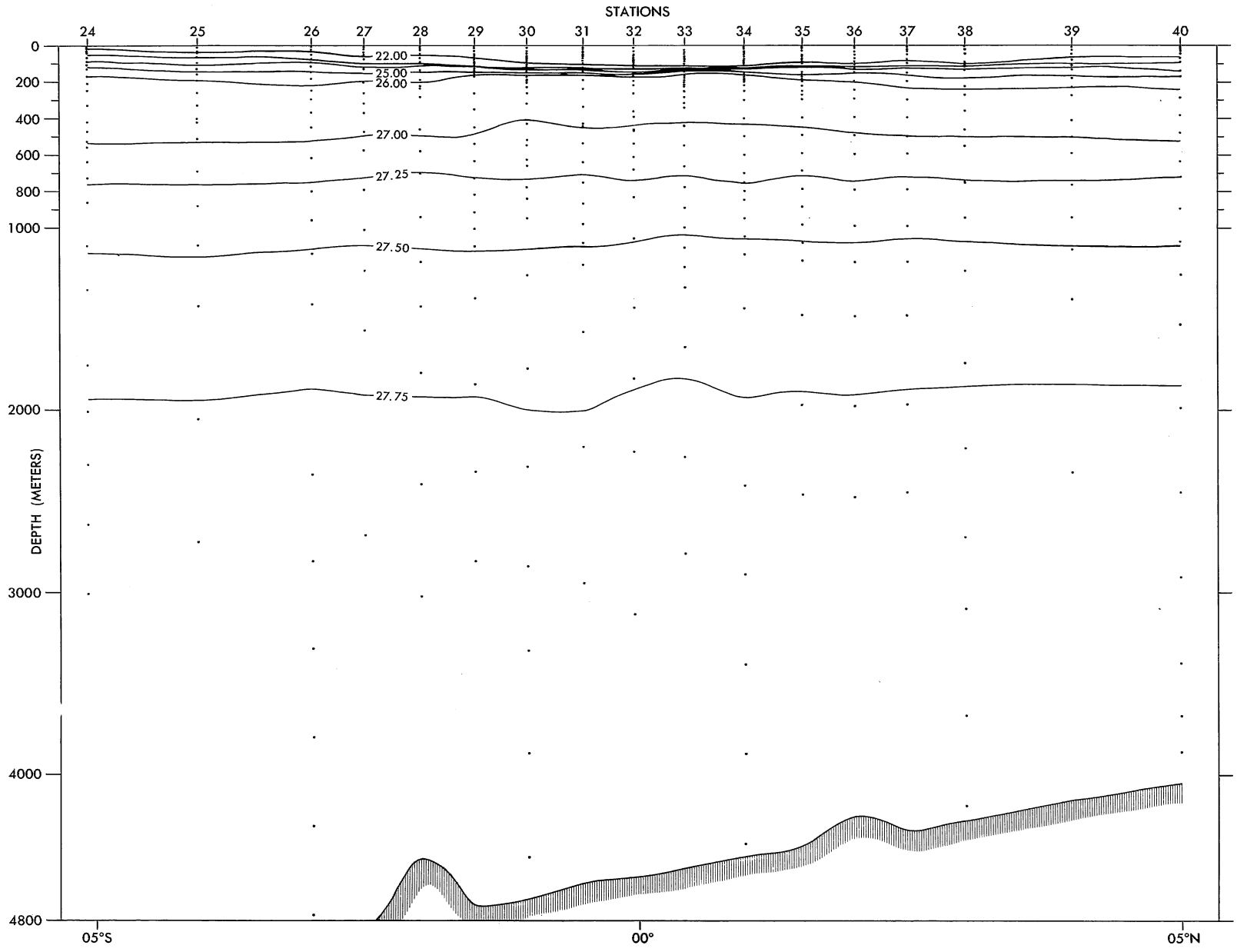


FIGURE 25.—Density distribution in $\sigma_t$ along 88°E from 5°S to 5°N, June 1964.

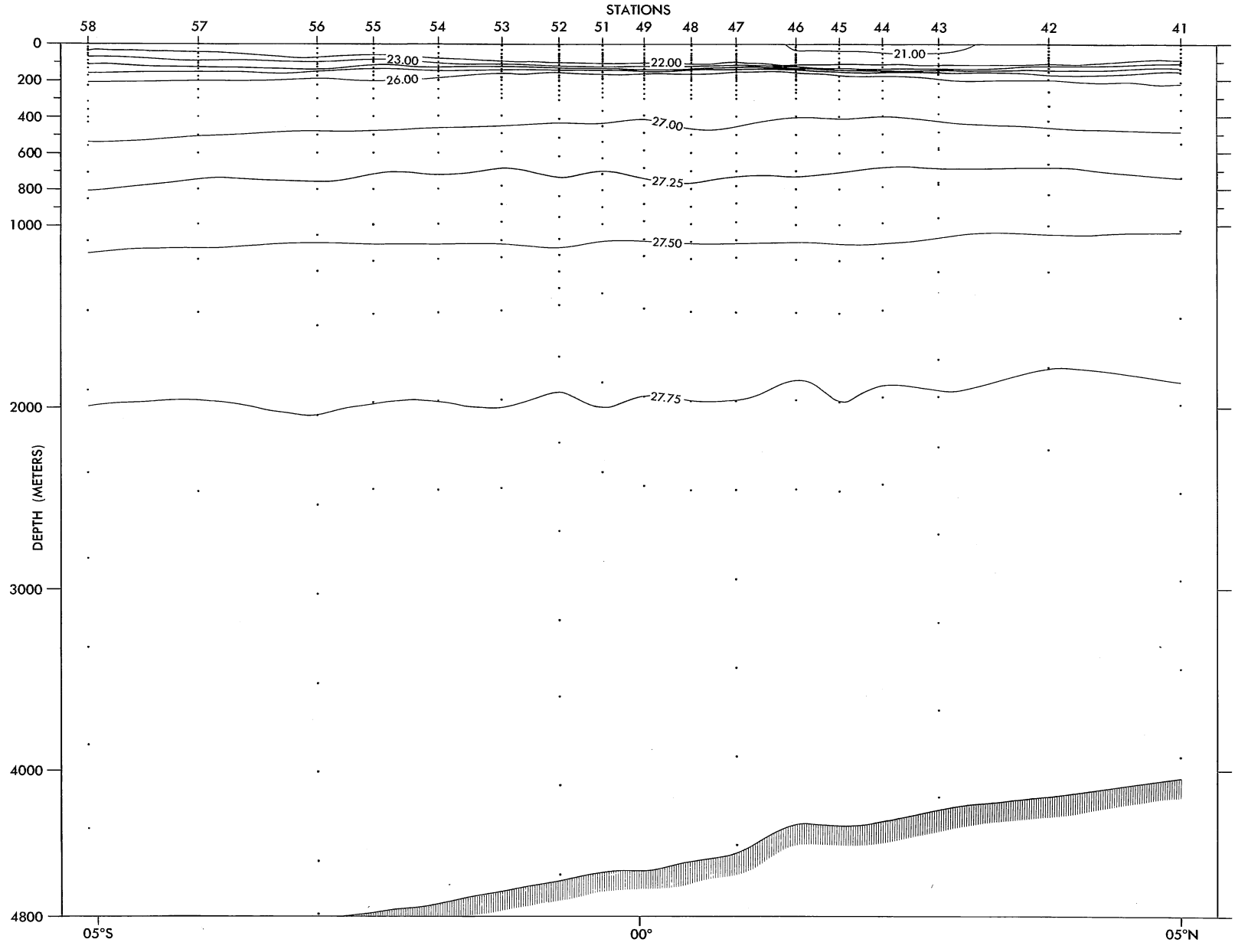


FIGURE 26.—Density distribution in $\sigma_t$ along 92°E from 5°S to 5°N, June 1964.

## Bathythermograph Observations

The *Pioneer* made 885 bathythermograph lowerings during the period February 14 to August 10, 1964—74 lowerings en route to Honolulu from San Francisco in February and 67 lowerings along this section of the return track in August; 306 lowerings in the western Pacific Ocean; and, 438 lowerings in the South China Sea, Strait of Malacca, Andaman Sea, Bay of Bengal, Indian Ocean, Java Sea, and Celebes Sea. A 250-m BT was used. Observations were made every 2 hours while underway. At least one lowering was made at every oceanographic station. BT traces and log sheets were forwarded to the National Oceanographic Data Center, Washington, D.C. Modified BT long sheets appear in volume 2 of this cruise report. Bathythermograph prints may be ordered—by the number shown on the log sheets—from NODC. Selected bathythermograph profiles (numbers 1–23; figs. 27–49) were prepared from the BT data obtained in the western Pacific, southeast Asian waters, and Indian Ocean. The trackline location and reference numbers of the profiles are shown on chart 1 (facing page 140).

In the western Pacific, bathythermograph observations were made between Hawaii and the Philippines during the months of February and March (profile numbers 1 through 7) while en route to the Indian Ocean and again in the month of July (profile numbers 17 through 23) on the return trip. A comparison of these winter and summer profiles shows the change brought about by summer heating. This effect can be seen very readily by comparing the February profile No. 7 (fig. 33) and July profile No. 23 (fig. 49) just west of Hawaii.

BT profile numbers 11, 12, and 13 correspond in position with the oceanographic-station sections across the Equator at 84°E, 88°E, and 92°E in the Indian Ocean and profile numbers 15 and 16 show the temperature distribution in the Macassar Strait and the Celebes Sea, respectively.

Bathythermograph lowerings numbered 473 to 477 were made on June 13, 1964 off the northwest coast of Sumatra as part of a special investigation to detect internal water movements that might be associated with zones of choppy water observed on the surface. The unusual phenomenon was first observed by the *Pioneer* on June 12 when five distinct, north-south trending, surface zones of choppy sea were sighted. These zones were 200 to 800 m in width, 3,200 m apart, and easily seen by their short, steep, randomly oriented, white-capped waves. Wave heights ranged from 0.3 to 0.6 m. On June 13, similar north-south bands of choppy water were sighted near 06°09′N, 94°37′E. Ten bands of approximately 200-m width and 800 m apart were observed (fig. 50). After crossing a number of the bands, the *Pioneer*'s course was altered and the bathythermograph lowerings were commenced. The observed phenomenon is described, and the results of the special investigation are discussed, by R. B. Perry and G. R. Schimke on pages 47 to 52.

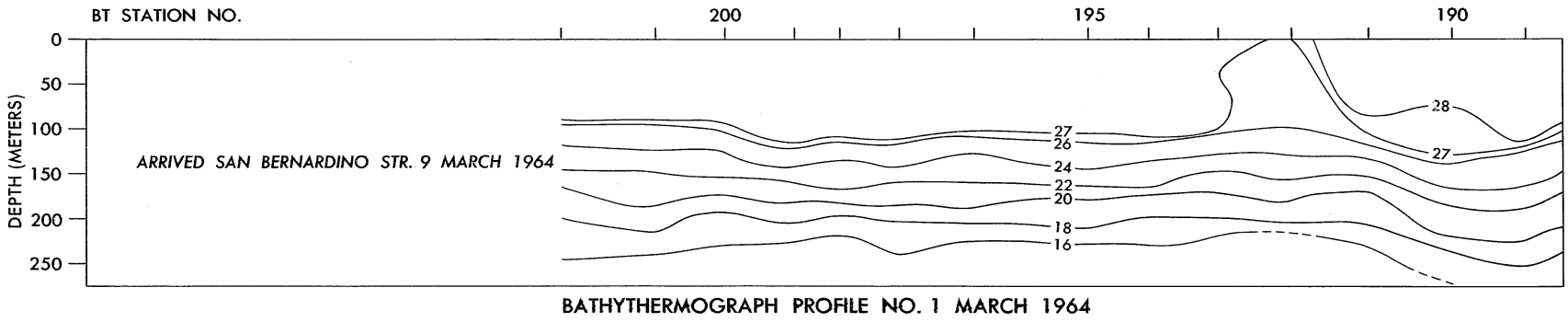


FIGURE 27.—Bathythermograph profile No. 1, western Pacific, March 1964.

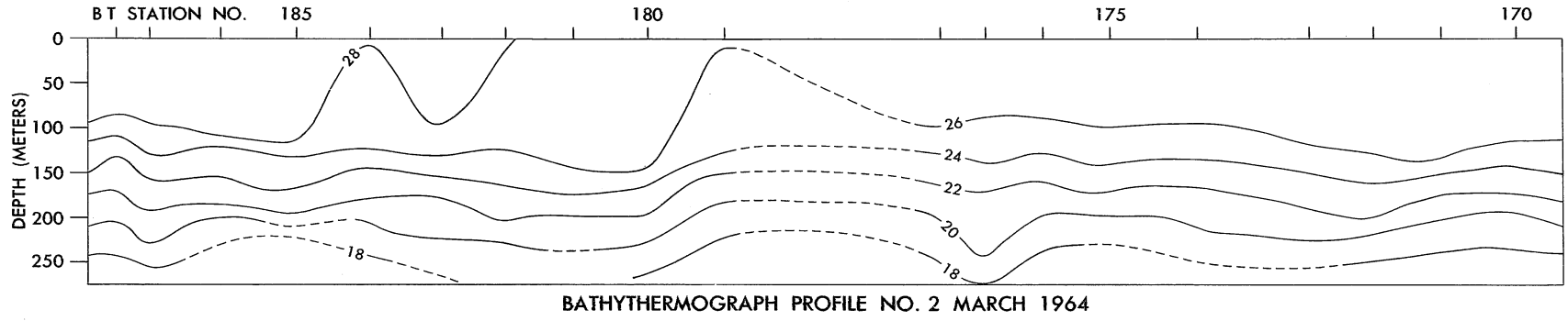


FIGURE 28.—Bathythermograph profile No. 2, western Pacific, March 1964.

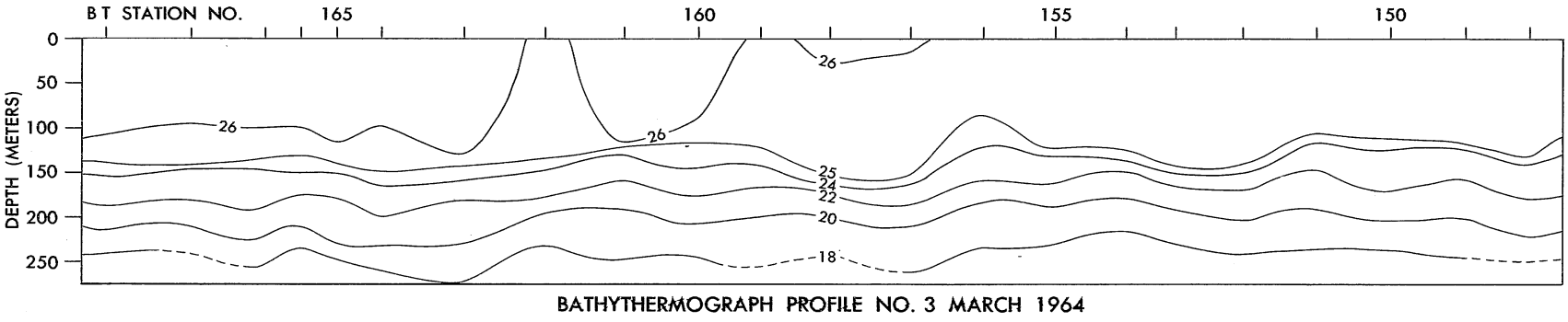


FIGURE 29.—Bathythermograph profile No. 3, western Pacific, March 1964.

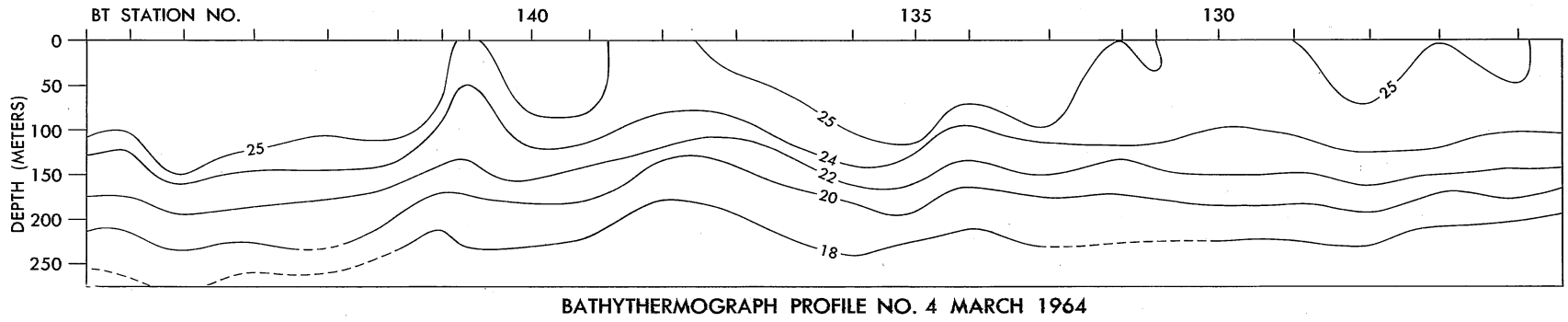


FIGURE 30.—Bathythermograph profile No. 4, western Pacific, March 1964.

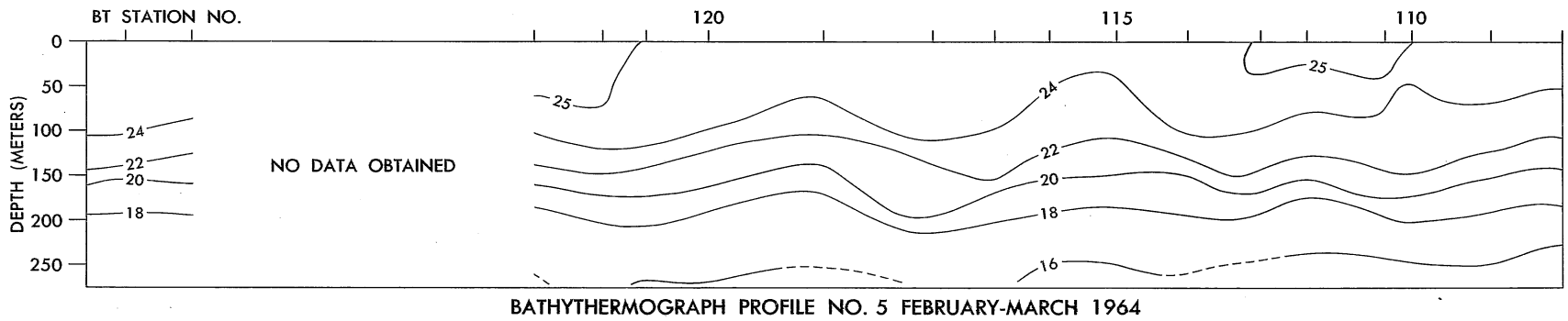


FIGURE 31.—Bathythermograph profile No. 5, western Pacific, February–March 1964.

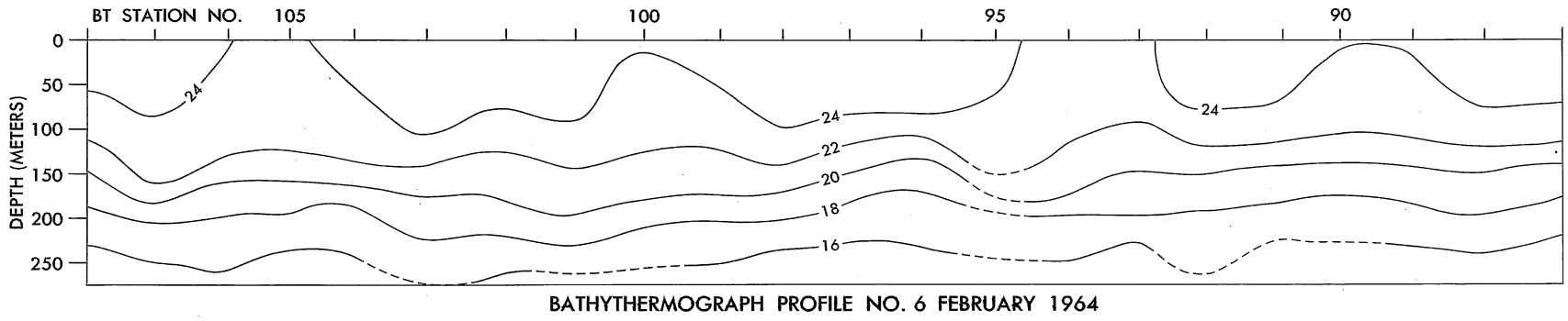


FIGURE 32.—Bathythermograph profile No. 6, western Pacific, February 1964.

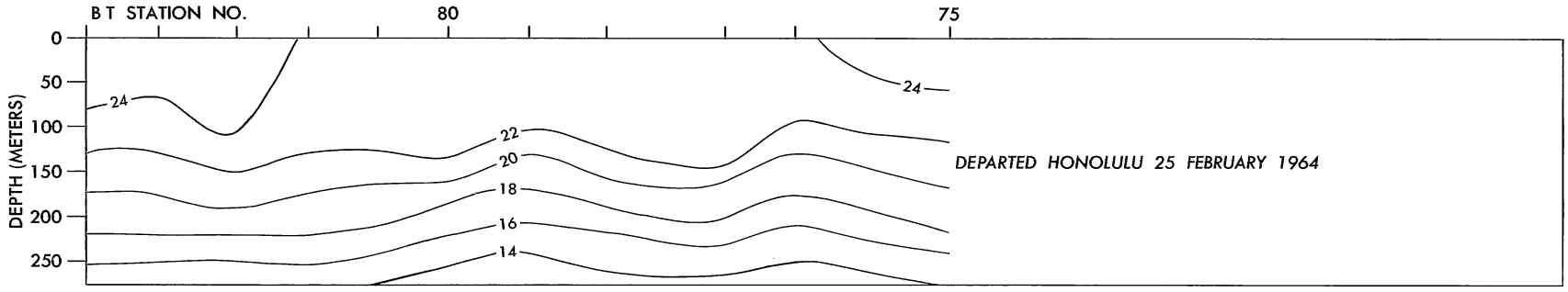


FIGURE 33.—Bathythermograph profile No. 7, western Pacific, February 1964.

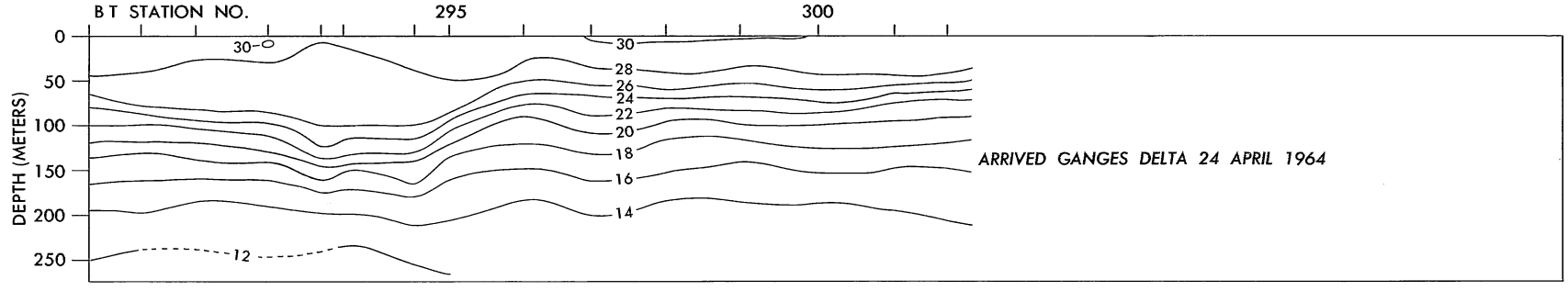


FIGURE 34.—Bathythermograph profile No. 8, Bay of Bengal, April 1964.

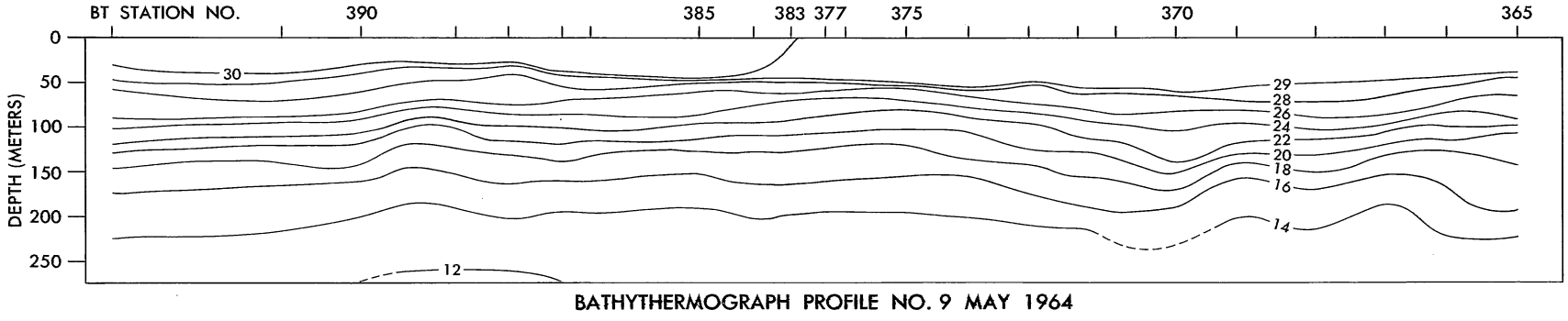


FIGURE 35.—Bathythermograph profile No. 9, Bay of Bengal, May 1964.

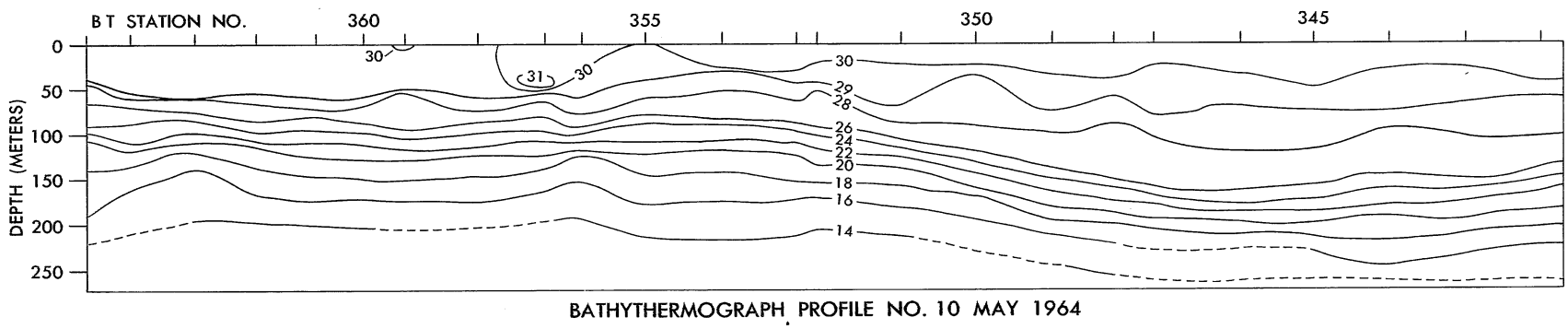


FIGURE 36.—Bathythermograph profile No. 10, Bay of Bengal, May 1964.

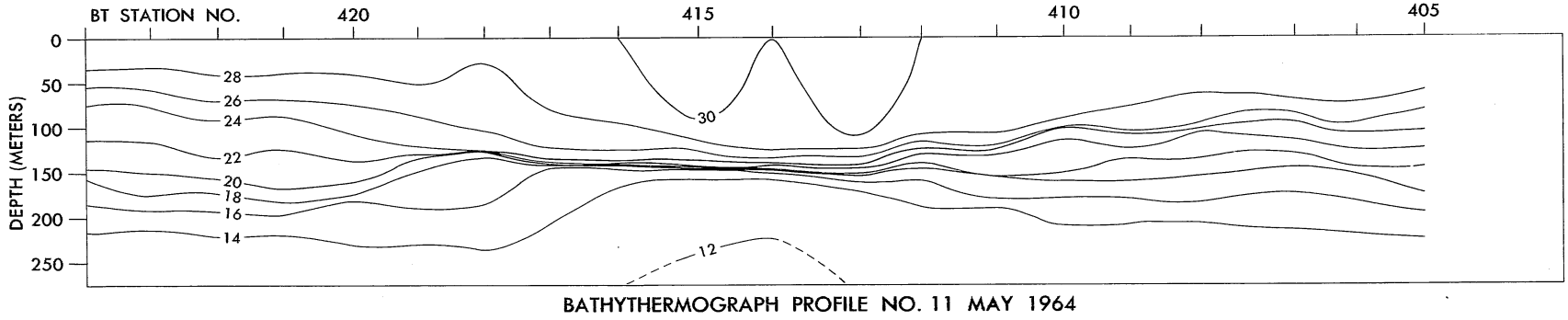


FIGURE 37.—Bathythermograph profile No. 11, Indian Ocean, May 1964.

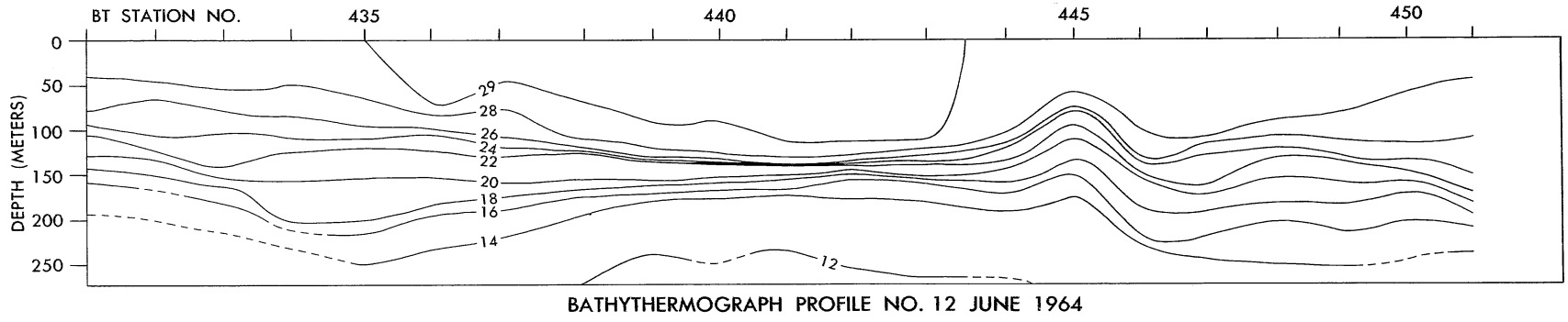


FIGURE 38.—Bathythermograph profile No. 12, Indian Ocean, June 1964.

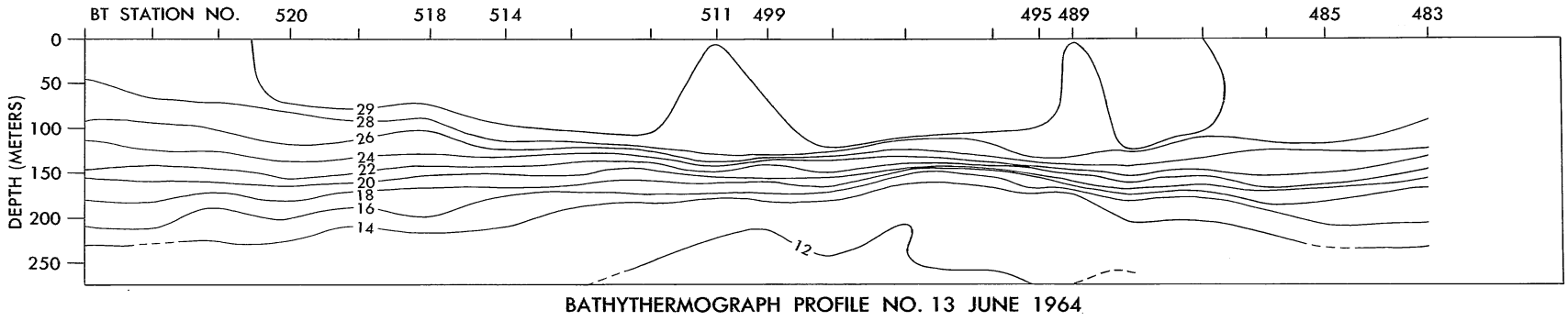


FIGURE 39.—Bathythermograph profile No. 13, Indian Ocean, June 1964.

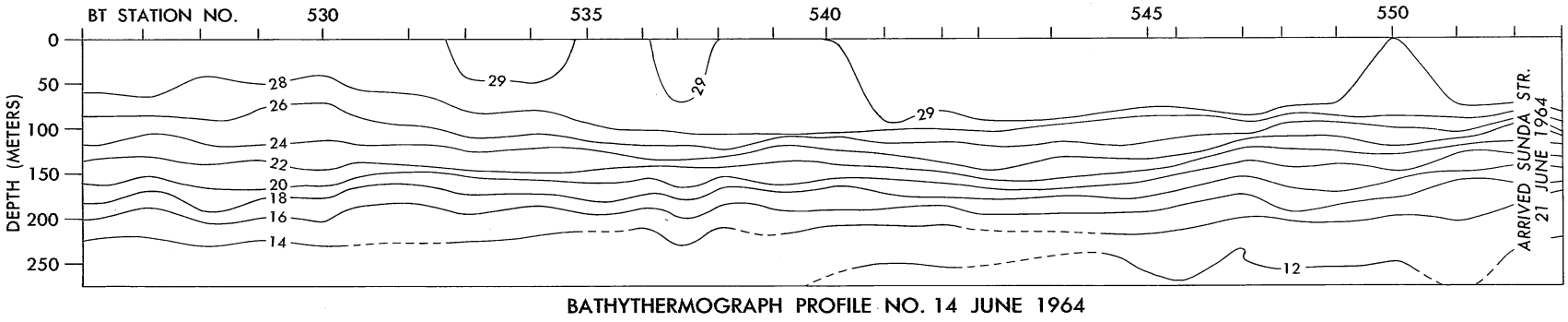


FIGURE 40.—Bathythermograph profile No. 14, Indian Ocean, June 1964.

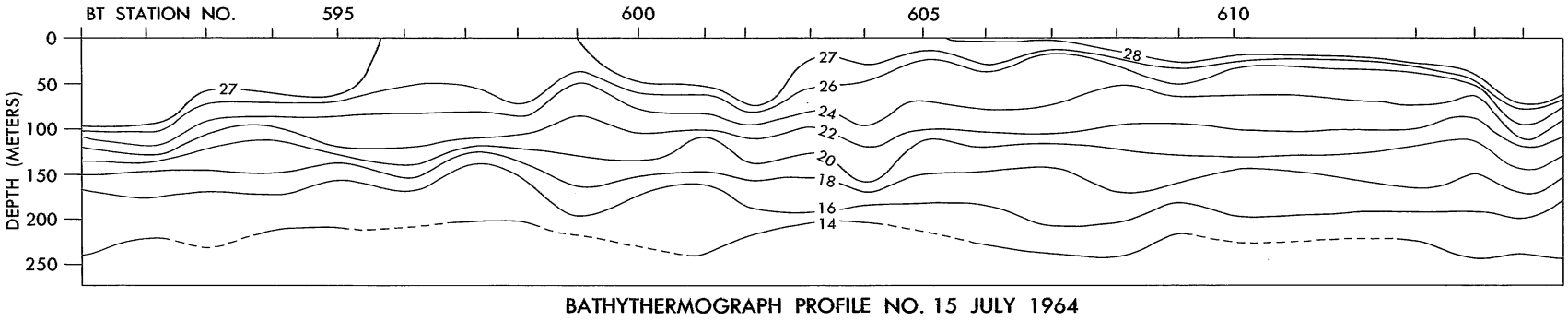


FIGURE 41.—Bathythermograph profile No. 15, Macassar Strait, July 1964.

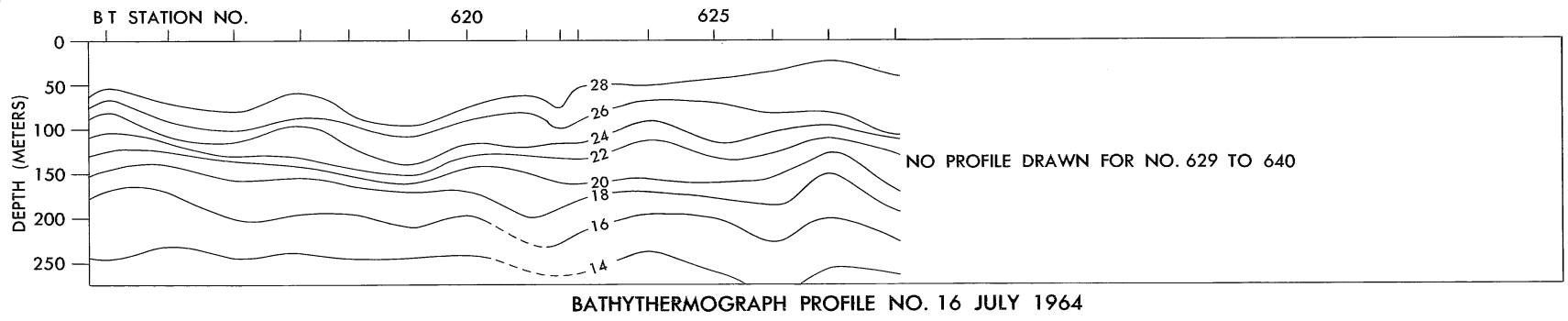


FIGURE 42.—Bathythermograph profile No. 16, Celebes Sea, July 1964.

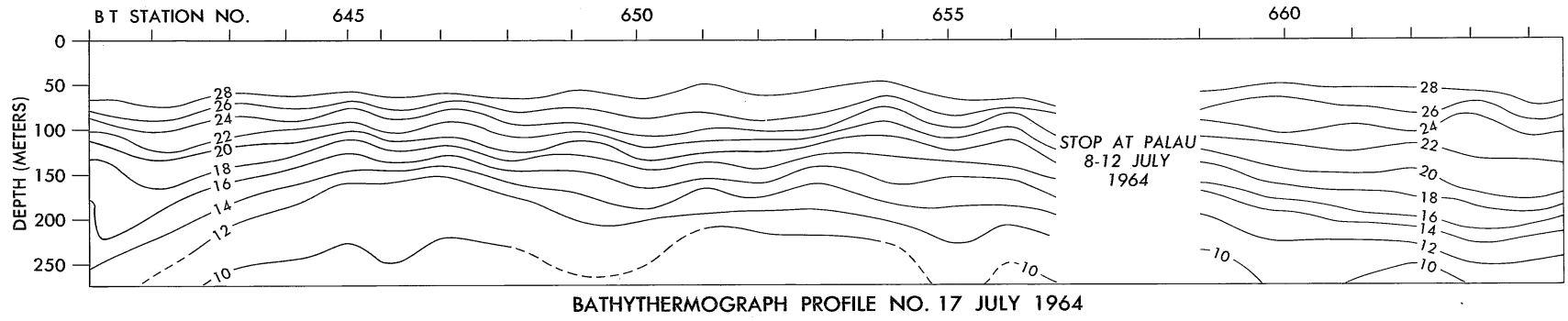


FIGURE 43.—Bathythermograph profile No. 17, western Pacific, July 1964.

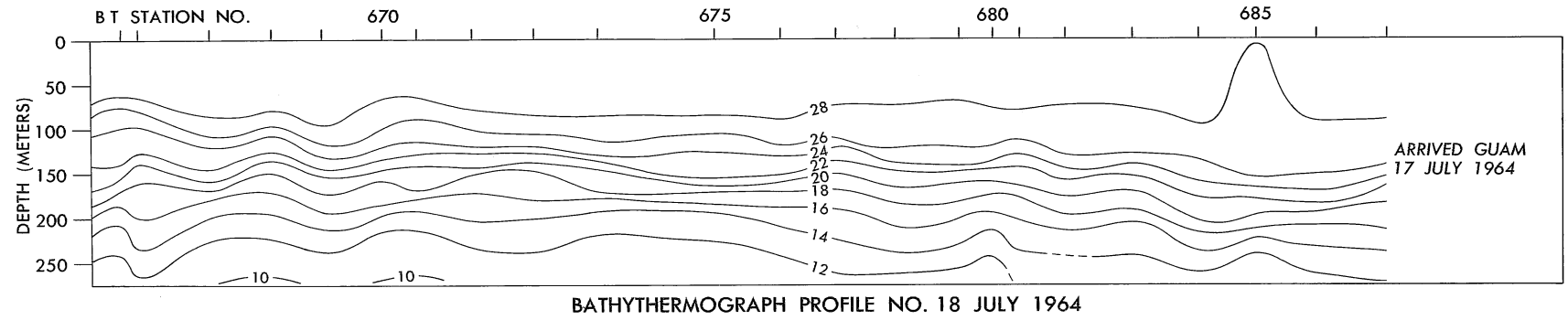


FIGURE 44.—Bathythermograph profile No. 18, western Pacific, July 1964.

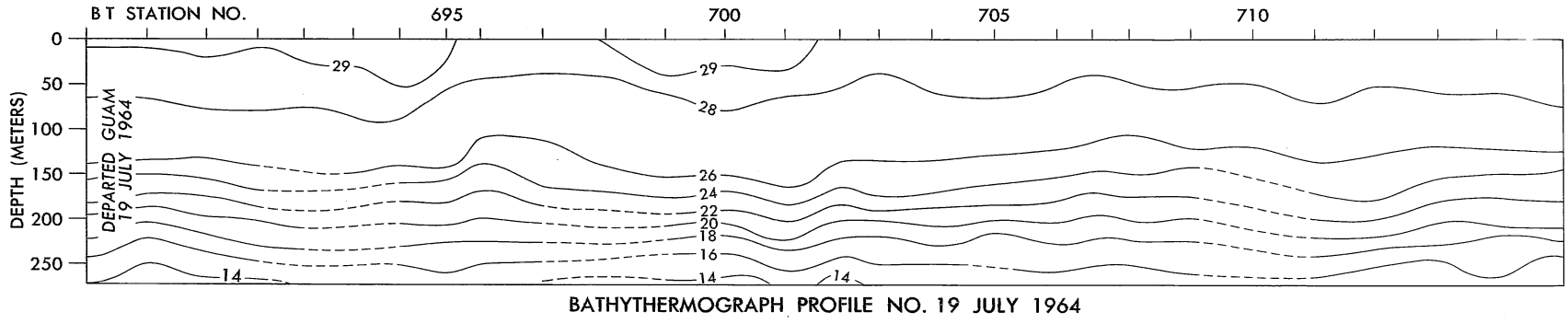


FIGURE 45.—Bathythermograph profile No. 19, western Pacific, July 1964.

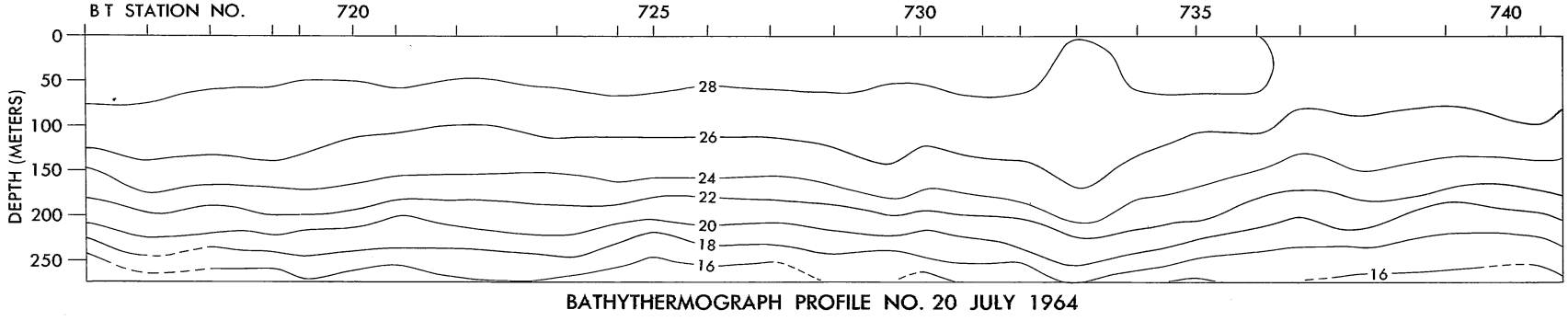


FIGURE 46.—Bathythermograph profile No. 20, western Pacific, July 1964.

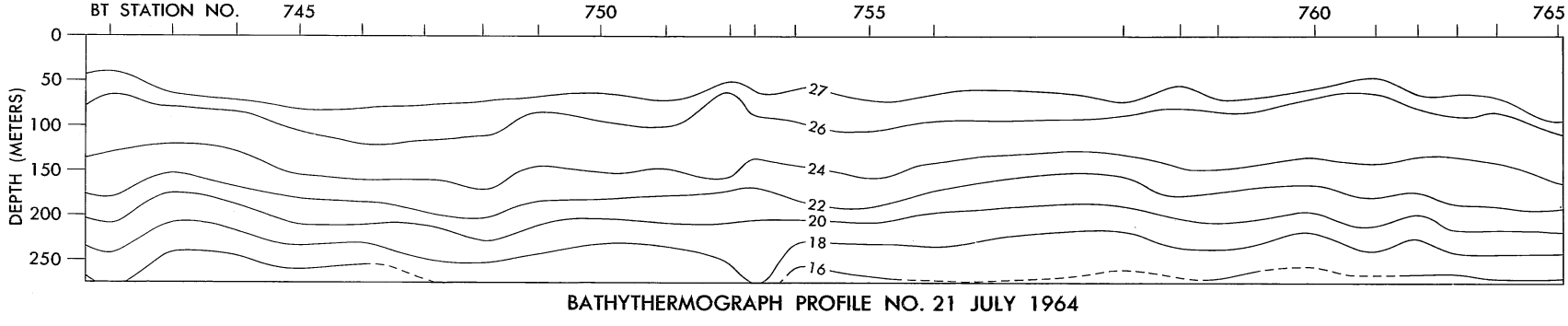


FIGURE 47.—Bathythermograph profile No. 21, western Pacific, July 1964.

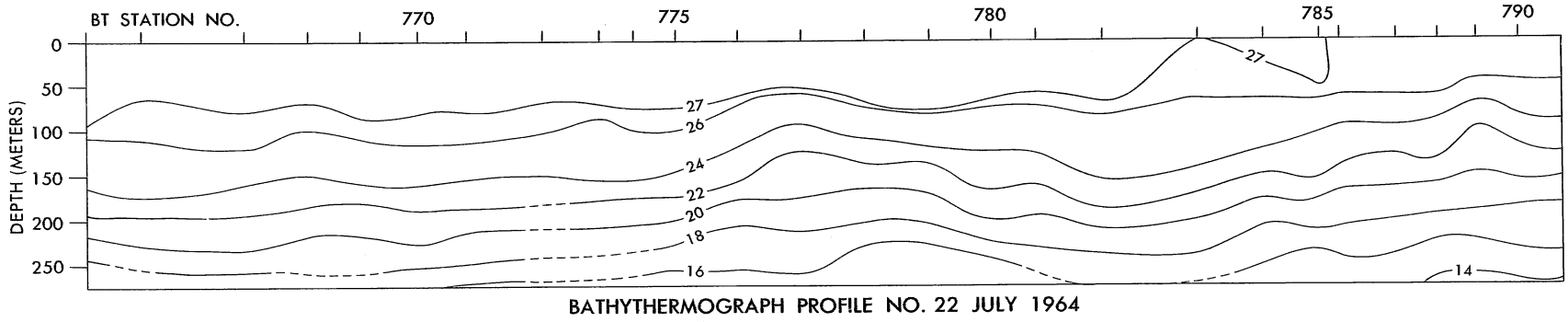


FIGURE 48.—Bathythermograph profile No. 22, western Pacific, July 1964.

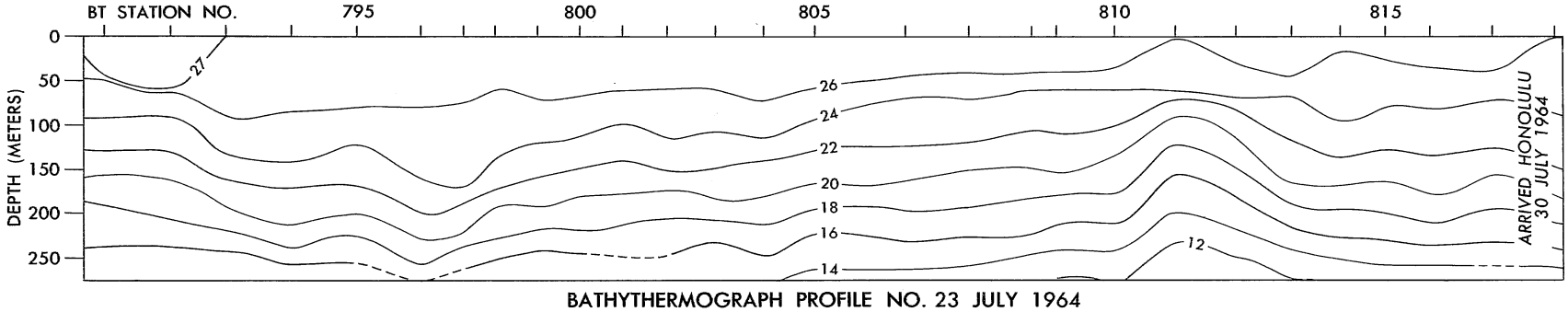


FIGURE 49.—Bathythermograph profile No. 23, western Pacific, July 1964.

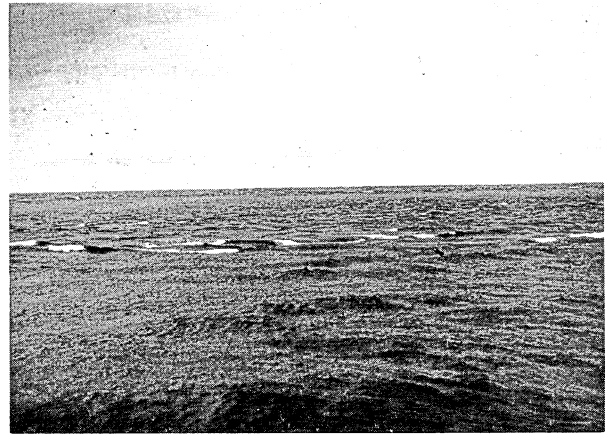

FIGURE 50.—Surface zone of choppy water observed northwest of Sumatra, June 13, 1964.

# A Comparison of Temperature and Salinity Data From the Central Portion of the Celebes Sea

ROBERT E. BURNS*

A replicate pair of oceanographic stations was observed on July 3, 1964 in the Celebes Sea as the USC&GS ship *Pioneer* returned to the United States from the 1964 Indian Ocean Expedition. The observed and interpolated values from the paired stations were compared and evaluated and the results were then compared with observations made in the same area by the *Snellius* in September 1929 (van Riel, 1934).

Instructions to the ship requested that paired stations—two stations at the same position and, as nearly as possible, at the same time—be obtained in the general area of the *Snellius* station at 3°N, 121°E in the center of the Celebes Sea. Each of the stations was to sample the whole of the water depth and to maintain as similar a spacing of sample bottles as possible. The second station of the pair was to follow immediately after completion of the first station in order to sample the identical water column and, presumably, the same distribution of water properties.

The *Pioneer* occupied the replicate stations, NODC station numbers 0062 and 0063, on July 3, 1964 at a mean position of 04°00.4′N, 122°36.0′E. The first station, 0062 (fig. 51[1]), consisted of three casts: cast I from 100 to 2,000 meters had a wire angle of 8 degrees; cast II from 2,000 to 5,100 m had a wire angle of 10 degrees; and, cast III from 0 to 75 m had a 0-degree wire angle. The second station, 0063 (fig. 52[2]), consisted of two casts: cast I from 0 to 800 m had a wire angle of 18 degrees; and, cast II from 950 to 5,050 m had a wire angle of 5 degrees. The entire operation was completed in less than five hours. For each station, a similar spacing of sample bottles was maintained over the first 800 m. On the second station, the wire angle was observed to change. For this reason, station 0063 was stopped short of the intended wire-out and the wire-depth of samples below 800 m differed from those of station 0062 by 50 m.

In the comparisons which follow, the data from the two stations are subjected to two analyses. First, there is an evaluation of observed and interpolated temperature and salinity values from the two paired stations to determine the best estimate of property distribution at the time the stations were occupied. Second, the accepted values for the *Pioneer* paired stations are then compared with the temperature and salinity values observed by the *Snellius* in 1929.

## COMPARISON OF "PIONEER" REPLICATE STATION DATA

Since neither of the replicate stations may be considered to be a standard, the initial analysis evaluates the reproducibility of the data obtained by each station of the pair. A direct comparison of observed values cannot be made because the sample depths are not identical. Consequently, the interpolated values for standard depths are compared. The standard depths selected for this comparison are the same as those reported by the *Snellius* in 1929.

The sources of possible errors in observed values for oceanographic stations are numerous and have not been fully evaluated in this analysis. Disregarding possible errors that were introduced in the observing and processing aboard the *Pioneer*, and accepting the "steady-state" premise, leaves two basic sources of error to be evaluated. These are: Errors introduced by the interpolation procedure itself, and errors introduced by the interaction of sample depths and the gradients of the parameters sampled. An examination of the differences in reported interpolated values gives insight into the relative magnitude of these two sources of error. Since the NODC values are the result of a machine interpolation, they are considered to be unique solutions and to have no variance. Hence, to compare the interpolated values reported for stations 0062 and 0063, it was decided to make the comparison by an interpolation technique which would not give unique solutions, that is, using the graphical interpolation technique of

*Institute for Oceanography, U.S. Environmental Science Services Administration.

| REFERENCE | | SHIP | LATITUDE | LONGITUDE | | MARSDEN SQUARE | | STATION TIME (GMT) | | | YEAR | ORIGINATOR'S | | DEPTH TO BOTTOM | MAX. DEPTH OF SAMPLES | WAVE OBSERVATIONS | | | | WEATHER CODE | CLOUD CODES | | | NODC STATION NUMBER |
|---|---|---|---|---|---|---|---|---|---|---|---|---|---|---|---|---|---|---|---|---|---|---|---|---|
| COUNTRY CODE | IDENTITY NUMBER | CODE | ° ' 1/10 | ° ' 1/10 | | 10° | 1° | MONTH | DAY | HR. 1/10 | | CRUISE NUMBER | STATION NUMBER | | | DIR. | HGT. | PER. | SEA AMT. | | TYPE | AMT. | | |
| 31 | 201 | PI | 04004N | 122360E | | 024 | 42 | 07 | 03 | 208 | 1964 | 442 | 062 | 4837 | 50 | 21 | | | 1 | X1 | 4 | 3 | | 0062 |

| WATER | | WIND | | BAROMETER (mbs) | AIR TEMP. °C | | VIS. CODE | NO. OBS. DEPTHS | SPECIAL OBSERVATIONS |
|---|---|---|---|---|---|---|---|---|---|
| SEA CODE | WAVE PER. (sec) | DIR. | SPEED OR FORCE | | DRY BULB | WET BULB | | | |
| | | 21 | S06 | 075 | 267 | 256 | 8 | | |

| MESSENGER TIME OR HR. 1/10 | CAST NO. | CARD TYPE | DEPTH (m) | T °C | S °/₀₀ | SIGMA-T | SPECIFIC VOLUME ANOMALY—X10⁷ | Σ Δ D DYN. M. X 10² | SOUND VELOCITY | $O_2$ ml/l | $PO_4$—P µg-at/l | TOTAL—P µg-at/l | $NO_2$—N µg-at/l | $NO_3$—N µg-at/l | $SiO_3$—Si µg-at/l | pH µg-at/l | SCC |
|---|---|---|---|---|---|---|---|---|---|---|---|---|---|---|---|---|---|
| | | STD | 0000 | 2895 | 3392 | 2129 | 0065092 | 0000 | 15425 | 452 | | | | | | | |
| 208 | | OBS | 0000 | 2895 | 3392 | 2129 | | | 15425 | 452 | | | | | | | |
| | | STD | 0010 | 2894 | 3390 | 2128 | 0065244 | 0065 | 15426 | 468 | | | | | | | |
| 208 | | OBS | 0010 | 2894 | 3390 | 2128 | | | 15426 | 468 | | | | | | | |
| | | STD | 0020 | 2880 | 3396 | 2137 | 0064407 | 0130 | 15425 | 457 | | | | | | | |
| 208 | | OBS | 0020 | 2880 | 3396 | 2137 | | | 15425 | 457 | | | | | | | |
| | | STD | 0030 | 2875 | 3403 | 2144 | 0063785 | 0194 | 15427 | 457 | | | | | | | |
| 208 | | OBS | 0030 | 2875 | 3403 | 2144 | | | 15427 | 457 | | | | | | | |
| | | STD | 0050 | 2870 | 3414 | 2154 | 0062917 | 0321 | 15430 | 457 | | | | | | | |
| 208 | | OBS | 0050 | 2870 | 3414 | 2154 | | | 15430 | 457 | | | | | | | |
| | | STD | 0075 | 2688 | 3445 | 2236 | 0055125 | 0468 | 15398 | 448 | | | | | | | |
| 208 | | OBS | 0075 | 2688 | 3445 | 2236 | | | 15398 | 448 | | | | | | | |
| 186 | | OBS | 0098 | 2610 | 3450 | 2265 | | | 15384 | 427 | | | | | | | |
| | | STD | 0100 | 2579 | 3451 | 2275 | 0051517 | 0602 | 15378 | 423 | | | | | | | |
| | | STD | 0125 | 2231 | 3465 | 2389 | 0040749 | 0717 | 15299 | 388 | | | | | | | |
| 186 | | OBS | T0147 | 1992 | 3472 | 2459 | | | 15240 | 370 | | | | | | | |
| | | STD | 0150 | 1972 | 3472 | 2464 | 0033604 | 0810 | 15235 | 371 | | | | | | | |
| 186 | | OBS | 0196 | 1689 | 3470 | 2533 | | | 15161 | 376 | | | | | | | |
| | | *STD | 0200 | 1650 | 3469 | 2541 | 0026361 | 0960 | 15149 | 375 | | | | | | | |
| | | *STD | 0250 | 1410 | 3457 | 2585 | 0022250 | 1081 | 15080 | 357 | | | | | | | |
| 186 | | OBS | 0294 | 1262 | 3450 | 2610 | | | 15038 | 334 | | | | | | | |
| | | STD | 0300 | 1242 | 3449 | 2613 | 0019663 | 1186 | 15032 | 328 | | | | | | | |
| 186 | | OBS | T0391 | 0982 | 3445 | 2657 | | | 14954 | 261 | | | | | | | |
| | | STD | 0400 | 0962 | 3446 | 2661 | 0015143 | 1360 | 14948 | 257 | | | | | | | |
| 186 | | OBS | T0489 | 0803 | 3450 | 2690 | | | 14904 | 234 | | | | | | | |
| | | STD | 0500 | 0792 | 3451 | 2692 | 0012278 | 1497 | 14902 | 236 | | | | | | | |
| 186 | | OBS | T0587 | 0709 | 3454 | 2706 | | | 14884 | 247 | | | | | | | |
| | | STD | 0600 | 0699 | 3454 | 2708 | 0010851 | 1613 | 14882 | 246 | | | | | | | |
| | | STD | 0700 | 0624 | 3455 | 2719 | 0009868 | 1717 | 14869 | 238 | | | | | | | |
| 186 | | OBS | T0783 | 0566 | 3455 | 2726 | | | 14860 | 233 | | | | | | | |
| | | STD | 0800 | 0552 | 3455 | 2728 | 0009025 | 1811 | 14857 | 232 | | | | | | | |
| | | *STD | 0900 | 0490 | 3457 | 2737 | 0008184 | 1897 | 14848 | 227 | | | | | | | |
| 186 | | OBS | 0980 | 0440 | 3458 | 2743 | | | 14841 | 224 | | | | | | | |
| | | STD | 1000 | 0435 | 3458 | 2744 | 0007517 | 1976 | 14842 | 224 | | | | | | | |
| | | STD | 1100 | 0415 | 3459 | 2747 | 0007288 | 2050 | 14851 | 222 | | | | | | | |
| 186 | | OBS | T1177 | 0402 | 3459 | 2748 | | | 14858 | 221 | | | | | | | |
| | | STD | 1200 | 0399 | 3459 | 2748 | 0007177 | 2122 | 14861 | 221 | | | | | | | |
| | | STD | 1300 | 0389 | 3459 | 2749 | 0007137 | 2193 | 14873 | 222 | | | | | | | |
| | | STD | 1400 | 0380 | 3459 | 2750 | 0007105 | 2265 | 14886 | 223 | | | | | | | |
| 186 | | OBS | T1474 | 0374 | 3459 | 2751 | | | 14896 | 224 | | | | | | | |
| | | STD | 1500 | 0372 | 3459 | 2751 | 0007083 | 2336 | 14900 | 225 | | | | | | | |
| | | STD | 1750 | 0362 | 3459 | 2752 | 0007146 | 2513 | 14938 | 231 | | | | | | | |
| 186 | | OBS | T1968 | 0358 | 3459 | 2752 | | | 14973 | 233 | | | | | | | |
| | | STD | 2000 | 0358 | 3459 | 2752 | 0007279 | 2694 | 14978 | 233 | | | | | | | |
| 202 | | OBS | T2043 | 0358 | 3459 | 2752 | | | 14986 | 233 | | | | | | | |
| | | STD | 2500 | 0358 | 3459 | 2752 | 0007640 | 3067 | 15063 | 227 | | | | | | | |
| 202 | | OBS | T2523 | 0358 | 3459 | 2752 | | | 15067 | 227 | | | | | | | |
| | | STD | 3000 | 0358 | 3460 | 2753 | 0007917 | 3456 | 15149 | 218 | | | | | | | |
| 202 | | OBS | T3008 | 0358 | 3460 | 2753 | | | 15151 | 218 | | | | | | | |
| 202 | | OBS | 3497 | 0360 | 3460 | 2753 | | | 15236 | 219 | | | | | | | |
| 202 | | OBS | 3988 | 0366 | 3460 | 2752 | | | 15324 | 217 | | | | | | | |
| | | STD | 4000 | 0366 | 3460 | 2752 | 0008718 | 4287 | 15327 | 217 | | | | | | | |
| 202 | | OBS | 4480 | 0373 | 3460 | 2752 | | | 15414 | 221 | | | | | | | |
| 202 | | OBS | 4679 | 0377 | 3460 | 2751 | | | 15451 | 218 | | | | | | | |
| 202 | | OBS | 4778 | 0377 | 3460 | 2751 | | | 15468 | 218 | | | | | | | |
| 202 | | OBS | 4828 | 0380 | 3460 | 2751 | | | 15478 | 219 | | | | | | | |
| 202 | | OBS | T4878 | 0380 | 3460 | 2751 | | | 15487 | 218 | | | | | | | |
| 202 | | OBS | T4928 | 0380 | 3460 | 2751 | | | 15496 | 218 | | | | | | | |
| 202 | | OBS | T4978 | 0382 | 3460 | 2751 | | | 15506 | 219 | | | | | | | |

FIGURE 51[1].—Oceanographic station 0062 data printout, Celebes Sea, July 1964.

| REFERENCE | | SHIP | LATITUDE | LONGITUDE | DRIFT | MARSDEN SQUARE | | STATION TIME (GMT) | | | YEAR | ORIGINATOR'S | | DEPTH TO BOTTOM | MAX. DEPTH OF SAMPLES | WAVE OBSERVATIONS | | | | WEATHER | CLOUD CODES | | | NODC STATION NUMBER |
|---|---|---|---|---|---|---|---|---|---|---|---|---|---|---|---|---|---|---|---|---|---|---|---|---|
| COUNTRY CODE | IDENTITY NUMBER | CODE | ° ′ 1/10 | ° ′ 1/10 | INDICATOR | 10° | 1° | MONTH | DAY | HR. 1/10 | | CRUISE NUMBER | STATION NUMBER | | | DIR. | HGT. | PER. | SEA AMT. | CODE | TYPE | AMT. | | |
| 31 | 201 | PI | 04004N | 122360E | | 024 | 42 | 07 | 03 | 226 | 1964 | 442 | 063 | 4837 | 50 | 00 | | | 0 | X1 | 4 | 3 | | 0063 |

| WATER | | WIND | | BAROMETER (mbs) | AIR TEMP. °C | | VIS. CODE | NO. OBS. DEPTHS | SPECIAL OBSERVATIONS |
|---|---|---|---|---|---|---|---|---|---|
| CRUISE CORR | TRANS. (m) | DIR. | SPEED OR FORCE | | DRY BULB | WET BULB | | | |
| | | 21 | S06 | 091 | 267 | 256 | 8 | | |

| MESSENGER TIME OF HR. 1/10 | CAST NO. | CARD TYPE | DEPTH (m) | T °C | S °/.. | SIGMA–T | SPECIFIC VOLUME ANOMALY–X10⁷ | Σ Δ D DYN. M. X 10² | SOUND VELOCITY | $O_2$ ml/l | $PO_4$–P µg-at/l | TOTAL–P µg-at/l | $NO_2$–N µg-at/l | $NO_3$–N µg-at/l | $SiO_3$–Si µg-at/l | pH µg-at/l | SCC |
|---|---|---|---|---|---|---|---|---|---|---|---|---|---|---|---|---|---|
| | | STD | 0000 | 2896 | 3389 | 2127 | 0065339 | 0000 | 15425 | 445 | | | | | | | |
| 226 | | OBS | 0000 | 2896 | 3389 | 2127 | | | 15425 | 445 | | | | | | | |
| 226 | | OBS | 0009 | 2898 | 3388 | 2125 | | | 15427 | 457 | | | | | | | |
| | | STD | 0010 | 2895 | 3389 | 2127 | 0065348 | 0065 | 15426 | 457 | | | | | | | |
| 226 | | OBS | 0019 | 2877 | 3398 | 2140 | | | 15425 | 457 | | | | | | | |
| | | STD | 0020 | 2877 | 3398 | 2140 | 0064167 | 0130 | 15425 | 457 | | | | | | | |
| 226 | | OBS | 0028 | 2873 | 3402 | 2144 | | | 15426 | 460 | | | | | | | |
| | | STD | 0030 | 2873 | 3403 | 2145 | 0063721 | 0194 | 15426 | 460 | | | | | | | |
| 226 | | OBS | 0047 | 2868 | 3412 | 2153 | | | 15429 | 457 | | | | | | | |
| | | STD | 0050 | 2846 | 3418 | 2165 | 0061869 | 0320 | 15425 | 457 | | | | | | | |
| 226 | | OBS | 0071 | 2716 | 3444 | 2227 | | | 15403 | 454 | | | | | | | |
| | | STD | 0075 | 2710 | 3445 | 2229 | 0055797 | 0467 | 15403 | 452 | | | | | | | |
| 226 | | OBS | T0094 | 2628 | 3448 | 2258 | | | 15388 | 439 | | | | | | | |
| | | *STD | 0100 | 2590 | 3452 | 2272 | 0051772 | 0601 | 15380 | 428 | | | | | | | |
| | | *STD | 0125 | 2290 | 3466 | 2373 | 0042283 | 0719 | 15314 | 392 | | | | | | | |
| 226 | | OBS | 0142 | 2023 | 3471 | 2450 | | | 15247 | 377 | | | | | | | |
| | | STD | 0150 | 1965 | 3471 | 2465 | 0033502 | 0813 | 15233 | 377 | | | | | | | |
| 226 | | OBS | 0189 | 1706 | 3468 | 2527 | | | 15164 | 376 | | | | | | | |
| | | STD | 0200 | 1643 | 3465 | 2540 | 0026495 | 0963 | 15147 | 367 | | | | | | | |
| | | STD | 0250 | 1388 | 3452 | 2586 | 0022169 | 1085 | 15073 | 329 | | | | | | | |
| 226 | | OBS | T0284 | 1245 | 3446 | 2610 | | | 15030 | 306 | | | | | | | |
| | | STD | 0300 | 1190 | 3445 | 2620 | 0018983 | 1188 | 15013 | 296 | | | | | | | |
| 226 | | OBS | T0380 | 0970 | 3442 | 2657 | | | 14948 | 256 | | | | | | | |
| | | STD | 0400 | 0934 | 3442 | 2663 | 0014979 | 1358 | 14938 | 248 | | | | | | | |
| 226 | | OBS | T0477 | 0822 | 3444 | 2682 | | | 14908 | 230 | | | | | | | |
| | | STD | 0500 | 0802 | 3446 | 2687 | 0012797 | 1497 | 14905 | 233 | | | | | | | |
| 226 | | OBS | T0575 | 0736 | 3451 | 2700 | | | 14892 | 239 | | | | | | | |
| | | STD | 0600 | 0712 | 3451 | 2704 | 0011260 | 1617 | 14887 | 237 | | | | | | | |
| | | STD | 0700 | 0626 | 3452 | 2716 | 0010117 | 1724 | 14870 | 232 | | | | | | | |
| 226 | | OBS | T0772 | 0571 | 3453 | 2724 | | | 14860 | 230 | | | | | | | |
| | | STD | 0800 | 0550 | 3453 | 2727 | 0009146 | 1820 | 14856 | 230 | | | | | | | |
| | | STD | 0900 | 0487 | 3455 | 2736 | 0008293 | 1907 | 14847 | 230 | | | | | | | |
| 241 | | OBS | 0946 | 0464 | 3455 | 2738 | | | 14845 | 230 | | | | | | | |
| | | STD | 1000 | 0447 | 3455 | 2740 | 0007889 | 1988 | 14847 | 230 | | | | | | | |
| | | STD | 1100 | 0421 | 3456 | 2744 | 0007584 | 2066 | 14853 | 230 | | | | | | | |
| 241 | | OBS | T1144 | 0411 | 3456 | 2745 | | | 14856 | 230 | | | | | | | |
| | | STD | 1200 | 0403 | 3456 | 2746 | 0007447 | 2141 | 14862 | 230 | | | | | | | |
| | | STD | 1300 | 0391 | 3457 | 2748 | 0007309 | 2215 | 14874 | 230 | | | | | | | |
| | | STD | 1400 | 0381 | 3457 | 2749 | 0007265 | 2287 | 14887 | 230 | | | | | | | |
| 241 | | OBS | T1442 | 0377 | 3457 | 2749 | | | 14892 | 230 | | | | | | | |
| | | STD | 1500 | 0373 | 3457 | 2749 | 0007243 | 2360 | 14900 | 229 | | | | | | | |
| | | STD | 1750 | 0361 | 3457 | 2751 | 0007279 | 2542 | 14937 | 228 | | | | | | | |
| 241 | | OBS | T1937 | 0355 | 3457 | 2751 | | | 14966 | 227 | | | | | | | |
| | | STD | 2000 | 0355 | 3457 | 2751 | 0007383 | 2725 | 14977 | 227 | | | | | | | |
| 241 | | OBS | 2432 | 0354 | 3458 | 2752 | | | 15050 | 227 | | | | | | | |
| | | STD | 2500 | 0354 | 3458 | 2752 | 0007653 | 3101 | 15062 | 225 | | | | | | | |
| 241 | | OBS | T2925 | 0355 | 3458 | 2752 | | | 15135 | 217 | | | | | | | |
| | | STD | 3000 | 0356 | 3458 | 2752 | 0008028 | 3493 | 15148 | 219 | | | | | | | |
| 241 | | OBS | 3415 | 0363 | 3458 | 2751 | | | 15223 | 225 | | | | | | | |
| 241 | | OBS | T3905 | 0367 | 3458 | 2751 | | | 15310 | 218 | | | | | | | |
| | | STD | 4000 | 0369 | 3458 | 2751 | 0008911 | 4340 | 15328 | 218 | | | | | | | |
| 241 | | OBS | 4395 | 0374 | 3458 | 2750 | | | 15399 | 218 | | | | | | | |
| 241 | | OBS | T4788 | 0378 | 3458 | 2750 | | | 15470 | 215 | | | | | | | |
| 241 | | OBS | T4935 | 0380 | 3458 | 2749 | | | 15497 | 221 | | | | | | | |
| 241 | | OBS | T4983 | 0382 | 3458 | 2749 | | | 15506 | 265Q | | | | | | | |

FIGURE 52[2].—Oceanographic station 0063 data printout, Celebes Sea, July 1964.

the precomputer era. This was done in the following steps.

1. For each station, 0062 and 0063, and for both temperature and salinity, five independently plotted graphs of observed water property versus depth were prepared. From each of these, interpolated values of the property were estimated for the standard depths. These values are tabulated in table 4[1] for temperature and in table 5[2] for salinity. In addition, mean values of the property, the range of values, and an estimate of standard deviation were calculated using the techniques for small samples outlined by Crow et al., in 1960.
2. Using data from table 4[1], a comparison was made of temperature values as given for stations 0062 and 0063.
   a. Interpolations at each standard depth were compared for comparable variance (see Crow et al., 1960, p. 74). Except when an interpolated value at one station was compared with an observed value at the other, all of the comparisons indicated an acceptance of the assumed comparable variance.

TABLE 4[1].—*Temperature in °C at standard depths for* Pioneer *oceanographic stations 0062 and 0063 in Celebes Sea, July 1964*

[Based on graphic interpolations to standard depths]

*Pioneer* 0062

| Depth, meters | 1 | 2 | 3 | 4 | 5 | Range T,°C | Mean T,°C | Standard deviation |
|---|---|---|---|---|---|---|---|---|
| 0 | 28. 95 | 28. 95 | 28. 95 | 28. 95 | 28. 95 | 0. 00 | 28. 95 | 0. 00 |
| 50 | 28. 70 | 28. 70 | 28. 70 | 28. 70 | 28. 70 | 0. 00 | 28. 70 | 0. 00 |
| 100 | 25. 50 | 25. 74 | 25. 87 | 25. 90 | 25. 96 | 0. 46 | 25. 79 | 0. 20 |
| 150 | 19. 74 | 19. 77 | 19. 32 | 19. 68 | 19. 54 | 0. 45 | 19. 61 | 0. 19 |
| 200 | 16. 46 | 16. 45 | 16. 53 | 16. 64 | 16. 42 | 0. 22 | 16. 50 | 0. 09 |
| 400 | 9. 66 | 9. 62 | 9. 75 | 9. 64 | 9. 75 | 0. 13 | 9. 68 | 0. 05 |
| 600 | 6. 97 | 6. 98 | 7. 02 | 6. 98 | 6. 98 | 0. 05 | 6. 99 | 0. 02 |
| 800 | 5. 52 | 5. 51 | 5. 51 | 5. 52 | 5. 53 | 0. 02 | 5. 52 | 0. 01 |
| 1000 | 4. 35 | 4. 32 | 4. 33 | 4. 31 | 4. 35 | 0. 04 | 4. 33 | 0. 02 |
| 1500 | 3. 75 | 3. 75 | 3. 74 | 3. 70 | 3. 76 | 0. 06 | 3. 74 | 0. 02 |
| 2000 | 3. 58 | 3. 58 | 3. 58 | 3. 58 | 3. 58 | 0. 00 | 3. 58 | 0. 00 |
| 3000 | 3. 58 | 3. 58 | 3. 58 | 3. 58 | 3. 58 | 0. 00 | 3. 58 | 0. 00 |
| 4000 | 3. 65 | 3. 65 | 3. 68 | 3. 68 | 3. 68 | 0. 03 | 3. 67 | 0. 01 |

*Pioneer* 0063

| Depth, meters | 1 | 2 | 3 | 4 | 5 | Range T,°C | Mean T,°C | Standard deviation |
|---|---|---|---|---|---|---|---|---|
| 0 | 28. 96 | 28. 96 | 28. 96 | 28. 96 | 28. 96 | 0. 00 | 28. 96 | 0. 00 |
| 50 | 28. 62 | 28. 61 | 28. 62 | 28. 52 | 28. 62 | 0. 10 | 28. 60 | 0. 04 |
| 100 | 25. 90 | 25. 75 | 25. 50 | 25. 23 | 25. 67 | 0. 67 | 25. 61 | 0. 29 |
| 150 | 20. 20 | 19. 65 | 19. 95 | 19. 50 | 19. 72 | 0. 70 | 19. 80 | 0. 30 |
| 200 | 16. 21 | 16. 38 | 16. 15 | 16. 06 | 15. 98 | 0. 40 | 16. 16 | 0. 17 |
| 400 | 9. 27 | 9. 40 | 9. 43 | 9. 34 | 9. 36 | 0. 16 | 9. 36 | 0. 07 |
| 600 | 7. 10 | 7. 15 | 7. 12 | 7. 12 | 7. 14 | 0. 05 | 7. 13 | 0. 02 |
| 800 | 5. 48 | 5. 52 | 5. 51 | 5. 50 | 5. 51 | 0. 03 | 5. 50 | 0. 01 |
| 1000 | 4. 45 | 4. 50 | 4. 46 | 4. 44 | 4. 44 | 0. 06 | 4. 46 | 0. 03 |
| 1500 | 3. 75 | 3. 75 | 3. 73 | 3. 70 | 3. 68 | 0. 07 | 3. 72 | 0. 03 |
| 2000 | 3. 55 | 3. 55 | 3. 56 | 3. 55 | 3. 55 | 0. 01 | 3. 55 | 0. 00 |
| 3000 | 3. 59 | 3. 57 | 3. 58 | 3. 59 | 3. 55 | 0. 04 | 3. 58 | 0. 02 |
| 4000 | 3. 70 | 3. 70 | 3. 68 | 3. 70 | 3. 69 | 0. 02 | 3. 69 | 0. 01 |

b. At each standard depth a comparison of the mean temperatures of stations 0062 and 0063 was made using the $\tau_d$ test (Crow et al., 1960, p. 57). Results are tabulated in table 6[3].

c. Similar comparisons were made for salinity using table 5[2] and tabulating the results in table 7[4].

The results of the tests indicated in tables 6[3] and 7[4] are not surprising. In those cases where the null-hypothesis is rejected, there is an implication that the error introduced by the sample-spacing is greater than that introduced by the graphic interpolation used here. This conclusion has been generally accepted for some time, but the present analysis lends some additional quantitative support. The acceptance of the null-hypothesis at 100 and 150 m is due to large variances in the original data resulting from interpolations in the area of the thermocline.

TABLE 5[2].—*Salinity in °/₀₀ at standard depths for* Pioneer *oceanographic stations 0062 and 0063 in Celebes Sea, July 1964*

[Based on graphic interpolations to standard depths]

*Pioneer* 0062

| Depth, meters | 1 | 2 | 3 | 4 | 5 | Range S, °/₀₀ | Mean S, °/₀₀ | Standard deviation |
|---|---|---|---|---|---|---|---|---|
| 0 | 33. 92 | 33. 92 | 33. 92 | 33. 92 | 33. 92 | 0. 00 | 33. 92 | 0. 00 |
| 50 | 34. 14 | 34. 14 | 34. 14 | 34. 14 | 34. 14 | 0. 00 | 34. 14 | 0. 00 |
| 100 | 34. 52 | 34. 51 | 34. 52 | 34. 51 | 34. 52 | 0. 01 | 34. 52 | 0. 00[1] |
| 150 | 34. 72 | 34. 72 | 34. 72 | 34. 72 | 34. 72 | 0. 00 | 34. 72 | 0. 00 |
| 200 | 34. 68 | 34. 68 | 34. 69 | 34. 69 | 34. 69 | 0. 01 | 34. 69 | 0. 00[1] |
| 400 | 34. 45 | 34. 45 | 34. 45 | 34. 45 | 34. 45 | 0. 00 | 34. 45 | 0. 00 |
| 600 | 34. 54 | 34. 54 | 34. 54 | 34. 54 | 34. 54 | 0. 00 | 34. 54 | 0. 00 |
| 800 | 34. 55 | 34. 55 | 34. 55 | 34. 55 | 34. 55 | 0. 00 | 34. 55 | 0. 00 |
| 1000 | 34. 58 | 34. 58 | 34. 58 | 34. 58 | 34. 58 | 0. 00 | 34. 58 | 0. 00 |
| 1500 | 34. 59 | 34. 59 | 34. 59 | 34. 59 | 34. 59 | 0. 00 | 34. 59 | 0. 00 |
| 2000 | 34. 59 | 34. 59 | 34. 59 | 34. 59 | 34. 59 | 0. 00 | 34. 59 | 0. 00 |
| 3000 | 34. 60 | 34. 60 | 34. 60 | 34. 60 | 34. 60 | 0. 00 | 34. 60 | 0. 00 |
| 4000 | 34. 60 | 34. 60 | 34. 60 | 34. 60 | 34. 60 | 0. 00 | 34. 60 | 0. 00 |

*Pioneer* 0063

| Depth, meters | 1 | 2 | 3 | 4 | 5 | Range S, °/₀₀ | Mean S, °/₀₀ | Standard deviation |
|---|---|---|---|---|---|---|---|---|
| 0 | 33. 89 | 33. 89 | 33. 89 | 33. 89 | 33. 89 | 0. 00 | 33. 89 | 0. 00 |
| 50 | 34. 16 | 34. 16 | 34. 15 | 34. 16 | 34. 15 | 0. 01 | 34. 16 | 0. 00[1] |
| 100 | 34. 50 | 34. 50 | 34. 49 | 34. 50 | 34. 50 | 0. 01 | 34. 50 | 0. 00[1] |
| 150 | 34. 71 | 34. 71 | 34. 71 | 34. 71 | 34. 71 | 0. 00 | 34. 71 | 0. 00 |
| 200 | 34. 66 | 34. 61 | 34. 65 | 34. 66 | 34. 65 | 0. 05 | 34. 65 | 0. 02 |
| 400 | 34. 42 | 34. 42 | 34. 42 | 34. 42 | 34. 42 | 0. 00 | 34. 42 | 0. 00 |
| 600 | 34. 52 | 34. 51 | 34. 52 | 34. 52 | 34. 52 | 0. 01 | 34. 52 | 0. 00[1] |
| 800 | 34. 53 | 34. 54 | 34. 54 | 34. 54 | 34. 53 | 0. 01 | 34. 54 | 0. 00[1] |
| 1000 | 34. 55 | 34. 56 | 34. 55 | 34. 55 | 34. 56 | 0. 01 | 34. 55 | 0. 00[1] |
| 1500 | 34. 57 | 34. 57 | 34. 57 | 34. 57 | 34. 57 | 0. 00 | 34. 57 | 0. 00 |
| 2000 | 34. 57 | 34. 57 | 34. 57 | 34. 57 | 34. 57 | 0. 00 | 34. 57 | 0. 00 |
| 3000 | 34. 58 | 34. 58 | 34. 58 | 34. 58 | 34. 58 | 0. 00 | 34. 58 | 0. 00 |
| 4000 | 34. 58 | 34. 58 | 34. 58 | 34. 58 | 34. 58 | 0. 00 | 34. 58 | 0. 00 |

[1] Variance of 0.004 noted.

TABLE 6[3].—*Test for comparability of station 0062 and station 0063 temperature means ($\tau_d$ test)*

[Test after Crow et al., *Statistics Manual*, 1960, p. 57]

| Depth, meters | Station 0062 | | Station 0063 | | $\tau_d$ | Test result |
|---|---|---|---|---|---|---|
| | $\overline{T}$ (°C) | Range | $\overline{T}$ (°C) | Range | | |
| 0 | 28. 95 | 0. 01⁻ | 28. 96 | 0. 01⁻ | 1. 00⁺ | Reject |
| 50 | 28. 70 | 0. 01⁻ | 28. 60 | 0. 10 | 1. 00 | Reject |
| 100 | 25. 79 | 0. 46 | 25. 61 | 0. 67 | 0. 16 | Accept (thermocline) |
| 150 | 19. 61 | 0. 45 | 19. 80 | 0. 70 | 0. 16 | Accept (thermocline) |
| 200 | 16. 50 | 0. 22 | 16. 16 | 0. 40 | 0. 55 | Reject |
| 400 | 9. 68 | 0. 13 | 9. 36 | 0. 16 | 1. 10 | Reject |
| 600 | 6. 99 | 0. 05 | 7. 13 | 0. 05 | 1. 40 | Reject |
| 800 | 5. 52 | 0. 02 | 5. 50 | 0. 03 | 0. 40 | Reject |
| 1000 | 4. 33 | 0. 04 | 4. 46 | 0. 06 | 1. 30 | Reject |
| 1500 | 3. 74 | 0. 06 | 3. 72 | 0. 07 | 0. 15 | Accept |
| 2000 | 3. 58 | 0. 01⁻ | 3. 55 | 0. 01 | 3. 00 | Reject |
| 3000 | 3. 58 | 0. 01⁻ | 3. 58 | 0. 04 | 0. 00 | Invalid ($s_1 \neq s_2$) |
| 4000 | 3. 67 | 0. 03 | 3. 69 | 0. 02 | 0. 40 | Reject |

Hypothesis tested $=[\overline{X}_1=\overline{X}_2]=[\overline{T}(\text{sta. } 0062)=\overline{T}(\text{sta. } 0063)]$

$$\tau_d=\frac{[\overline{X}_1-\overline{X}_2]}{[\text{Range}_1+\text{Range}_2]}.$$

Critical value of $\tau_d=0.39$, when $\alpha=0.01$

TABLE 7[4].—*Test for comparability of station 0062 and station 0063 salinity means ($\tau_d$ test)*

[Test after Crow et al., *Statistics Manual*, 1960, p. 57]

| Depth, meters | Station 0062 | | Station 0063 | | $\tau_d$ | Test result |
|---|---|---|---|---|---|---|
| | $\overline{S}$(°/₀₀) | Range | $\overline{S}$(°/₀₀) | Range | | |
| 0 | 33. 92 | 0. 01⁻ | 33. 89 | 0. 01⁻ | 3. 00⁺ | Reject |
| 50 | 34. 14 | 0. 01⁻ | 34. 16 | 0. 01 | 2. 00 | Reject |
| 100 | 34. 52 | 0. 01 | 34. 50 | 0. 01 | 1. 00 | Reject |
| 150 | 34. 72 | 0. 01⁻ | 34. 71 | 0. 01⁻ | 1. 00⁺ | Reject |
| 200 | 34. 69 | 0. 01 | 34. 65 | 0. 05 | 0. 67 | Reject |
| 400 | 34. 45 | 0. 01⁻ | 34. 42 | 0. 01⁻ | 3. 00⁺ | Reject |
| 600 | 34. 54 | 0. 01⁻ | 34. 52 | 0. 01 | 2. 00 | Reject |
| 800 | 34. 55 | 0. 01⁻ | 34. 54 | 0. 01 | 1. 00 | Reject |
| 1000 | 34. 58 | 0. 01⁻ | 34. 55 | 0. 01 | 3. 00 | Reject |
| 1500 | 34. 59 | 0. 01⁻ | 34. 57 | 0. 01⁻ | 2. 00⁺ | Reject |
| 2000 | 34. 59 | 0. 01⁻ | 34. 57 | 0. 01⁻ | 2. 00⁺ | Reject |
| 3000 | 34. 60 | 0. 01⁻ | 34. 58 | 0. 01⁻ | 2. 00⁺ | Reject |
| 4000 | 34. 60 | 0. 01⁻ | 34. 58 | 0. 01⁻ | 2. 00⁺ | Reject |

Hypothesis tested $=[\overline{X}_1=\overline{X}_2]=[\overline{S}$ (sta. 0062) $=\overline{S}$ (sta. 0063)]

Critical value of $\tau_d=0.39$, when $\alpha=0.01$

In view of the dissimilar information obtained for stations 0062 and 0063, several comparisons were made to determine if any systematic differences are present. Signs-test comparisons of the means of the graphic interpolations and the NODC interpolations indicated no significant differences resulting from the choice of interpolation technique. The temperatures indicated for station 0062 are not systematically different from those of station 0063, but the salinities indicate a systematic error of $\approx 0.02$°/₀₀ with station 0062 showing higher values than station 0063.

The best estimate for conditions in the Celebes Sea when the *Pioneer* occupied the replicate pair of stations is tabulated in table 8[5]. These values are based on the information from the two parts of the paired stations as tabulated by NODC, and using NODC interpolated values for the standard depths listed.

TABLE 8[5].—*Best estimate of temperature and salinity distribution for* Pioneer *stations 0062 and 0063*

[Based on NODC interpolated values]

| Depth, meters | $\bar{T}$ (°C) | Standard deviation | $\bar{S}$ (°/₀₀) | Standard deviation |
|---|---|---|---|---|
| 0 | 28. 96 | 0. 01 | 33. 90 | 0. 03 |
| 50 | 28. 58 | 0. 21 | 34. 16 | 0. 04 |
| 100 | 25. 84 | 0. 10 | 34. 52 | 0. 01 |
| 150 | 19. 68 | 0. 06 | 34. 72 | 0. 01 |
| 200 | 16. 46 | 0. 06 | 34. 67 | 0. 04 |
| 400 | 9. 48 | 0. 25 | 34. 44 | 0. 04 |
| 600 | 7. 06 | 0. 12 | 34. 52 | 0. 03 |
| 800 | 5. 51 | 0. 02 | 34. 54 | 0. 02 |
| 1000 | 4. 41 | 0. 11 | 34. 56 | 0. 03 |
| 1500 | 3. 72 | 0. 01 | 34. 58 | 0. 02 |
| 2000 | 3. 56 | 0. 03 | 34. 58 | 0. 02 |
| 3000 | 3. 57 | 0. 02 | 34. 59 | 0. 02 |
| 4000 | 3. 68 | 0. 03 | 34. 59 | 0. 02 |

## COMPARISON OF "PIONEER" AND "SNELLIUS" STATION DATA

The pair of stations obtained by the *Pioneer* has permitted some evaluation of probable error in the determination of standard depth values of temperature and salinity. The *Snellius* data are reported for a single station and no proper estimate of sample variance can be made. Consequently, the evaluation of possible differences in water characteristics between the 1929 *Snellius* and 1964 *Pioneer* stations is made by comparing the reported *Snellius* values with a 95-percent confidence interval as derived from the *Pioneer* paired stations. From the data tabulated in table 8[5], a 95-percent confidence interval has been calculated for both temperature and salinity values at each standard depth. These are tabulated in table 9[6], along with the *Snellius* values reported by van Riel (1934).

The evaluation of possible water characteristics is made simply by comparing the *Snellius* values with the limits listed for the *Pioneer* values. If the *Snellius* value is outside the limits of the *Pioneer* values, it is indicated with a plus or a minus sign; if it is within the limits, it is indicated with a zero. The sign notation is such that a plus indicates warmer or more saline water in 1964, a minus indicates cooler or less saline water in 1964, and a zero indicates no significant net change between 1929 and 1964.

The water mass characteristics of the Celebes Basin are basically controlled by the characteristics of the Western North Pacific Central Water (Sverdrup, Johnson, and Fleming, 1942, p. 737 ff.), which fills the basin from the northeast. Below sill depth (≈ 1,400 m), the control of the sill is imposed since this is a subtropical basin, and the comparison of the *Pioneer* and *Snellius* data indicates no significant differences. Between the sill and the depth of the characteristic salinity maximum (≈150 m), changes in conditions should be related to changes resulting from longer-

TABLE 9[6].—*Comparison of 1964* Pioneer *and 1929* Snellius *oceanographic station data in Celebes Sea*

| Depth, meters | *Pioneer* 95-percent confidence interval [1] T, °C | *Snellius* T, °C | Comparison [2] | *Pioneer* 95-percent confidence interval [1] S, °/₀₀ | *Snellius* S, °/₀₀ | Comparison [2] |
|---|---|---|---|---|---|---|
| 0 | 28. 94 to 28. 98 | 28. 4- | + | 33. 84 to 33. 96 | 34. 22 | − |
| 50 | 28. 16 to 29. 00 | 27. 33 | + | 34. 08 to 34. 24 | 34. 33 | − |
| 100 | 25. 64 to 26. 04 | 24. 41 | + | 34. 50 to 34. 54 | 34. 68 | − |
| 150 | 19. 56 to 19. 80 | 20. 44 | − | 34. 70 to 34. 74 | 34. 81 | − |
| 200 | 16. 34 to 16. 58 | 17. 26 | − | 34. 59 to 34. 75 | 34. 70 | 0 |
| 300 | 8. 98 to 9. 98 | 8. 99 | 0 | 34. 36 to 34. 52 | 34. 42 | 0 |
| 600 | 6. 82 to 7. 30 | 6. 90 | 0 | 34. 46 to 34. 58 | 34. 52 | 0 |
| 800 | 5. 47 to 5. 55 | 5. 54 | 0 | 34. 50 to 34. 58 | 34. 52 | 0 |
| 1000 | 4. 19 to 4. 63 | 4. 49 | 0 | 34. 50 to 34. 62 | 34. 55 | 0 |
| 1500 | 3. 70 to 3. 74 | 3. 78 | − | 34. 54 to 34. 62 | 34. 58 | 0 |
| 2000 | 3. 50 to 3. 62 | 3. 61 | 0 | 34. 54 to 34. 62 | 34. 57 | 0 |
| 3000 | 3. 53 to 3. 61 | 3. 60 | 0 | 34. 55 to 34. 63 | 34. 58 | 0 |
| 4000 | 3. 62 to 3. 74 | 3. 72 | 0 | 34. 55 to 34. 63 | 34. 59 | 0 |

[1] The 95-percent confidence interval is based on data in table 8[5]. Confidence interval 95 = mean value ± (2 × standard deviation).

[2] Sign notation:

+ = *Pioneer* value warmer or more saline than *Snellius* value.

− = *Pioneer* value cooler or less saline than *Snellius* value.

0 = No significant difference between *Pioneer* and *Snellius* value.

period variability in the western Pacific Basin itself. The comparison indicates no significant differences, other than a possible slight warming at a depth of 200 m as indicated by the more recent *Pioneer* observations. Above the salinity maximum, the differences in conditions may be related to surface exchange processes within the Celebes Sea, or may merely reflect changes in the Western North Pacific Central Water related to seasonal variability in the Pacific itself. The upper 100 m, as observed by the *Pioneer* stations, is warmer and less saline than the *Snellius* observations. There also is slight indication of greater surface mixing (0 to 50 m) in the *Pioneer* data. The data analyzed in this study do not permit an adequate evaluation of where—such as the Pacific Basin or Celebes Basin—any of the observed differences may have been imposed upon the water column. In both cases the thermocline is between 100 and 150 m with the *Pioneer* data showing a stronger gradient, and both sets of data indicating the base of the thermocline to be close to the salinity maximum at 150 m.

## References


Crow, E. L., F. A. Davis, and M. W. Maxfield, *Statistics Manual*, 288 pp., Dover Publications, Inc., New York, 1960.

Sverdrup, H. U., M. W. Johnson, R. H. Fleming, *The Oceans, Their Physics, Chemistry, and General Biology*, 1087 pp., Prentice-Hall, Inc., New York, 1942.

van Riel, P. M., Chapter II. The bottom configuration in relation to the flow of the bottom water in *The Snellius-Expedition in the eastern part of the Netherlands East-Indies 1929–1930;* Vol. 2. Oceanographic Results; Part II. Soundings and Bathymetric Charts; 63 pp., E. J. Brill, Leiden, 1934.

# Large-Amplitude Internal Waves Observed off the Northwest Coast of Sumatra*

RICHARD B. PERRY† AND GERALD SCHIMKE‡

*Abstract.* Internal waves of large amplitude were observed north of Sumatra by the U.S. Coast & Geodetic Survey ship *Pioneer* in June 1964. The bathythermograph investigation which defined these waves was initiated after observation of curious periodic surface phenomena resembling tide rips. Analysis of bathythermograph records indicates that internal waves with a maximum observed wave height of 82 meters are the probable cause of the surface disturbances.

*Introduction.* The existence of internal waves in the sea, along surfaces separating layers of contrasting density, has been inferred from oceanographic observations for many years. A better understanding of these waves is important because of their effect on dynamic height computations, current measurements, marine life, undersea navigation, and submarine warfare. Large internal waves, and surface disturbances believed to be associated with these waves, were observed in the Andaman Sea area between Great Nicobar Island and Sumatra by the U.S. Coast & Geodetic Survey ship *Pioneer* in June 1964 during the vessel's participation in the International Indian Ocean Expedition.

*Setting.* The Andaman Sea is separated from the Bay of Bengal by the Andaman and Nicobar islands (fig. 53[1]) and a submerged, north-south trending ridge from which the exposed island peaks rise, the Andaman-Nicobar ridge (fig. 54 [2]). The sea is bordered by Burma, Thailand, the northern end of the Strait of Malacca, and the northwest coast of Sumatra. Between Great Nicobar Island, the southernmost island of the group, and Sumatra, the waters of the Andaman Sea connect with those of the Indian Ocean through the Great Channel, a passage in the submerged ridge characterized by rugged sea-bottom topography and depths greater than 2,000 m.

General summaries of meteorological and oceanographic conditions in the Bay of Bengal-Andaman Sea area are given in *U.S. Navy Hydrographic Office Special Publication 53* [1960] and by Sewell [1932]. They indicate that in June a well-mixed surface layer of water, having lower salinity and higher temperature than the surface waters in the Bay of Bengal, flows southwest, through the Great Channel. Temperature profiles taken by the *Pioneer* in June 1964 showed a well-mixed layer extending to a depth of about 100 m. A recent analysis of oceanographic conditions in the area indicates that surface currents in the Great Channel set to the west at about 0.8 m/sec during much of the year and that a subsurface flow sets to the east, into the Andaman Sea, below the thermocline depth (R. H. Sullivan, Jr., U.S. Navy Fleet Weather Service, personal communication).

*Observations.* On the morning of June 12, 1964, distinct zones of whitecaps ranging from 200 to 800 m in width and stretching from horizon to horizon (approximately 30 km) in a north-south direction were observed in the Andaman Sea north of Sumatra (fig. 54[2]). At least five of these zones, with a spacing of about 3,200 m between each zone, were observed. The observed zones or bands of choppy water had short, steep, randomly oriented waves with heights of about 0.3 to 0.6 m. Each band stood out distinctly in an otherwise undisturbed sea. A 4-m/sec NNW wind and a surface water temperature of 29°C were observed, but neither changed significantly as the ship crossed the bands of choppy water. Detailed salinity measurements were not made while crossing the bands; however, routine bi-hourly salinity samples showed a maximum regional salinity gradient of $0.03°/_{oo}$ per km. Later in the day, several other bands of similar dimensions, but having smaller waves, were observed.

On June 13, similar north-south trending bands of choppy water were seen farther to the west in the Great Channel, near 06°09′N, 94°37′E. Ten bands, each approximately 200 m wide and 800 m apart, were observed. In some instances, the water between the bands of choppy water

*Published originally in *Journal of Geophysical Research*, vol. 70, no. 10, pp. 2319–2324, May 15, 1965.
†Institute for Oceanography, U.S. Environmental Science Services Administration.
‡Coast and Geodetic Survey, U.S. Environmental Science Services Administration.

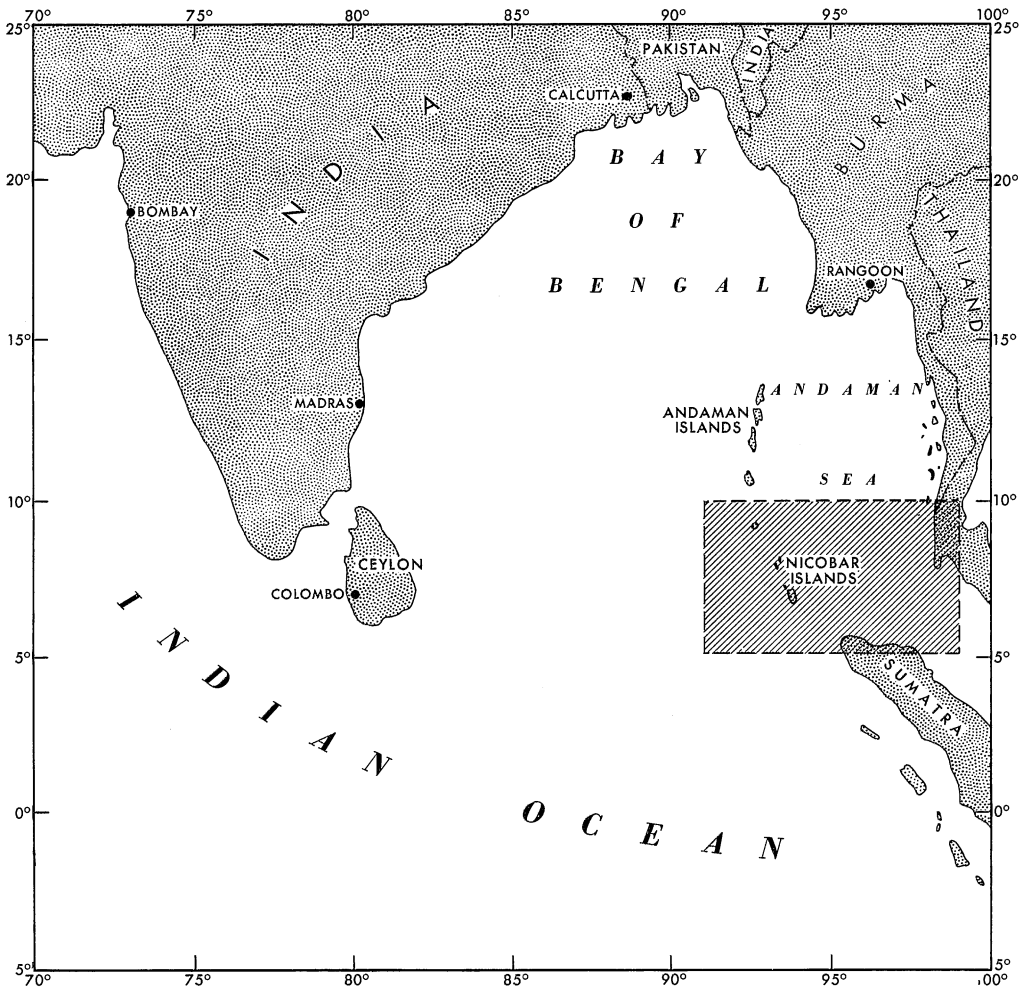


FIGURE 53[1].—Indian Ocean area in which bands of choppy sea were observed.

had a slicked appearance despite a 9–m/sec SSW wind. Similar slicks were not apparent on the preceding day when the bands of choppy water were farther apart. Boundaries of the choppy water were all well defined. After crossing a number of the bands, the ship changed course to an easterly direction to initiate a bathythermograph (BT) investigation of the observed phenomenon. The time at which the bow of the ship entered a chop line and the time the stern entered the same line was observed. By using the ship's course and average speed as determined by visual fixes on land, it was possible to compute the rate at which the bands were moving, assuming their direction of progress to be perpendicular to their long axis. The bands were computed to be moving eastward at 2.6 m/sec. A series of five BT observations was obtained by repeatedly lowering the instrument while the ship steamed west at 4.7 m/sec, approximately perpendicular to the long axis of the chop lines. Four well-defined bands of choppy water were crossed during the BT observations (fig. 55[3]). Each BT record taken while crossing the chop lines showed a split trace in the thermocline region. A maximum separation of nearly 15 m was recorded on one lowering. Since the bathythermograph functioned properly on previous and subsequent measurements, the cause of the split trace was attributed to pronounced horizontal temperature gradients, possibly associated with internal waves.

The temperature profile in figure 55[3] was derived by plotting the depth of the isotherms from the five BT traces against the time elapsed during the observations. The temperatures recorded during the descent of the BT are separated from those

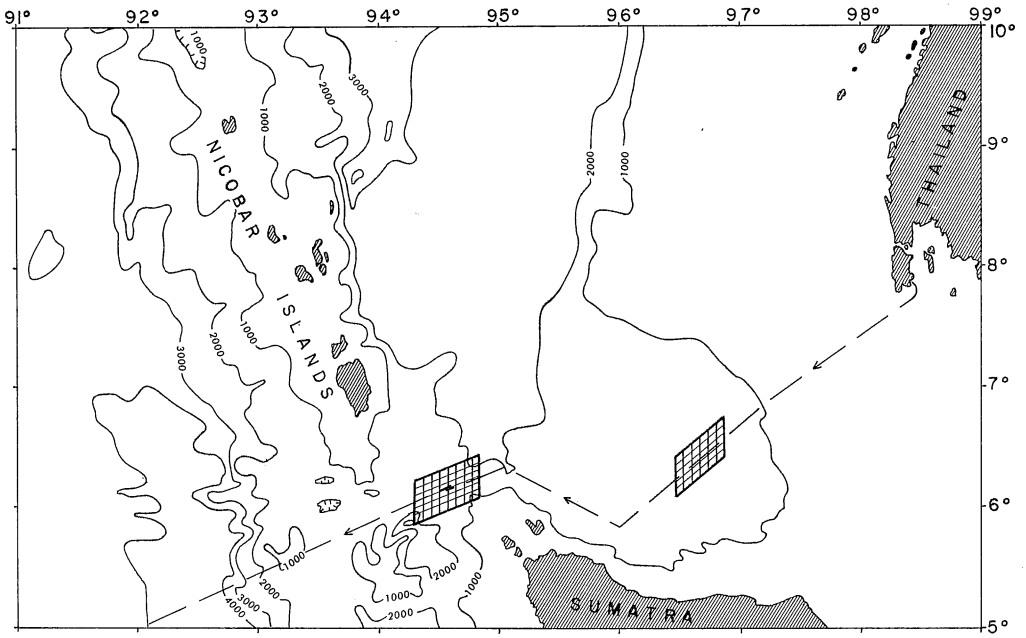


FIGURE 54[2].—Trackline of USC&GS ship *Pioneer*, June 12–13, 1964. Crosshatched areas indicate places where surface disturbances were observed. Depth contours in meters.

recorded during the ascent. In the resulting profile the periodic undulations of the closely spaced isotherms, which depict the depth of the thermocline, strongly suggest the presence of internal waves. The maximum height of the apparent waves is approximately 80 m. If they are indeed internal waves, and moving at the same speed and in the same direction as the surface chop lines, then the wavelength is calculated to be about 2000 m.

Upon completing the special BT observations, the *Pioneer* resumed its westward course through the Great Channel into the Bay of Bengal. As the ship proceeded westward, the surface waves in the bands of choppy water were observed to increase in size. The last and westernmost chop line sighted, at 06°03′N, 94°21′E, was a very choppy north-south zone characterized by seas of 1.8 to 2.1 m and extending from horizon to horizon.

During the ship's westward course through the area where the internal waves were found, the routine bi-hourly BT observations indicated an intensification of the temperature gradient in and a rising of the thermocline. From the point where the last line of surface chop was observed, and westward into the Bay of Bengal, the thermocline depth gradually increased and its temperature gradient became somewhat less intense.

*Discussion.* In the Bay of Bengal and adjacent waters, surface phenomena similar to that observed aboard the *Pioneer* have been previously observed and variously described as current rips, tide rips, lines of demarcation, and disturbed and rippled water [*Marine Observer*, 1958, 1959, 1962*a*, 1962*b*, 1963, 1964]. Alternate bands of rough and smooth water passed the R.V. *Anton Bruun* at four oceanographic stations in the Andaman Sea in March 1963 while that ship was operating under the National Science Foundation Program in Biology for the International Indian Ocean Expedition. At one of these stations a low roar accompanied by breaking whitecaps was observed as the bands passed the ship in a flat calm sea (E. C. LaFond, U.S.N. Electronics Laboratory, 1965, written communication).

In more restricted areas similar but smaller-scale, elongated surface features occasionally are caused by converging currents, by tide rips, or by the influence of bottom topography. Pickard [1961] has observed similar surface phenomena on a much reduced scale in certain inlets along the British Columbia mainland. His surface phenomena were related to progressive internal waves associated witht a shear zone between inflowing bottom water and outflowing surface water in a positive estuarine situation.

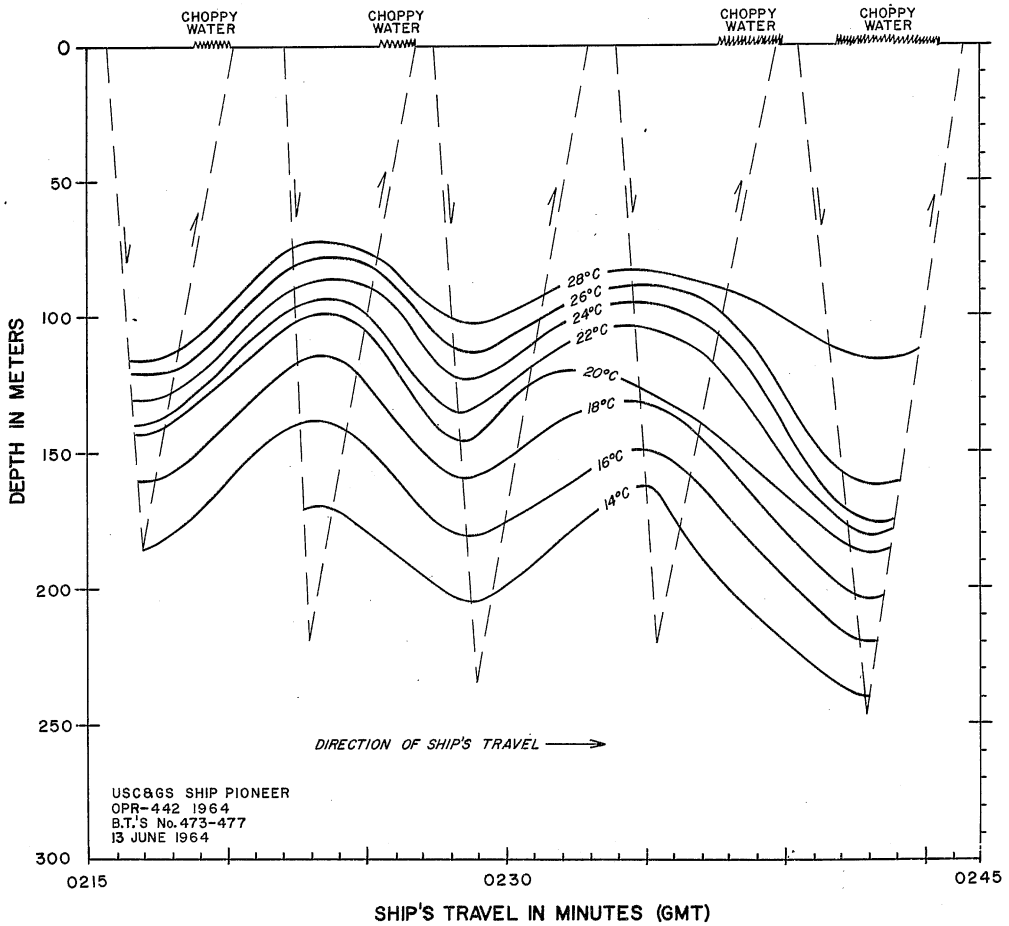


FIGURE 55[3].—Temperature profile as defined by bathythermograph. Dashed lines indicate path followed by bathythermograph.

Bands of surface chop have also been associated with oceanic fronts. Such fronts are generally characterized by strong horizontal temperature gradients at the surface and by marked faunal and color changes [Knauss, 1963]. A pronounced lateral shear in the surface flow is often in evidence as the observing ship crosses the disturbed band of water. The *Pioneer* experienced no difficulty in maintaining a true course while crossing the bands of disturbed water. There were no noticeable horizontal temperature or salinity gradients at the surface for a distance of more than 145 km on either side of the five special BT observations taken on June 13. Therefore, the possibility that the observed phenomena were directly associated with an oceanic front can be dismissed.

The possibility of bottom topographical influence as a causative factor has been considered because remarkable correlations have been made between sightings of disturbed water and sharp rises in the bottom topography at relatively great depths. Such a correlation was noted aboard the *Pioneer* earlier in the expedition while in the Andaman Sea. However, the jumbled and rugged topographical features and great depth of the sea floor in the immediate vicinity of the chop lines (fig. 54[2]) make it hard to conceive of the bottom features giving rise to long, straight, narrow surface disturbances stretching from horizon to horizon.

Surface slicks have been related to internal waves in shallow water areas [Ewing, 1950; Dietz and LaFond, 1950]. In many cases, slicks are particularly noticeable in waters close to shore, where they usually are associated with wave heights of 10 m or less. Pickard [1961] pointed out

the basic difference between these slicks and the bands of choppy water which we observed.

Internal waves of greater height than 10 m have been observed in the deep oceans by means of Nansen bottles with reversing thermometers, BT's, and, more recently, thermistor chains. Generally, these internal waves have been long waves with periods of the same order of magnitude as the tidal period. Slicks or disturbed surface conditions have not been associated with internal waves in deep water far from shore before these observations.

The mechanism for generating internal waves is frequently in question. In coastal areas the rise and fall of the tides over the continental shelf [Rattray, 1960] and shear caused by one mass of water flowing over another [Proudman, 1953] are among the mechanisms proposed for the generation of internal waves. The internal waves observed by the *Pioneer* were of such short wavelength that tidal generation hardly seems to be a reasonable explanation. On the other hand, because of their large amplitude, it seems somewhat speculative in the absence of direct current measurements to propose that shear flow was the generating mechanism. However, investigations by R. H. Sullivan, Jr., U.S. Navy Fleet Weather Service (personal communication, 1964), indicate that a strong shear flow may occur in the vicinity of the observed phenomena during most of the year. If this is the case, the situation seems directly analogous to that observed by Pickard [1961].

Defant [1961] wrote, "the appearance of waves at the boundary surface between two water layers has for a long time escaped the attention of observers because, even when the amplitude of the oscillation at the boundary surface is large, the free surface of the upper layer is only slightly disturbed and remains practically at rest." In the case at hand, the density of $\rho'$ of the upper well-mixed layer was 1.021 g/cm$^3$. From the previous observations of Sewell [1932] and *USN H. O. Special Publication 53* [1960], the density $\rho$ of the lower layer can be reckoned as 1.026 g/cm$^3$. Using 40 m for the amplitude of the internal wave, and the formula $\eta_0 = -Z(\rho-\rho')/\rho$ [Defant, 1961], where $\eta_0$ is the amplitude of the wave at the free surface and $Z$ is the amplitude of the internal wave, we compute a 0.2-m amplitude for the wave at the free surface.

The generating mechanism of the highly agitated bands of chop is not clear, but they probably are caused by a redistribution of mass that takes place with the passage of the internal wave. Pickard's observations in Canadian waters indicate that his "ruffled bands" are associated with the convergence taking place at the surface just behind the advancing internal wave crest. As seen in figure 55[3], it was not possible to establish a clear relationship between the bands of chop at the surface and a particular phase of the wave.

There is no direct correlation of wind effects and the observed phenomena since they were observed on June 12 in a relatively calm sea. Also the waves of the chop zone showed variable heights under relatively constant wind conditions on June 13. A topographic influence seems unlikely because of the irregular character and depth of the bottom.

Owing to the prevailing oceanographic conditions north of Sumatra during much of the year, and reported sightings of disturbed bands of water stretching from horizon to horizon, we believe that the existence of the phenomenon reported herein may be common in this part of the world, and its occurrence on June 13, 1964, probably was not unique.

More comprehensive investigations of this phenomenon might include the use of aircraft for aerial reconnaissance and aerial photography to chart the extent and periodicity of the surface disturbances. Current measurements and detailed thermal investigations should also be made using at least two ships equipped with thermistor chains.

*Conclusions.* The zones or narrow bands of choppy water sighted by the USC&GS ship *Pioneer* in the Andaman Sea area are believed to have been caused by internal waves. Internal waves, which were observed to occur simultaneously with the choppy surface phenomena, had uncommon dimensions of approximately 80 m in height and 2,000 m in length.

Although the limited observational data preclude any conclusive demonstrations of a generating mechanism for these waves, the cause may be related to a shear zone resulting from a well-mixed upper layer of warm, low-salinity water flowing westward over cooler, higher-salinity water flowing eastward through Great Channel north of Sumatra.

## References


Defant, A., *Physical Oceanography*, vol. 2, Pergamon Press, New York, 1961.

Dietz, R. S., and E. C. LaFond, Natural slicks on the ocean, *J. Marine Res.*, *9*(2), 69–76, 1950.

Ewing, G., Slicks, surface films, and internal waves, *J. Marine Res.*, *9*(3), 161–187, 1950.

Knauss, J. A., Equatorial current systems, in *The Sea*, vol. 2, edited by M. N. Hill, pp. 235–252, Interscience (Wiley), New York, 1963.

*The Marine Observer*, Meteorological Office, London: vol. 28, no. 179, p. 5, 1958; vol. 29, no. 183, p. 183, 1959; vol. 32, no. 197, p. 117, 1962; vol. 32, no. 198, p. 178, 1962; vol. 33, no. 200, p. 64, 1963; vol. 33, no. 202, p. 186, 1963.

Pickard, G. L., Oceanographic features of inlets in the British Columbia mainland coast, *J. Fisheries Res. Board Can.*, *18*(6), 907–999, 1961.

Proudman, J., *Dynamical Oceanography*, John Wiley & Sons, New York, 1953.

Rattray, M., Jr., On the coastal generation of internal tides, *Tellus*, *12*(1), 54–62, 1960.

Sewell, R. B. S., Geographic and oceanographic research in Indian waters, *Mem. Asiatic Soc. Bengal*, *9*(6), 357–424, 1932.

U.S. Navy Hydrographic Office, Summary of oceanographic conditions in the Indian Ocean, *Spec. Publ. 53*, 1960.

# Geology and Geophysics

The geological and geophysical program of the International Indian Ocean Expedition was directed toward securing a better understanding of this ocean basin, particularly its sea-floor boundary and the underlying structure. The primary responsibilities for the U.S. effort in this phase of the work were shared by the Woods Hole Oceanographic Institution, the Scripps Institution of Oceanography, and the Lamont Geological Observatory, with additional support in this effort being provided by Stanford University, the U.S. Navy, and the U.S. Coast and Geodetic Survey.

Among the questions for which specific answers were sought are the following. What are the major crustal features of the Indian Ocean basin? What are the characteristics of the trenches, mid-ocean ridges, rift zones, basin floor, and continental margins? Is the Indian Ocean basically an Atlantic- or Pacific-type ocean basin? What is the relationship between the structural, geomorphological, and sedimentary provinces? What information about the geologic history of the region can be obtained by sampling the marine sediments? What mineral resources are present? What picture will measurements of the earth's terrestrial force fields provide in this vast region, and how do the anomalous distributions in these fields correlate with local geologic features? What tectonic forces have acted to produce the region's tectonic patterns? What is the present status of tectonic activity and continuing geologic change? To provide answers to these questions and greater insight concerning the problems peculiar to the Indian Ocean basin and its continental margins, the *Pioneer* carried out a program of continuous precision depth soundings, gravity and magnetic measurements, and, along selected sections, continuous acoustic reflection surveys of the subbottom structure. The nature of the sea floor and sediments was studied by various bottom sampling methods and by underwater photography. In certain special areas, as the depth permitted, underwater investigations were carried out by diving scientists with SCUBA gear. Measurements also were made of the heat flux in the ocean floor at several sites by means of thermoprobes and sediment sampling.

## Bathymetry and Position Control

A continuous record of water depth, or ocean bottom profile, was obtained during the *Pioneer*'s Indian Ocean Expedition. The route along which the depth soundings were made is shown by the generalized trackline on chart 1 (facing page 140). Gaps in the continuous sounding record occurred whenever the ship stopped to make observations at oceanographic, deep-sea camera, and bottom-sample stations. However, additional soundings were made as the ship drifted on station to provide the needed depth information for station observations.

*Sounding equipment.* The *Pioneer's* depth finding and recording equipment during the 1964 cruise included two EDO-type 185 (Navy AN/UQN–I) echo sounders, two Timefax Precision Depth Recorders (fig. 56) that operate with the EDO equipment, and two Raytheon Survey Fathometers (DE–723B). The EDO–185 transducer has the capability to sound in the deepest water and to provide a graphic trace of the bottom profile on any of three sounding scales with the following resolutions: 0–600 feet, ±1 ft; 0–600 fathoms, ±1 fm; and, 0–6,000 fms, ±10 fms. The PDR records accurately throughout the entire depth range on an expanded scale in increments or phases of 400 fms with a trace resolution of ±1 fm. The Raytheon Survey Fathometer, which was used in shoal water and when entering and leaving ports, presents a graphic record of depth from 0 to 250 ft, or fms, in six phases of 50 ft or fms as follows: 0–50, 40–90, 80–130, 120–170, 160–210, and 200–250. Its accuracy from 1–100 ft is ±0.25 ft, and from 100 ft to 250 fms ±0.25 percent of indicated depth.

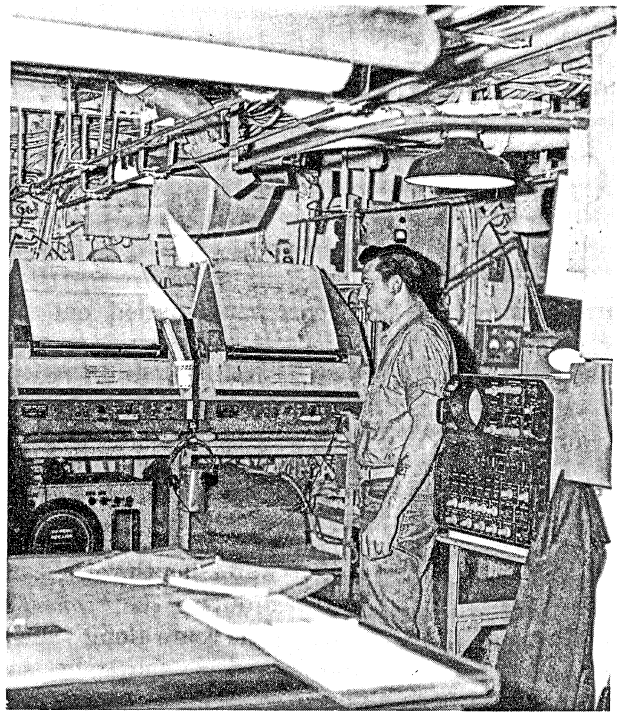

FIGURE 56.—Precision Depth Recorders aboard *Pioneer*.

*Position control.* The best available means was utilized for navigation and position control. Between San Francisco and the Philippine Islands, control was accomplished by Loran A, Loran C, and astronomical fixes. From the Philippines to a point about 500 miles to the southwest, and in the northern Celebes Sea, Loran A control was available. Astronomical, visual, and radar fixes were used in the South China Sea, Strait of Malacca, Andaman Sea, Bay of Bengal, northeast Indian Ocean, Java Sea, and Macassar Strait. Use of Loran C was limited to a relatively small area in the mid-Pacific near the Hawaiian Islands. The ship's two Sperry MK2 Model 2 Loran A and two Sperry AN/SPN 32 Loran C units were operable at all times during the cruise. A Sperry Mark II, Model 6 Gyrocompass was used with repeater units located in each of the two radar units, in the gravity room, in the chart room, and on the bridge, as well as on each bridge wing for visual bearings.

The radar equipment consisted of a Sperry MK III unit with 1, 2, 6, 15, and 40-mi ranges and a Decca 404 unit with 0.75, 1.5, 3, 6, 12, 24, and 48-mi ranges. Less than 5 percent of the trackline was within range of visual or radar control.

Astronomic sights were made in accordance with standard Coast and Geodetic Survey procedures. These procedures require at least 6 observations of each star by two observers. The weather during the 6-month cruise was exceptionally good and adequate astronomic sights were obtained as necessary. Dead-reckoning between fixes was accomplished with the aid of the ship's electromagnetic log. In the smooth-plotting of the ship's position, all Loran and astronomic sight computations were check computed. All the checked lines of position and radar and visual ranges and bearings were replotted in determining the accepted positions and trackline of the ship.

*Sounding records.* A total of 31,507 nautical miles of trackline bathymetry was obtained during the expedition. The results are contained in 35 sounding volumes and on 95 boat sheets at the U.S. Coast and Geodetic Survey. The geophysical profiles (figs. 67 through 70) show the bathymetry along selected sections of trackline. Figure 57 is a composite photograph of the PDR record northeast of Ceylon. Five scale shifts were used to record this portion of the continental slope near Trincomalee. This slope is one of the steepest sections of continental slope discovered to date. It exceeds 45° between depths of 472 and 1,095 fms. The portion of slope between 40 and 275 fms was photographed with the Coast and Geodetic Survey's deep-sea camera system—camera lowering No. 6 in table 16, deep-sea camera stations (see Bottom Photography). A dredge haul (No. 19) was made at 440 fms on this slope. Figure 58 is a composite photograph of the PDR record across the submarine canyons that are incised in the continental shelf south of Trincomalee Canyon, along the east coast of Ceylon. The submarine canyons off the Ganges Delta are described by Drs. H. B. Stewart, Jr., R. S. Dietz, and F. P. Shepard on pages 77 to 79. Other interesting aspects of the bathymetric records with respect to geological and geophysical investigations are discussed in several papers at the end of this chapter.

## Bottom Sampling

During the Indian Ocean Expedition of the *Pioneer*, 104 bottom samples were collected. The general location of the sample sites is shown in figures 1 through 3 by the tracklines and the key to data collected. The geographic positions of the samples, together with the serial and sample-type number of each, are given in table 10. Core samples were obtained with the Phleger and

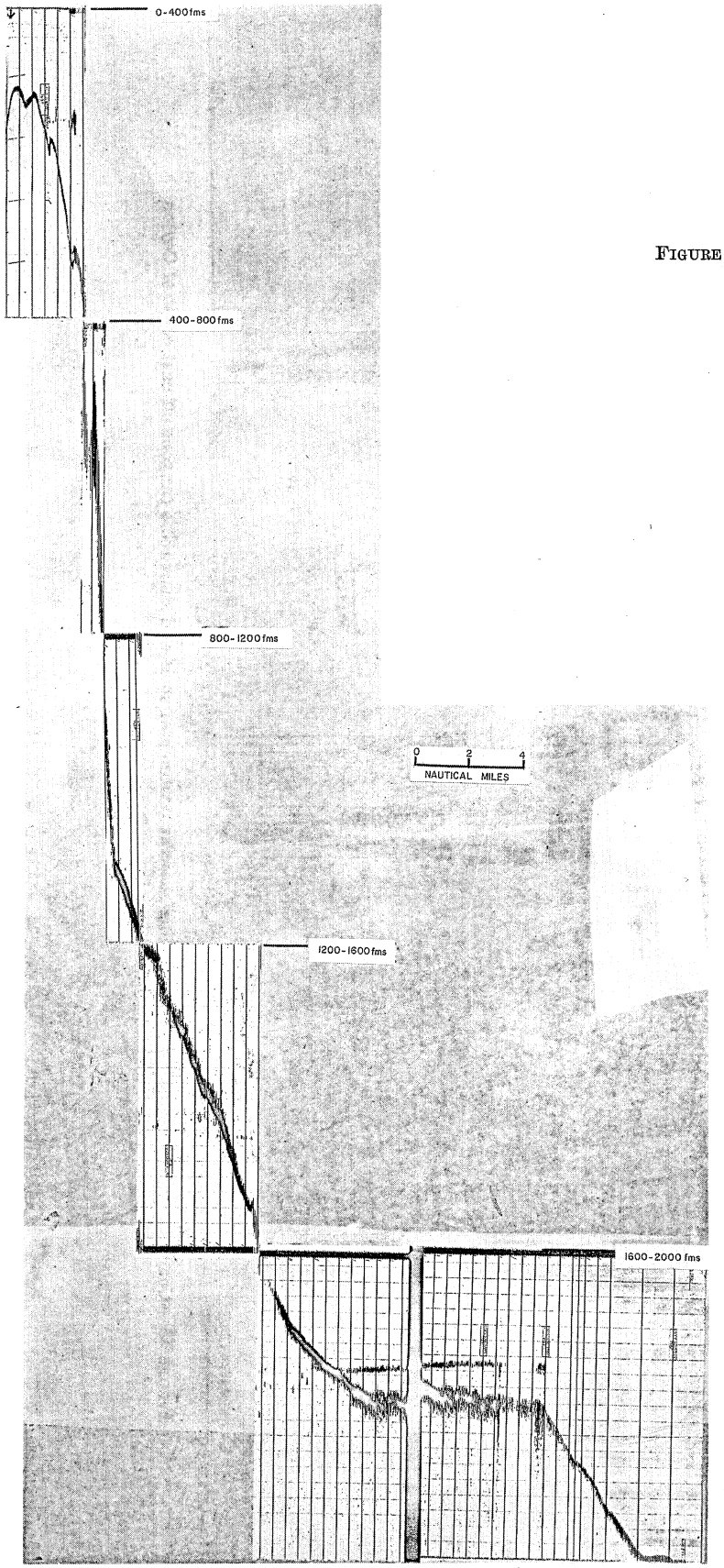


FIGURE 57.—Composite photograph of depth recording across continental slope northeast of Ceylon.

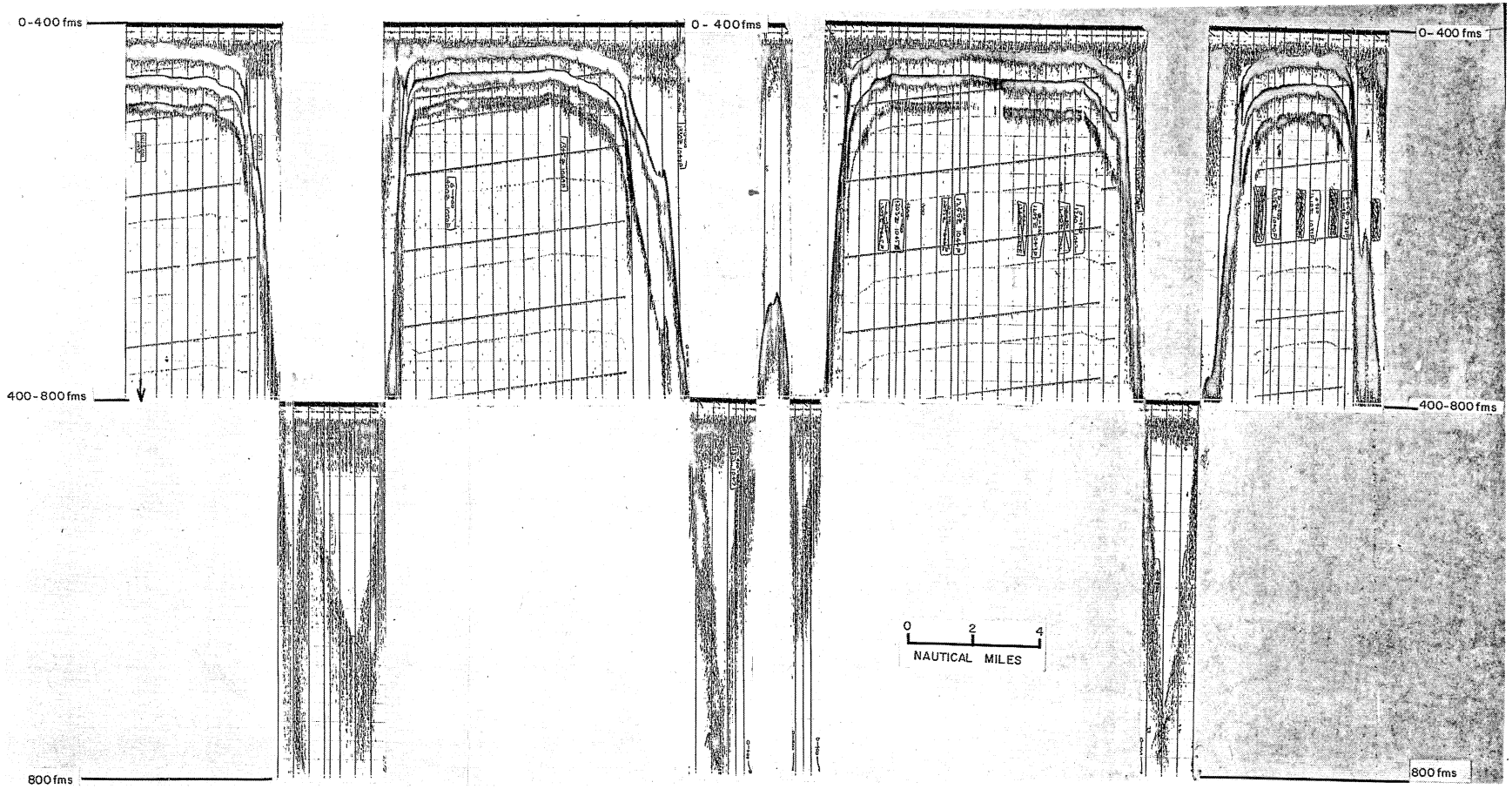


FIGURE 58.—Composite photograph of depth recording showing continental shelf and submarine canyons off east coast of Ceylon.

TABLE 10.—*Bottom sample locations and numbers**

| Serial No. | Sample No. | Latitude ° ′ | Longitude ° ′ | Serial No. | Sample No. | Latitude ° ′ | Longitude ° ′ |
|---|---|---|---|---|---|---|---|
| 306 | Dredge 1 | 10 46. 4 N | 117 44. 6 E | 630 | Core 21 | 10 09. 8 N | 92 27. 0 E |
| 307 | Dredge 2 | 10 49. 4 N | 117 51. 3 E | 637 | Core 22 | 10 02. 6 N | 93 12. 3 E |
| 339 | Core 1 | 06 59. 0 N | 115 16. 6 E | 681 | Core 23 | 09 54. 1 N | 93 44. 7 E |
| 358 | Core 2 | 01 55. 7 N | 101 50. 0 E | 690 | Dredge 11 | 10 01. 8 N | 96 23. 1 E |
| 359 | Core 3 | 01 54. 9 N | 101 50. 2 E | 709 | Core 24 | 10 58. 7 N | 93 42. 0 E |
| 360 | Grab 1 | 01 51. 4 N | 101 51. 3 E | 710 | Dredge 12 | 11 12. 9 N | 93 34. 7 E |
| 361 | Grab 2 | 01 46. 7 N | 101 51. 9 E | 717 | Core 25 | 09 47. 6 N | 93 55. 7 E |
| 362 | Grab 3 | 01 41. 8 N | 101 52. 4 E | 737 | Dredge 13 | 11 50. 7 N | 93 33. 0 E |
| 364 | Core 4 | 02 13. 7 N | 101 35. 8 E | 766 | Core 26 | 12 48. 6 N | 93 57. 3 E |
| 365 | Core 5 | 02 13. 9 N | 101 36. 7 E | 772 | Dredge 14 | 12 50. 4 N | 94 44. 4 E |
| 366 | Grab 4 | 02 14. 1 N | 101 36. 9 E | 821 | Grab 27 | 20 55. 8 N | 88 36. 0 E |
| 368 | Grab 5 | 02 18. 1 N | 101 42. 2 E | 822 | Grab 28 | 20 55. 8 N | 88 25. 9 E |
| 371 | Grab 6 | 02 48. 0 N | 100 27. 0 E | 823 | Grab 29 | 20 54. 0 N | 88 14. 3 E |
| 372 | Core 6 | 02 48. 3 N | 100 26. 7 E | 826 | Grab 30 | 21 12. 8 N | 89 27. 2 E |
| 373 | Core 7 | 02 30. 8 N | 100 28. 7 E | 827 | Core 27 | 21 12. 8 N | 89 27. 2 E |
| 381 | Core 8 | 03 15. 5 N | 101 10. 4 E | 829 | Core 28 | 21 13. 8 N | 89 29. 0 E |
| 382 | Grab 7 | 03 15. 6 N | 101 10. 2 E | 830 | Dredge 15 | 21 13. 1 N | 89 22. 8 E |
| 383 | Grab 8 | 03 19. 2 N | 101 06. 4 E | 858 | Dredge 16 | 19 15. 3 N | 89 04. 9 E |
| 384 | Grab 9 | 03 25. 7 N | 100 59. 4 E | 859 | Core 29 | 19 17. 1 N | 89 10. 2 E |
| 385 | Grab 10 | 03 28. 4 N | 100 56. 3 E | 860 | Core 30 | 19 21. 7 N | 89 17. 1 E |
| 386 | Grab 11 | 03 36. 7 N | 100 49. 0 E | 970 | Dredge 17 | 08 44. 0 N | 81 22. 6 E |
| 387 | Grab 12 | 03 46. 3 N | 100 40. 8 E | 971 | Core 31 | 08 50. 5 N | 81 22. 6 E |
| 388 | Grab 13 | 04 09. 5 N | 100 29. 1 E | 972 | Core 32 | 08 51. 7 N | 81 24. 8 E |
| 390 | Grab 14 | 04 09. 5 N | 100 22. 4 E | 979 | Dredge 19 | 08 29. 7 N | 81 31. 3 E |
| 393 | Grab 15 | 04 09. 2 N | 99 52. 1 E | 3791 | Core 33 | 05 53. 2 S | 101 10. 8 E |
| 394 | Core 10 | 04 09. 4 N | 99 52. 3 E | 3815 | Grab 31 | 06 11. 0 S | 104 56. 2 E |
| 396 | Grab 16 | 04 01. 1 N | 99 24. 1 E | 3816 | Grab 32 | 06 11. 0 S | 104 56. 2 E |
| 398 | Grab 17 | 04 29. 9 N | 99 54. 3 E | 3817 | Grab 33 | 06 15. 9 S | 104 50. 1 E |
| 400 | Grab 18 | 04 52. 2 N | 100 14. 6 E | 3891 | Grab 35 | 08 46. 9 S | 115 42. 4 E |
| 401 | Core 12 | 04 52. 5 N | 100 14. 5 E | 3892 | Grab 36 | 08 42. 2 S | 115 41. 9 E |
| 404 | Grab 19 | 04 42. 9 N | 99 09. 3 E | 3893 | Grab 37 | 08 42. 2 S | 115 41. 9 E |
| 410 | Grab 20 | 05 46. 4 N | 98 13. 7 E | 3906 | Grab 38 | 08 37. 9 S | 115 36. 8 E |
| 411 | Core 14 | 05 46. 5 N | 98 13. 3 E | 3907 | Grab 39 | 08 30. 7 S | 115 45. 3 E |
| 416 | Grab 21 | 05 31. 7 N | 99 14. 9 E | 3921 | Grab 40 | 08 31. 2 S | 115 43. 7 E |
| 417 | Core 15 | 05 31. 2 N | 99 14. 3 E | 3922 | Grab 41 | 08 23. 7 S | 115 49. 1 E |
| 422 | Grab 22 | 05 48. 6 N | 97 28. 8 E | 3146 | Core 35 | 05 24. 7 N | 127 46. 8 E |
| 423 | Grab 23 | 05 48. 6 N | 97 28. 8 E | 3181 | Dredge 21 | 07 35. 5 N | 134 26. 2 E |
| 424 | Grab 24 | 05 48. 0 N | 97 28. 0 E | 3182 | Dredge 22 | 07 39. 3 N | 134 26. 8 E |
| 429 | Core 16 | 05 44. 5 N | 96 31. 3 E | 3200 | Dredge 23 | 07 37. 6 N | 134 44. 3 E |
| 440 | Dredge 3 | 06 14. 0 N | 94 59. 5 E | 3202 | Dredge 25 | 07 41. 9 N | 134 41. 7 E |
| 472 | Core 17 | 05 52. 5 N | 92 33. 0 E | 3229 | Core 36 | 11 16. 0 N | 141 58. 5 E |
| 497 | Dredge 4 | 06 44. 8 N | 98 09. 9 E | 3239 | Grab 42 | 13 14. 8 N | 144 29. 9 E |
| 505 | Core 18 | 05 46. 6 N | 97 00. 7 E | 3240 | Grab 43 | 13 13. 0 N | 144 27. 9 E |
| 507 | Dredge 5 | 05 46. 5 N | 97 31. 4 E | 3241 | Grab 44 | 13 13. 6 N | 144 26. 6 E |
| 521 | Grab 25 | 05 25. 5 N | 100 21. 3 E | 3242 | Grab 45 | 13 13. 6 N | 144 26. 6 E |
| 540 | Dredge 6 | 08 50. 4 N | 94 31. 4 E | 3243 | Grab 46 | 13 13. 6 N | 144 26. 6 E |
| 575 | Core 19 | 09 21. 3 N | 93 56. 2 E | 3244 | Grab 47 | 13 13. 2 N | 144 26. 7 E |
| 582 | Dredge 8 | 08 57. 0 N | 93 33. 0 E | 3246 | Grab 48 | 13 14. 6 N | 144 26. 8 E |
| 589 | Grab 26 | 09 21. 0 N | 92 44. 8 E | 3247 | Dredge 26 | 13 39. 0 N | 144 25. 3 E |
| 590 | Dredge 9 | 09 24. 2 N | 92 34. 6 E | 3248 | Dredge 27 | 13 39. 1 N | 144 25. 6 E |
| 625 | Core 20 | 10 09. 4 N | 91 06. 9 E | 3251 | Core 37 | 13 32. 4 N | 144 33. 4 E |
| 628 | Dredge 10 | 10 07. 6 N | 91 37. 9 E | 3252 | Dredge 28 | 13 17. 1 N | 144 37. 2 E |

*Unsuccessful attempts (failure to obtain a sample) are not listed.

Hydroplastic corers. The Hydroplastic coring apparatus was often rigged with a Phleger corer serving as a tripping weight. The Shipek grab sampler (fig. 59) and chain bag dredge (fig. 60) also were used to sample the bottom. Field descriptions—published in volume 2 of this series—were recorded as the samples were brought aboard. The samples then were divided and packed for later distribution and laboratory analysis.

*Strait of Malacca samples.* Selected bottom samples and splits of samples have been sent to various laboratories for analysis. Mr. George Keller of the U.S. Naval Oceanographic Office at Suitland, Md., retained splits of 25-grab, 5-dredge, and 10-core samples taken in the Strait of Malacca. Dr. J. B. Alexander, Director of the Geological Survey of the Federation of Malaysia, Ipoh, Perak, Malaysia also retained splits of samples taken in the Strait of Malacca. Results of the laboratory examination for 22 of these samples appear in tables 11 and 12. Table 11 describes the samples and gives the results of heavy mineral separations. Table 12 is an analysis of mineral contents after the clay-size fraction was removed by washing. Mr. Kelvin S. Rodolfo of the Geology Department, University of Southern California, Los Angeles, Calif. prepared field descriptions of all samples. These are published in volume 2. He also retained splits of 7-grab, 8-dredge and 6-core samples, obtained in the Strait of Malacca, Andaman Sea, Bay of Bengal, and Indian Ocean, for further laboratory analysis.

FIGURE 59.—Grab sampler used to sample surface of sea floor.

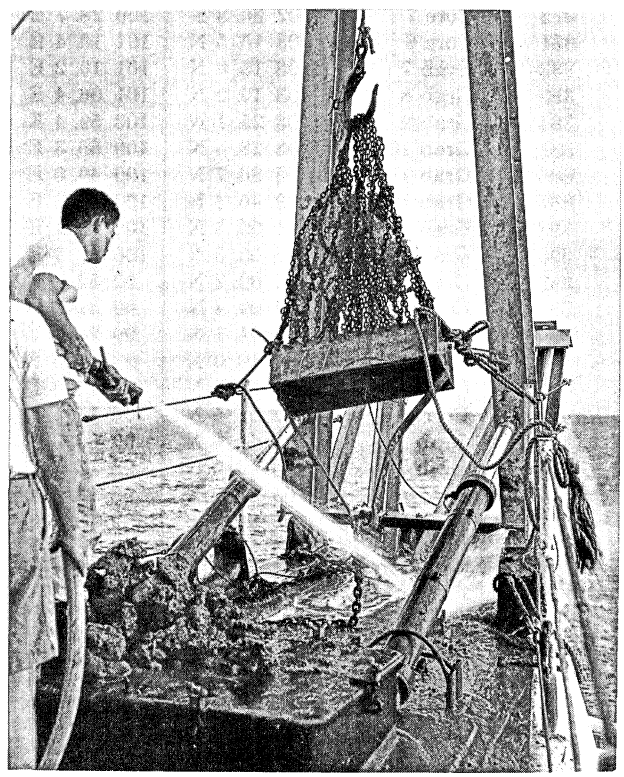

FIGURE 60.—Emptying contents of chain bag dredge.

TABLE 11.—*Descriptions and heavy-mineral separations of sediment samples from Strait of Malacca*

| Grab sample number | Description and heavy-mineral separation of sample | |
|---|---|---|
| 1 | Gray, clayey to silty sediment; organic remains, including gastropods, present; limonite nodules occur. | |
| | Total weight of sample: | 435. 6 gm |
| | Bromoformed lights: | 99. 4% |
| | Bromoformed heavies: | 0. 6% |
| 2 | Gray, clayey to silty sediment; organic remains include plant and microshells. | |
| | Total weight of sample: | 446.7 gm |
| | Bromoformed lights: | 74.9% |
| | Bromoformed heavies: | 25.1% |
| 3 | Gray, clayey to silty sediment with micro-organic remains. | |
| | Total weight of sample: | 539.4 gm |
| | Bromoformed lights: | 100.0% |
| | Bromoformed heavies: | tr |
| 4 | Light brown, sandy sediment; virtually quartz, subangular to rounded; organic remains, including pelecypods, present; limonite nodules occur. | |
| | Total weight of sample: | 177.3 gm |
| | Bromoformed lights: | 100.0% |
| | Bromoformed heavies: | tr |
| 5A | Gray, clayey to silty sediment wlth micro-organic remains. | |
| | Total weight of sample: | 725.0 gm |
| | Bromoformed lights: | 98.3% |
| | Bromoformed heavies: | 1.7% |
| 5B | Gray, sandy sediment with micro-organic remains. | |
| | Total weight of sample: | 164.6 gm |
| | Bromoformed lights: | 99.7% |
| | Bromoformed heavies: | 0.3% |
| 6 | Similar to 5B, except slightly more clayey material present with small gastropod shells. | |
| | Total weight of sample: | 922.8 gm |
| | Bromoformed lights: | 100.0% |
| | Bromoformed heavies: | tr |
| 7 | Gray, clayey to sandy sediment; organic remains, including brachiopod, present. | |
| | Total weight of sample: | 1, 094.3 gm |
| | Bromoformed lights: | 99.3% |
| | Bromoformed heavies: | 0.7% |
| 8 | Similar to 7; includes decayed plant remains. | |
| | Total weight of sample: | 763.5 gm |
| | Bromoformed lights: | 99.4% |
| | Bromoformed heavies: | 0.6% |
| 9 | Similar to 7. | |
| | Total weight of samples: | 257.7 gm |
| | Bromoformed lights: | 99.0% |
| | Bromoformed heavies: | 1.0% |
| 10 | Similar to 7. | |
| | Total weight of sample: | 697. 0 gm |
| | Bromoformed lights: | 100. 0% |
| | Bromoformed heavies: | tr |
| 11 | Gray, clayey to silty sediment; organic remains, mainly gastropods and brachiopods. | |
| | Total weight of sample: | 687. 7 gm |
| | Bromoformed lights: | 100. 0% |
| | Bromoformed heavies: | tr |
| 12 | Olive gray sediment, mainly silt; abundant organic remains include brachiopods and pelecypods. | |
| | Total weight of sample: | 837. 4 gm |
| | Bromoformed lights: | 100. 0% |
| | Bromoformed heavies: | tr |
| 13 | Similar to 12. | |
| | Total weight of sample: | 1, 054. 2 gm |
| | Bromoformed lights: | 100. 0% |
| | Bromoformed heavies: | tr |
| 14 | Light gray, sandy sediment with abundant organic remains. | |
| | Total weight of sample: | 869. 8 gm |
| | Bromoformed lights: | 100. 0% |
| | Bromoformed heavies: | tr |
| 15 | Olive gray, silty sediment with micro-organic remains. | |
| | Total weight of sample: | 608. 3 gm |
| | Bromoformed lights: | 99. 7% |
| | Bromoformed heavies: | 0. 3% |
| 16 | Olive gray, silty sediment; organic remains include pelecypods and gastropods. | |
| | Total weight of sample: | 789. 9 gm |
| | Bromoformed lights: | 99. 7% |
| | Bromoformed heavies: | 0. 3% |
| 17 | Sandy sediment of variable color with abundant organic remains. | |
| | Total weight of sample: | 588. 2 gm |
| | Bromoformed lights: | 99. 7% |
| | Bromoformed heavies: | 0. 3% |
| 18 | Olive gray, silty sediment with micro-organic remains, including gastropods. | |
| | Total weight of sample: | 686. 3 gm |
| | Bromoformed lights: | 100. 0% |
| | Bromoformed heavies: | tr |
| 19 | Gray, silty to sandy sediment with organic remains. | |
| | Total weight of sample: | 522. 1 gm |
| | Bromoformed lights: | 99. 7% |
| | Bromoformed heavies: | 0. 3% |
| 20 | Gray, silty sediment with organic remains. | |
| | Total weight of sample: | 837. 2 gm |
| | Bromoformed lights: | 100. 0% |
| | Bromoformed heavies: | tr |
| 21 | Gray, clayey to silty sediment with organic remains, including gastropods. | |
| | Total weight of sample: | 696. 9 gm |
| | Bromoformed lights: | 99. 7% |
| | Bromoformed heavies: | 0. 3% |
| 22 | Sandy sediment of variable color with organic remains. | |
| | Total weight of sample: | 839. 4 gm |
| | Bromoformed lights: | 98. 3% |
| | Bromoformed heavies: | 1. 7% |

TABLE 12.—*Approximate mineral-content analyses of sediment samples from Strait of Malacca* [1]

[Percent of sample by weight]

| Mineral content | Grab sample number | | | | | | | | | | | | | | | | | | | | | | |
|---|---|---|---|---|---|---|---|---|---|---|---|---|---|---|---|---|---|---|---|---|---|---|---|
| | 1 | 2 | 3 | 4 | 5A | 5B | 6 | 7 | 8 | 9 | 10 | 11 | 12 | 13 | 14 | 15 | 16 | 17 | 18 | 19 | 20 | 21 | 22 |
| Quartz | 99 | 74 | 99 | 100 | 97½ | 99½ | 98 | 98½ | 84½ | 84 | 90 | 60 | 70 | 60 | 70 | 96½ | 94½ | 50 | 90 | 93 | 95 | 98½ | 97½ |
| Organic remains | ½ | 1 | 1 | --- | 1 | ---- | 2 | 1 | 15 | 15 | 10 | 40 | 30 | 40 | 30 | 3 | 4 | 49½ | 10 | 4½ | 5 | 1 | 1 |
| Iron oxides | ½ | ½ | -- | tr [2] | tr | tr | tr | tr | ---- | tr | tr | -- | tr | -- | -- | tr | ---- | ---- | -- | tr | -- | ---- | tr |
| Tourmaline | tr | ---- | tr | tr | ¼ | tr | tr | tr | ¼ | ¼ | tr | tr | tr | tr | tr | tr | tr | ---- | tr | 1½ | tr | tr | 1¼ |
| Ilmenite | tr | tr | tr | tr | ---- | ½ | tr | tr | ¼ | ½ | tr | tr | tr | tr | tr | tr | tr | ---- | tr | tr | tr | tr | ¼ |
| Amphibole | tr | ---- | -- | --- | tr | ---- | tr | ---- | ---- | ---- | -- | -- | -- | -- | -- | tr | tr | ---- | -- | tr | tr | tr | tr |
| Zircon | tr | ---- | -- | tr | tr | tr | tr | tr | tr | tr | tr | tr | tr | tr | -- | tr | tr | tr | tr | tr | -- | tr | tr |
| Topaz | tr | ---- | -- | tr | ¼ | tr | tr | tr | tr | tr | tr | tr | tr | tr | -- | tr | tr | ---- | tr | tr | -- | tr | tr |
| Rutile | tr | ---- | -- | --- | ---- | tr | tr | tr | tr | ---- | tr | tr | tr | -- | -- | tr | ---- | ---- | tr | tr | -- | tr | ---- |
| Pyrite | ---- | 24½ | -- | --- | ½ | ---- | -- | tr | tr | tr | -- | -- | -- | -- | tr | ---- | ---- | ---- | -- | ---- | -- | ---- | ---- |
| Leucoxene | tr | ---- | -- | --- | ---- | tr | tr | ---- | ---- | ---- | -- | -- | -- | -- | -- | ---- | ---- | ---- | -- | ---- | -- | ---- | ---- |
| Cassiterite(?) | tr | ---- | -- | --- | ---- | ---- | -- | ---- | ---- | ---- | -- | -- | tr | tr | -- | tr | ---- | ---- | -- | ---- | -- | tr | ---- |
| Calcite | tr | ---- | -- | --- | ---- | ---- | -- | ---- | ---- | ---- | -- | -- | -- | -- | -- | ---- | ---- | ---- | -- | ---- | -- | ---- | ---- |
| Muscovite | ---- | ---- | -- | tr | tr | ---- | -- | ---- | ---- | tr | tr | -- | tr | -- | -- | ---- | ---- | ---- | -- | ---- | -- | ---- | ---- |
| Anatase | ---- | ---- | -- | --- | tr | ---- | -- | tr | ---- | ---- | -- | -- | -- | -- | -- | ---- | ---- | ---- | -- | ---- | -- | ---- | ---- |
| Biotite | ---- | ---- | -- | --- | ½ | ---- | tr | tr | tr | ---- | tr | tr | tr | tr | -- | ½ | 1½ | ½ | tr | ½ | -- | ½ | tr |
| Fluorite | ---- | ---- | -- | --- | tr | ---- | -- | ---- | ---- | ---- | -- | -- | -- | -- | -- | ---- | ---- | ---- | -- | ---- | -- | ---- | ---- |
| Garnet | ---- | ---- | -- | --- | ---- | tr | -- | ---- | ---- | ---- | -- | -- | -- | -- | -- | ---- | ---- | ---- | -- | ---- | -- | ---- | ---- |
| Monazite | ---- | ---- | -- | --- | ---- | tr | -- | tr | tr | tr | -- | -- | tr | tr | tr | ---- | ---- | ---- | -- | ---- | -- | ---- | ---- |
| Siderite | ---- | ---- | -- | --- | ---- | ---- | tr | ½ | tr | ¼ | tr | -- | -- | -- | -- | tr | ---- | ---- | tr | ---- | -- | tr | ---- |
| Allanite | ---- | ---- | -- | --- | ---- | ---- | tr | ---- | tr | tr | -- | -- | -- | -- | -- | ---- | ---- | ---- | -- | ½ | -- | tr | tr |
| Epidote | ---- | ---- | -- | --- | ---- | ---- | -- | tr | tr | ---- | tr | -- | tr | -- | -- | ---- | ---- | ---- | tr | ---- | -- | ---- | ---- |
| Andalusite | ---- | ---- | -- | --- | ---- | ---- | -- | ---- | ---- | ---- | tr | tr | -- | -- | -- | tr | ---- | ---- | tr | ---- | -- | ---- | ---- |

[1] After removal of clay-size fraction by washing.

[2] tr denotes trace present.

*Java, Mindanao, and Mariana Trench samples.* Core number 33 was obtained from the northern slope of the Java Trench, core number 35 from the flank of the Mindanao Trench, and core number 36 from an estimated depth of 5,700 fms in the Mariana Trench. These core samples were sent to the Marine Science Center, U.S. Coast and Geodetic Survey Regional Office, Seattle, Wash. where the cores were opened, photographed, and examined megascopically for gross structures as indicated by marked changes in lithology, color, texture, and consistency, and for water content, cohesiveness, and modal grain size. Descriptions of the megascopic analysis of these cores (tables 13, 14, and 15) were prepared by Mr. William Anikouchine, marine geologist, at the Seattle Laboratory.

TABLE 13.—*Description of core sample from Java Trench*

Core No. 33; Length 249 cm; Intervals in cm measured from top.

| Unit | Interval | Description |
|---|---|---|
| 1 | 0–27 | Light olive gray (5Y6/1), fine-grained, uniform clay with darker (5Y4/1) streaks and blotches. The streaks are less than 1 mm thick and are in 1 to 2 cm zones spaced about 4 cm apart. Very pale orange (10YR8/2) galls of more compact clay, 1.5 by 4 cm in size, occur at 8 and 11 cm from the top of this unit. |
| 2 | 27–63 | Greenish gray (5GY6/1) with streaks and mottling of light olive gray (5Y6/1) and dark greenish gray (5GY4/1) in the upper half, and 1 cm layers of dark greenish gray (5GY4/1), silty clay spaced 1.5 cm apart. The silty clay layers are found at 34 and 50 cm. Two streaks of dark yellowish brown (10YR4/2) clay occur at about 42 cm. The lower contact is transitional. The unit is 36 cm thick. |
| 3 | 63–108 | Greenish gray (5GY6/1), slightly silty clay. The upper half of this unit has streaks of dark greenish gray (5GY4/1), fine sand spaced 1 to 2 cm apart and lying at steep angles to the bedding. Moderate yellowish brown (10YR5/4) bands up to 1 cm thick occur at 70 and 86 cm. The upper band is in the shape of a parabola, opening laterally, and the lower band is subhorizontal and has a sharp upper and gradational lower contact. Between 75 and 80 cm, the streaks of fine sand have a cross-bedded configuration with tangents to the lower contact and truncations at the top. The lower half of the unit is uniform greenish gray (5GY6/1), slightly silty clay. A fragment of the core catcher was lodged at 100 cm and a void was present between 106 and 108 cm. The unit is 43 cm thick. |
| 4 | 108–251 | Greenish gray (5GY6/1) clay, streaked and banded with dark greenish gray (5GY4/1), silty clay. The bands are typically 1 cm thick and are spaced between 2 and 10 cm apart. Light olive brown (5Y5/6) bands, 1 cm thick, occur at 116 and 120 cm and moderate yellowish brown (10YR5/4) streaks occur at 174 and 178 cm. The material between 108 and 131 cm shows evidence of disruption by the core catcher, fragments of which occur at 126 cm and at the bottom of the core. The bedding planes are distorted to produce arc-shaped traces which are concave downward. This is true of the entire core but is especially pronounced in this unit. Many small voids (2 by 10 mm) occur throughout this unit. This unit is 143 cm thick. |

TABLE 14.—*Description of core sample from Mindanao Trench*

Core No. 35; Length 498 cm; Intervals in cm measured from top.

| Unit | Interval | Description |
|---|---|---|
| 1 | 0–5 | Dark yellowish orange (10YR6/6), uniform-textured clay. Contained wood fragments (samples 35–W3 and 35–W4). The lower contact is irregular, and below it there is a layer 5 cm thick of oxidized blotches and greenish black (5GY2/1) streaks. This unit is the oxidized surface layer. It is 5 cm thick. |
| 2 | 5–329 | Dark greenish gray (5GY4/1) clay of apparent uniform texture and composition in layers, 2 to 8 cm thick, randomly intercalated with like-colored, irregular layers, lenses, and streaks of rough-textured, "curdled" clay, ranging in thickness between 5 mm and 13 cm with an average thickness of about 2 cm. Contacts between intercalations are either abrupt or gradational in no apparent pattern. The entire unit is streaked, banded, and variegated |

TABLE 14.—*Description of core sample from Mindanao Trench*—Continued

| Unit | Interval | Description |
|---|---|---|
| | | with lighter (5GY5/1) and darker (5GY3/1) colors; dark to medium dark gray (N3 to N4) carbonaceous smears; streaks and mottlings of olive gray (5Y4/1), brownish gray (5YR4/1), and dark greenish gray (5GY4/1). The color variations are both sharp and gradational, and occur at random but mainly in the layers of fine-textured clay. The color bands have a typical thickness of 3 cm. A twiglike piece of wood, 2 mm in diameter (not sampled), occurs at 305 cm. There are greenish black (5GY2/1) streaks, 5 mm thick above and below the twig, at a distance of 2 cm. The unit is 324 cm thick. |
| 3 | 329–383 | Dark greenish gray (5GY4/1) clay slurry consisting of 1-mm curds of compact, cohesive, and uniform clay in a flocculated clay-water suspension. This unit undoubtedly was disrupted during core handling. However, cohesive lumps distributed throughout the slurry show layers up to 2 mm thick of dark gray (N3) and greenish black (5GY2/1) uniform clay. This unit increases in liquid content toward the top, probably due to settling and compaction after disruption. Two pieces of wood, a branch about 1 cm in diameter and 5 cm long and a fragment 5 mm in diameter and 2 cm long, were found within this unit (samples 35–W1 and 35–W2). The upper contact of this unit is abrupt. The lower contact coincides with the place where the core was cut into middle and lower sections so that it appears abrupt. The unit is 54 cm thick. |
| 4 | 383–405 | Clay similar to unit 2. Approximately 2 and 3.5 cm from the top of this unit are 1-cm lenses of greenish black (5GY2/1) clay which contain pyrite (or marcasite) nodules up to 1 cm in diameter. The lower 10 cm shows color banding 1 to 2 cm thick. The lower contact is abrupt. The unit is 22 cm thick. |
| 5 | 405–498 | Dark greenish gray (5GY4/1) clay of uniform consistency that serves as a matrix for clay galls up to 3 mm in diameter. The galls are of the same color, uniform, compact, and covered with a dark gray (N3) carbonaceous film. The upper 3.5 cm are banded with medium dark gray (N4) and dark gray (N3). Below this, the unit is streaked vertically with dark gray (N3). The unit is 93 cm thick. |

TABLE 15.—*Description of core sample from Mariana Trench*

Core No. 36; Length 328.5 cm; Intervals in cm measured from top.

| Unit | Interval | Description |
|---|---|---|
| 1 | 0–10 | Pale yellowish brown (10YR6/2), fine-grained clay of uniform texture containing moderate brown (5YR-3/4) mottling in the upper half of the unit and olive gray (5Y3/2), silty lenses in the lower half. The lenses are typically 2 mm thick. The lower contact is wavy, abrupt, and marked by 1 cm of thin (less than 1 mm) color banding, alternating between dark yellowish orange (10YR6/6) and moderate yellowish brown (10YR5/4). |
| 2 | 10–35 | Uniform, fine-grained, dark yellowish brown (10YR4/2) clay showing subhorizontal bands, about 2 cm thick, that are a moderate yellowish brown (10YR5/4 and 10YR3/2). The lower contact is irregular and subparallel to the bedding. The unit is 25 cm thick. |
| 3 | 35–71.5 | Light yellowish brown (10YR5/2) clay, similar to the unit above but showing irregular mottling instead of banding. The mottling is dark yellowish brown (10YR4/2) and pale yellowish brown (10YR6/2). Between 40 and 50 cm and at 69 cm there are silty-clay lenses lying at various steep angles to the bedding. These lenses are marbled in olive gray (5Y3/2), dark yellowish orange (10YR6/6), pale yellowish brown (10YR6/2), and grayish orange (10YR7/4). The lower contact is abrupt, although marked only by a slight darkening of the sediment color. The unit is 36.5 cm thick. |
| 4 | 71.5–102.5 | Dark yellowish brown (10YR4/2) clay, similar to unit 2 but with subtle color layering about 3 cm thick and |

TABLE 15.—*Description of core sample from Mariana Trench*—Continued

| Unit | Interval | Description |
|---|---|---|
| | | having vague lighter streaks about 1 mm thick. The unit is 31 cm thick. |
| 5 | 102. 5–121 | Dark yellowish brown (10YR4/2), uniform clay containing moderate yellowish brown (10YR5/4) clay galls up to 1 mm in diameter. The galls become fewer and finer toward the top. The upper contact is gradational and the lower is abrupt. The unit is 18.5 cm thick. An air void, extending the length of the unit, indicates stretching of the core during coring operations. |
| 6 | 121–142 | Lightly mottled, fine-grained clay; flecks of moderate yellowish brown (10YR5/4) in a matrix of moderate brown (5YR3/4). In the lower 5 cm, an irregular subhorizontal layer contains clay galls about 1 mm in diameter rather than flecks. The unit is 21 cm thick. |
| 7 | 142–369. 5 | Moderate brown (5YR3/4), uniform, fine-grained clay, streaked vertically with moderate yellowish brown (10YR5/4) and a little dusky yellowish brown (10YR2/2). The streaks close at the upper part of the unit to assume the configuration of a series of parabolas opening downward. Voids are present between 251 and 256 cm and between 277.5 and 313.5 cm (a total of 41 cm). Subtracting the voids, the thickness of this unit is 186.5 cm. |

Core 33, Java Trench: Obvious stretching and disruption of this core sample must be borne in mind in any interpretation.

The variation in color of the sediment probably represents changing conditions in the chemical nature of the sedimentary environment. However, it is difficult to tell whether these variations were produced during or after sedimentation, that is, whether or not they result from diagenesis.

The fine-grained nature of the bulk of the sample suggests quiescent deposition. The silty and sandy layers and streaks indicate that quiet periods were punctuated with "showers" of coarser material, presumably derived from terrestrial sources.

If the layers and bands of apparently oxidized clay—found at depth in the core—are not the result of sampling, then they represent zones of incomplete reduction. This suggests that either the rate of reduction was slow or that deposition of the overlying material was rapid and irregular, or possibly both.

In many ways core 33 resembles core 35 from the Mindanao Trench. The major differences are the lack of "curdled" clay layers, organic materials, and carbonaceous smears which appear as streaks and mottlings. The lack of the latter may contribute to the incomplete reduction already mentioned.

A tentative interpretation of the sedimentary record provided by this core is that it represents deposition in a quiet area in which periodic, short bursts of coarser sediments were introduced, probably by storm-generated or earthquake-triggered turbidity currents.

Core 35, Mindanao Trench: The alteration of texture, water content, bands, streaks, and lenses in this core sample indicate pronounced variations in the nature of sedimentation. Clay of uniform composition indicates deposition and compaction during quiescent periods. The presence of clay galls indicates a different mode of formation, possibly the settling of violently disrupted preexisting clay deposits or flocculated clay that has been rolled about on the bottom. The presence of wood suggests rapid transport and burial. Carbonaceous streaks, mottlings, and films on clay galls indicate an abundance of organic material in the sediment. This correlates well with the oxidation-reduction characteristics of the sediment as evidenced by the presence of pyrite (marcasite) nodules. It seems likely that the banded arrangement of coloring is closely related to changes in the chemical nature of the sediments and that the coloring matter itself may reflect variations in the redox potential. A tentative interpretation of the core is that the sediments in this area were deposited by a turbidity current generated by flooded rivers. Submarine slumping also may have contributed to deposition in the area.

Core 36, Mariana Trench: This sample is typical deep-sea (pelagic) red clay. The only pronounced structures in the sample are the sharp color bands in unit 1, which might have been caused by disruption of the upper part of core during handling, and the mottling and silty layers in unit 3, which may be the remains of burrows produced by benthonic organisms, although it is unusual to find them so deep (70 cm) in core samples. The voids

and vertical streaks indicate stretching of the core during the coring operation. It seems likely that all of unit 7, which had an actual thickness of only 186.5 cm after subtracting the voids, was "sucked" into the core barrel from a single horizon. If this was the case, this portion of the sample does not adequately represent the vertical sequence of sediment that should have been penetrated by the core barrel at this depth.

*Palau and Guam samples.* Mr. Gilbert Corwin and Dr. Joshua I. Tracey, Jr. of the U.S. Geological Survey, Washington, D.C., participated in the Palau to Guam leg. Dredge hauls, numbered 21 through 25, were taken in the vicinity of the Palau Islands. Grab samples, numbered 42–48, core sample 37, and dredge samples 26–28 were taken west of Guam. The collection and analysis of these samples together with the results of depth soundings, acoustic reflecting profiling, and gravity and magnetic measurements were part of a special marine geological investigation near the Palau and Guam Islands. Results of this study are reported by Corwin and Tracey on pages 81 to 90.

*Other analyses.* Microscopic examination and size analysis of the core samples from the Java, Mindanao, and Mariana Trenches—numbers 33, 35, and 36—are being conducted by the Marine Science Center, USC&GS Regional Office, Seattle, Wash. The clay fractions from representative samples were submitted to the Department of Oceanography, University of Washington, Seattle, for X-ray diffraction identification of clay minerals. Splits of the three cores were sent to Dr. D. P. Kharkar, Tata Institute of Fundamental Research, Colaba, Bombay, India, for Io-Pa age-determination and to Dr. J. D. M. Wiseman of the British Museum, London, for examination of *Ethnodiscus* in the sediments. Plant material from one core was given to the Department of Botany, University of Washington. Micropaleontological studies of Radiolaria and Formaninifera in the cores have been begun by Mr. John Holdon of the Coast and Geodetic Survey. Coarse fractions of the three cores samples have been provided Professor Hsin-Yi Ling, Department of Oceanography, University of Washington.

Mr. John Kofoed of the Coast and Geodetic Survey is examining splits of grab samples 35–41 from the Lombok Strait, Indonesia area.

A rock sample from dredge haul no. 19 off Ceylon was presented to the Geological Survey of Ceylon for analysis.

## Bottom Photography

Nine lowerings were made with the Coast and Geodetic Survey's stereo deep-sea camera system (fig. 61). More than 4,000 photographs were made on 1,600 ft of exposed film. Table 16 gives the geographic location of each lowering and other information about it. The locations of camera stations also are shown in figures 1 to 3. A photograph from camera lowering number 8, north of Sumatra, and three photographs from camera lowering number 9, in the Mindanao Trench, are shown in figures 62 and 63.

The 35-millimeter cameras are operated by automatic timing devices as the cameras reach the

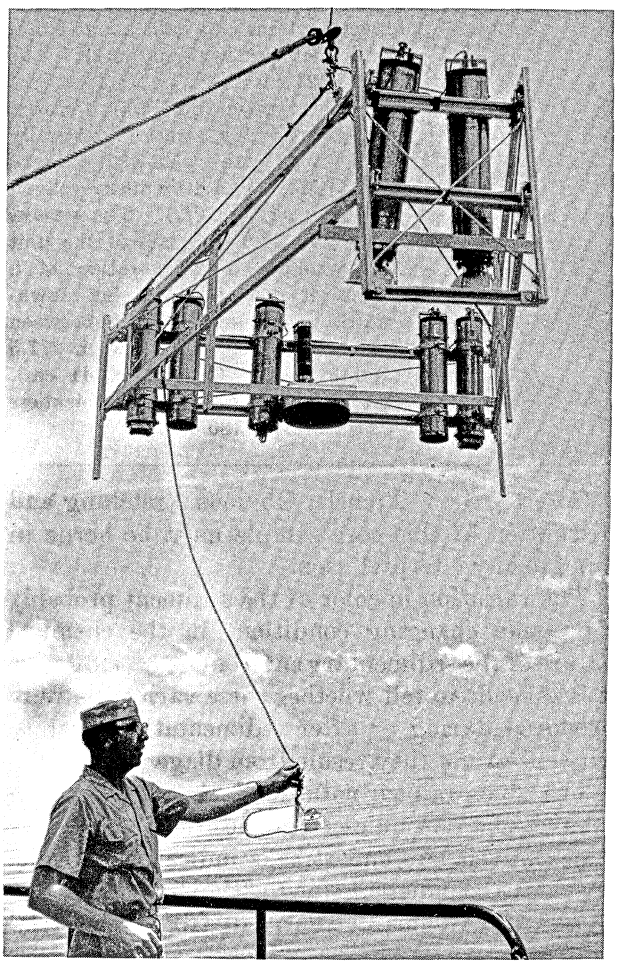

FIGURE 61.—Deep-sea camera equipment. Pendant contains magnetic compass for orienting bottom photographs.

TABLE 16.—*Deep-sea camera stations*

| Lowering number | Date 1964 (month/day) | Position | Depth (meters) | Cable out (meters) | Time (hours) | Remarks |
|---|---|---|---|---|---|---|
| 1 | 3/18 | 06°58′N 115°13′E | 1,862 | 2,105 | 4.6 | South China Sea; color film. |
| 2 | 3/29 | 02°17′N 101°44′E | 33 | 28 | 2.0 | Strait of Malacca; color film; 180 ft exposed. |
| 3 | 4/1 | 04°42′N 99°07′E | 49 | 52 | 2.3 | Strait of Malacca; black and white film; one camera inoperative. |
| 4 | 4/20 | 11°48′N 93°36′E | 596 | 585 | 2.6 | Andaman Sea; color film. |
| 5 | 5/6 | 19°04′N 89°28′E | 1,563 | -------- | 2.1 | Bay of Bengal; color film; depth control difficult. |
| 6 | 5/17 | 08°28′N 81°30′E | 45–278 | -------- | 3.3 | Off Trincomalee; black and white film; bottom pinger faded. |
| 7 | 5/18 | 05°46′N 81°11′E | 1,463 | 366 | 2.5 | Southeast coast of Ceylon; color film; lowering made to study deep scattering layer; pictures blank. |
| 8 | 6/8 | 05°44′N 97°26′E | 250–310 | 290 | 2.3 | North of Sumatra; color film; camera watches not synchronized; frequent variations in depth as noted on oscilloscope. |
| 9 | 7/6 | 05°27′N 127°27′E | 6,898–7,058 | 7,111 | 6.5 | Mindanao Trench; color film; one camera clock inoperative; frequent shoaling and irregular bottom made depth control difficult. |

desired depth. The camera units do not have shutters but depend on the absence of light at depth to prevent fogging of the film. Two 400-watt-second units are used for the light source. Self-contained batteries provide the power for these units and to advance the film. As many as 500 stereo pairs can be exposed during a single lowering. Either color or panchromatic film can be used. The cameras are equipped with Hopkins wide-angle 4.5 f lenses that have been corrected for operation through a quartz window and through water.

The system is designed to be used 15 ft above the ocean floor and to photograph 400 square feet of the bottom. The distance between the camera and the bottom is maintained by using a pinger on the camera and an oscilloscope attached to the echo sounder aboard ship. The battery-powered pinger consists of a "driver," coil, and transducer, and simultaneously sends a sound signal upward toward the ship and downward to the ocean floor every second. Both the direct signal from the pinger and the reflected signal from the ocean floor are picked up and displayed on the oscilloscope aboard ship. The signals are compared for accurate positioning of the cameras above the bottom as the ship drifts over the area of interest.

A magnetic compass is attached to a pendant below the camera frame. The compass face is photographed on one of the stereo pairs and provides a means of orienting photographs of the sea floor.

The developed film is held by the Institute for Oceanography, U.S. Environmental Science Services Administration.

## Gravity

Measurements of the acceleration of gravity, $g$, yield valuable information about the gross geological structure of the ocean basins, and the configuration of the crust-mantle interface. Reconnaissance marine gravity surveys, such as those made during the *Pioneer*'s International Indian Ocean Expedition, also provide data that are essential to the determination of the exact shape and size of the Earth's equipotential surface, or *geoid*.

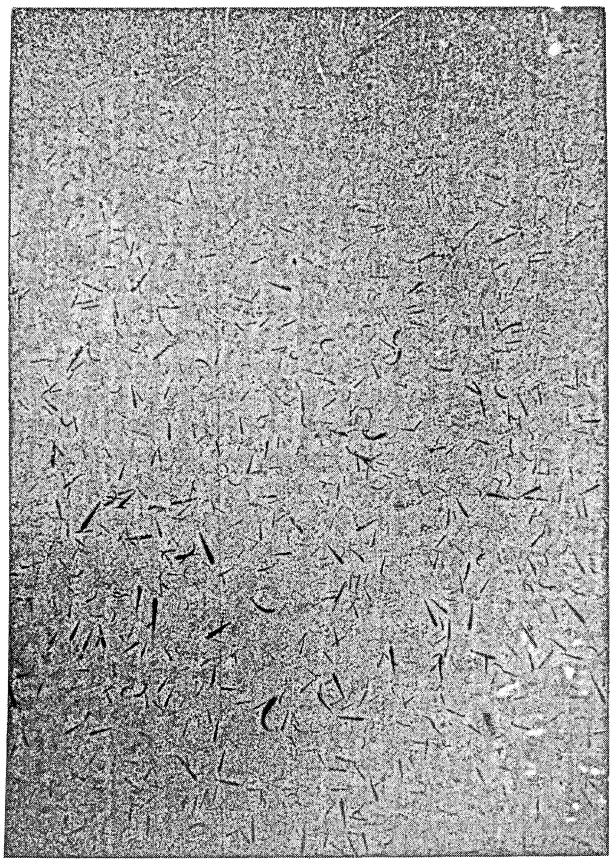

FIGURE 62.—Camera lowering number 8 north of Sumatra showing school of small fish.

*The sea gravity meter.* Continuous underway measurements of the acceleration of gravity were made aboard the *Pioneer* with the LaCoste & Romberg Air-Sea Gravity Meter No. S–11 (fig. 64). The sensing element of this instrument is a horizontal, pivoted beam, suspended by a spring. Under static conditions, a change in the acceleration of gravity, $\Delta g$, causes a deflection of the beam from null. The beam is restored to null by adjusting the tension on the spring. The amount of adjustment, measured as turns on a screw, is proportional to $\Delta g$.

Under operating conditions at sea, the deflection of the beam changes constantly as it responds to short-period accelerations caused by the ship's motion. In the later LaCoste & Romberg instruments, such as No. S–11, the motion of the beam is averaged electronically in order to filter out the short-period oscillations, and the signal is fed to a series of servo systems which continuously adjust the measuring screw tension to drive the "average" deflection to zero. The input to the servo systems is averaged over a 1–10 minute period selected by the operator. The output from the servo systems is recorded graphically; raw gravity, corrected for horizontal accelerations as explained below, can be scaled directly from this trace.

To reduce the effects of short-period, large-amplitude accelerations induced by sea motion, the gravity meter is mounted on a gimbal suspension. Accelerations which affect the measuring element are resolved into an angular displacement between the axis of the instrument and the vertical. This angle is measured by a pair of long-period, horizontal pendulums (HAM) which are mounted on the meter case at right angles to each other. A voltage output from each HAM, which is proportional to the acceleration component sensed by it, is averaged and converted to a shaft rotation which is continuously added to the measuring screw.

Since the LaCoste & Romberg instrument measures only differences in gravity and not the absolute value, a survey must begin from a point where the value of $g$ is established. In the case of marine surveys, this value is determined by making a connection with a portable land gravity meter between the pier and a gravity reference station. Such connections are made, where possible, each time the ship puts into port.

The difference between the gravity value determined by the land connection and the value determined by static observation with the sea meter (based on the previous port connection) is considered to be caused by instrument drift. To correct observations taken during the cruise, the drift is assumed to be time-linear. IIOE port connections were made at Honolulu, Manila, Singapore, Calcutta, Colombo, Djakarta, Palau, Guam, and again at Honolulu.

*Reduction of data.* Raw gravity values measured on a moving platform must be corrected for the component of the platform's motion which adds to or subtracts from the east-west velocity of the Earth's rotation. This correction, known as the *Eötvös correction*, is given approximately by EC, mgal$= 7.5 \cdot \cos \phi \cdot s \cdot \sin a$ where $\phi$ is the latitude of the observation, $s$, the ship's speed in knots, and $a$, the ship's heading (1 mgal$=1\times10^{-3}$ cm/sec/sec). The correction is positive if the ship is heading east and negative if the ship is heading west.

Gravity values may be reported as *observed gravity*, corrected for Eötvös effect and drift, or *free-air anomaly*, which is the difference between

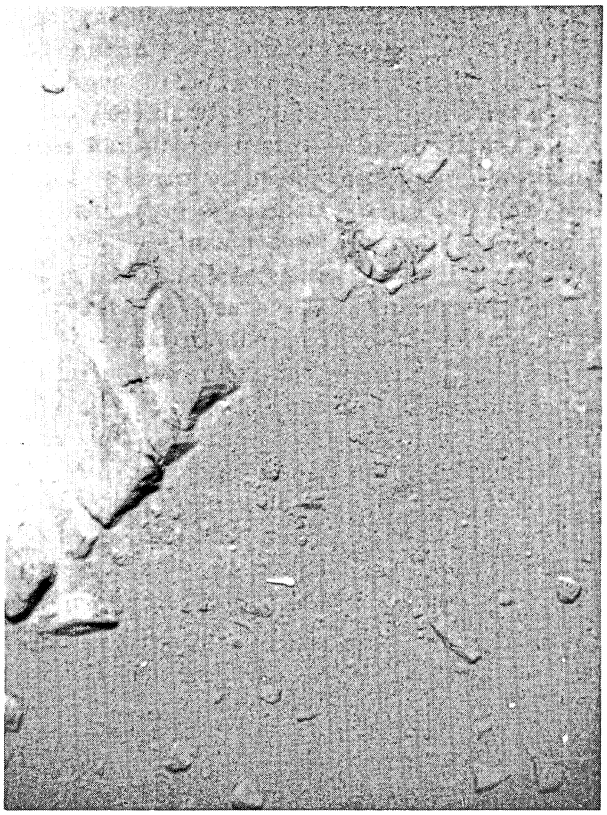

a

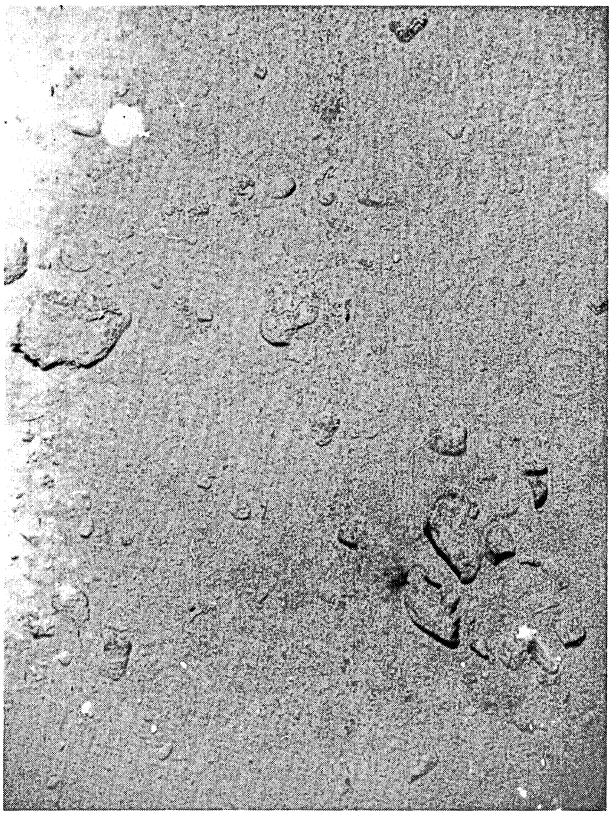

b

c

FIGURE 63.—Camera lowering number 9 in Mindanao Trench. Depth at which photographs were taken was approximately 7,000 meters. (a) Outcrop of angular jointed rock. (b) Worm burrows, loose rocks, and brittle star at upper left. (c) Loose stone and gravel-like appearance may be due to current.

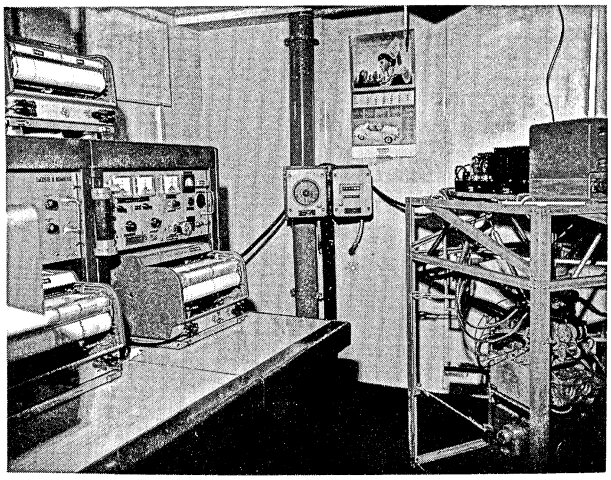

FIGURE 64.—Shipborne gravity meter and recording units.

the observed gravity value reduced to sea level, and the "normal", or theoretical gravity, which would be produced by a homogeneous ellipsoid of revolution of a given equatorial radius and flattening. The *Pioneer* data were reduced using the parameters of the 1930 International Ellipsoid. The free-air anomoly may be further reduced by applying the *simple Bouguer correction* which in the case of marine data is computed by assuming that the distance between the ocean floor and sea level is filled with material of a given density, extending infinitely in all directions.

*Accuracy of data.* Static readings with the LaCoste & Romberg Air-Sea Gravity Meter are accurate to at least ±0.5 mgal. Underway measurements, however, involve uncertainties in navigational control as well as in compensation for sea accelerations. At the present time, the best accuracy expected from marine gravity surveys is about ±5 mgal; the estimated mean probable error in the *Pioneer* IIOE gravity measurements is ±12–15 mgal.

As shown by the formula for the Eötvös correction, marine gravity data are especially sensitive to variations in ship's course and speed. An error of 2 knots in speed on a 090° heading in the Indian Ocean would, for example, result in a 12–15 mgal error in the corrected observed gravity value. Since course and speed cannot be determined accurately during steering maneuvers, bathythermograph casts, and biological casts, gravity data collected during these activities were not processed.

The effects of sea state on the accuracy of the gravity value depends on the time lag selected for the average beam position, period and damping of the HAM pendulums, "overloading" of the HAM correction circuits, and the presence of long-period swells which are not effectively filtered out or compensated. Under certain circumstances, sea conditions may cause systematic errors on the order of 30–150 mgal. Generally, instrument performance was satisfactory under sea conditions up through Beaufort scale 4, and marginal in scale 5 and scale 6 conditions; the meter was shut down when heavier seas were encountered.

*Results.* The sea gravity meter was operational approximately 80 percent of the survey time during *Pioneer*'s Indian Ocean cruises. This represents a total of about 26,000 nm of trackline. The reduced gravity values and magnetics data, taken at 5-minute intervals, will be tabulated in another volume of this series. Part of the data in the Andaman Sea area have been utilized in a geological study by Peter, Weeks, and Burns, pages 91 to 107.

## Magnetics

Marine magnetic measurements, made by ships at sea, are used in the compilation of magnetic charts and in geophysical studies of the earth's crust. Magnetic charts must be revised periodically because of slow changes which continually take place in the earth's magnetic field. Data for this purpose are received from magnetic observatories all over the world, but an accurate representation of the global magnetic field requires that observations also be obtained in oceanic areas. Detailed analysis of the underlying structural characteristics of the earth's crust in oceanic areas also depends in part upon magnetic-survey traverses in the area of investigation.

*The earth's magnetic field.* The magnetic field surrounding the earth is a vector field, having direction as well as magnitude. At any point, it can be fully described by giving its direction and magnitude or by resolving it into three mutually perpendicular components. The main features of the earth's magnetic field show total field intensities—the length of the magnetic vector—ranging from 0.25 gauss near the geomagnetic equator, where the total intensity vector is horizontal, to 0.6 gauss near the magnetic poles, where the total intensity vector is vertical (1 gauss = $1g^{1/2}\ cm^{-1/2}\ sec^{-1}$; 0.25 gauss = 25,000 gammas). Since the magnetic field of the earth is not a simple dipole field, there are regional discrepancies from the

main centered dipole field by as much as 0.13 gauss. Deviations from the dipole field, or from the smooth true magnetic field, are called magnetic anomalies. It is generally agreed that the large regional characteristics of the earth's magnetic field are caused by sources within the core of the earth, and that the local anomalies are caused by lithological structures within the crust.

Slow changes in the magnetic field, called secular variations, and the cumulative effect of these variations after a few years make it necessary to revise the magnetic charts. In addition to these slow changes, there are many variations of shorter period. These are associated with the seasons, lunar periods, rotation of the earth on its axis, and with flares and other disturbances on the sun. Magnetic data, obtained on survey ships, are usually checked against the effect of these time variations of the magnetic field. The world charts display only the large regional characteristics in the earth's magnetic field. The smaller localized anomalies, up to a few hundred miles in extent, are suppressed. For the study of the geological structure of the ocean floor, however, these local anomalies must be investigated. The most important causes of local anomalies are: Change of magnetic mineral content in the underlying rocks, change of the direction of magnetization, and structural displacement and faulting of igneous rocks which contain magnetic minerals. These changes in the crust may cause anomalies as large as 2,000 gammas. The instrument sensitivity of the marine magnetometer is $\pm$ 1 gamma.

*Principles of the marine magnetometer.* The marine magnetometer (Varian model V–4931) measures the total strength (intensity) of the magnetic field. In the measurement of the magnetic field strength, use is made of the effect of the magnetic field on the spinning proton, which forms the nucleus of the hydrogen atom. The spinning proton of the hydrogen atom, like the spin of a charged particle, forms a magnetic dipole similar to a tiny permanent magnet. An external field exerts a torque on the proton and tends to align its axis parallel to the external field. However, the mass of the spinning proton gives it the character of a gyroscope. Torque on a gyroscope causes its axis to tilt or precess in a plane perpendicular to the force which causes the torque. The rate of precession is directly proportional to the magnitude of the external force. This principle is utilized by the marine magnetometer. The sensing element or fish, which is towed 500 feet astern to avoid the magnetic effect of the ship, contains a coil immersed in kerosene (fig. 65). A direct current is sent through the coil which creates a large magnetic field and aligns the protons in the direction of the axis of the coil. After approximately 3 seconds, the (polarizing) current is turned off and the protons begin to precess in step with each other under the influence of the earth's magnetic field. The precessing protons, like an oscillating magnet in a coil, induce an alternating current in the coil. This current passes through the towing cable and enters the shipboard system where it is amplified and its frequency is counted and converted to the magnetic field value in gammas. The $H=23.4874(f)$ equation, where $H$ is the total magnetic field and $f$ the proton precession frequently, represents the relationship be-

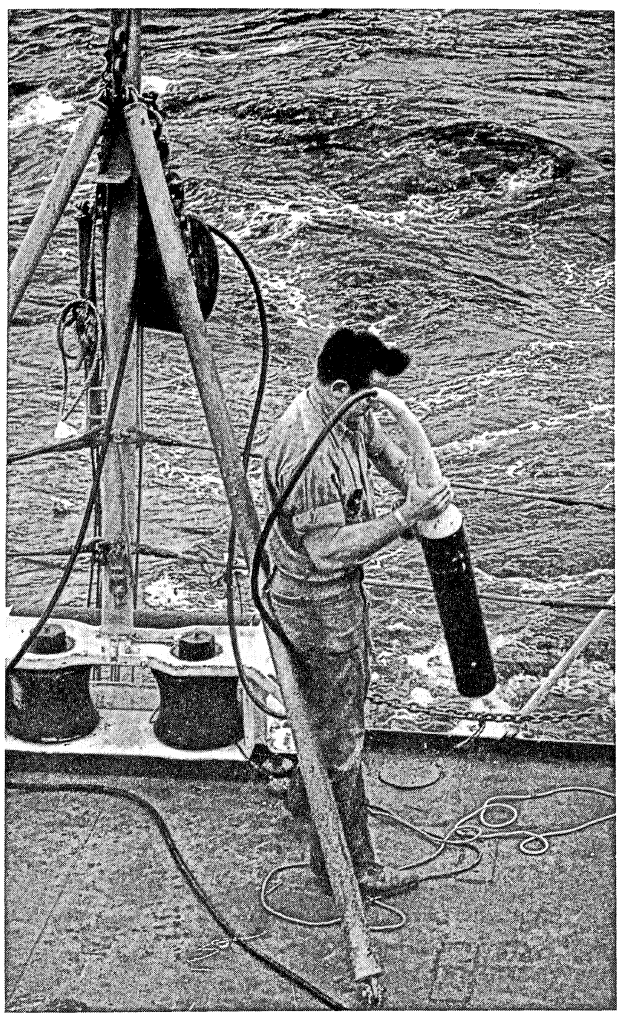

FIGURE 65.—Sensing element or fish of the towed marine magnetometer.

tween the two parameters. Because collisions between atoms in the kerosene tend to disrupt the phase and the spin-axis orientation of the protons, the kerosene is polarized every 6 seconds for 3 seconds. Thus the sampling of the magnetic field strength may be obtained at 6-second intervals

The principal outputs of the marine magnetometer are a strip-chart record of the magnetic field strength variations (100 gamma or 1,000 gamma full scale) and a digital printout strip of the total field strength; both are sampled once every minute. In addition, the gravity meter output values, the time (GMT), date, and the total magnetic field strength in gammas are all recorded every minute on a punched paper tape.

*Results.* The magnetometer was operational approximately 92 percent of the total underway time during the expedition. A total length of 29,112 nm of magnetic survey was obtained. Although the instrument accuracy was ±1 gamma, the measurements were affected by diurnal variations which may have been as large as 35 gammas in parts of the survey area. Because the diurnal variations are different from one area to another, records from nearby magnetic observatories must be used to correct the observed shipboard data. In case of a single trackline or a reconnaissance survey, the diurnal effect of the magnetic field may be neglected in the geological interpretation because its period is much larger than the observational period of the crustal anomalies.

Marine magnetic data, together with other geophysical information, have been used to study the geological structure of the Andaman Sea region. Results of this study, by G. Peter, L. A. Weeks, and R. E. Burns, appear on pages 91 to 107.

## Geophysical Profile Sections

Four profile sections showing bathymetry, magnetics, and gravity were plotted along the *Pioneer* tracklines in the Bay of Bengal and Indian Ocean. The locations of the profiles A–A′, B–B′, C–C′, and D–D′, are shown in figure 66. Depths of the sea floor are given in fms, free-air gravity anomalies in mgal based on the International Gravity Formula, and total intensity of the earth's magnetic field in gammas.

Section A–A′ (fig. 67) was observed in the northern part of the Bay of Bengal in the vicinity of the Ganges Canyon, 20°55.9′N, 88°36.2′E, to the Preparis Channel at 14°29.8′N,94°51.8′E. The magnetic profile reflects the regional magnetic gradient of approximately 2,270 gammas for the interval of 15° to 21°N. The zone, 19°52.0′N, 89°22.8′E to 18°44.8′N, 90°15.8′E, beginning just off the Ganges Shelf, is topographically a smooth easterly slope with a depth range of 730 to 1,020 fms. It is marked by a broad gravity anomaly of −56 mgal and a broad negative magnetic anomaly of 80 gammas. At 17°32.4′N, 91°09.8′E, in a zone of flat topography of 1,220 fms depth, a gravity high of +9 mgal is associated with a minor magnetic low.

In the vicinity of the "Ninety-east Ridge," between 17°19.6′N, 91°19.7′E, and 15°09.6′N, 93°03.2′E, the ocean bottom continues to slope moderately eastward within a depth range of 1,225 to 1,495 fms, the gravity field is smooth with increasing negative values eastward, and the irregular magnetic field has a maximum displacement of 120 gammas.

Section B–B′ (fig. 68) extends from a point off the east coast of Ceylon (08°29.8′N, 81°43.7′E) to a point off the west coast of Little Andaman Island (10°37.6′N, 92°14.3′E). Section C–C′ (fig. 69) extends between 04°59.7′N, 87°56.5′E and a point off northwestern Sumatra at 06°06.1′N, 94°59.3′E. Section D–D′ (fig. 70) extends from position 05°06.0′S, 92°10.5′E across the northern limit of the Java Trench to the Sunda Strait at 05°51.4′S, 106°42.1′E. Table 17 is a tabular summary of the geophysical relationships observed along sections B–B′, C–C′, and D–D′.

## Geological Echo Profiling

The Coast and Geodetic Survey's Geological Echo Profiler (GEP) was used on numerous occasions to obtain a continuous seismic reflection record of the subbottom geologic structure. This device utilizes a towed sound source (sparker) to generate low-frequency signals. The signals travel to the ocean bottom, penetrate the sediment and underlying rock, and are reflected from the surfaces or interfaces that separate materials of varying acoustic properties (impedance). The reflected signals are detected by a hydrophone array towed from the ship and registered on one or more recording devices aboard the vessel.

During the *Pioneer* operations, the receiving unit (hydrophone array) was connected to a

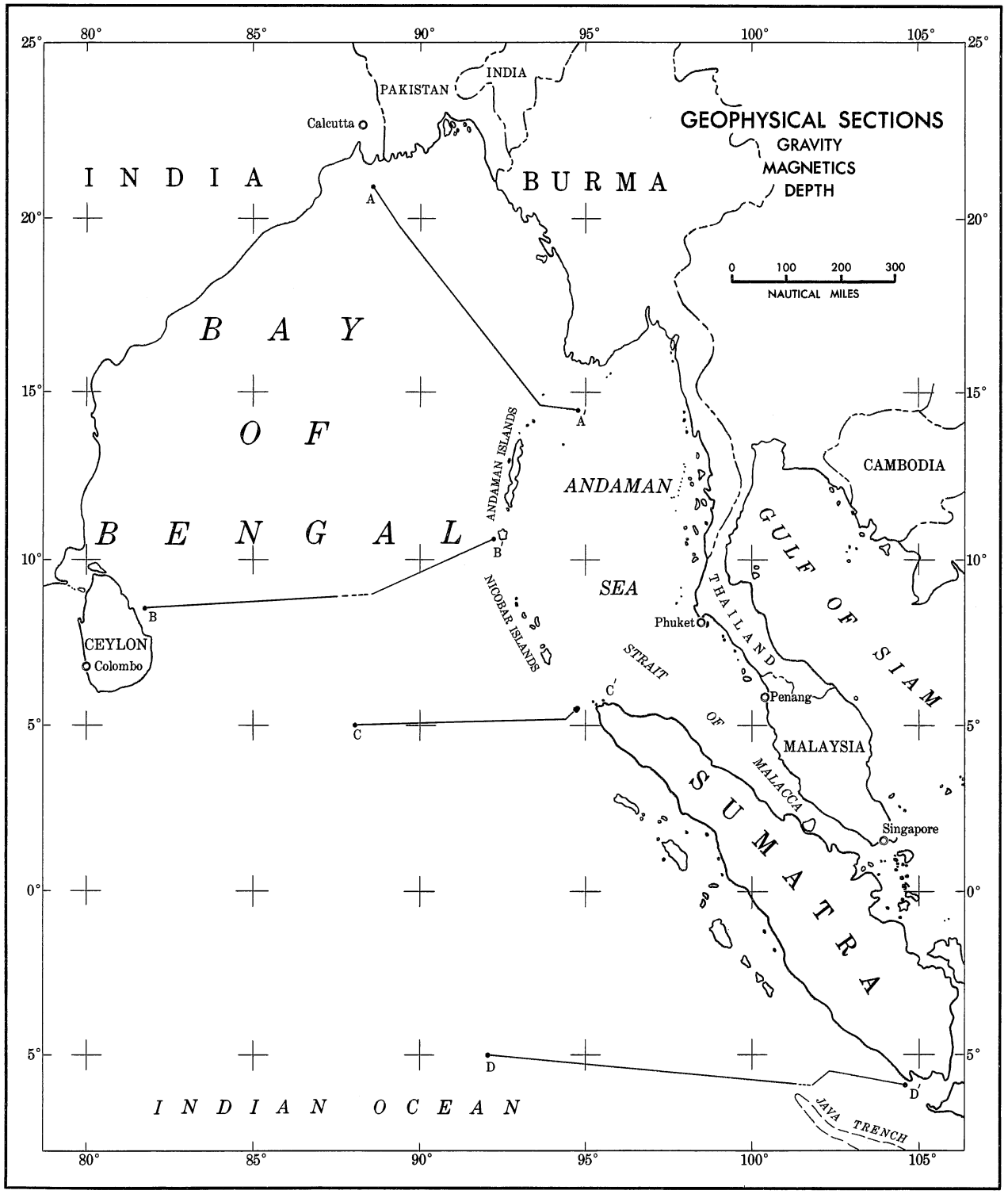


FIGURE 66.—Location of geophysical profile sections in Andaman Sea, Bay of Bengal, and northeast Indian Ocean.

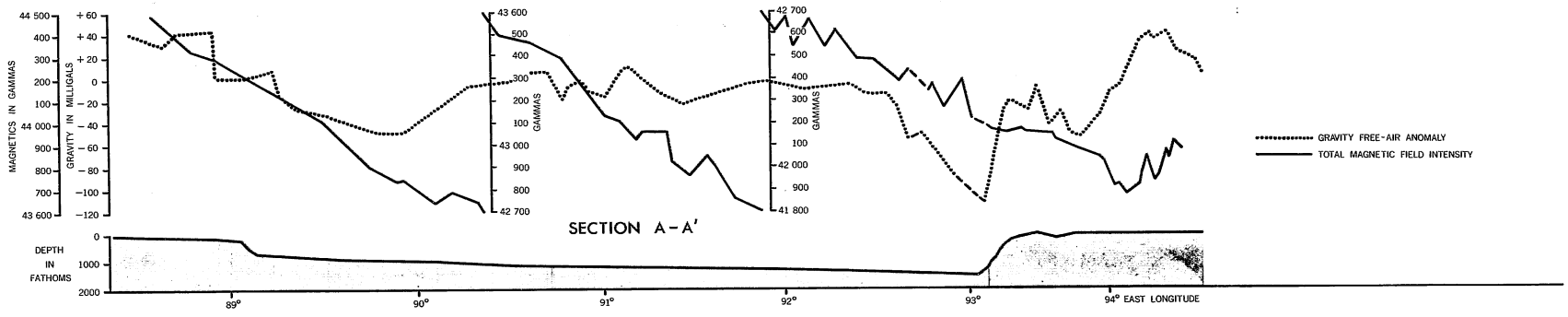


FIGURE 67.—Geophysical profile section A–A'.

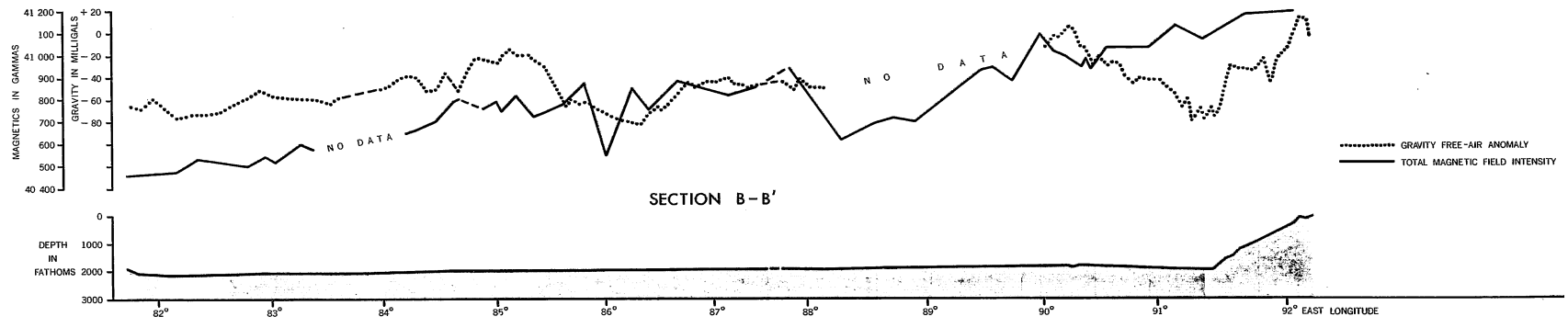


FIGURE 68.—Geophysical profile section B–B'.

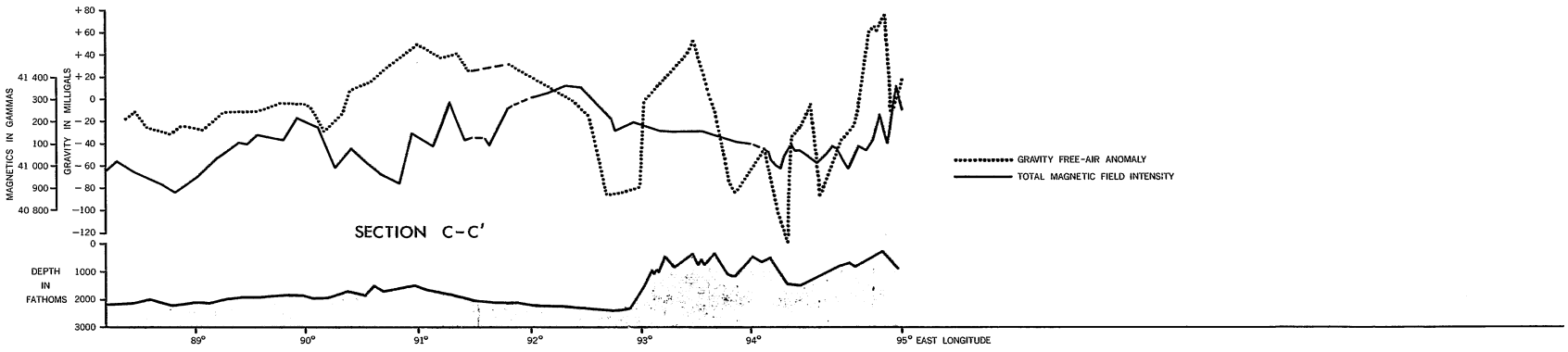


FIGURE 69.—Geophysical profile section C–C'.

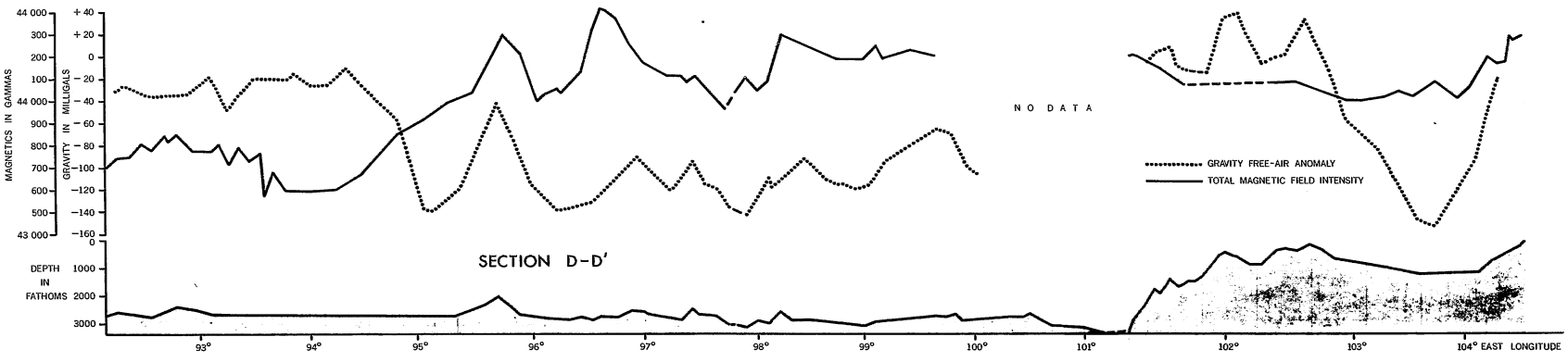


FIGURE 70.—Geophysical profile section D–D'.

TABLE 17.—*Summary of geophysical data along selected profile sections in Andaman Sea, Bay of Bengal, and northeast Indian Ocean*

| Position | Bathymetry (depth in fathoms) | Magnetics (total intensity in gammas) | Gravity (free-air anomaly in milligals) |
|---|---|---|---|
| *Section B–B'* | | | |
| 08°30.9'N 82°08.7'E | 2,075 (Ceylon slope) | ---------- | −73* |
| 08°53.3'N 85°07.8'E | 2,005 | 40, 778 | −15 (high) |
| 08°55.8'N 86°01.0'E | 1,975 | 40,550 (low) | −72* |
| 08°57.7'N 86°19.5'E | 1,980 | 40,809 | −83 (low) |
| 08°57.3'N 88°18.4'E | 1,930 | 40,615 (low) | ---------- |
| 09°44.1'N 90°12.0'E | 1,810 (high, Ninety-east Ridge) | 41,110 (minor high) | +7 (high) |
| 10°10.0'N 91°11.2'E | 1,905 | 41,128 | −80 (low) |
| 10°12.9'N 91°17.8'E | 1,930 (low) | 41,068 | −76 |
| *Section C–C'* | | | |
| 05°00.8'N 88°47.2'E | 2,200 | 40,878 | −30 |
| 05°02.0'N 89°58.2'E | 1,830 | 41,216 | ±0 |
| 05°02.2'N 90°06.8'E | 1,955 | 41,076 | −30 (low) |
| 05°02.7'N 90°39.7'E | 1,505 (high, Ninety-east Ridge) | 40,964 | −23* |
| 05°02.8'N 90°48.3'E | 1,715 | 40,920 | +35* |
| 05°03.1'N 91°01.2'E | 1,460 (high, Ninety-east Ridge) | 41,065 | +49 (high) |
| 05°03.7'N 91°22.3'E | 1,950 | 41,296 | +40 |
| 05°06.0'N 92°19.6'E | 2,255 | 41,363 (high) | ±0 |
| 05°01.8'N 92°50.8'E | 2,405 (low) | 41,207 (high) | −86 (low) |
| *Section D–D'* | | | |
| 05°17.0'S 93°54.7'E | 2,740 | 43,580 | −20* |
| 05°24.5'S 95°07.4'E | 2,735 | 43,950 | −140 (low) |
| 05°28.2'S 95°42.2'E | 1,250 (high) | 44,290 | −42 (low) |
| 05°30.2'S 96°01.5'E | 2,760 | 43,990 (low) | −118* |
| 05°31.6'S 96°14.4'E | 2,885 | 44,043 | −140 (low) |
| 05°33.2'S 96°37.9'E | 2,750 | 44,415 (high) | −128* |
| 05°36.0'S 96°54.5'E | 2,355 (high) | 44,248 | −92 (high) |

* Indicates interpolated value.

TABLE 17.—*Summary of geophysical data along selected profile sections in Andaman Sea, Bay of Bengal, and northeast Indian Ocean*—Continued

| Position | Bathymetry (depth in fathoms) | Magnetics (total intensity in gammas) | Gravity (free-air anomaly in milligals) |
|---|---|---|---|
| *Section D–D'* | | | |
| 05°40.0'S 97°56.1'E | 3,140 (low) | 43,955 (low) | −144 (low) |
| 05°41.6'S 98°14.4'E | 2,570 (high) | 44,295 (high) | −120* |
| 05°42.8'S 98°28.1'E | 2,830 | 44,233 | −94 (high) |

*Indicates interpolated value.

Rayflex vertical-feed paper recorder and to a sound-tape recorder (fig. 71). The paper recorder provided the graphic trace or profile of the subbottom structure; the sound-tape recorder was a back-up system for recording the initial and reflected sound signals, the time intervals, and position fixes. To minimize ship noise and water turbulence, both the sparker unit and hydrophone array were towed 300 ft aft of the *Pioneer* from 16-ft booms extending from opposite sides of the ship. The speed of the vessel was reduced to 5 knots during geological echo profiling operations.

A 10-kilowatt generator was used to supply electrical power to capacitor banks. Twenty thousand joules of energy were discharged every 4 seconds through two No. 19 electrical cables. The positive and negative terminals of the cables were towed in contact with the sea. By this means, a spark or arc of explosive nature was produced between the submerged cable terminals, which in turn generated underwater sound waves in the low-frequency range of 90 to 120 cycles per second.

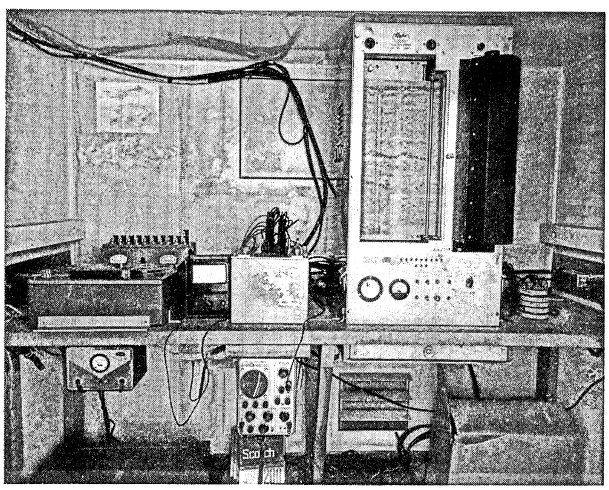

FIGURE 71.—Geological Echo Profiler recording equipment. Sound-tape recorder on left and vertical-feed paper recording on right.

The hydrophone array consisted of 20 hydrophones, each with its own preamplifier and rechargeable cadmium sulfide battery. Each hydrophone had two terminals connected to the amplifier junction box so that any number of combinations of the hydrophones could be used. The array also was enclosed in a 340-ft plastic tube filled with diesel oil to provide neutral buoyancy and minimize water noise. To minimize ship noise further, the hydrophones were placed 15 ft apart (approximately quarter wavelength). Such an array is more sensitive to sound waves reflected from the ocean bottom than it is to the sound waves traveling parallel to the array axis (ship noise). Position fixes were marked on the graphic record and repeated orally for recording on the sound-tape record. The number assigned to each fix and the Greenwich time were recorded in a log book.

The Geological Echo Profiler proved to be a valuable tool in the geophysical investigations, especially in the Andaman Sea area where the underlying rocks are buried by great thicknesses of sediments. The results of subbottom profiling in this area, together with an interpretative analysis of the GEP data and related geological and geophysical data, are described in the papers at the end of this section by Peter, Weeks, and Burns (pages 91 to 107) and by Weeks, Harbison, and Peter (pages 109 to 118). During the expedition, approximately 1,000 nm of subbottom profiling

were accomplished. In addition to the profiles in the Andaman Sea, GEP surveys were conducted in the northern Bay of Bengal, off Ceylon, off Sumatra, and around the islands of Palau and Guam in the western Pacific Ocean (see papers by Stewart, Dietz, and Shepard, pages 77 to 79, and by Corwin and Tracey, pages 81 to 90).

## Heat-Flow Measurements

During the *Pionner*'s geophysical investigations in the Andaman Sea, the thermoprobe (fig. 72) was used at selected sites to obtain a record of the temperature gradient in the bottom sediment and to secure a core sample of the sediment from which its coefficient of thermal conductivity could be measured. From the combined data, the heat flux of the ocean bottom was computed. The amount of heat flowing from the earth's interior outward through the surface layers has an important bearing upon many geological and geophysical problems. Answers to some of these problems are being sought by the correlation of heat-flow measurements with observed distributions of gravity and magnetic field strength, rock composition, bottom topography, and subbottom geologic structure. The method used and the results of the heat-flow measurements are described by Dr. Robert E. Burns in the paper "Sea Bottom Heat-Flow Measurements in the Andaman Sea," pages 119 and 120.

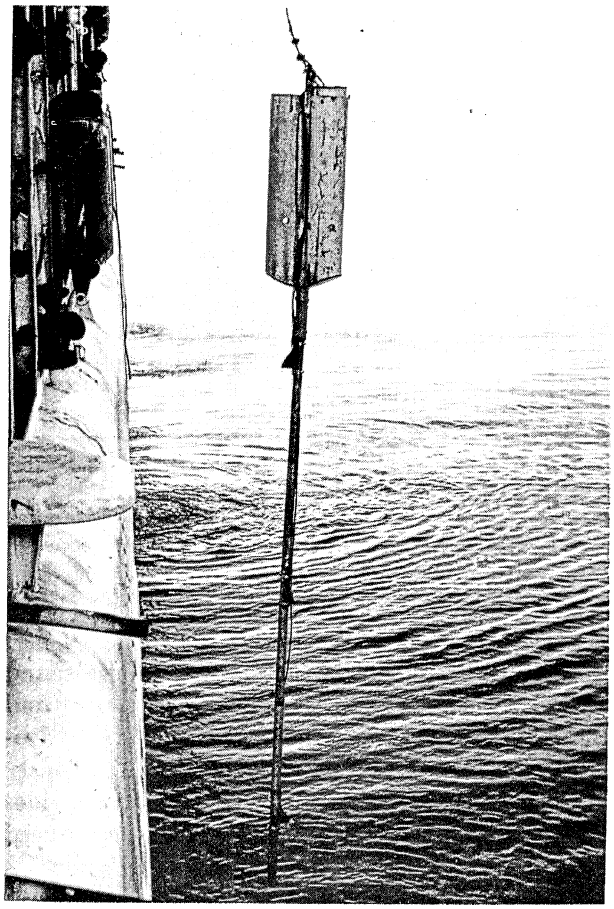

FIGURE 72.—Thermoprobe for measuring temperature in sea floor sediment.

# Submarine Valleys off the Ganges Delta

H. B. Stewart, Jr.,* R. S. Dietz,* and F. P. Shepard†

The Swatch of No Ground, sometimes called the Ganges Submarine Canyon, has been known to exist for many years, and the inner part—well up on the shelf at the head of the Bay of Bengal—has been surveyed in detail by the Pakistan Navy (Hayter, 1960). The *Galathea*, during the Danish Deep-Sea Expedition of 1950–52, made five crossings of the Swatch of No Ground which showed the canyon to extend at least to 19°9′N, some 150 kilometers south of the shelf break (Kilerich, 1958). A crossing of a leveed channel at 5°N by the Swedish vessel *Albatross* in 1948 led Dietz (1953) to suggest that this channel was formed by turbidity currents, possibly originating at the head of the Bay of Bengal, although Koczy (1954) did not agree. The southerly extent of the Swatch of No Ground was not known. Also, evidence to indicate any connection between the leveed channel and the larger canyon feature at the head of the Bay was lacking. To learn more about these features and to determine the relationship, if any, of the leveed channel at 5°N to the Swatch of No Ground, a detailed geological investigation was carried out in the Bay of Bengal.

Results from depth soundings showed that the Swatch of No Ground is a long narrow trough incised in the continental shelf at the head of the Bay of Bengal. It differs from any submarine canyons in that it has no major tributaries and is generally U-shaped in cross section rather than having the V-shape of typical canyons. In addition, the trough does not extend directly down the shelf normal to the slope, but crosses the slope at an angle of 45°, trending NE–SW. The floor of the trough is as much as 800 meters below the surrounding shelf surface and averages 15 km in width. A sparker—continuous seismic-reflection, or GEP—profile (fig. 73[1]) across the trough at 55 km below its head suggested the possibility that the Swatch of No Ground is bounded by faults on both sides. If this is the case, then the trough is a graben or a faultline valley. Faulting is common in the Bengal Basin to the north, and the nearest known fault trace, at Khulna, some 120 km due north (Morgan and McIntire, 1956), is parallel to the trend of the Swatch of No Ground. A fault origin for this feature provides a logical explanation for its NE–SW trend of 45° to the slope. It also accounts for the U-shape of the trough and the lack of tributaries. However, the sparker profiles also can be interpreted as showing deep valley fill subsequent to the original formation of the trough. This is a second possible interpretation. Both views should be retained until more information is available.

Delta-building, turbidity current flow, and submarine slumping also may play an important role in accounting for the observed features of the trough. Two other known troughs of this type occur off major deltas, namely, those of the Indus and Mississippi Rivers. It is probable that the trough results in part from the action of turbidity currents along a fault valley. The sparker (GEP) profile taken 55 km below the head of the canyon showed that the sediment layers on the northwestern side of the trough dip toward the trough as they near the edge of the northwest canyon wall. Similar sedimentary characteristics have been described as occurring at the edges of the Hudson Canyon (Ewing et al., 1960). This evidence supports the view of Shepard (1934) that the present relief of submarine canyons is attributable in part to the accumulation of sediments along their flanks, subsequent to formation of the original feature.

The sparker profile also indicated considerable fill within the trough. A core sample taken in the center of the trough at a depth of 513 m had fine silt in its surface layer underlain by fine to medium sand. A dredge haul on the steep northwest wall of the canyon contained stiff, blue-green clay. In following the profile features of the canyon to the south, the general U-shaped cross section gave way to a series of terraces usually along only one side (fig. 74[2]). These steplike features, however, could not be correlated on adjacent profiles. Neither the depth of the steps nor their number could be satisfactorily related. This suggests that the apparent terrace features more probably are

*Institute for Oceanography, U.S. Environmental Science Services Administration.
†Scripps Institution of Oceanography, La Jolla, Calif.

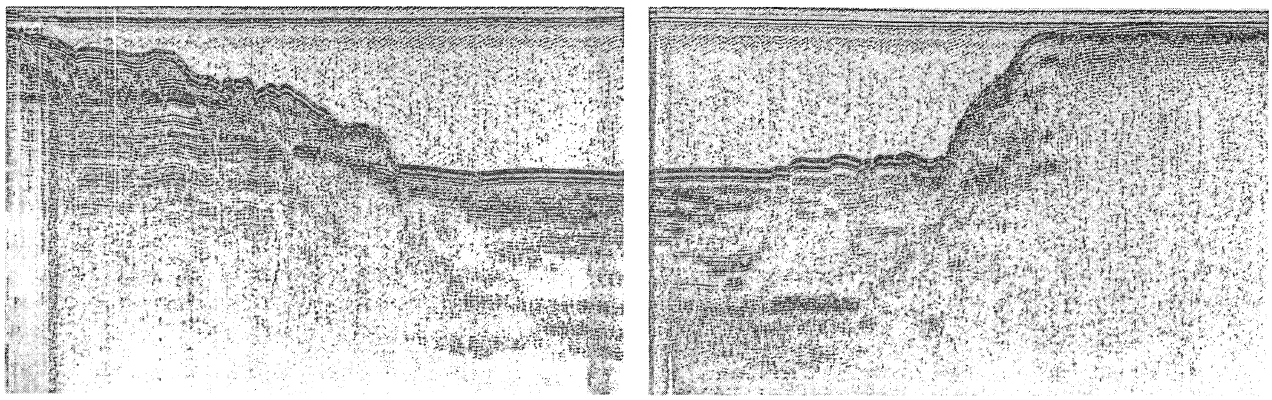

FIGURE 73[1].—Continuous seismic-reflection profile across Swatch of No Ground at 55 km below the head of the canyon.

slump blocks. This conclusion also is borne out by three additional sparker profiles which show sharp structural discontinuities associated with the apparent terraces.

Farther south from the head of the canyon the width becomes narrower and the relief less until broad natural levees are found along both sides

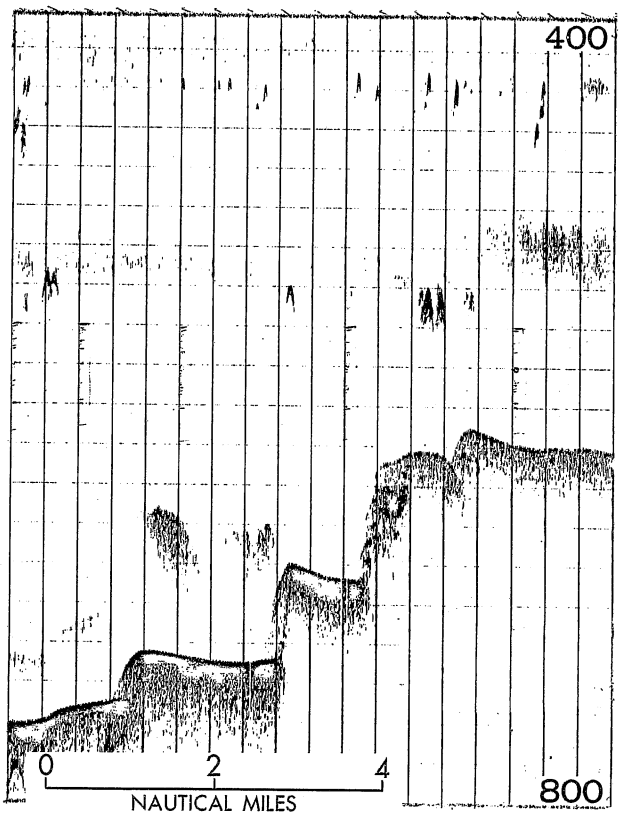


FIGURE 74[2].—PDR record showing steplike terraces of Swatch of No Ground.

(fig. 75[3]). At a distance of 155 km, the depth of the trough axis was 1,500 m and the break or edge of the canyon walls, 1,190 m. Over the next 220 km, 17 crossings were made. The relief indicated by successive profile sections at these points became further subdued until all that remained was a leveed channel or valley, similar to those found on broad fans seaward of many submarine canyons. A core sample from the axis of this leveed fan valley, at a depth of 1,757 m, contained fine sand in its lower portion and silty clay in its surface layer. A core from the top of the adjacent levee, at a depth of 1,565 m, consisted of 5.5 m of silty clay. At 430 km from the head of the canyon, the fan valley turned eastward and a similar valley was observed nearby. The ship's trackline was changed to a large box pattern to follow this second channel. It was found to be a bifurcation of the main channel, and from this point southward, the number of fan valleys increased and their pattern became increasingly complex. A detailed survey of a small area of this sea floor indicated that some of the valleys coalesced to form single valleys farther downslope. At a distance of 450 km, the pattern of fan valleys was so complex that a very detailed survey along closely spaced and accurately positioned tracklines would have been required to trace the pattern southward across the gently sloping floor of the Bay of Bengal. However, a long profile section across the Bay, at about 9°N and approximately 1,300 km south of the head of the Swatch of No Ground, showed many leveed channels (fig. 76[4]). These varied considerably in

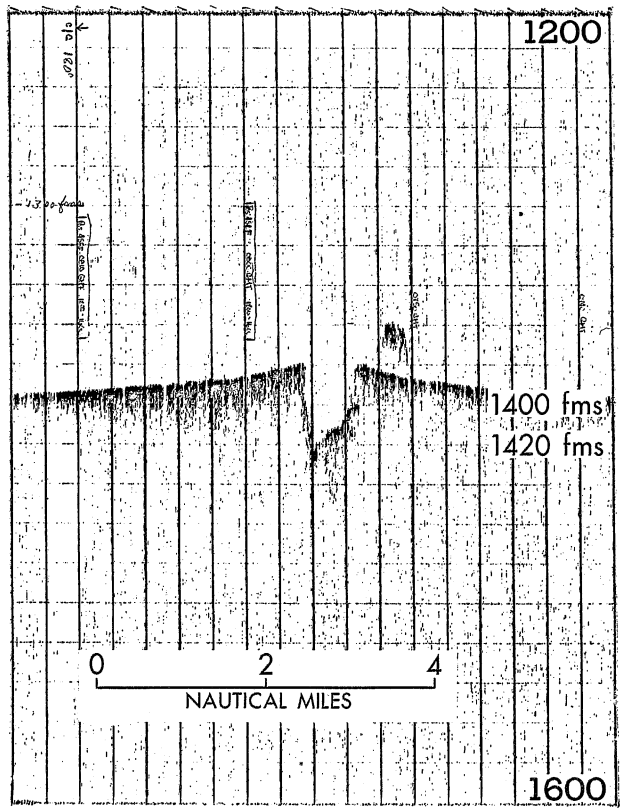


FIGURE 75[3].—PDR record showing broad natural levees along southern reaches of Swatch of No Ground.

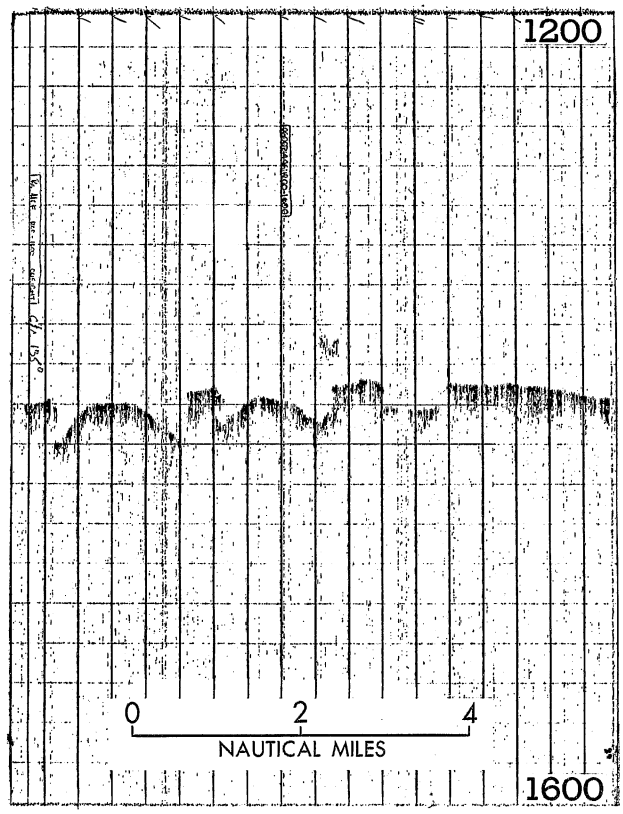


FIGURE 76[4].—PDR record showing leveed channels near southern limits of Swatch of No Ground.

size and shape, ranging from 10 to 80 m in depth and up to 9 km across. Thus it would seem highly probable that the leveed channel, plotted 440 km farther to the south during the cruise of the Swedish ship *Albatross*, is a part of this complex and far-reaching system of fan valleys.

The most logical explanation for the Bay of Bengal fan valleys is that they were formed by the action of turbidity currents. Since the *Pioneer* survey of 1964 was concentrated mainly on the Swatch of No Ground and the system of fan valleys which it apparently feeds, other sources of supposed turbidity currents along the northwest side of the Bay were not investigated. For example, profiles of the outer Trincomalee Canyon off northeast Ceylon show the beginning of what may be a leveed fan valley at a depth of 3,350 m. It is possible that similar features, terminating in fan valleys, will be found once the Bay of Bengal is adequately surveyed. The present survey adequately established the Swatch of No Ground as the principal source of the system of fan valleys observed during this survey.

## REFERENCES


Dietz, R. S., Possible deep-sea turbidity-current channels in the Indian Ocean, *Bull. Geol. Soc. Am.*, vol. 64, pp. 375–378, 1953.

Ewing, J., M. Ewing, and C. Fray, Buried erosional terrace on the edge of the continental shelf east of New Jersey, Abstract of paper, *Bull. Geol. Soc. Am.*, vol. 71, p. 1860, 1960.

Hayter, P. J. D., The Ganges and Indus submarine canyons, *Deep-Sea Research*, vol. 6, pp. 184–186, 1960.

Kilerich, A., The Ganges Submarine Canyon, *Andhra Univ. Memoirs in Oceanography*, Series No. 62, vol. 2, pp. 29–32, 1958.

Koczy, F. F., A survey on deep-sea features taken during the Swedish Deep-Sea Expedition, *Deep-Sea Research*, vol. 1, pp. 176–184, 1954.

Morgan, J. P., and W. G. McIntire, *Quaternary Geology of the Bengal Basin*, Tech. Report No. 9, Coastal Studies Inst., Louisiana State Univ., 1956.

Shepard, F. P., Canyons off the New England coast, *Amer. Jour. Sci.*, vol. 27, pp. 24–36, 1934.

# Marine Geologic Investigations Near the Palau Islands and Guam, Mariana Islands*

GILBERT CORWIN AND JOSHUA I. TRACEY, JR.†

The intersecting arcuate submarine ridges and associated trenches that bound the east and southeast sides of the Philippine Sea are among the most spectacular and puzzling features of the world's oceans (fig. 77[1]). Early explorers noted marked differences between islands that rise from the crests of the ridges and those of the central basins. As knowledge of the islands and submarine topography accumulated, controversy arose over the origin and history of these arcs. In contrast to islands of the basins, many of those on the arcs have been uplifted so that former reef deposits now stand high above sea level. Also, the geologic and tectonic features of these island arcs resemble those of the continental margins rather than those characteristic of the ocean basins in the following ways: The volcanic suites and geologic structures of the islands; the unique occurrence of metamorphic rocks on the Yap Islands; the numerous deep earthquakes of the northern arcs; and, the trenches, including the Challenger and Nero Deeps. Many writers, therefore, have considered the arcs to be the true margin of the Asiatic Continent and have drawn the boundary between the continent and Pacific Basin along the trenches associated with the arcs. However, recent geophysical studies suggest that the earth's crust beneath the Philippine Sea has oceanic characteristics and that continental properties are confined to the arcs themselves. Much additional information is needed to resolve the many problems relating to the origin and history of this portion of the western North Pacific Ocean. This is particularly true for the marine areas where new data is needed to supplement that obtained on land.

The U.S. Geological Survey mapped and studied the geology, soils, and mineral resources of islands on the Mariana, Yap, and Palau Arcs and the Eastern Caroline Swell for the U.S. Army Corps of Engineers between 1947 and 1957. Geologic maps and preliminary results of these investigations were published by the Corps of Engineers (Cloud et al., 1955; Corwin et al., 1957; Doan et al., 1960; Johnson et al., 1960; Mason et al., 1956; Stark et al., 1958; Tracey et al., 1959). Laboratory and office investigations and syntheses are continuing, and the results are being published in journals and by the Geological Survey.

## PALAU ISLANDS AREA

The Palau Ridge and associated Palau Trench constitute the southern and westernmost arc. The ridge can be traced northward from the Palau Islands through the Philippine Sea nearly to Kyushu, Japan; Parece Vela reef near the center of the Philippine Sea rises from the crest of the ridge (fig. 77[1]). South of the Palau Islands, the ridge trends southwestward and westward toward Halmahera, Indonesia. The associated Palau Trench on the southeast convex side of the ridge is distinct and well developed from Helen Reef, southwest of the Palau Islands, to the northern end of the Palau Islands where it ends abruptly. The deepest part of the trench lies between the north end of Babelthuap, the largest of the Palau Islands, and the west end of the intersecting Yap Arc. Unlike most other arcs of the circumpacific region, the Palau Arc has no known active volcanoes, no reports of associated major earthquake loci along it, and no other evidence of present structural activity.

A broad, actively growing coral reef, partly fringing but mostly barrier, encloses most of the Palau Islands. The small limestone island of Anguar to the south and two small low atolls, Kayangel and Ngaruangel to the north, are separated from the remainder of the island group by channels (fig. 78[2]).

Within the main Palau reef, the islands are of two types: The northern islands are composed chiefly of early Tertiary volcanic deposits, and the

*Publication of this report is authorized by the Director, U.S. Geological Survey, Washington, D.C.

†The authors are the geologists in charge of the U.S. Geological Survey's studies of the Palau and northern Mariana Islands area, and Guam, respectively. Both scientists boarded the *Pioneer* at Palau on July 11, 1964, and debarked at Guam on July 16, 1964, after the special marine geological investigations were completed.

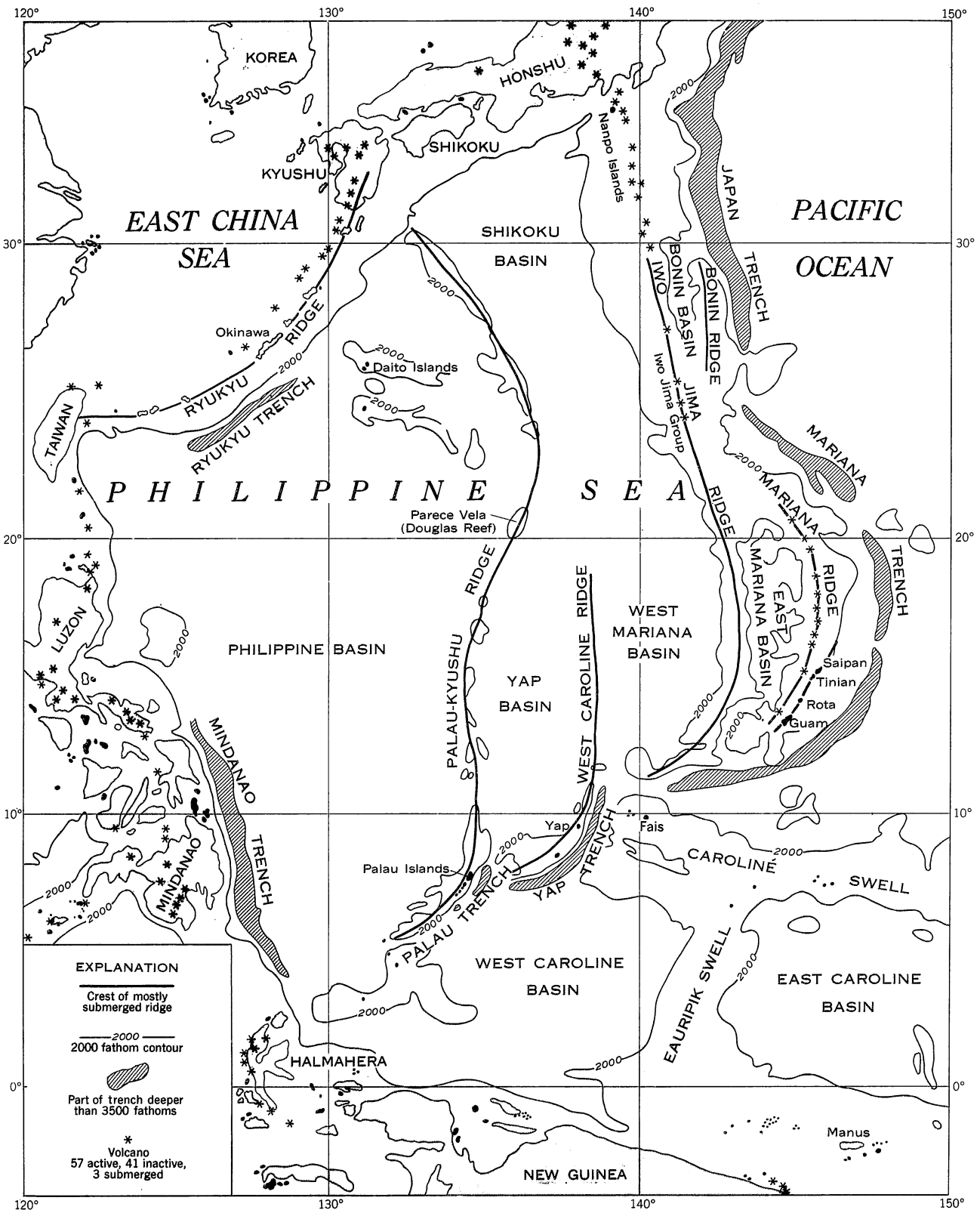


FIGURE 77[1].—Regional relations in the western North Pacific Ocean. After: Hess, 1948, pl. 1; and, Cloud, Schmidt, and Burke, 1956, fig. 2.

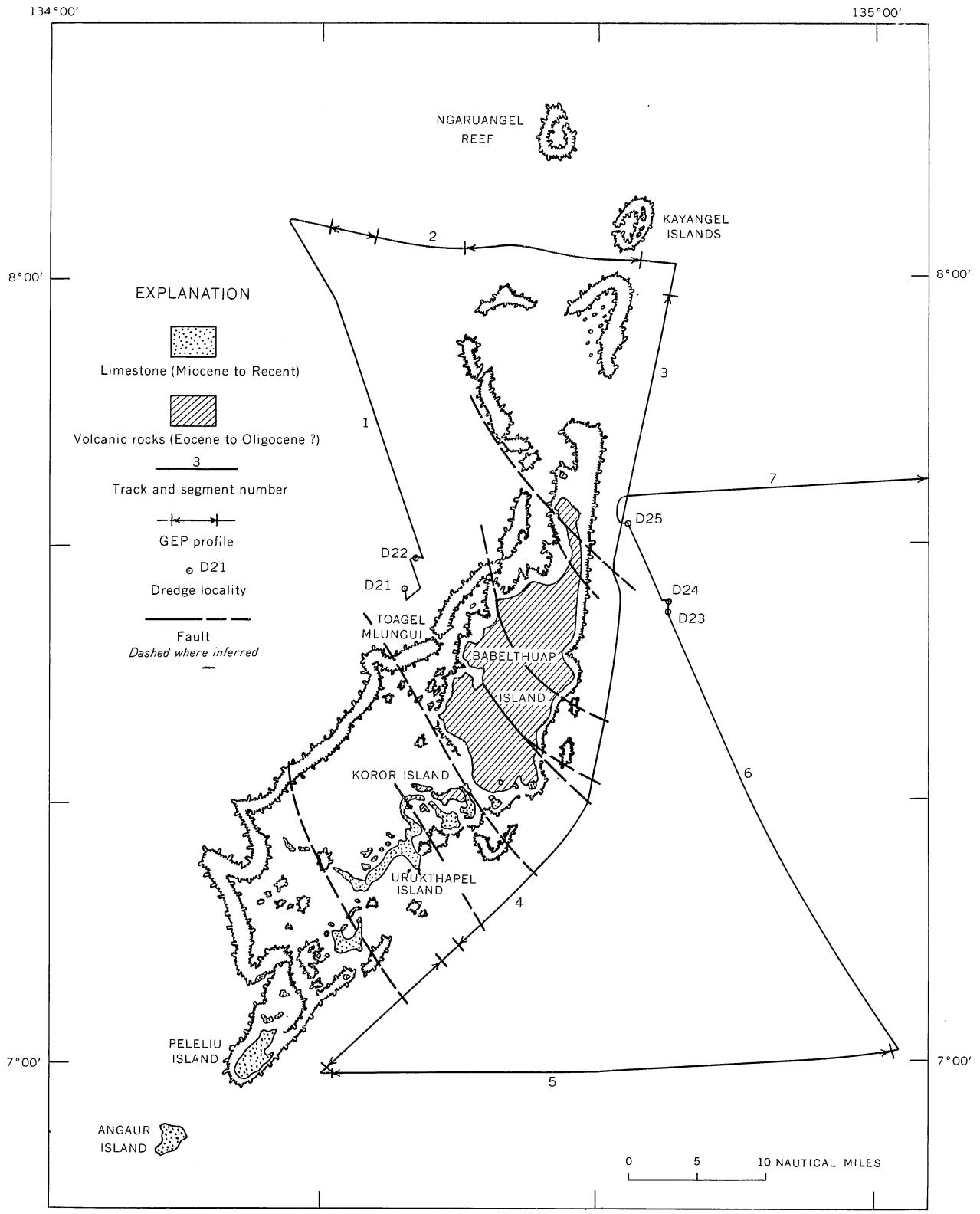


FIGURE 78[2].—Palau Islands and vicinity showing 1964 geophysical trackline of USC&GS ship *Pioneer* and dredge localities. The inferred faults connect the observed topographic features of the trackline with selected major faults of Babelthuap (Mason et al., 1956, pl. 1) and postulated faults to the south.

southern ones are high limestone islands. High ridges of limestone overlie volcanic deposits at the south end of Babelthuap, on Koror and Auluptagel, and on some small islands near the center of the island group. No raised limestones are found north of the southern end of Babelthuap, and no volcanic rocks are exposed south of Malakal Harbor.

The exposed volcanic rocks are predominately pyroclastic deposits which have been separated into three major formations (Mason et al., 1956). The two older formations are marine deposits. These apparently were erupted from a large vent located near the west-central coast of Babelthuap, and possibly from a subsidiary vent near the southeast coast; fossils indicate a late Eocene age for these units. The uppermost formation consists largely of unfossiliferous subaerial deposits that were erupted from several vents, mostly located within a presumed caldera in the older formations near the west-central coast of Babelthuap. Since their deposition, the volcanic deposits have been deformed by faulting and deeply weathered and eroded.

At Urukthapel, near the center of the Palau Islands, the limestones rise from below sea level to more than 700 feet above. The highest limestones of Urukthapel are lagoonal deposits of an upper Miocene coral reef (Cole, 1950). These "core" limestones appear to be flanked by younger reef limestones at successively lowered elevations, suggesting intermittent uplift. (Based on his observations in the Palau Islands and the state of knowledge at the time, Carl Semper had good reasons to believe that coral reefs were formed on rising foundations, and to become the chief opponent of Darwin's coral reef theory.) The nature and distribution of these limestones and their relation to the underlying volcanic deposits suggest differential uplift and faulting. The limestones show little deformation; therefore, it is assumed that major faults occupy the channels between the islands.

Objectives of the marine geophysical investigations in the Palau Islands area, as conducted during the USC&GS ship *Pioneer* cruise of 1964, were as follows:

1) to compare the tectonically inactive Palau Arc with active arcs elsewhere;
2) to study the structural trends at the intersection of two major arcs—the Palau and Yap Arcs;
3) to interpret the structural evolution of the Palau Islands;
4) to date the latest volcanic activity in the vicinity of the islands; and,
5) to provide a basis for future marine geological and geophysical work in the Palau Islands area.

To accomplish these objectives, a cruise trackline consisting of seven major segments was followed as shown in figure 78[2]. The program of measurements, observations, and bottom sampling for each segment of this trackline is summarized in table 18[1].

Northwest of West Passage (Toagel Mlungui), bathymetric charts (Hess, 1948; Dietz, 1954) show relatively steep slopes between 500 and 1,500 fms (about 1,000 and 2,500 meters), suggesting the possibilities of a fault scarp and outcrops of older volcanic rocks near its crest. The primary objective of dredge hauls D21 and D22 was to obtain samples that might be used in dating the youngest volcanic rocks of the islands. Although no vol-

TABLE 18[1].—*Summary of records obtained and stations occupied near Palau Islands during 1964 cruise of USC&GS ship* Pioneer

| Geophysical trackline | | Remarks |
|---|---|---|
| Segment | Records obtained [1] | |
| 1 | PDR, G, M: | |
| | D21 | 440–320 fathoms, mud in eyebolts and chain links. |
| | D22 | 650–575 fms, 5 kilogram soft calcareous globigerinid sandstone. |
| 2 | PDR, G, M, GEP. | GEP record discontinuous. |
| 3 | PDR, G, M, GEP. | GEP record poor and discontinuous to northern Babelthuap. |
| 4 | PDR, G, M. GEP. | GEP, 1-nautical mile break in record. |
| 5 | PDR, G, M, GEP. | |
| 6 | PDR, G, M: | |
| | D23 | Mud-silt in eyebolts and chain links. |
| | D24 | No recovery. |
| | D25 | 3 kg limestone with some pebbles and fragments of volcanic rocks. |
| 7 | PDR, G, M. | |

[1] PDR, Precision Depth Recorder; G, Seaborne Gravimeter; M, Towed Magnetometer; GEP, Geological Echo Profiler subbottom record; D21, Dredge Station Number.

canic fragments were recovered, the blocks of impure calcareous silty sand appear to have unusual significance with respect to the late geologic history of the islands and adjacent reefs. The induration and structures of the blocks, numerous borings, manganese encrustations, and abundant clastic grains suggest the possibility of a Pleistocene or older age for the sediment.

The sample from dredge station D22 has been prepared for laboratory study to determine its age, the depth and temperature of water at the time of its deposition, and the nature of the clastic grains. If the material proves to be of Pleistocene age, then results of the other analyses of the sample should have direct application to morphologic studies of the existing Palau reefs and lagoons, and in determining what the climatic and weathering conditions were like at the time when important bauxite deposits of the islands may have formed. At best, studies of the sample will provide only partial answers to these and related questions. More information is needed about the deposits from which the sample was derived, including their distribution, thickness, and geologic relations. Future sampling to provide this information can be accomplished best by grab sampling and coring operations.

Two dredge sites were planned for the steep submarine slopes to the east of northern Babelthuap. Objectives of dredging at these sites were similar to those west of the islands, to obtain samples for dating the youngest volcanic rocks of the islands. Between the two sites, three hauls were attempted—dredge stations D23, D24, and D25. The first two attempts produced no significant recovery, apparently because the bottom was smooth and hard or because it was covered with fine, loose material that was washed from the dredge as it was raised. Small amounts of fine mud were obtained by scraping the chains and eye bolts of the dredge. The third attempt produced about 3 kg of broken limestone, some gravel, and small amounts of white clay. The predominant limestone contained small pebbles and fragments of volcanic rocks, and the gravel contained a few discrete pebbles of tuff and other volcanic rocks.

Unbroken surfaces of the limestone and the volcanic pebbles were coated with manganese oxides as much as 1 millimeter thick. The limestone is an impure, porous, medium-grained, detrital deposit composed of skeletal fragments and molds with few identifiable fossils. Volcanic detritus within the limestone consists mostly of scattered crystals and lithic fragments of sand size; larger fragments range up to 2 centimeters in maximum dimension and include pieces of basalt, andesite, and tuff. The limestone and enclosed tuff fragments, for the most part, are soft and appear to be altered or composed of secondary minerals.

The discrete volcanic fragments range in size from a few mm to more than 3 cm in maximum dimension. The larger fragments are subangular to round pieces of tuff breccia that may originally have been deposited in water. This material resembles that found in the limestone and may have broken from the soft limestone matrix, or it may be from an accumulation of closely associated volcanic detritus.

The tuff breccia dredge samples differ from similar rocks on the islands chiefly in their abundance of bright red lithic fragments. Because the color reflects the oxidation state of the iron, the abundance of red particles in the marine deposits may merely reflect depositional environments. Further study of the tuffs may permit their correlation with the volcanic sequence of the islands.

Based on the bottom topography and dredge samples, the limestone and associated volcanic materials appear to be detrital deposits that accumulated on a bench on steep submarine slopes having outcrops of volcanic rocks. The deposits can be compared to talus or scree deposits of steep slopes on land. The manganese coatings, alteration of the material, and lack of cementation suggest the possibility of a pre-Recent age and the probability that the deposits have never been exposed to subaerial weathering.

The trackline adjacent to the Palau Islands was planned to include a traverse across the Palau Ridge, a longitudinal profile along the ridge, and two transverse crossings of the adjacent Palau Trench. One of the latter crossings was at the southern end of the Palau Islands where the bathymetry indicates little influence of tectonism associated with the Yap Arc. The other crossed the deepest part of the Palau Trench, which lies between the Palau Arc and the west end of the Yap Arc. In addition to continuous echo sounding, gravimeter, and magnetometer profiling along the planned and connecting tracks, subbottom (GEP) profiles were obtained across the

ridge along the longitudinal profile and on the southern crossing of the trench (segments 2–5).

Because of various malfunctions, GEP records are lacking for about 25 percent of the track along segments 2–5. Preliminary shipboard analyses of the records were made as received and after plotting the data on base sheets. In general, penetration was shallow, and few subbottom reflections were received from shortly after beginning the run until the *Pioneer* had crossed the trench near the end of the run.

At the beginning of the run, relatively deep penetrations of apparently uniform sediments were obtained in the basin northwest of the Palau Islands. Here surficial layers conform to the bottom slopes and overlie sediments that are moderately deformed and appear to converge or thin on the lower slopes of the ridge. A buried north-trending fault or steep monoclinal fold can be noted as an offset in the subbottom reflections. Upward movement on the east side of the offset conforms to the predominant direction of movement of north-south longitudinal faults mapped on Babelthuap.

The upper west flank and crest of the ridge are characterized by several steep-sided hills or ridges that appear to have a close genetic relation to the configuration of coral reefs surrounding the main portion of the Palau Islands to the south. The subbottom profiles suggest the possibility of faults bounding these hills or ridges, and the presence of a uniform surficial layer more than 100 ft thick on the crests of the ridges and in adjacent lower areas. The relief and subbottom records together suggest that the crest of the arch represents a faulted terrain. The relief features of this terrain were accentuated by the growth of coral reefs and subsequently drowned.

The surface relief of the longitudinal profile along the east side of the Palau Islands was much greater than had been anticipated on the basis of existing bathymetric information. Numerous side echoes, shallow penetration, an apparent lack of well-defined subbottom reflecting layers, and discontinuities in the GEP record resulted in records that provide little geologic information other than that which can be deduced from the relief. A probable thin layer of sediment was identified on the floor of a grabenlike valley off the north-central coast of Babelthuap; elsewhere it appeared that the bottom is hard and lacks surficial sediments. Based on the relief, several mapped faults on the islands have been extended to the line of the track on figure 78[2]. The profusion of mapped faults on land permits various possibilities in correlating the land features with the relief features of the profile; therefore, the extensions are necessarily tentative. The reasonable correlation of some faults with profile features suggests that at least part of the offshore relief can be attributed to movements along the prominent northwest-southeast fault system of the land areas. The relief does not provide support for the existence of several faults that previously were postulated to explain the distribution of some geologic units on land and the configuration of the limestone islands. As a result, the significance of some of the previously postulated faults is being reevaluated.

Along segment 5, eastward from Peleliu, steep slopes on the west side of the trench are interrupted at several depths by nearly level and westward-sloping benches. Subbottom profiles suggest thin sediments on the benches and the presence of faults at their inner margins. Because deeper reflecting horizons were lacking, it was not possible to confirm the existence of the faults or to determine their attitudes. On the east side of the trench, near the end of the GEP run, two distinct subsurface reflections were obtained. The uppermost was relatively smooth and the lower, irregular. Both reflecting surfaces appear to dip gently toward the trench. These surfaces and their terminations on the east wall of the trench merit further field study.

Comparative studies of the bottom relief, gravity, and magnetic profiles for the Palau area must be completed before generalizations can be drawn concerning the geologic structure and its relation to the structural trends of the western Pacific. The track eastward from northern Babelthaup should be particularly significant. It includes the deepest part of the Palau Trench, a longitudinal profile of the west end of the Yap Ridge, a traverse across the southern part of the Yap Trench, and a longitudinal profile along the crest of the East Caroline Swell. The track along the crest of the swell was continued eastward to longitude 139°E, at which point the course was changed to the NNE to permit a nearly right-angle crossing of a prominent longitudinal escarpment on the crest of the swell and a subsequent land fix on the island of Fais, one of the few coral islands of the Pacific Basin that shows evidence of Recent uplift.

From Fais, the tract was directed across the Challenger Deep where additional geophysical data concerning trenches and a core from near the deepest part of the southern Mariana Trench were obtained.

From the Challenger Deep, the ship proceeded to the west side of Guam, the southernmost island on the arcuate ridge of the Mariana Arc. As shown by Hess (1948, fig. 3 therein) and by Cloud, Schmidt, and Burke (1956, p. 18), a curved line through the active and inactive volcanic islands of the northern Mariana Islands passes through an intermittent sulfur boil about 25 nm west of Saipan and through a submerged peak having the shape of a volcanic cone about 20 nm west of Guam (fig. 77[1]). The older southern Mariana Islands, from Guam to Farallon de Medinilla, form a second curve arc east of the line of volcanos. The volcanic rocks of Guam and Saipan include dacite, andesite, and tholeiitic basalt, whereas those of the northern Mariana Islands are high-alumina basalts and andesites.

## Guam Area

Guam consists of a southern dissected upland of volcanic rocks fringed by limestone and a northern upraised plateau of limestone (fig. 79[3]). Water-laid tuff, volcanic breccia, lava, and limestone-bearing breccia of late Eocene and Oligocene age make up the central structural block of the island. The rocks dip generally southeast and grow progressively finer grained to the southeast, indicating a volcanic source to the northwest where a collapsed caldera, called the Northwest Collapse Area, is inferred from the submarine topography (Tracey et al., 1964, p. A53). The axes of small tight folds in the central structural block trend northeast, and block faults trend generally northeast and southeast. These are interpreted as resulting from submarine slumping and sliding on the southeast flank of the volcano during its growth and subsequent collapse in Eocene and Oligocene time. Later volcanism produced the Northwest Cone. The southern structural block of the island consists of northeasterly-dipping lava flows, pyroclastic breccia, and interbedded limestone of early Miocene age that appear to be remnants of a now-collapsed Miocene volcano. The inferred caldera is called the Southwest Collapse Area. The Southwest Cone, west of the collapse area, likewise is presumed to have resulted from later eruptions.

The work of the *Pioneer* west of Guam was planned to investigate the collapse-caldera hypothesis by sampling the cones and collapse areas, and by making continuous gravity, magnetic, subbottom (GEP), and bottom (PDR) profiles along the lines of two of the structure sections inferred by Tracey et al., (1964, figs. 25, 26, 28, and 29 therein). The sample locations and the trackline of the geophysical profiles (positions 324K to 364K) are shown in figure 79[3], and the samples are listed in table 19[2].

The continuous seismic profiles and echosounder profiles show a generally hard bottom and sharp breaks in slope at the base of the island and the base of each cone. Layers of sediment were not apparent in the GEP profile, except for horizontal layers more than 100 ft thick in the Northwest Collapse Area. Fault traces could not be detected in the GEP profile, but the sharp breaks in slope may represent the surface trace of faults which bound the caldera. Further interpretation must await analysis of the gravity and magnetic data.

Core 37 in the Northwest Collapse Area was intended to sample the layered sediments indicated on the GEP profile. However, only a 4-cm sample of unconsolidated light brown calcareous silt and fine sand was obtained. This contained abundant globigerinid Foraminifera, presumably Recent. Dredge haul D28 was taken near the base of the steep southwest slope of the island to sample the Miocene volcanic sequence at the lowest possible stratigraphic level. Only a few rounded pebbles of basalt were recovered, and these were probably wave-worn fragments carried downslope from the beach.

The Southwest Cone has a flattened top about ½ mi in diameter and a minimum depth of 11 fms. Seven grab samples were obtained across the cone (fig. 79[3], G42 to G48). These yielded small amounts of calcareous globigerinid sand from the slopes, and calcareous sand containing *Halimeda* as well as broken limestone fragments from the top. No volcanic fragments were recovered and no volcanic mineral grains were found in preliminary examinations of the samples; thus the volcanic origin of the Southwest Cone remains unproven. If it is volcanic, it apparently has not been active in Recent time. It was presumably truncated at sea level, submerged, and capped by

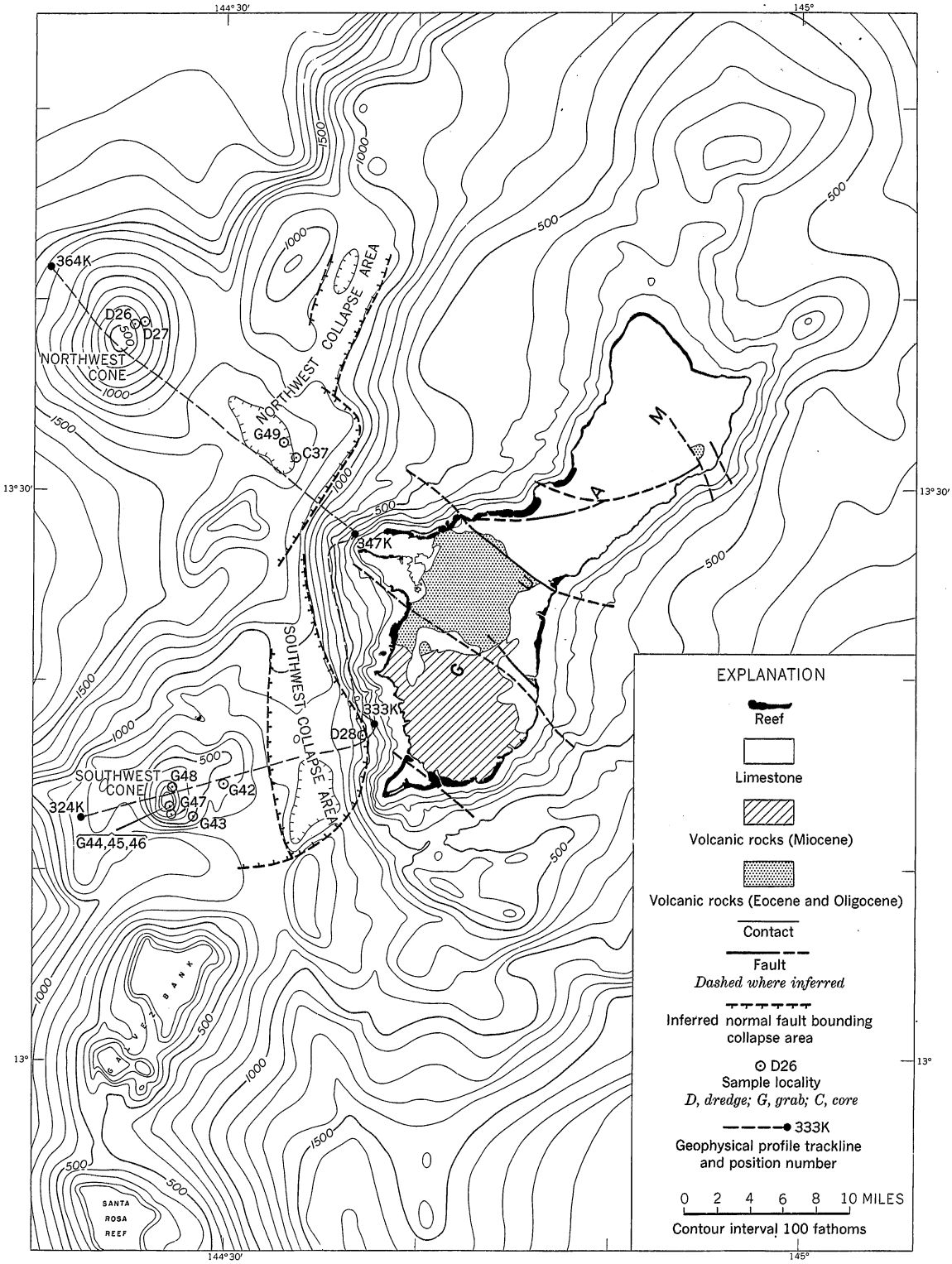


FIGURE 79[3].—Bathymetric chart of Guam and vicinity showing 1964 geophysical trackline of USC&GS ship *Pioneer* and sampling localities. Major structural features of the island and inferred submarine features are from Tracey et al., 1964, fig. 25. Bathymetry compiled by Emery in 1952 from USS *Bowditch* survey of 1944–45.

TABLE 19[2].—*Bottom sampling records west of Guam, 1964 cruise of USC&GS ship* Pioneer

| Sample number | Position number (fix) | Depth (fathoms) | Remarks |
|---|---|---|---|
| G42 | 310K | 500 | Globigerinid sand: globigerinid Foraminifera, 75%; very fine calcareous sand, 5%; manganese-coated limestone fragments 1–10 mm, 20%. |
| G43 | 313K | 422 | Sand, fine to very fine, calcareous; contains planktonic Foraminifera. |
| G44 | 315K | 28 | Sand, unsorted organic detrital; contains *Halimeda*, coral, shells, Foraminifera, also 2 large fragments (10 cm) of porous limestone coated with encrusting organisms. |
| G45 | 316K | 26 | Organic matter (mostly green and brown algae), limestone fragment (1 cm), some fine calcareous sand. |
| G46 | 316K | 24 | Few *Halimeda* segments; a little very fine calcareous sand. |
| G47 | 317K | 200 | *Halimeda* sand, coarse, unsorted, *Halimeda*, 10%; large fragment of limestone (18 cm) brought up on top of grab sampler. |
| G48 | 319K | 400 | Sand, calcareous, fine- to medium-grained, with small foraminiferal shell fragments. |
| D26 | 371K | 585–540 | Pumice, yellowish-brown. |
| D27 | 376K | 790–710 | Pumice, light to dark brown. |
| C37 | 388K | 1, 490 | Sand, fine, and silt, mostly carbonate, medium brown; contains pelagic Foraminifera and sparse volcanic mineral grains. |
| D28 | 396K | 540–440 | Basalt pebbles, largest 9 cm, some rounded; small coral and organic fragments. |

calcareous reef or bank deposits that now cover the slopes. Further inferences about the history of the Southwest Cone will require a detailed program of dredging and coring to obtain volcanic material that might be compared with that of Guam.

The Northwest Cone rises 1,000 fms from the sea floor to a depth of less than 460 fms. Two dredge hauls were made on its upper slopes. The first haul, D26, from a depth of 585 to 540 fms, recovered a small amount of yellowish-brown weathered pumice, one piece of which was 9 cm in largest dimension. The second haul, D27, from 790 to 710 fms, recovered several kg of light brown to dark brown pumice—must of it in small fragments, 5 mm to 3 cm in size, and less weathered in appearance than that from haul D26. Preliminary examination showed that the index of retraction of the glass is close to 1.52, indicating a probable andesitic composition. The pumice contained scattered small acicular crystals, probably augite and hypersthene, and small crystals of feldspar. One piece of pumice, 5 cm long, contained a feldspar crystal 1 cm on each side.

The darker pieces of pumice appear to be coated with a very thin film of manganese oxide. Scattered small fragments of red earthy material, probably altered volcanic tuff, are coated with as much as 0.1 mm of manganese oxide. A few small marine organisms occupied cavities in the pumice, but there was no organic incrustation such as would be expected if the material had been exposed on the sea floor for any considerable time. The minor amount of manganese oxide and the dearth of organisms indicate a Recent age for the dredged material, although the cone probably dates back into the Pleistocene.

The Northwest Cone may have been the source of the volcanic mineral grains of feldspar, augite, hypersthene, and magnetite found in insoluble residues of Mariana Limestone of Pliocene and Pleistocene age by Hathaway and Carroll (in Schlanger, 1964, p. D43) and attributed by them to ashfalls from a source away from the island, inasmuch as major volcanism on the island ended in mid-Miocene time. Ash from the cone may be the source of the thin red lateritic soil that overlies the Mariana Limestone on the northern plateau of Guam, since the lateritic deposits occur at a considerable distance from any other source of weathered volcanic material on the island. If the laterite formed wholly from weathering of volcanic minerals in the underlying nearly pure limestone, the solution of a greater thickness of limestone would be required than is apparent from field observations. Upper Quaternary ash, derived from the Northwest Cone and deposited on the emerged limestone surface, would have provided a source for the laterite, although as Carroll and Hathaway (1963, p. F35) indicate, no independent evidence for late ashfalls was

found in their mineralogical studies of the soil profiles.

Studies of the composition of the pumice, and of the feldspar and other minerals in the pumice, may provide clues that will help relate the Recent volcanism of the Northwest Cone to both the older volcanism of the southern Mariana Islands and the younger volcanism of the northern islands. Pumice alters so readily that chemical analyses may not be particularly diagnostic. For this reason, future marine work in the area should include dredge hauls from the base of the Northwest Cone to obtain, if possible, lava from flows that may have issued from the lower slopes of the volcano.

## References


Carroll, Dorothy, and John Hathaway, "Mineralogy of Selected Soils From Guam," *U.S. Geol. Survey Prof. Paper 403–F*, pp. F1–F53, 1963.

Cloud, Preston E., Jr., R. G. Schmidt, and R. W. Burke, "Geology of Saipan, Mariana Islands," *General Geology: U.S. Geol. Survey Prof. Paper 280–A*, pp. 1–126, 1956.

Cloud, Preston E., Jr., et al., *Military Geology of Saipan, Mariana Islands—Introduction and Engineering Aspects: U.S. Army, Chief Eng., Intelligence Div., Office Eng., Headquarters, U.S. Army Forces Far East*, 67 pp., map, 1955.

Cole, W. S., "Larger Foraminifera From the Palau Islands," *U.S. Geol. Survey Prof. Paper 221–B*, pp. 21–31, pls. 5–6, fig. 1, 1950.

Corwin, Gilbert, et al., *Military Geology of Pagan, Mariana Islands: U.S. Army, Chief Eng., Intelligence Div., Office Eng., Headquarters, U.S. Army Japan*, 259 pp., illus., maps, 1957.

Dietz, R. S., "Marine Geology of Northwestern Pacific—Description of Japanese Bathymetric Chart 6901," *Bull. Geol. Soc. Am.*, vol. 65, pp. 1199–1224, 1954.

Doan, D. B., et al., *Military Geology of Tinian, Mariana Islands: U.S. Army, Chief Eng., Intelligence Div., Office Eng., Headquarters, U.S. Army Pacific*, 149 pp., illus., maps, 1960.

Hess, H. H., "Major Structural Features of the Western North Pacific—An Interpretation of H. O. 5485, Bathymetric Chart, Korea to New Guinea," *Bull. Geol. Soc. Am.*, vol. 59, pp. 417–446, 1948.

Johnson, C. G., et al., *Military Geology of Yap Islands, Caroline Islands: U.S. Army, Chief Eng., Intelligence Div., Office Eng., Headquarters, U.S. Army Pacific*, 164 pp., 10 figs., 20 tables, 64 photos, maps, 1960.

Mason, A. C., et al., *Military Geology of Palau Islands, Caroline Islands: U.S. Army, Chief Eng., Intelligence Div., Office Eng., Headquarters, U.S. Army Forces Far East*, 285 pp., illus., maps, 1956.

Schlanger, S. O., "Petrology of the Limestones of Guam," *U.S. Geol. Survey Prof. Paper 403–D*, pp. D1–D52, 1964.

Stark, J. T., et al., *Military Geology of Truk Islands, Caroline Islands: U.S. Army, Chief Eng., Intelligence Div., Office Eng., Headquarters, U.S. Army Pacific*, 81 pp., illus., maps, 1958.

Tracey, J. I., Jr., et al., *Military Geology of Guam, Mariana Islands: U.S. Army, Chief Eng., Intelligence Div., Office Eng., Headquarters, U.S. Army Pacific*, 282 pp., 49 pls. (5 maps), 19 figs., 21 tables, 1959.

Tracey, J. I., Jr., et al., "General Geology of Guam," *U.S. Geol. Survey Prof. Paper 403–A*, pp. A1–A104, 1964.

# A Reconnaissance Geophysical Survey in the Andaman Sea, and Across the Andaman-Nicobar Island Arc*

G. Peter, L. A. Weeks, and R. E. Burns†

*Abstract.* A marine geophysical study of the Andaman Sea has been conducted as part of the International Indian Ocean Expedition. A combination of magnetic, gravity, bathymetric, and sea floor heat-flux measurements, seismic sparker reflection profiles, and bottom sediment samples has been used to study the seaward continuity of major subaerial tectonic trends. The data indicate positive continuity of the structural trend of the Barisan Range of northern Sumatra and the Burma Range. It was found that the central graben of the Barisan Range of northern Sumatra extends into the Andaman Sea north to latitude 10°N. A previously unreported interdeep has been observed between the outer sedimentary island arc and the inner igneous trend of the major primary arc, which forms the western boundary of the Andaman Sea. Continental thickness of the crust is indicated under the sedimentary island platform. In the area of the backdeep, the north-northeast trends of the Malay peninsula are prominent.

*Introduction.* As part of its participation in the International Indian Ocean Expedition, the U.S. Coast and Geodetic Survey ship *Pioneer* conducted a reconnaissance geophysical survey in the Andaman Sea and across the Andaman-Nicobar island arc (fig. 80[1]). The basic survey consisted of a major underway series of simultaneous measurements of the earth's magnetic and gravity fields. These were supplemented by the continuous recording of water depth, a series of subbottom seismic reflection profiles, and associated programs of sea floor heat-flux measurements and bottom sediment sampling.

Measurements of the magnetic field were made with a towed Varian proton-precession magnetometer which measures the total intensity of the earth's magnetic field with a sensitivity of ±1 gamma. The sensing unit was towed far enough behind the ship to keep the ship's influence smaller than ±5 gamma. Because of the location of the survey area on the geomagnetic equator, the measurements were subject to diurnal variation as high as ±35 gamma. On the other hand, short-period variations related to magnetic storms appear to be absent from the record, since the U.S. Coast and Geodetic Survey Honolulu Magnetic Observatory records indicate that the survey was conducted during a quiet period.

The gravity measurements were made with a LaCoste & Romberg air-sea gravity meter. The meter was checked at the San Francisco gravity meter evaluation range both before and after the Indian Ocean operations. These checks indicate that rms errors are smaller than ±5 milligals when the seas are calm (Browne corrections smaller than 100 mgal). Because the average Browne correction during the Andaman Sea operations was approximately 50 mgal and frequently was smaller than 10 mgal, the data are considered to be accurate within the ±5 mgal limit.

A continuous record of water depth was obtained with the Precision Depth Recorder during all underway operations. The bathymetric profiles in this report represent uncorrected soundings obtained from the PDR record for points of inflection and gradient changes in the indicated bottom slopes.

The seismic-reflection profiles were obtained with a Rayflex sparker, utilizing a 20,000-joule electrical spark as a sound source. This spark source was towed about 100 meters behind the ship and was energized every 4 seconds. The hydrophone array consisted of 20 hydrophones spaced about 4.5 m apart and enclosed in a long plastic tube filled with diesel oil. The oil-filled tube provided a neutral buoyancy during towing and minimized water noise around the hydrophones. The reflected signal received by the hydrophone array was recorded both on paper strip-chart and on magnetic tape. On the reflection profiles presented in this report, the form lines of structures and faults were interpreted from the original rec-

*Published originally in *Journal of Geophysical Research*, vol. 71, no. 2, pp. 495–509, January 15, 1966.
†Institute for Oceanography, U.S. Environmental Science Services Administration.

790-089 O—66——8

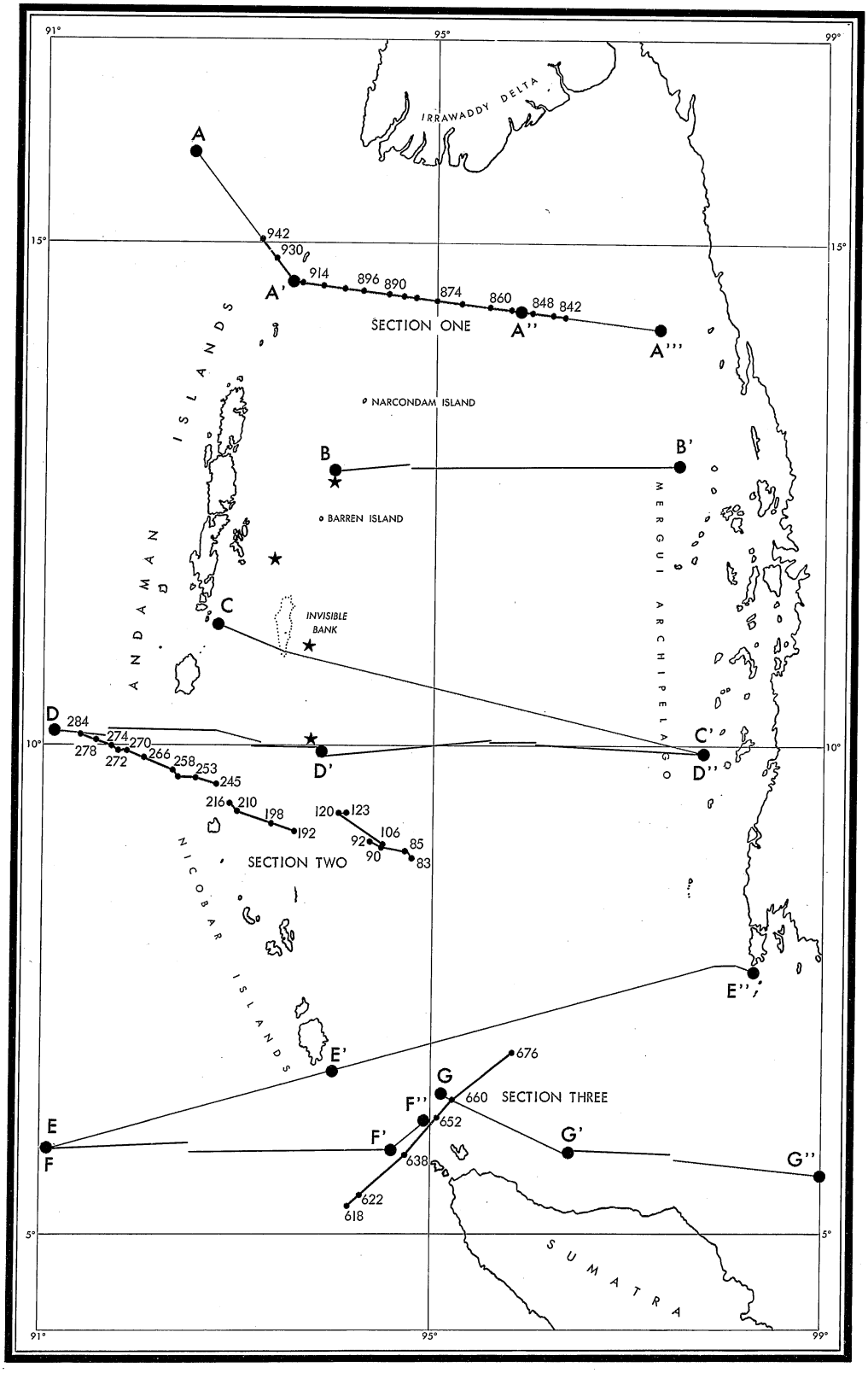


FIGURE 80[1].—General location of subbottom profile sections and bathymetry, magnetics, and gravity profiles.

ords. The horizontal scale on the sections is based on 30-minute fix-positions at a ship's speed of about 5 knots. Each fix-point marked on the sections is 30 minutes from the adjacent fix, regardless of the specific number assigned to it. Because of the small speed changes in the various parts of the sections, the assigned distance scale must be considered only approximate. The vertical scale is shown in meters so that the first reflection can be related directly to bathymetric profiles. This scale was based on an assumed sound velocity of 1.6 kilometers per second, and the depths indicated for the subbottom horizons are probably deeper by as much as 40 percent.

The measurements of sea floor heat-flux were made in association with the bottom-sediment sampling program. Bottom sediment samples were collected with several types of coring, grab, and dredge sampling devices. The results of the heat-flux measurements have been reported separately (Burns, 1964—pages 119 and 120). The detailed description of the bottom sediment composition and distribution will be the topic of another paper.

*Geologic and tectonic framework.* The principal objective of the reconnaissance geophysical survey in the Andaman Sea was to examine the seaward continuity of the major geologic trends of this area. These trends are schematically indicated in figure 81[2], which is based on a geologic map prepared by the Geological Survey of the Federation of Malaya (Alexander, 1962). A generalized representation of the principal bathymetric features of the area (fig. 82[3]) has been compiled from several sources, including the bathymetric program of the *Pioneer*.

The dominant structural features in this area are related to the Indonesian arc which is part of the system of young primary arcs of southeastern Asia. The field program of the *Pioneer* was designed to provide a series of traverses of the Andaman Sea, from the Mergui Archipelago in the east and extending westward across the Andaman-Nicobar island arc.

To the east of the Andaman Sea, the geologic structure belongs to the fold-mountain system which extends from Burma, through Thailand and Malaysia, and eastward into Borneo. The major orogeny of this eastern folded belt occurred during the Triassic and Jurassic periods.

The Indonesian arc in this area consists of a primary double arc with a recognized inner volcanic trend and an outer sedimentary arc. The inner volcanic trend is well-defined in central Burma and also in Sumatra. It consists of a belt that was originally folded during the Cretaceous and developed during the late Tertiary and Quaternary into a volcanic arc system, which is still marked by active volcanism. In Sumatra, this volcanic trend is represented by the Barisan Range, which is split longitudinally by the Semangko fault, a graben or rift valley extending the full length of Sumatra. In northern Sumatra, the trend of the fault zone is identified by the Atjeh graben which extends offshore into the Andaman Sea. On both sides of the graben there are members of the pre-Tertiary and Lower Tertiary Block Mountain system, composed mainly of metamorphic rocks with diabase and serpentine. On the northeast side of the graben there are additional young volcanic rocks, generally identified as andesite effusives. On the basis of recent active volcanism reported at Barren and Norcondam Islands, it has been postulated previously that this volcanic trend extends through these islands northward into Burma. In Burma, a major fault zone separates the Triassic-Jurassic fold-mountain system of eastern Burma from the Cretaceous Burma Range.

The only clear subaerial indication of the outer sedimentary arc is the island arc formed by the Andaman and Nicobar Islands which form the western border of the Andaman Sea. Orogenic activity in this belt began as early as the Cretaceous, but the elevation of the islands did not occur until the Oligocene and Miocene (Karunakaran et al., 1964).

Van Bemmelen (1949) proposes that the geologic development of the area has been from east to west. The relationship of a rapidly developing outer sedimentary arc to an inner volcanic arc has not changed, although the double arc system has shifted progressively to the west. The inner volcanic arc of today was the sedimentary arc of an earlier period, and what is now an uplifted platform started as an outer depressed belt.

*Trends paralleling the island arc.* The Cretaceous to Oligocene and Miocene orogenic belt is represented in this area by major trends which are generally indicated by the morphologic trends indicated in figure 82[3]. The basic elements of a primary double island arc may be identified. The inner igneous arc runs east of the Andaman and Nicobar Islands, through Narcondam Island, Bar-

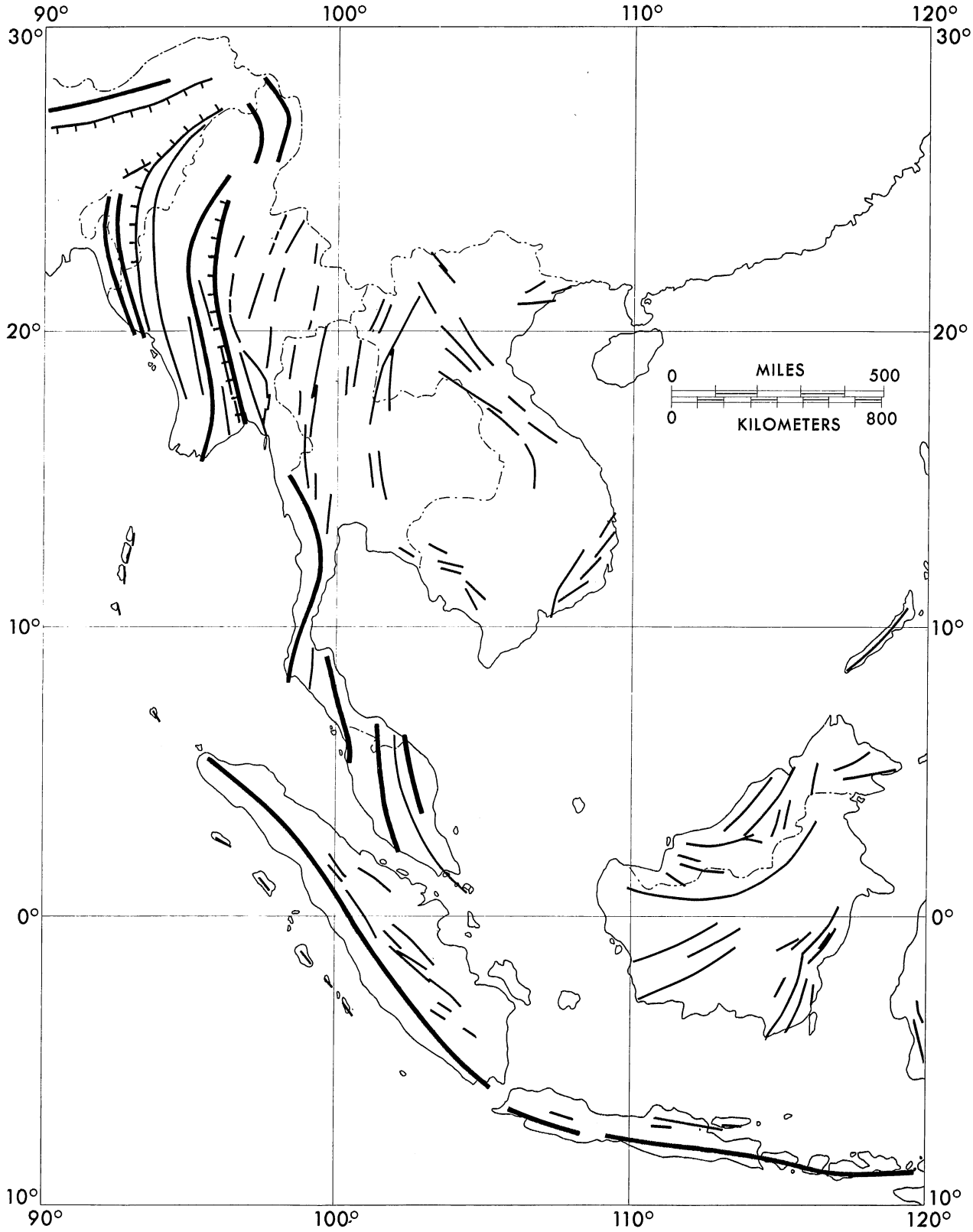


FIGURE 81[2].—Major geologic trends adjacent to the Andaman Sea.

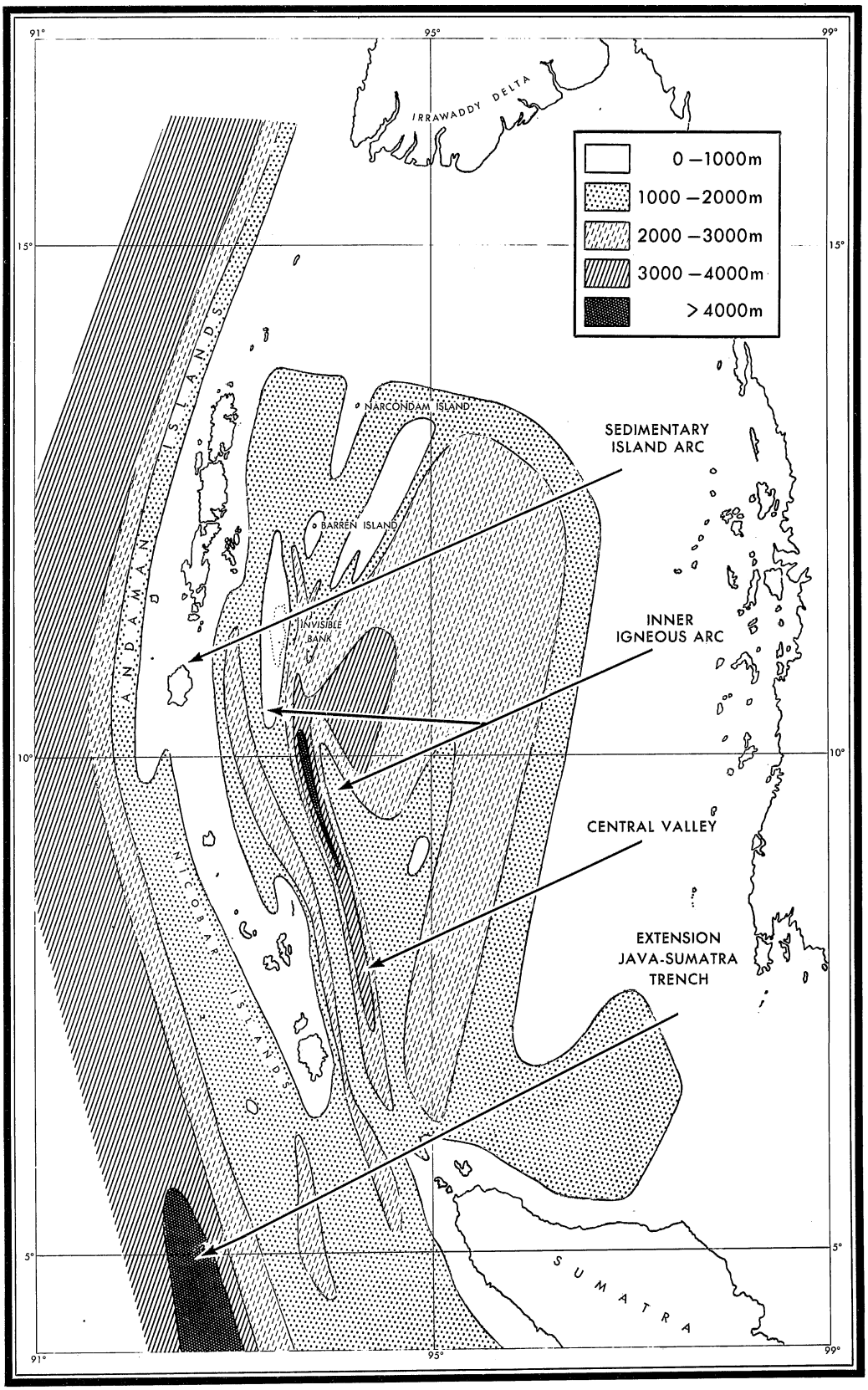


FIGURE 82[3].—Schematic presentation of principal bathymetric features in Andaman Sea area.

ren Island, and Invisible Bank, and connects the Cretaceous orogenic ranges of Burma and Sumatra. A structurally depressed belt separates the inner igneous arc from the outer sedimentary arc. The trend of the sedimentary island arc is represented by the Andaman-Nicobar platform and passes south of Sumatra through Simalur and Nias Islands (outside the area shown on the base map). The fourth trend is indicated by the northern extension of the Java-Sumatra Trench which is locally a weak trough west of the sedimentary island platform with depths in excess of 4,000 m at the south and greater than 2,500 m at the north.

The free-air gravity anomalies are presented in chart form (fig. 83[4]) and may be compared with the general trends indicated above. The inner igneous arc is indicated by generally high positive free-air anomalies, specifically prominent at the northern tip of Sumatra, Invisible Bank, and near Barren and Narcondam Islands. A parallel belt of negative anomalies indicates the trend of the sedimentary island platform. The axis of this belt passes through the Nicobar Islands but shifts to the inner (eastern) side of the Andaman Islands. A belt of slightly positive free-air anomalies in the west is generally associated with the outer limit of the island arc in the southern part of the area, but moves up onto the insular shelf and disappears just north of 10°N latitude. The westernmost belt of negative anomalies is coincident with the axis of the foredeep.

Four profiles based on simultaneous measurement of gravity, magnetic field, and water depth cross the entire arc system and are shown in figure 84[5]. The magnetic field measurements generally indicate minor anomalies associated with the extension of the Java-Sumatra Trench. The magnetic field is relatively smooth over the sedimentary island platform, and the relatively large and sharp anomalies are clear indications of the igneous belt to the east. Most of the anomalies associated with the igneous belt are negative, indicating induced magnetization of the rocks in this equatorial region. Several sharp positive peaks suggest reverse remanent magnetization (Girdler and Peter, 1960).

The postulated continuity of the igneous belts of Burma and Sumatra is strengthened by this set of profiles. Although on profile A′–A″ there is complete lack of bathymetric indication, owing to burial by the encroaching Irrawaddy Delta from the north, the igneous trend is clearly indicated by both the positive free-air anomaly and the magnetic anomalies. In the south, the igneous trend is best indicated by the magnetic anomalies. The seismic-reflection profile section 3 (fig. 85[6]) indicates almost a direct correlation with the subaerial geological trends of northern Sumatra, and section 2 (fig. 86[7]) farther to the north also shows significant similarity. The continuity is further strengthened by the very high sea floor heat-flux measured in the deepest portion of the Andaman basin (fig. 87[8]), which is directly on the axis of the igneous trend (note the deep area near the eastern end of profile D–D′). Two other measurements of the heat-flux along the axis of the igneous trend also are somewhat higher than the world average, and the only low value was measured in a sediment-filled basin (interdeep) between the sedimentary island arc and the igneous belt.

The extension of this igneous belt with its known seismicity, high heat-flux, volcanic activity, and central graben appears to be somewhat similar to the extension of the East African rift system into the Gulf of Aden, the extension of the Iceland graben into the Mid-Atlantic Ridge, or possibly the extension of the Great Alpine Fault of New Zealand into the Tonga-Kermadec Ridge. In each case, it appears that the same tectonic forces operate both on land and at sea. The Iceland and the East African graben systems are established as tensional features of the earth's crust, connected to the mid-oceanic ridge systems. The Barisan Range, which has been discussed by van Bemmelen (1949) as a tensional relaxation feature, may indicate through some of these similarities that the island arc systems represent another manifestation of global crustal tension.

*North-northeast trends.* With the exception of the major trends of the arc system which have already been discussed, the trends in the Andaman basin itself tend to strike north-northeast. The most prominent north-northeast trend indicated in figure 87[8] is formed by continuity of magnetic and positive free-air anomalies with the shelf-break along the Malay peninsula in the northern half of the Andaman Sea. The profiles shown in figure 88[9] indicate that this trend was detected on each crossing of the basin. In the northern part of the basin, the trend was detected

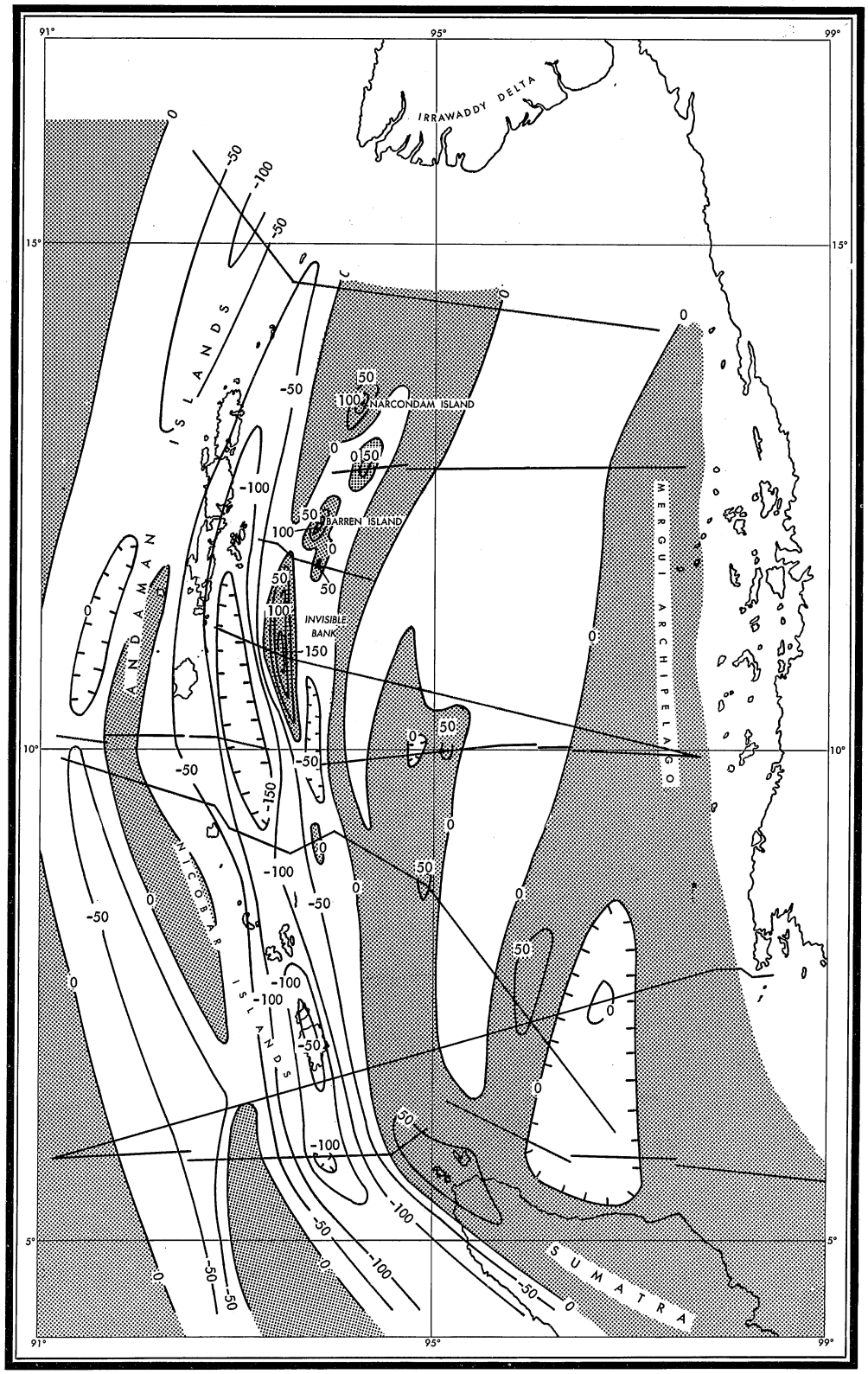


FIGURE 83[4].—Free-air gravity anomalies, Andaman Sea. (Contour interval 50 mgal. Control lines indicated.)

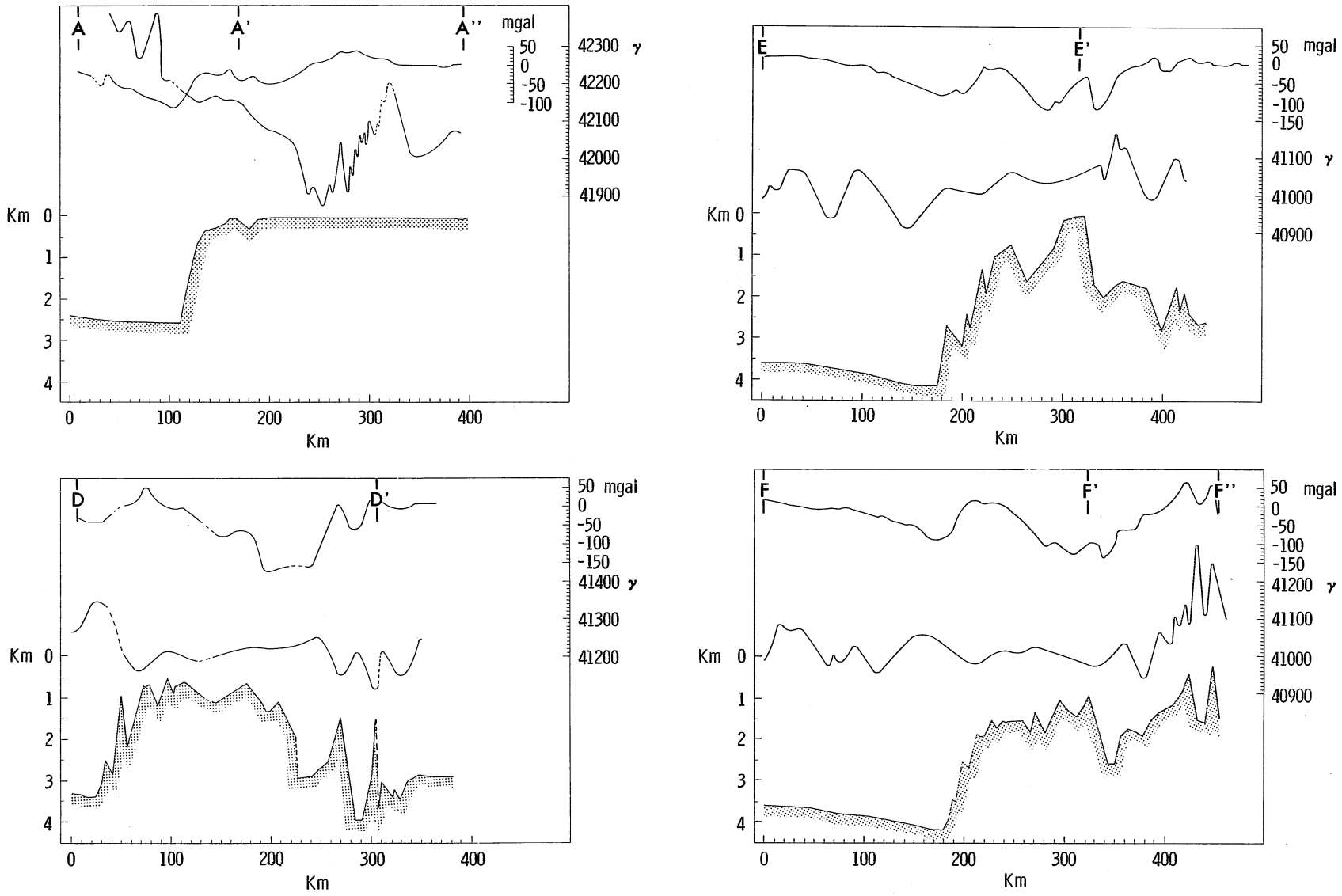


FIGURE 84[5].—Bathymetric, magnetic, and free-air gravity anomaly profiles A–A′–A″, D–D′, E–E′, and F–F′–F″.

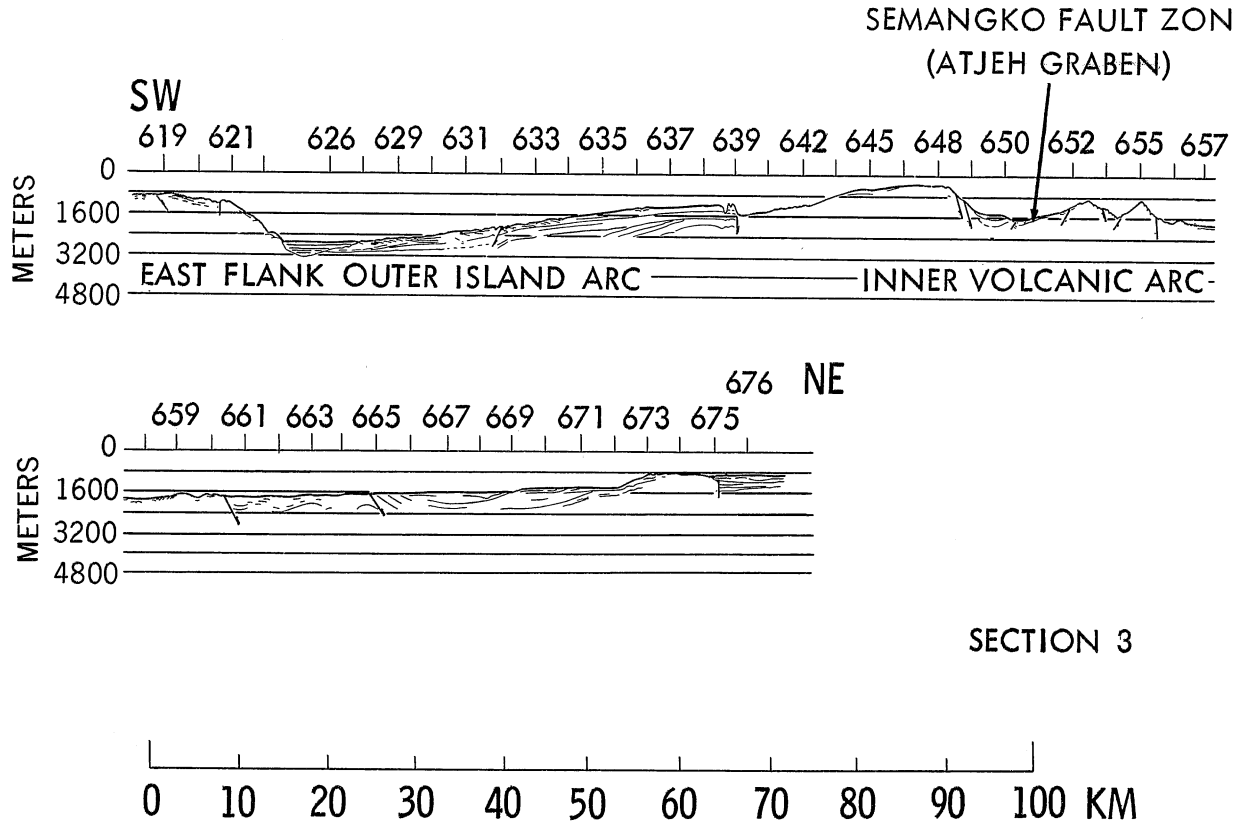


FIGURE 85[6].—Subbottom profile along section three.

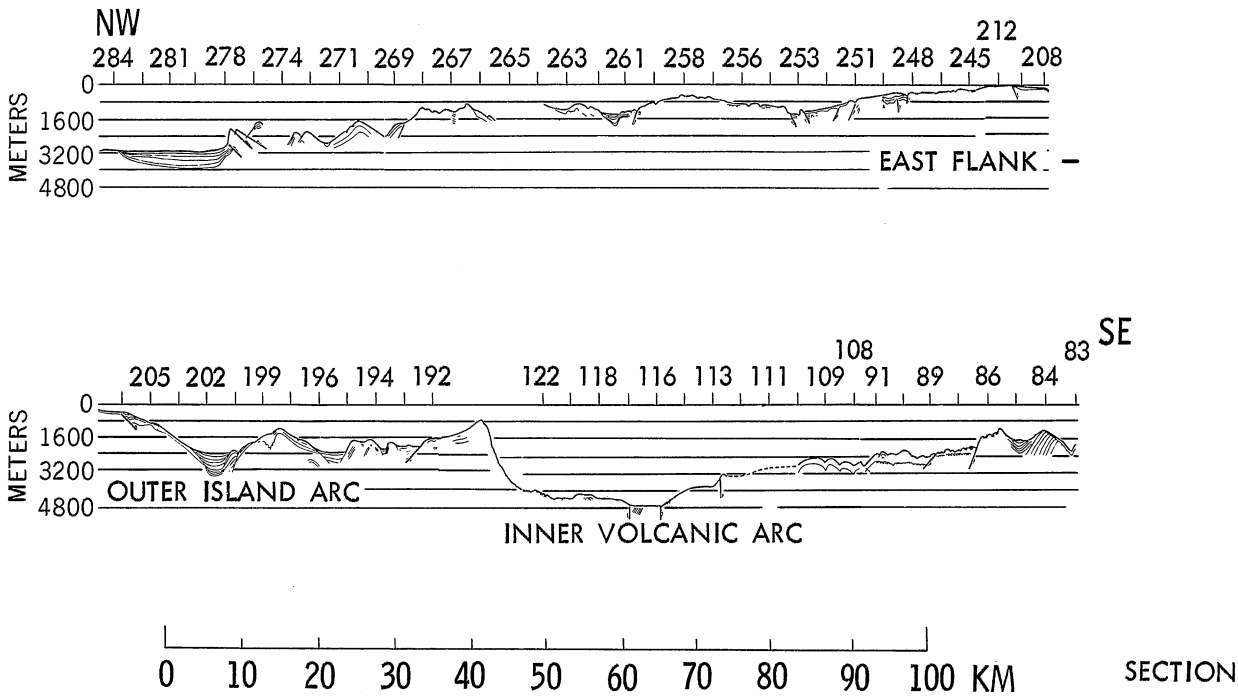


FIGURE 86[7].—Subbottom profile along section two.

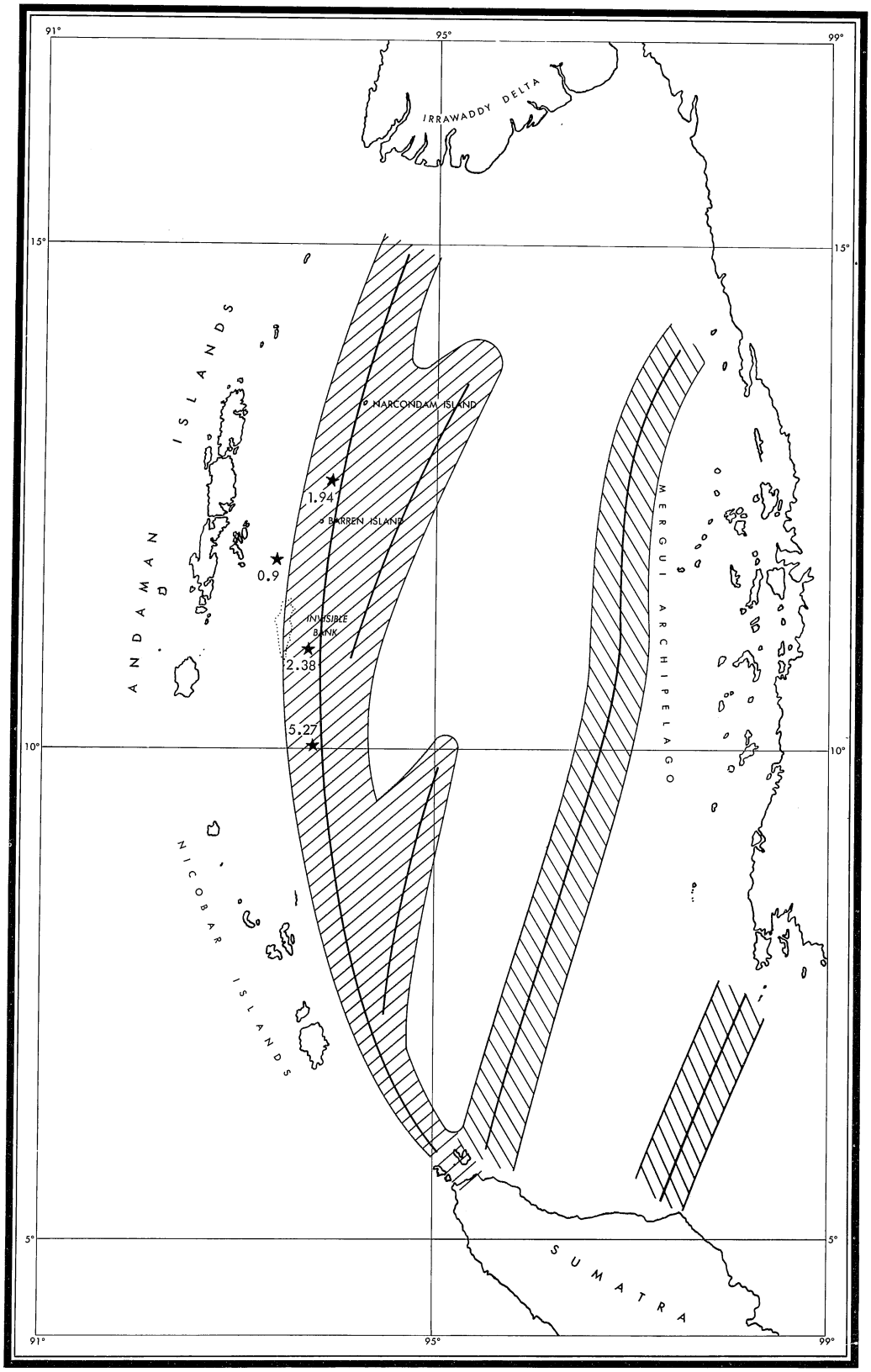


FIGURE 87[8].—Magnetic anomaly trends and measured sea-floor heat flux ($10^{-6}$ cal cm$^{-2}$ sec$^{-1}$).

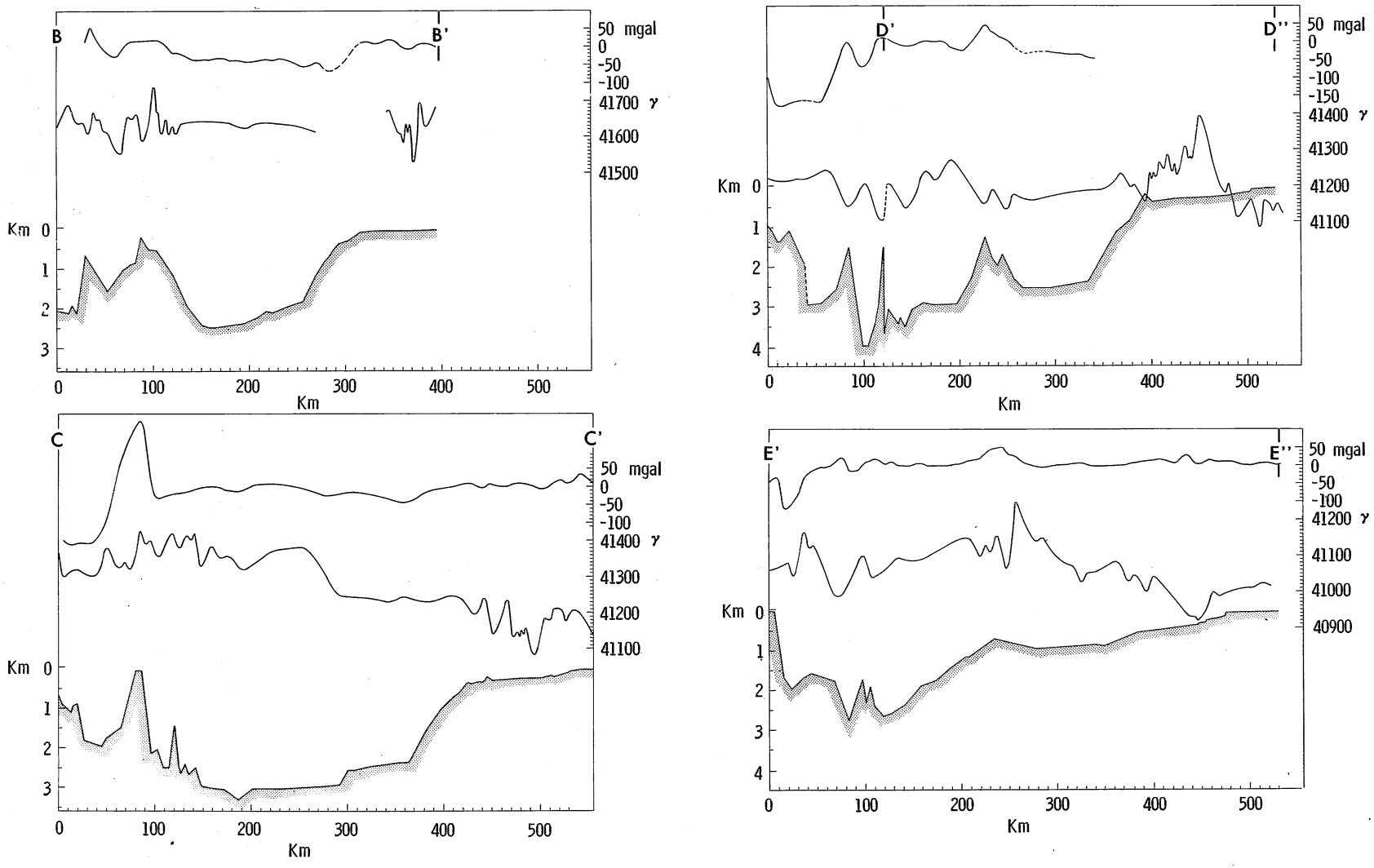


FIGURE 88[9].—Bathymetric, magnetic, and free-air gravity anomaly profiles B–B′, C–C′, D′–D″, and E′–E″.

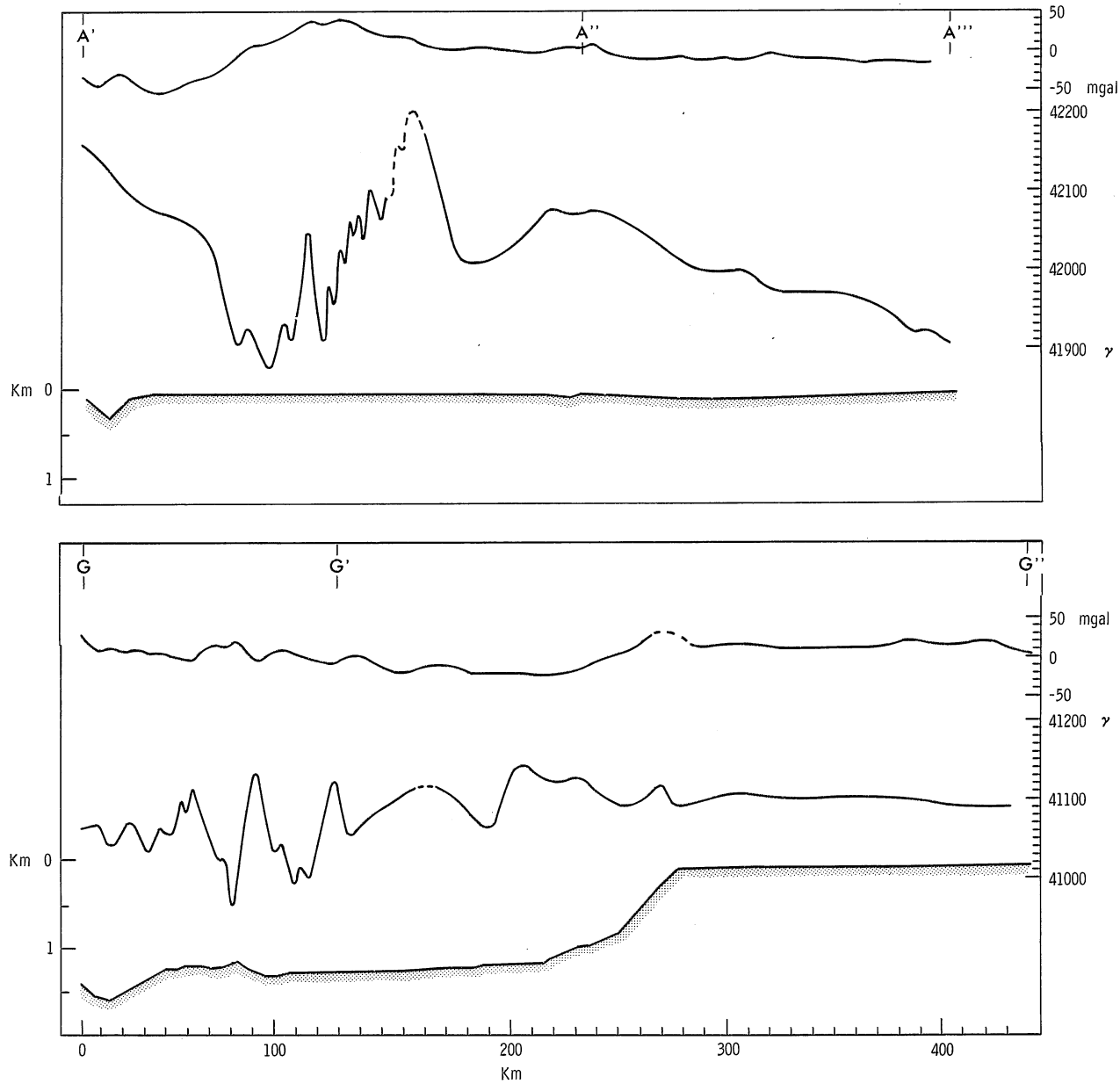


FIGURE 89[10].—Bathymetric, magnetic, and free-air gravity anomaly profiles A'–A''–A''' and G–G'–G''.

a few kilometers south of point A''' (on a section not included in this report), and profiles B–B', C–C', and D'–D'' indicate similar associations with the shelf immediately to the east of the shelf-break. In the southern portion of the basin, profile E'–E'' shows the trend in deeper water about 250 km west of the poorly defined shelf-break and associated with a minor rise that may be a slope terrace. Still farther south, profile G–G' (fig. 89[10]) indicates that similar anomalies were detected in deeper water (>1,000 m) off the northern tip of Sumatra. The anomalies may reflect the underlying Triassic-Jurassic tectonic trends of the Malay peninsula, or may be similar to anomaly trends of this type frequently associated with the appearance of intrusive and effusive rocks along the shelf-break in other parts of the world (Drake et al., 1958; Peter et al., 1965). This latter interpretation is partially supported by the occurrence of igneous rocks brought up by several dredge hauls made from the *Pioneer*.

In the southern half of the Andaman Sea, cross-

ing the 200-m shelf-break, indications of normal faulting were observed. On profile G′–G″ (fig. 89[10]), there is a distinct change in the magnetic field character from smooth to moderately active at the shelf-break over the inferred fault. These geophysical anomalies, together with the fault observed near fix-position 675 on the southernmost seismic-reflection profile (fig. 85[6] and fig. 90[11]), seem to support our second conclusion, and suggest that the shallow southeastern portion of the Andaman Sea is underlain by a downfaulted portion of the west Malayan shelf.

There is an abrupt change in the depth of the seafloor (from 2,700 m to 3,000 m), indicated in profiles C–C′ and D′–D″ (fig. 88[9]), which may be another indication of a fault zone. The associated steplike change in the magnetic anomaly also appears to support this conclusion. The trend of the inferred fault is also NNE, parallel to the shelf-break anomaly trend mentioned above.

South of profile C–C′ the actual fault plane cannot be observed. Profile D′–D″ indicates that it is overlain by a mountain range which merges with the igneous inner arc at the latitude of the south Nicobar Islands (fig. 82[3]).

Toward the north there is no indication of this fault on profile B–B′ (fig. 88[9]). The fault indications in profile section 1 (fig. 91[12]) are probably due to sediment settling, since A″–A‴ (fig. 89[10]) lacks significant geophysical anomalies which usually indicates deep-seated tectonic control.

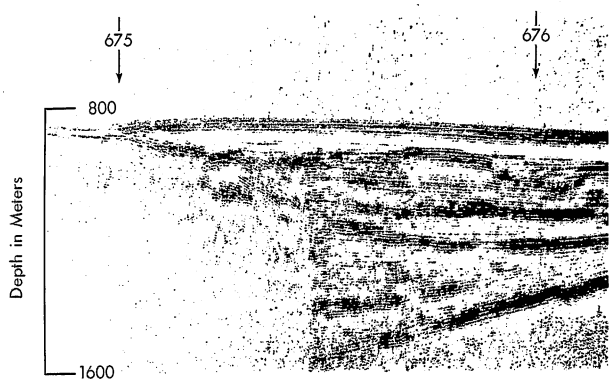


FIGURE 90[11].—Subbottom profile record showing detail at position 675 along section three.

Northeast of Invisible Bank, another NNE trend, a mountain range, merges with the igneous arc. The range is less than 250 km long, and the geophysical data along profile A″–A‴ do not indicate that other mountains are buried under the Irrawaddy Delta along this trend.

*Bouguer and isostatic anomalies.* Bouguer anomalies have been calculated for sections C–C′ and E–E′–E″ (figs. 92[13] and 93[14]). The calculations are based on an assumed crustal density of 2.84 g/cm³ and a two-dimensional model of the bottom topography (Talwani et al., 1959). The 2.84 g/cm³ density is the average density of the

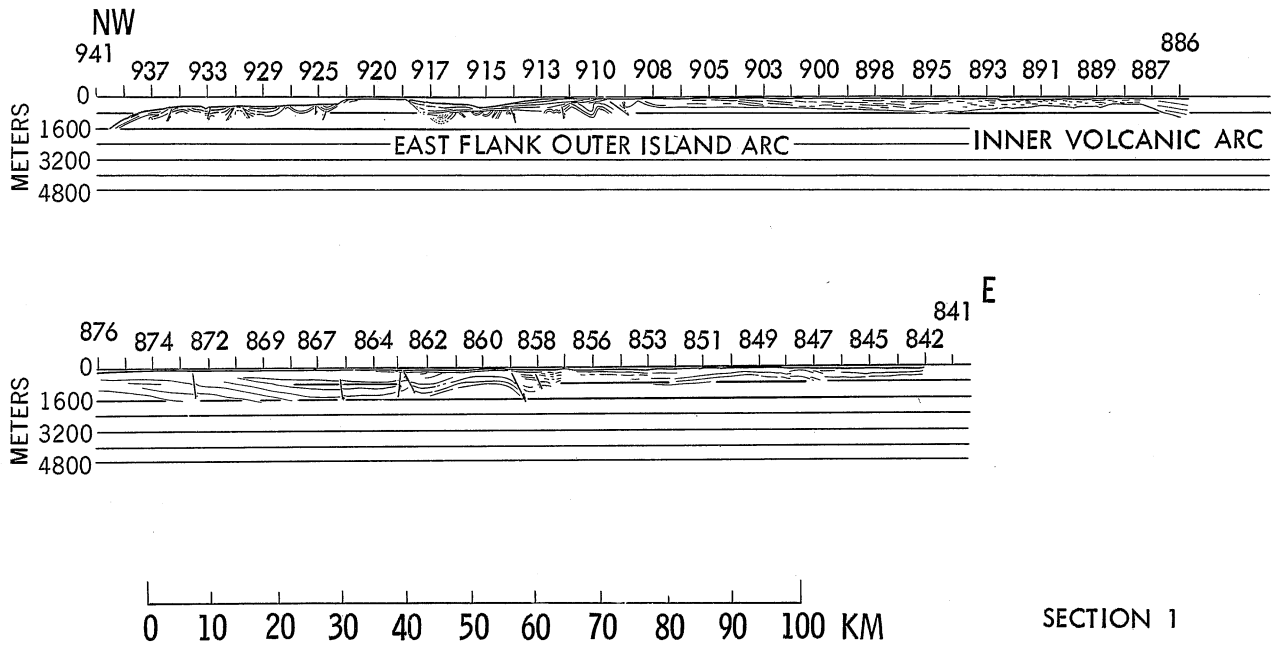


FIGURE 91[12].—Subbottom profile along section one.

combined "low velocity basement" and "high velocity basement" as derived by marine seismic refraction measurements (Talwani et al., 1959; Peter et al., 1965). Similar high values can be obtained by averaging the densities in that part of the crust which lies below sea level (Woollard, 1959). Because the local sections are primarily marine areas below sea level, it is appropriate to use the 2.84 g/cm$^3$ density for Bouguer corrections rather than the customary 2.67 g/cm$^3$—which is more appropriate for the average density of continental rocks above sea level.

In figure 92[13], the Bouguer anomaly over Invisible Bank indicates that the bank may be composed of rocks of higher density than the assumed 2.84 g/cm$^3$, and that a large density contrast exists deep into the crust in the area along the trend of the igneous arc.

In figure 93[14], a crustal section has been calculated from the Bouguer anomalies. In this calculation, the mantle density was assumed as 3.3 g/cm$^3$ and the depth to the mantle surface was adjusted through successive computations until its gravitational attraction matched the Bouguer anomalies. Besides the assumption that the structure is two-dimensional perpendicular to the profile, it was assumed that at the point where the free-air anomaly and the Bouguer anomaly are each zero (the continental shelf), the crustal thickness is 30 km. Through successive calculations, the crust under the Andaman Islands was lowered to 40 km and the mismatch between the calculated and the observed curves was reduced to only 30 mgal. In additional calculations the crust-mantle interface was lowered below 40 km, but the computed curve had started to broaden, indicating a shallow rather than a deep source for the anomaly.

Generally, the fit between the gravitational attraction of the mantle in the calculated crustal section and the Bouguer anomalies is good. The departures at the eastern flank of the outer (sedimentary) island arc and over the igneous arc are within the errors of the assumptions of the model. This is certainly true for the sedimentary island platform (area west of E′ on figure 93[14]) where the use of the 2.84 g/cm$^3$ density in the Bouguer corrections was obviously too high.

The derived crustal cross section, because it is based solely on the gravity data, does not represent

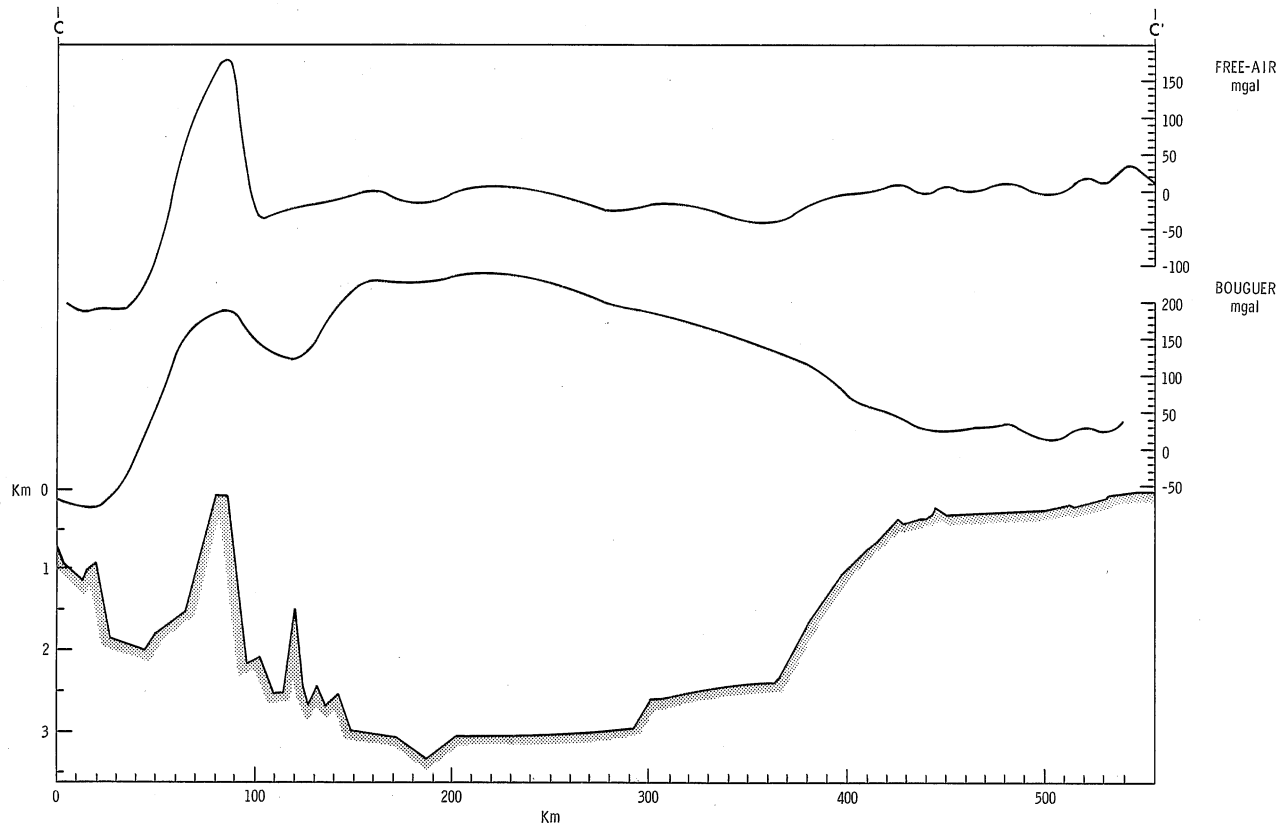


FIGURE 92[13].—Bathymetric and free-air and Bouguer gravity anomaly profile C–C′.

a unique solution. On the basis of similar calculations by Woollard (1959), the estimated error in the crustal thickness of the model is ±10 percent. It is entirely possible that sedimentary material plays a much greater role in the Bouguer anomalies than is implied in figure 93[14] (a mismatch of only 30 mgal). However, more detailed treatment of this possibility would be purely speculative without additional seismic information. Regardless of the possible magnitude of these corrections for a thick accumulation of sedimentary material, the present conclusions should be still applicable; the crustal thickness under the sedimentary island platform is far in excess of normal oceanic crust, and appears to be of continental type.

The Airy-Heiskanen two-dimensional isostatic anomalies (Talwani et al., 1959) are shown for profile E–E′–E″ in figure 94[15]. These show a close resemblance to the free-air anomalies along

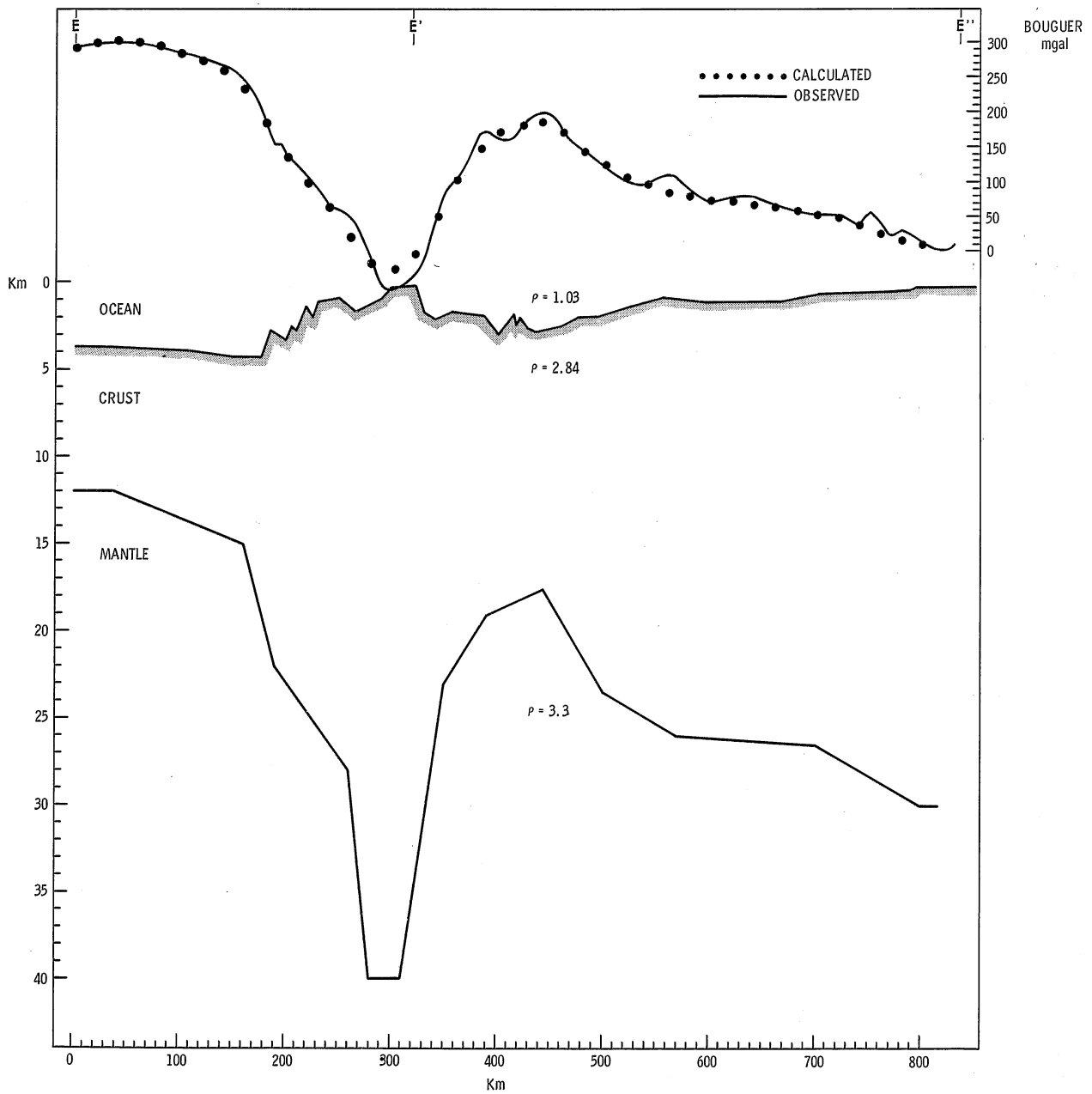


FIGURE 93[14].—Bathymetric and Bouguer gravity anomaly profile E–E′–E″. (Includes calculated crustal model).

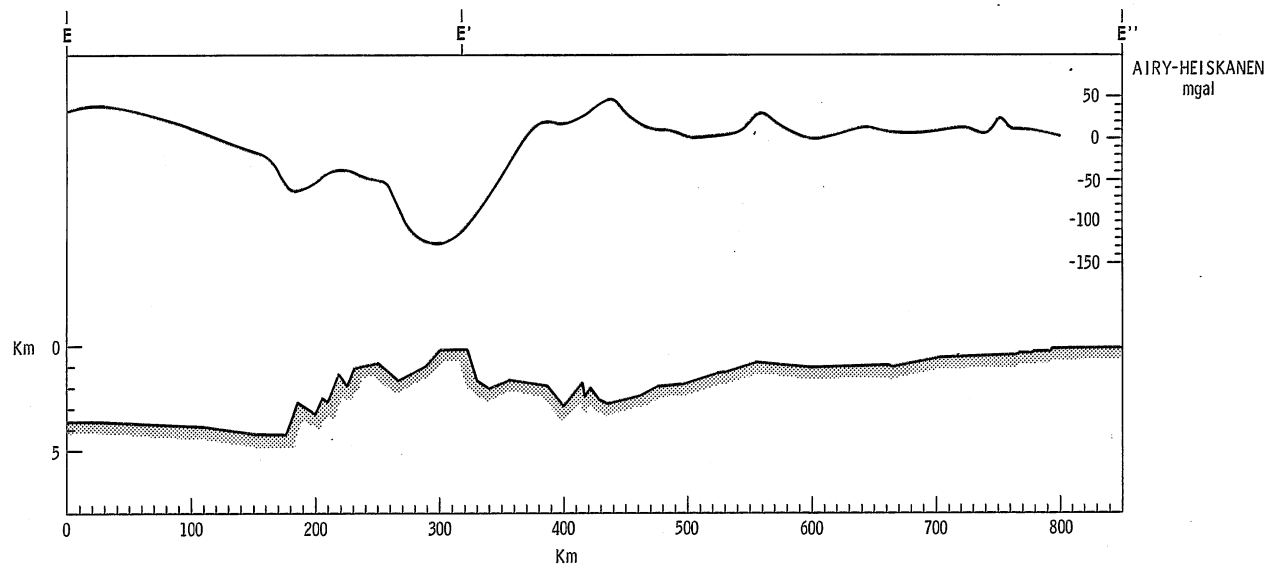


FIGURE 94[15].—Bathymetric and Airy-Heiskanen isostatic anomaly profile E–E'–E''.

the section (figs. 84[5] and 88[9]). The negative isostatic anomaly includes not only the local extension of the Java-Sumatra Trench (Woollard and Strange, 1962), but also the sedimentary island arc itself. A similar phenomenon was observed by Lyons (published in Eardley, 1962) and Talwani (personal communication) in the Antilles arc, where the large negative anomalies of the Puerto Rico Trench continue into the Barbados-Trinidad Ridge. Although this phenomenon is still not well understood, it is most likely connected to the relative age or state of development of the different parts of the island arc.

*Conclusions.* On the basis of the data available from the reconnaissance survey by the *Pioneer*, a detailed quantitative interpretation is impossible. The principal objective of this paper, other than the reporting of the data, has been to indicate the continuity of the subaerial geological and tectonic trends through the Andaman Sea area. This continuity is particularly well-supported for the extension of the structural trends of northern Sumatra northward through the igneous belt. The geophysical data verify the connection between the Cretaceous belts of the Barisan Range in Sumatra and the Burma Range, which was formerly postulated principally on evidence of bathymetry and of volcanism at Barren and Narcondam Islands. There is strong evidence that the southeast Andaman Sea is underlain by the downfaulted Sunda shelf (west Malayan shelf).

The Bouguer anomalies indicate continental thickness of the crust under the Andaman-Nicobar island platform, and the Airy-Heiskanen anomalies suggest that future elevation of the islands may be expected.

*Acknowledgments.* The authors wish to thank Dr. H. B. Stewart, Jr. of the Coast and Geodetic Survey for his efforts in incorporating the many measurements required by this study into the scientific program of the *Pioneer*, and Dr. J. B. Alexander and his colleagues at the Geological Survey of the Federation of Malaysia for their helpful assistance in the program. In addition, both Dr. Stewart and Captain E. B. Brown of the *Pioneer* have been instrumental in providing needed support during the measurement and data-processing phases of this study.

## REFERENCES

Alexander, J. B., A short outline of the geology of Malaya with special reference to Mesozoic Orogeny, in *The Crust of the Pacific Basin*, Am. Geophys. Union, Geophysical Monograph 6, 81–86, 1962.

Burns, R. E., Sea bottom heat-flow measurements in the Andaman Sea, *J. Geophys. Res.*, *69*(22), 4918–4919, 1964.

Drake, C. L., M. Ewing, and G. H. Sutton, Continental margins and geosynclines: The east coast of North America, north of Cape Hatteras, *Physics and Chemistry of the Earth*, vol. 3, pp. 110–198, Pergamon Press, London, 1958.

Eardley, A. J., *Structural Geology of North America*, Harper and Row, New York, 1962.

Girdler, R. W., and G. Peter, An example of the importance of natural remanent magnetization in the interpretation of magnetic anomalies, *Geophys. Prosp.*, *8*(3), 474–483, 1960.

Karunakaran, C., K. K. Ray, and S. S. Saha, A new probe into the tectonic history of the Andaman and Nicobar Islands, *International Geological Congress, Report on the Twenty-Second Session, India*, 1964, ed. B. C. Roy, Volume of Abstracts, Section 4, p. 45, New Delhi, 1964.

Peter, G., D. Elvers, and M. Yellin, Geological structure of the Aleutian trench southwest of Kodiak Island, *J. Geophys. Res.*, *70*(2), 353–366, 1965.

Talwani, M., G. H. Sutton, and J. L. Worzel, A crustal section across the Puerto Rico Trench, *J. Geophys. Res.*, *64*(10), 1545–1555, 1959.

van Bemmelen, R. W., *The Geology of Indonesia*, Government Printing Office, The Hague, 1949.

Woollard, G. P., Crustal structure from gravity and seismic measurements, *J. Geophys. Res.*, *64* (10), 1521–1544, 1959.

Woollard, G. P., and W. E. Strange, Gravity anomalies and the crust of the Earth in the Pacific Basin, in *The Crust of the Pacific Basin*, Am. Geophys. Union, Geophysical Monograph 6, 60–80, 1962.

790–089 O—66——9

# The Island Arc System in the Andaman Sea

L. A. Weeks, R. N. Harbison, and G. Peter*

As part of the International Indian Ocean Expedition, the U.S. Coast and Geodetic Survey ship *Pioneer* conducted geological subbottom profiler surveys in the Andaman Sea. These surveys were designed to study the nature of the great Indonesian island arc system between Sumatra and Burma, and to show the possible relationship of these areas as common members of a great structural geologic system.

*Geologic history and tectonic development.* The Indonesian arc has developed landward of its associated submarine trench. This feature is typical of all arc-shaped island chains. For this reason, the origin of island arc trenches is believed to be closely associated with crustal movement. This view is further substantiated by the fact that earthquakes commonly occur along trenches, with their foci deepening markedly landwards to over 200 miles in depth. Volcanoes also occur in parallel lines along many of the trenches, and lie approximately over the zones of intermediate focus earthquakes or landward of the trenches. In the Andaman Sea, volcanoes are present landward of the outer sedimentary island arc. The tectonic development and patterns of the Andaman Sea region are discussed in an east-to-west direction.

The Malay peninsula is the tectonic continuation of the eastern Burma fold-mountain system, which eventually swings eastward, parallel to the island arc system, into Borneo. The main fold axes in the south trend a little west of north, changing perceptibly to east of north at the Thailand-Burma border. These structural trends are at an acute angle to those of the island arc and are nowhere exactly parallel to them. The Mergui Archipelago along the coast of Burma is moderately faulted, and has been slightly submerged in geologically recent times (Chhibber, 1934). The Malacca Strait and adjoining Sunda shelf also were submerged during Recent times.

A large fault, striking north-south through central Burma, extends seaward in the Gulf of Martaban. In the 1964 *Pioneer* survey, the subbottom profiler sections did not extend far enough east to detect this fault under the Andaman Sea. However, the bathymetry of the eastern Andaman Sea shelf and the magnetic observations suggest its presence. Differences in structural grain between the Malay peninsula and trends of the island arc to the west could be accounted for by such a fault, downthrown to the west.

The Malay peninsula came into existence in the Mesozoic by cycles of diastrophism radiating out from an older center of orogeny to the east. This Triassic-Jurassic orogeny is evidenced by folding of earlier sediments and intrusions of granites.

The sedimentary oil-producing basins of Sumatra and Burma (backdeep) are interconnected through the Andaman Sea, and terminated on the east by a common fault or by the abruptly sloping "basement rocks" of the Malay peninsula. According to Krishnan (1960), the Andaman Sea probably took shape at the end of the Cretaceous.

West of the peninsula and the backdeep basin zone is the Cretaceous-folded belt or inner volcanic arc. This belt is traceable from central Burma, across the Irrawaddy delta, through Narcondam and Barren Islands and Invisible Bank, into the volcanic Barisan Range of Sumatra, and through Krakatoa and the Indonesian islands. The main orogeny, at the end of the Cretaceous, folded and thrusted the pre-Tertiary sediments to the southwest. Uplift and emplacement of batholiths followed. In Sumatra, the whole length of the Barisan Range was affected by later elevation during the Plio-Pleistocene (van Bemmelen, 1949). The Semangko graben (rift) zone developed as a post-elevation collapse feature. The whole inner volcanic-arc belt comprises a positive isostatic anomaly.

Across an intervening inner sedimentary trough or interdeep, the next belt west is the nonvolcanic outer-island arc. It is traceable from the eastern Himalayan arc southward through eastern India, Burma, the Andaman and Nicobar Islands, and the islands west of Sumatra. This Tertiary-folded belt is the outer island arc of today. The rocks are predominantly marine sediments which

*Institute for Oceanography, U.S. Environmental Science Services Administration.

have been uplifted, folded, and faulted. The belt is isostatically negative, indicating a deficiency of mass—in direct contrast to the inner volcanic arc.

West of the outer island arc is the foredeep. In the south this feature is called the Java Trench. As a morphological feature the trench does not extend north of Simalur Island (3°N). It is not present off the Andaman and Nicobar Islands (van Bemmelen, 1949). However, based on the 1964 *Pioneer* survey work, the trench appears to be present as a buried structural feature off the Andaman and Nicobar Islands. Horizontal movements in the northern part of the Andamans are believed to have occurred earlier than in the southern part. There is a definite gradation from coarse to fine sediments in Eocene beds from north to south. Therefore, these beds are believed to be older than the equivalent belt farther south along the Indonesian chain. Westward thrusting of the outer-island-arc geanticlines had more or less ceased prior to the Miocene—as indicated by Miocene sediments that rest unconformably on older rocks and are hardly folded (van Bemmelen, 1949). Subsequent elevation of the outer island arc in the Quaternary has resulted from vertical uplift combined with a post-glacial eustatic rise in sea level.

Van Bemmelen (1949), in his classic synthesis of the geology of Indonesia, ascribed variations along various portions of the same structural belt to the fact that different orogenic centers or foci were involved. He believed the Andaman Sea belts developed from a different orogenic focus than did the areas to the south and north. Northern Sumatra (Atjeh section), near which the *Pioneer* ran several geophysical tracklines, belongs to the same orogenic focus as the Andaman Sea.

*Subbottom profiling results.* Subbottom profiling was accomplished along five sections that cross the structural belts of the island arc system in the Andaman Sea (fig. 95 [1]). Figure 96[2] shows sections 1, 2, and 3 in the northern part of the Andaman Sea at approximately 10°N, 12°N, and 15°N, respectively. Figure 97[3] shows sections 4 and 5 just north of Sumatra. Section 5, the southernmost, is confined to the backdeep. Section 4 extends from the backdeep to the axis of the outer island arc. Section 1, a discontinuous profile section, extends from the backdeep to the foredeep along the Ten Degree Channel just north of Car Nicobar Island. Section 2 extends from the backdeep to the east flank of the outer island arc at Ritchie's Archipelago, just east of Middle Andaman Island. Section 3, the northernmost, extends from the backdeep in the vicinity of the Tenasserim coast of Burma, across the submerged Irrawaddy Delta to a point just south of Preparis Island, and then northwest across the outer island arc.

The sections, as interpreted, show form lines of the structure and approximate thicknesses of sedimentary layers. Some of the faults indicated on the sections were obvious on the subbottom profile records. Others were inferred because of the attitude of the beds and the structurally complex geology of the area. Fault planes and the direction of movement along faults are less definite.

The horizontal scale of the interpreted sections is based on the ship's position fixes. These were made at 30-minute intervals while traveling at a speed of about 5 knots. Hence, each fix-point marked on the sections is separated from the adjacent fix by a 30-minute time interval—regardless of the number assigned to it—and the horizontal scale is approximately 5 nautical miles between every two fix-marks. Analysis and interpretation of the GEP results preceded the receipt of adjusted fix-locations by many months, but the differences between the true or corrected trackline and the section tracklines (as illustrated) are relatively slight.

Penetration depths are uncorrected for sound velocity. The scale of the sections is based on a velocity of 5,248 feet per second or 1,600 meters per second. Where "lower velocity" sediments overlie or are adjacent to "high velocity" rocks, any single velocity assumption is incorrect. A higher estimated velocity would increase the thicknesses of sediments penetrated, perhaps as much as 50 percent in some cases. Bottom depths varied greatly throughout the Andaman Sea, therefore instrumental scale shifts were frequent. The results of the Geological Echo Profiler survey are discussed from south to north.

*Northern Sumatra—Sections 4 and 5.* The two profiles across the northern tip of Sumatra were made in order to cross known trends of major proportions. Section 4 starts on the east flank of the outer island arc, which can be seen to plunge steeply into the interdeep. Perhaps clear evidence of sedimentation is lacking due to the ruggedness

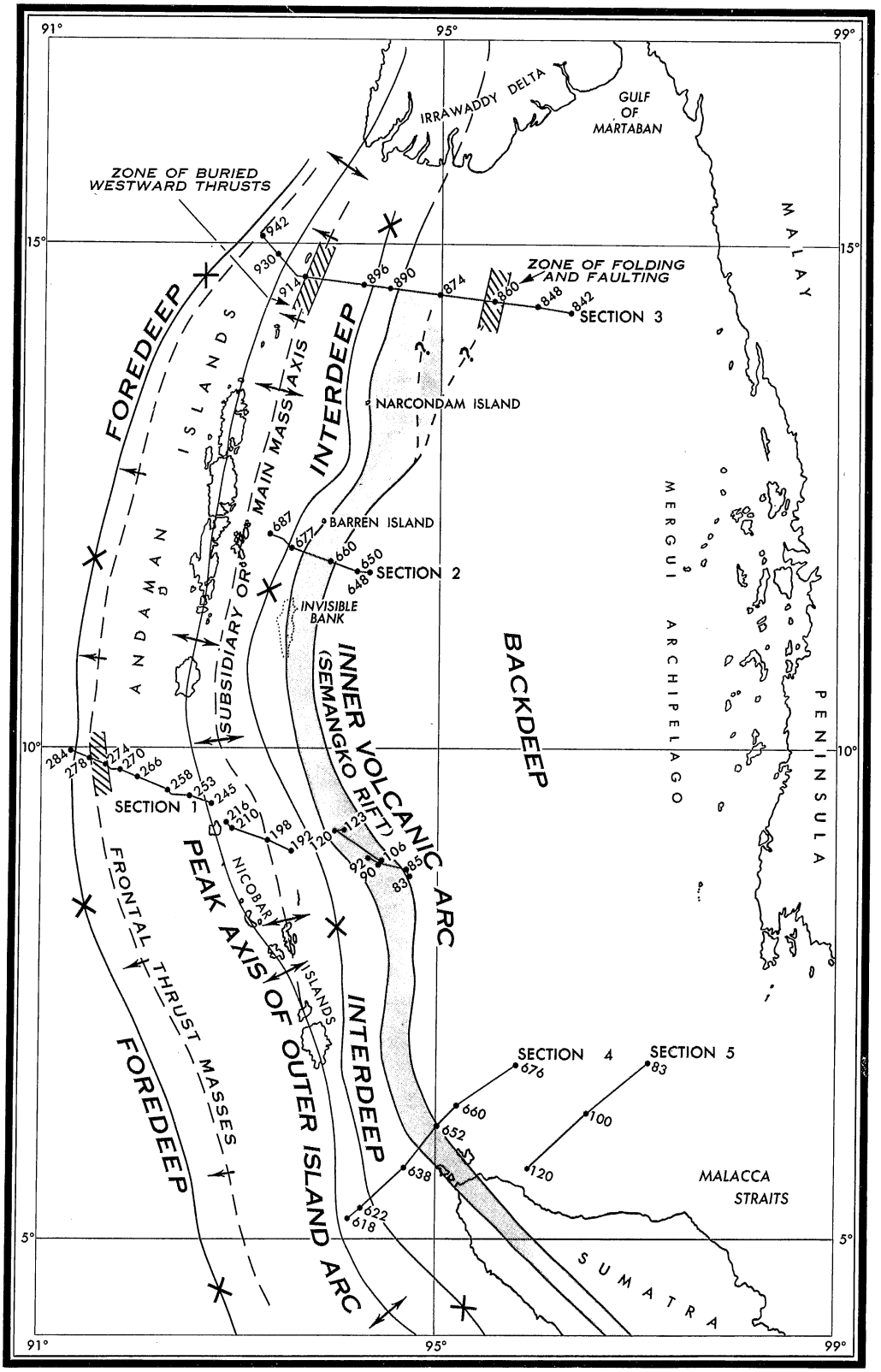


FIGURE 95[1].—Diagram showing structural belts of the Andaman Sea region and location of subbottom profile sections.

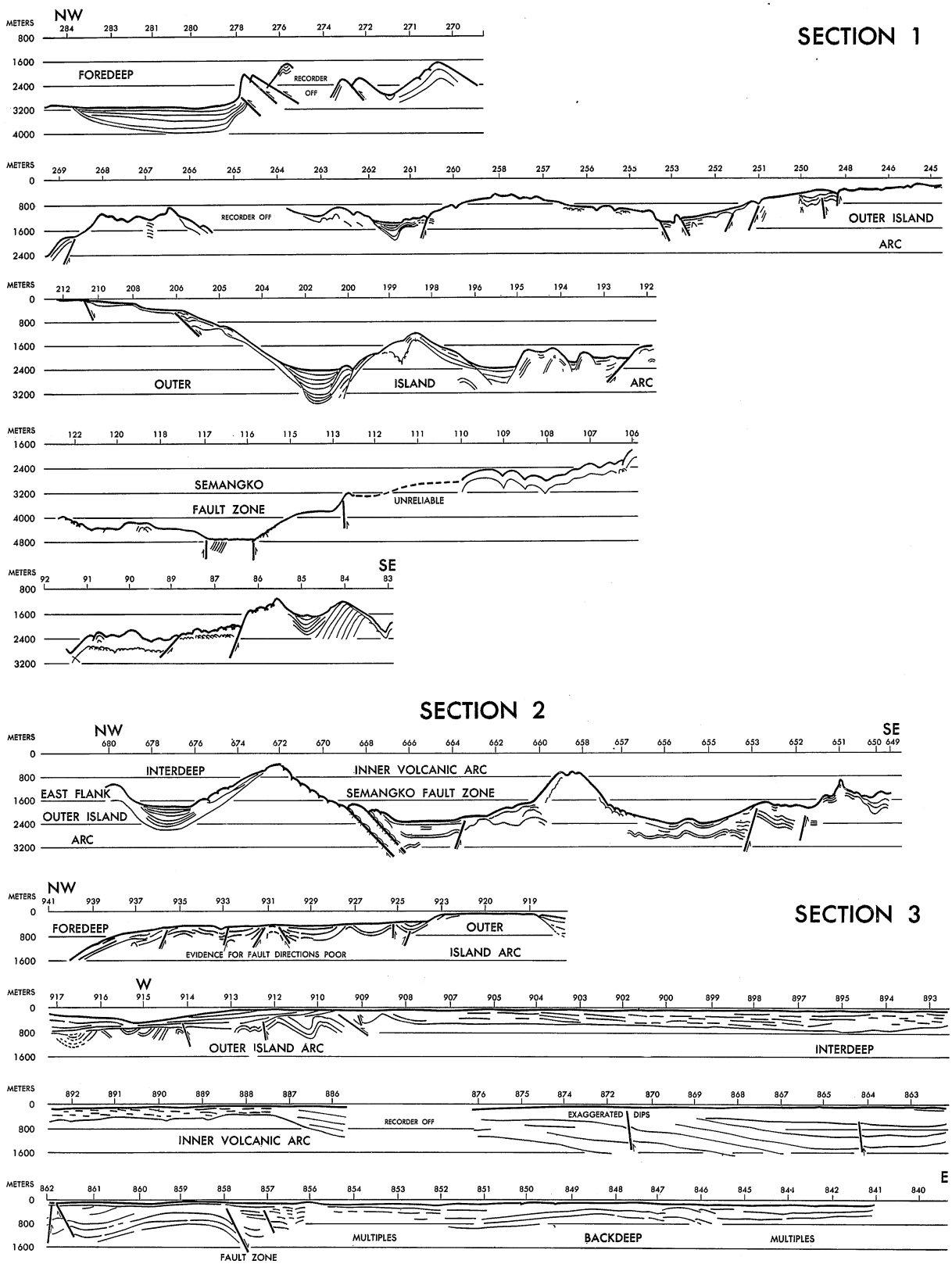


FIGURE 96[2].—Subbottom profile sections: 1, along Ten Degree Channel; 2, at Ritchie's Archipelago; and 3, south of Irrawaddy Delta.

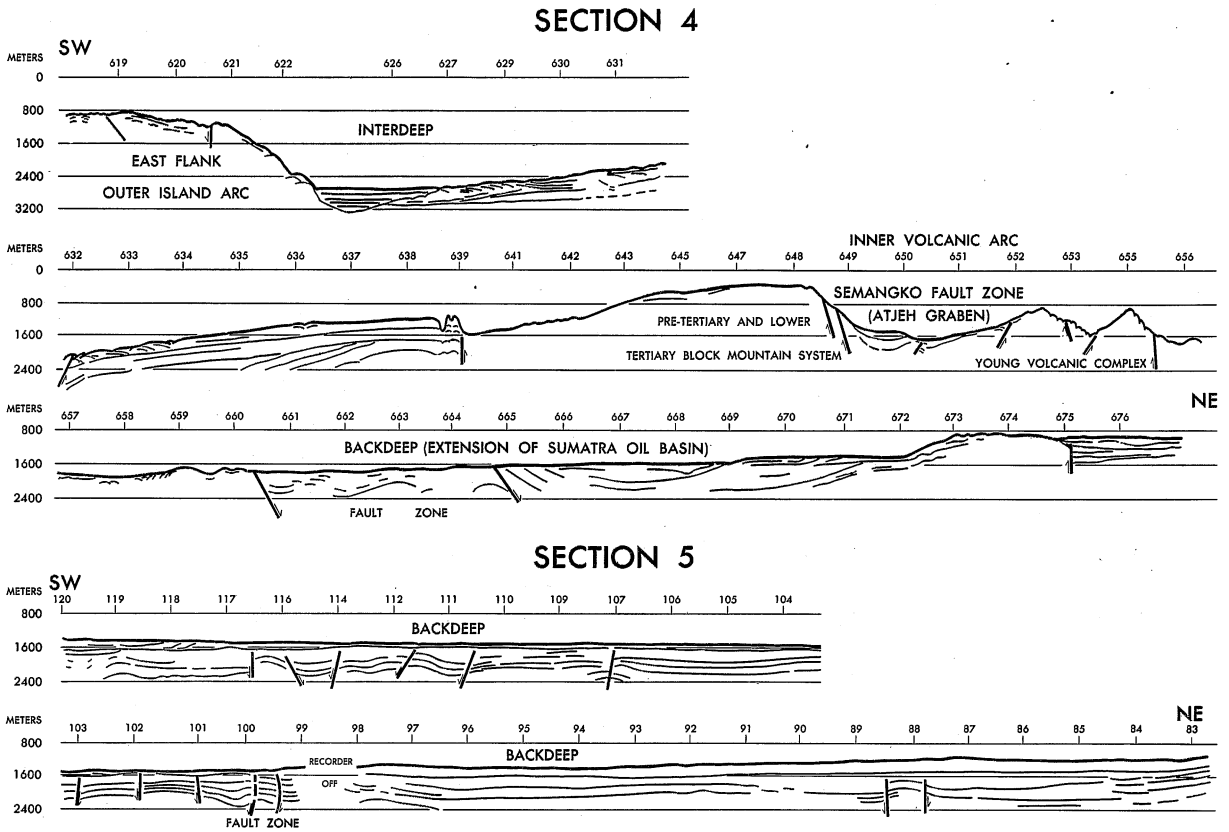


FIGURE 97[3].—Subbottom profile sections 4 and 5 north of Sumatra.

and steepness of the slope, but bedding can be seen at the top of the arc along with some indications of faulting. Simalur Island, to the south, is a geanticline cut by north-south trending transverse faults (van Bemmelen, 1949). From the interdeep to fix 639, several unconformities are detectable between upper and lower beds. Sediments to the southwest of fix 639 in section 4 disappear against hard bedrock or volcanics to the northeast (see subbottom profile, fig. 98[4]). The mass to the northeast is the western block of the inner volcanic arc—a horst. A fault is postulated, upthrown to the northeast.

The portion of section 4 from fix 639 to 648 represents the offshore continuation of the Pre-Tertiary and Lower Tertiary Block Mountain System of northern Sumatra. The block is represented by the western side of the Atjeh graben and the islands west of the Bengal Passage. There is a lack of obvious bedding on the GEP records, probably owing to the dense nature of the rocks which on Sumatra are primarily Permo-Carboniferous (undoubtedly metamorphosed) with diabase and serpentines (Geologic Maps of Indonesia). The Atjeh graben, part of the Semangko fault zone which runs the length of Sumatra, shows up very clearly. It is considered to be a relaxation feature after the Plio-Pleistocene uplift in the Barisan Range (van Bemmelen, 1949). On Sumatra, the graben is filled with Neogene (Pliocene and Mio-

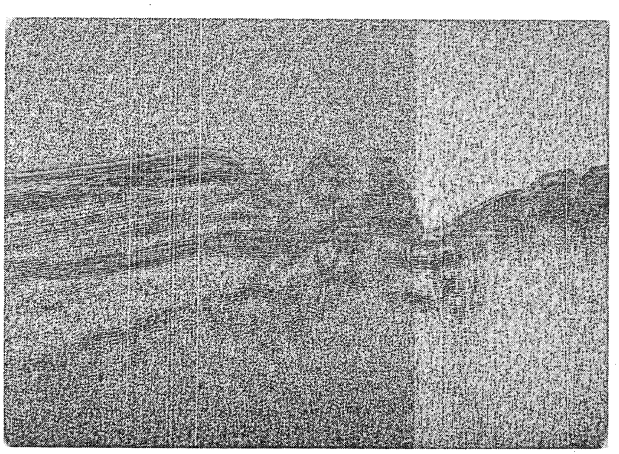

FIGURE 98[4].—Subbottom profile at fix 639 of section 4. Sediments to the southwest (left) disappear against hard bedrock or volcanics to the northwest (right).

cene) sediments overlain by Quaternary and alluvial deposits, and extends into the Bengal Passage. East of the graben in Northern Sumatra, the rocks are primarily young volcanics, identified as andesite effusives, and as block mountain structures similar to those on the west side. The whole belt from fix 639 to 656 represents the inner volcanic arc, complicated by the Semangko fault zone.

To the northeast of the inner volcanic arc lies the backdeep. This is the Andaman Sea extension of the Sumatra oil basin. Folding and faulting are evident. In this area, and in Sumatra also, the tendency is for structural complexity to decrease away from the inner volcanic arc. The area between fixes 660 and 665 is more contorted than to the northeast. Fix 665 to 673 represents a broad synclinal trough, although the bottom rises gradually to the northeast. Beyond fix 673, northeast to the large fault at fix 675 (see subbottom profile, fig. 99[5]), subbottom reflections disappear. This leads to the interpretation that the "basement" or volcanic rocks are faulted against approximately 1,600 m of sediments. The fault does not reach the sea floor, which is often the case within the areas of survey in the Andaman Sea. Northeast of the fault, the basal sediments can be seen to dip into the fault, whereas the upper beds overlap the fault and the so-called "basement" or volcanic rocks. The records show an old channel above the fault plane that probably was cut into the softer materials at that point. The fault is an older feature covered by younger sediments.

Section 5 lies about 50 nm (93 kilometers) southeast of section 4. It was planned to cover the backdeep, to include trends found on section 4, and to detect the fault found at the end of the more northern section (fix 675). The southwestern part of the section shows subbottom folding and faulting unconformably beneath a thin veneer of surface deposits. The surface veneer is relatively flat, except at fix 118. Between fixes 99 and 100 a large fault zone was encountered. The large fault encountered on section 4 (fix 675) does not appear to be present on section 5. A similar relationship of "basement" or volcanic rocks to sediments was not found. If the fault were present, it would intersect section 5 between fixes 95 and 105, providing it remained parallel to the trend of the other structures. On the other hand, if the fault, which appears to be a major feature, paralleled the eastern shelf of the Andaman Sea and then veered southwest, it would be possible for it to intersect section 4 but not section 5. That would indicate that the fault was controlled by the Malay peninsula structural grain, rather than by the younger structural grain of the island arc. However, one would expect such a fault to be downthrown to the west, rather than to the east. A scissors fault, alternately downthrown to east and west, is one possible explanation. Section 1 to the north did not extend far enough east to record the fault feature. Consequently, its extent and true significance are not known.

FIGURE 99[5].—Subbottom profile at fix 675 of section 4. Basement or volcanic rocks on left abut against sediments on right. A fault separates the contrasting subbottom structural features at depth, but is covered by overlying sediments at the sea floor.

Northeast of fix 99, the remainder of the backdeep section shows a folded subbottom, in part unconformably overlain by surface deposits. At the northeast end of the section, the bottom and subbottom deposits show a conformable relationship and rise onto the Andaman Sea shelf.

*Ten Degree Channel—Section 1.* Section 1, the first profile run in the area, frequently was interrupted for oceanographic stations. Consequently, this profile was not continuous and some important features were missed. The section from fixes 245 to 284 includes structural features of the western outer-island arc (Nicobar Islands), west of the Ten Degree Channel. From fix 272 to 284, the GEP record indicates block structures that are thrust to the west against a basin, the ancient foredeep. The bathymetry west of fix 284 indicates gradual shoaling. The greatest depths are adjacent to the thrust blocks. The Java Trench (foredeep) terminates considerably south of this area and does not appear as a deep trench on any crossings of the foredeep. However, the deepest water

is always adjacent to the western limit of the outer island arc. It seems probable that later sedimentation filled the foredeep west of the Andaman and Nicobar Islands.

From fix 245 to the thrusted blocks at fix 278, the nature of the western flank of the outer island arc is evident. The shelf is rugged and youthful in appearance, both structurally and topographically, which one would expect from an island mass which has emerged so recently. Bottom depth increases approximately 2,400 m between fixes 245 and 284, in a distance of 92 nm (170 km).

There is a 16½-nm gap (31 km) between fixes 245 and 212. Both positions represent the same structural trend along the outer island arc and can be considered essentially equivalent. The youthful and structurally complex area from fix 192 to 212 is the eastern flank of the outer island arc. Bathymetric data show its continuation a short distance southeast of fix 192. The total width of the outer island arc in this sector is about 100 nm (185 km). The maximum width of Car Nicobar Island, near which the survey passed, is 7 nm (13 km). The sea floor base of the outer island arc is many times this width. East of the outer island arc, the bottom is rough and the subbottom structure has a youthful appearance. Just south of this traverse the Nicobar Islands are broken up into several groups with trends that apparently extend northward.

Fixes 192 and 122 were 30 nm (56 km) apart. Subbottom profiles were not obtained between these fixes, but continuous depth soundings were made.

Bathymetric data indicate that the bottom rises rapidly to a depth of less than 180 m just southeast of fix 192. The bottom then plunges rapidly towards the interdeep where depths of about 4,100 m were observed. It rises again to the western block of the inner volcanic arc west of fix 120. The bottom of the graben valley (Semangko Rift) is found between fixes 116 and 117 at a depth of around 4,800 m. This is deeper than the interdeep by about 700 m. Lack of subbottom penetration prevented delimiting the graben valley between the faults. Also, the survey line did not cross structural trends at right angles. This gives the section the appearance of greater width. The peak of the eastern block of the inner volcanic arc appears at fixes 84 to 86. The western block lies between fixes 120 and 192, as does the interdeep. The backdeep lies a short distance east of fix 83.

*Ritchie's Archipelago—Section 2.* Section 2 was run south of Barren Island and extends west to Ritchie's Archipelago, which lies just east of the Andaman Islands. This section and section 4 show the structure of the inner volcanic arc and associated rift valley very well. Fix 680 is over the east flank of the outer island arc. The interdeep is evident, with some 800 m of sediments in its structural trough. The peak at fix 672 is the western part of the inner volcanic arc. This feature lies approximately halfway between Invisible Bank and Barren Island, both of which are part of the inner volcanic arc (western flank). The area between fix 672 and 658 is a continuation of the Semangko rift valley found both onshore and offshore Sumatra (section 4). A large fault may be present at fix 660 along the steep slope, but the records provide inconclusive evidence. Tipper (1911) is of the opinion that Barren and Narcondam Islands have emerged along a master fault zone east of the Andaman Islands. However, both Barren and Narcondam Islands, as well as Invisible Bank, form only one side of the inner volcanic arc.

Southeast of fix 658, the GEP profile and bathymetric data indicate another ridgelike area. Sediments are more abundant than on the flanks of the volcanic arc. Except for a possible small intrusive at fix 651, volcanic or basement-type rocks appear to be lacking. This ridge does not extend very far either north or south of this section.

*Irrawaddy Delta—Section 3.* Section 3, the northernmost traverse made in the Andaman Sea, crossed the submerged extension of the Irrawaddy Delta from the Tenasserim coast of Burma. At a point just south of Preparis Island, the east-west traverse turned northwest to its termination.

The western part of section 3 shows the western slope of the outer island arc. At the western limit, the slope plunges steeply seaward in the foredeep area. Faulting and folding are not noticeable along the flat sea floor of this slope. This is typical of the northern traverse of the Andaman Sea, even where the underlying structure is complex. A small channel at fix 933 is the only indication of any structural control between fixes 923 and 935. Subbottom profiling shows the structural complexity of the wide belt from fix 937 to 909, a distance of 38 nm (70 km). This is the outer island arc, with its apex apparently

at fix 920 (see subbottom profile, fig. 100[6]). East of fix 919, the subbottom features are even more complex. Here younger sediments lie unconformably on the older folded rocks of the outer island arc. Perhaps this is the pre-Miocene unconformity. Thrusting presumably ended before Miocene time in the outer island arc (van Bemmelen, 1949). The younger beds are undoubtedly part of the massive Irrawaddy Delta. The Irrawaddy River deposits two-thirds of a million tons of silt per day on its rapidly building delta. Protection from the open sea and lack of effective longshore currents are favorable to the delta's advance to the south.

Fixes 908 to 888 show the gradual descent of the bedrock to the interdeep at about fix 895, and gradual rise of the bedrock to the inner volcanic arc at fix 888. The deepest or basal reflection is a composite, and is not intended to be construed as a continuous reflection. Single beds cannot be followed very far. The highest free-air gravity value along the entire traverse occurs at fix 888. The extent of the traverse is covered by deltaic deposits. Lack of subbottom penetration beneath the bedrock prevents any interpretation of the underlying features.

East of fix 886, GEP equipment failure prevented obtaining data for 16 nm (30 km). Hence, it was impossible to define the rift valley (Semangko fault zone), which may be buried at depth by overlying sediments. The inner volcanic arc does not appear to be as well-developed here as it is farther to the south (sections 2 and 4). Attenuation of sparker energy through the soft overburden can mask some features, but the main reason could be the volcanic arc's more mature topography to the north. There are several indications that the island arc becomes younger to the south. Deltaic deposits are not likely to have covered a youthful feature of such relief.

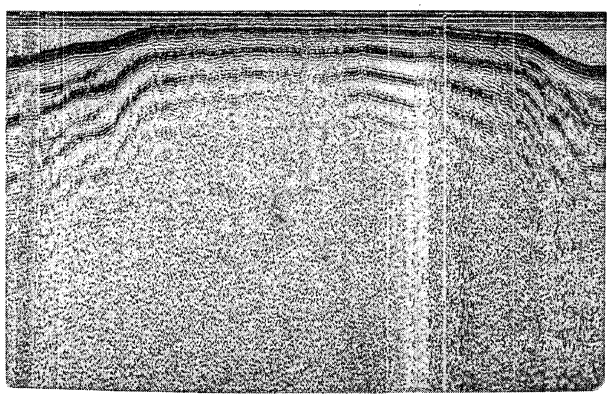

FIGURE 100[6].—Subbottom profile at fix 920 of section 3 showing apparent ridge crest of outer island arc in northern Andaman Sea.

East of fix 887, the beds appear to dip gently to the east with occasional faults. The uppermost or surface beds lie unconformably on the older sediments. Whether all the reflections represent deltaic deposits is uncertain. If the basal beds are of deltaic origin, the faults, although older than the surface sediments, must be very recent. Between fixes 857 and 862, an interesting subbottom structure was developed. Conclusions about this feature are not definite. Several possibilities exist. It may be just a folded section of the backdeep or it may represent the eastern segment of the inner volcanic arc, whose "twin nature" was noted to the south. Free-air gravity and magnetic intensity both show an increase at this point. Thin surface beds unconformably overlie the folded sediments.

If this folded section is the eastern block of the inner volcanic arc, then there is considerable divergence going north from the Ritchie's Archipelago traverse (section 2). Off Sumatra and off Ritchie's Archipelago, the distance between segments was similar, about 20 nm (37 km). On this traverse, the segments may be separated by as much as 61 nm (113 km), or three times as much. However, it appears more likely that the eastern segment, if still existent, lies within the 16-nm (30 km) area of no records between fixes 876 and 886.

The remainder or eastern portion of the traverse is not particularly striking. It contains gently folded beds, presumed to be deltaic deposits. The records contain multiple reflections and these may mask some features.

*Conclusions.* The comparison of subbottom profiles, bathymetry, and gravity and magnetic measurements in the Andaman Sea leads to some interesting conclusions. Again, each structural belt is discussed from east to west.

I. The Backdeep: The typical structure of the backdeep is shown in sections 4 and 5. In section 3, which also traverses the backdeep, the subbottom features are masked by the cover of deltaic sediments. In general, the structural features of the backbelt are less complex than those of the belts to the west, but some large anticlines, synclines, and fault zones are present. The largest anticline was recorded off the Sumatra coast between fixes 100 and 105 of section 5. Its width

was about 14 nm (26 km). This feature could be of impressive size—depending on its extent normal to the section. Numerous faults were recorded across this anticline and it appeared to terminate against a fault zone to the northeast at fix 100. A smaller anticline is present between fixes 111 and 115. This feature is about 7 nm (13 km) wide and also is faulted. In the backdeep portion of section 3, two anticlinal structures were observed, one 12½ nm (23 km) wide between fixes 845 and 851 and the other 8 nm (15 km) wide between fixes 858 and 861. Both are overlain by flat-lying beds of sediment which rest unconformably on the subjacent beds.

The backdeep consists primarily of sedimentary beds. In most instances, the sedimentary sequences exceed 800 m in thickness. Suspected volcanic or "basement" rocks were found only between fixes 673 and 675, section 4. The greatest water depths at which the backdeep was observed occur at fix 658 of section 4 and at fix 656 of section 2, adjacent to the inner volcanic arc.

II. The Inner Volcanic Arc and Semangko Rift Valley: The inner volcanic arc and Semangko rift valley was the most interesting structural feature observed in the Andaman Sea area. On land, the rift valley can be traced some 1,100 nm (2,040 km) through the entire length of Sumatra. During the 1964 *Pioneer* cruise, by means of geological echo profiling, it was traced nearly 600 nm (1,110 km) north of Sumatra through the Andaman Sea. Free-air gravity values also indicated the presence of the rift valley beneath the sediments of the Irrawaddy Delta, but the subbottom structural detail along the traverse in this area (section 3) could not be resolved beneath some 400 m of sediments.

The width of the rift valley, as determined by the east-west traverses between northern Sumatra and Ritchie's Archipelago, was observed to be 5 to 10 nm (9¼–18½ km) between the bounding faults and 20 to 25 nm (37–46 km) between the bounding ridge crests. The valley relief, between adjacent ridge crest and valley floor, was observed to be 1,200 m off Sumatra (section 4) and nearly 2,000 m at section 2. The western ridge of the inner volcanic arc rises higher above the sea floor and is a more massive feature than the eastern ridge. Narcondam and Barren Islands and Invisible Bank are part of the western structural elements of the inner arc system.

The magnetic and gravity results in the Andaman Sea area provide further evidence of the submarine continuation of the inner volcanic arc. A broad magnetic high belt extends from the tip of Sumatra to section 3 (see paper by Peter, Weeks, and Burns, pages 91 to 107). This belt broadens northward to Narcondam Island and then narrows before it crosses section 3. Gravity maxima of over 50 milligals occur just off the tip of Sumatra and at Invisible Bank, Barren Island, and Narcondam Island. The highest free-air values of over 100 mgal were observed at Invisible Bank and Barren and Narcondam Islands—a value of over 150 mgal being found at the south end of Invisible Bank. Interesting structural similarities of the Andaman Sea inner volcanic arc and the Mid-Atlantic Ridge are compared in table 20[1]. The Mid-Atlantic Ridge is a much longer structural feature and is not part of an island arc development, but the rift valleys and many related tectonic features are common to both the Mid-Atlantic Ridge and Andaman Sea inner volcanic arc.

III. The Interdeep: The interdeep is the structurally depressed belt between the two major up-

TABLE 20[1].—*Similarities of Andaman Sea inner volcanic arc and central part of Mid-Atlantic Ridge*

| Andaman Sea Inner Volcanic Arc | Mid-Atlantic Ridge |
|---|---|
| Volcanic rock types—serpentine, diabase, andesite. | Volcanic rock types—serpentine, basalt, diabase. |
| Earthquake belt—zone of epicenters. | Earthquake belt—zone of epicenters. |
| Prominent rift valley. | Prominent rift valley. |
| Adjacent high mountains. | Adjacent high mountains. |
| Peaks above sea level—Narcondam and Barren Islands. | Peaks above sea level—Iceland, Tristan da Cunha. |
| Considerable relief between rift valley and adjacent peaks. | Considerable relief between rift valley and adjacent peaks. |
| Width of rift valley 20 to 25 mi from peak to peak. | Width of rift valley 15 to 30 mi from peak to peak. |
| Depth to floor of valley varies between 5,000 and 15,000 ft where crossed by profiler. | Depth to floor of valley averages 12,000 ft. |
| Caused by normal faulting due to extension or relaxation of the crust. | Caused by normal faulting due to extension or relaxation of the crust. |
| High ratio of length to width. | High ratio of length to width. |

lifts of the island arc system. Its appearance is similar along the north-south extent of the arc except in the north where deltaic deposits have masked many of its features. Just off Sumatra (section 4), some 700 m of flat-lying sediments fill the depression (interdeep) between the two arcs. The eastern slope of the outer island arc is steeper than the western slope of the inner volcanic arc and may have been the source of most of the sediment. To the south, the interdeep separates Sumatra and the offshore Mentawai Islands. The interdeep was not profiled in the Ten Degree Channel (section 1), but is indicated by the bathymetry on several other traverses made by the ship.

Off Ritchie's Archipelago, east flank of outer island arc in section 2, the narrow and downwarped interdeep is filled with sediments that appear to have been deposited from both flanks and folded in the form of a syncline as the downwarping continued. In section 3 off the Irrawaddy Delta, the broad interdeep lies between flanks with very slight slope and is filled with sediments that mask its topographic expression on the sea floor.

IV. The Outer Island Arc: The outer island arc is composed of predominantly sedimentary rocks. It is the youngest geologic feature of the whole Andaman Sea structural system. It continues north of section 3 as the Arakan Yoma Mountains of western Burma, and finally abuts against the eastern Himalayan arc along the Burma-India border. To the south, the outer arc includes the Mentawai Islands off Sumatra and submarine ridge landward of the Java Trench.

The outer arc is structurally complex. It has the overall features of a large geanticline. Its width exceeds 100 nm (185 km) in places. Near the Irrawaddy Delta the width narrows before entering Burma, but to the south, between Barren and Narcondam Islands, a distinct bulge to the east is indicated by the bathymetric data taken by the *Pioneer*. The subbottom profiles of sections 1 and 3 suggest westward thrusting of the outer arc. The apparent thrust ridges of section 1 can be traced northward by the bathymetric data. The presence of other ridges with long, straight, east-dipping slopes also suggests westward thrusting.

Gravity measurements show a negative free-air anomaly approximating the peak axis of the outer island arc. The peak axis of the arc and the negative gravity axis correlate exactly at the south end of the index map (fig. 95[1]). At 8°00′N and 93°30′E, the negative gravity axis veers east of the Nicobar Islands. It continues east of the islands and again joins the peak axis of the outer islands as it enters Burma. The trend labeled "subsidiary or main mass axis" on the index map marks the negative gravity axis north of 8°N. A belt as wide as the outer island arc and tilted westward would be expected to have its main mass axis lying eastward of its surface peaks (Nicobar and Andaman Islands). The zone of westward thrusts on section 3, Ritchie's Archipelago (southwest of Barren Island) and the cluster of islands at 8°00′N and 93°30′E, are considered part of the subsidiary trend, coinciding with the negative free-air anomaly.

Results of survey: The geophysical investigations of the 1964 USC&GSS *Pioneer* Indian Ocean Expedition provided much new data about the geologic features of the Andaman Sea area, particularly the submarine tectonic patterns and crustal development of the area. The subbottom profiles made it possible to delineate the major segments of the island arc system over a distance of more than 600 nm (1,110 km) and provided detailed information about the structural relationships of the basement and overlying rock complexes in the major structural belts—foredeep, outer sedimentary island arc, interdeep, inner volcanic island arc, and backdeep. Continued detailed analysis of the vast amount of geophysical data obtained in the Andaman Sea area and correlation of the 1964 results with results of other surveys can be expected to yield many new discoveries of scientific significance.

## References


Chhibber, H. L., *The Geology of Burma*, Macmillan & Co., 1934.

Geologic Maps of Indonesia, Scale 1:1,000,000.

Krishnan, M. S., *Geology of India and Burma*, 1960.

Tipper, G. H., Geology of Andaman Islands with reference to Nicobars; *Mem. Geol. Surv. Ind.*, vol. 35, pt. 4, pp. 195–213, 1911.

van Bemmelen, R. W., *The Geology of Indonesia*, vol. 1A, Government Printing Office, The Hague, 1949.

# Sea Bottom Heat-Flow Measurements in the Andaman Sea*

ROBERT E. BURNS †

The participation of the USC&GSS *Pioneer* in the International Indian Ocean Expedition included a major geophysical investigation of the Andaman Sea during April and May of 1964. A program of heat-flow measurements was motivated by known volcanism within the basin, indications of warmer bottom water than can be explained by simple adiabatic heating, and a general lack of data on the major seismic belt that runs through the Andaman-Nicobar area from Burma into Sumatra.

As part of operations in the area, four successful measurements were made of the heat flow associated with the inner or volcanic trend of the primary arc that encloses the Andaman Sea (see fig. 87[8]). A modified form of the thermograd [Gerard et al., 1962] was used to obtain a recording of the temperature gradient in the bottom sediment and a core, from which the coefficient of thermal conductivity of the bottom sediment can be determined. The heat flow defined here is a flow per unit area; it is determined as the product of the temperature gradient in the bottom sediment and the thermal conductivity of the sediment.

The temperature gradient in the sediment is determined by three thermistors fastened to the barrel of a coring tube at a fixed vertical separation of 104 cm. The thermistors are switched into a Wheatstone bridge circuit in alternating sequence with fixed-calibration resistors. The temperature at the penetration depth of each thermistor is determined as a function of the current flow in the bridge circuit, which is recorded on film.

The thermistors were calibrated both before and after the operation in the Andaman Sea. On the basis of these two calibrations, an error in absolute temperature of 0.05°C could be present in the measurements. However, an additional calibration of the thermistors was made at each station by comparing the thermistor-indicated temperatures of the near-bottom water both before and after the coring device penetrated the bottom. The maximum range of indicated temperatures in these comparisons was 0.02°C. Hence, the temperatures used to determine the temperature gradient in the sediment are considered to be precise within ±0.02°C. The separation of the thermistors is known to within 1%.

Since equipment was lacking to make direct measurements of the thermal conductivity of sediment from the core [Von Herzen and Maxwell, 1959], an indirect determination based on the water content of the core sample was used [Ratcliffe, 1960]. Sections were cut from the core at positions corresponding to the location of the thermistors. These samples were then capped and sealed with paraffin. Subsequently, the mean value of thermal conductivity was determined for each station on the basis of water content of the samples and on corrections for bottom temperature and pressure. Special precautions were taken during the procedure to prevent drying of the sediment sample, which might result in related errors in the conductivity values. Such errors are difficult to evaluate, but higher water content in the in-situ sediment samples would result in lower values of thermal conductivity than those given in this report. Examination of the thermal conductivity values indicates that they are comparable at the four stations and are lower than the average reported from other areas [see for example Foster, 1962; Uyeda et al., 1962; Von Herzen and Uyeda, 1963; Yasui et al., 1963]. At each of the stations in the Andaman Sea, all determinations of thermal conductivity were within ±10% of the mean value listed for the station.

The heat flow measured at the four stations in the Andaman basin is shown in table 21[1].

Although significant regional interpretation of the limited data is hardly possible, several observations of interest are noted:

1. The highest heat flow is associated with the deepest portion of the basin (station A-I), and, for the measurements available, it correlates with depth. Von Herzen and Uyeda [1963] considered the effect of irregular rock surface buried by sediments and proposed that heat from the interior will flow out preferentially from the thinly cov-

*Published originally in *Journal of Geophysical Research,* vol. 69, no. 22, pp. 4918–4919, November 15, 1964.

† Institute for Oceanography, U.S. Environmental Science Services Administration.

TABLE 21[1].—*Heat-flow measurements in the Andaman basin*

| Station no. | Location | Depth, meters | Temperature gradient* | Thermal Conductivity† | Heat flow‡ |
|---|---|---|---|---|---|
| A–I | 10°01′N 93°45′E | 4, 206 | 31 | 1. 70 | 5. 27 |
| A–II | 11°01′N 93°42′E | 2, 562 | 13 | 1. 83 | 2. 38 |
| A–III | 11°56′N 93°22′E | 1, 390 | 5 | 1. 79 | 0. 90 |
| A–IV | 12°44′N 93°58′E | 2, 151 | 11 | 1. 76 | 1. 94 |

*$10^{-4}$ °C $cm^{-1}$.
†$10^{-3}$ cal °$C^{-1}$ $cm^{-1}$ $sec^{-1}$.
‡$10^{-6}$ cal $cm^{-2}$ $sec^{-1}$.

ered areas. The deep basin at station A-I would normally be expected to have relatively thick sedimentary fill and consequently a relatively low heat flow. The fact that the heat flow is high indicates a possible lack of thick sedimentary fill in the deeper portions of the Andaman basin.

2. There is no apparent effect reflecting the volcanism at Barren Island (12°16′N, 93°50′E).

3. Initial conclusions on the relationship of heat flow to island arcs [Uyeda et al., 1962; Yasui et al., 1963] have been based on traverses generally normal to the structural trend. The measurements in the Andaman Sea are, on the other hand, all parallel to the major Indonesian primary arc system and have as great a variability as those on which these initial conclusions have been based.

These considerations indicate that the systematic collection of many more heat-flow measurements will be required if the relationships between heat flow and the tectonic patterns and geophysical processes of island-arc structures are to be more fully understood.

## REFERENCES


Foster, T. D., Heat-flow measurements in the northeast Pacific and in the Bering Sea, *J. Geophys. Res.*, *67*(7), 2991–2993, 1962.

Gerard, R., M. G. Langseth, Jr., and M. Ewing, Thermal gradient measurements in the water and bottom sediment of the western Atlantic, *J. Geophys. Res.*, *67*(2), 785–803, 1962.

Ratcliffe, E. H., The thermal conductivities of ocean sediments, *J. Geophys. Res.*, *65*(5), 1535–1541, 1960.

Uyeda, S., K. Hôrai, M. Yasui, and H. Akamatsu, Heat-flow measurements over the Japan trench, *J. Geophys. Res.*, *67*(3), 1186–1188, 1962.

Von Herzen, R., and A. E. Maxwell, The measurement of thermal conductivity of deep-sea sediments by a needle-probe method, *J. Geophys. Res.*, *64*(10), 1557–1563, 1959.

Von Herzen, R. P. and S. Uyeda, Heat flow through the eastern Pacific Ocean floor, *J. Geophys. Res.*, *68*(14), 4219–4250, 1963.

Yasui, M., K. Hôrai, S. Uyeda, and H. Akamatsu, Heat flow measurements in the western Pacific during the JEDS–5 and other cruises in 1962 aboard M/S Ryofu-Maru, *Oceanog. Mag., Japan Meteorol. Agency*, *14*(2), 147–156, 1963.

# Biology

The biological program carried out aboard the *Pioneer* during the vessel's 1964 participation in the International Indian Ocean Expedition consisted mainly of primary marine productivity studies by the Department of Botany, University of Hawaii, Honolulu; horizontal plankton-net tows for the Honolulu Laboratory of the U.S. Bureau of Commercial Fisheries; and vertical plankton-net tows for the Indian Ocean Biological Center, Ernaculam, India. Sightings of birds, aquatic mammals, and fish were recorded on a biological sighting log. One hundred and twenty-nine of these log sheets were annotated and sent to the Honolulu Laboratory of the Bureau of Commercial Fisheries. Vicente B. Alvarez and Quintin Stephen-Hassard of the University of Hawaii joined the *Pioneer* at Honolulu en route to the Indian Ocean to carry out the primary productivity studies and to assist in making horizontal and vertical plankton-net tows (fig. 101). A summary of the accomplishments from the time the *Pioneer* departed Honolulu on February 25, 1964 until it returned there on July 30, 1964 is given in table 22.

TABLE 22.—*Summary of biological sampling accomplishments*

| | |
|---|---|
| Primary productivity stations | 750 |
| Morning | 92 |
| Underway | 643 |
| In situ | 15 |
| Primary productivity samples | 4,688 |
| Seston samples | 784 |
| Pigment samples | 784 |
| BCF horizontal net tows | 116 |
| IIOE vertical net tows | 45 |
| UH 45-centimeter vertical net tows | 92 |

The zooplankton samples collected in the horizontal tows for the U.S. Bureau of Commercial Fisheries were sent to the Department of Zoology at the University of Hawaii for sorting. Material collected from the vertical tows was shipped—from Calcutta, India and Djakarta, Indonesia—to Dr. Vahn Hansen, Curator of the Indian Ocean Biological Center, University Oceanographic Laboratory, Ernaculam 6, South India. Additional biological sampling was accomplished during the dredging operations, SCUBA-diving investigations, and during plankton tows through the deep scattering layer (DSL) in May and June in the Bay of Bengal.

On May 14, the PDR record off the east coast of Ceylon showed the dawn descent of the deep scattering layer. As the layer descended, it separated into three distinct layers at 30, 95, and 150 fathoms. These layers were traced westward to the Ceylon shelf to observe what happened when the layers intersected the steeply rising sea floor. Figure 102 is a photograph of the PDR trace showing the three layers. The top layer, at 30 fms, cleared the bottom and extended shoreward over the outer shelf edge. The middle layer, at 95 fms, intersected the steeply rising sea floor. At this point, the trace was darker and gave the appearance of a dense concentration or "piling up" of organisms on the sea bottom. The bottom layer disappeared at a depth of about 150 fms. The differences noted in the two bottom layers led to investigating the possibility that different organisms might be in-

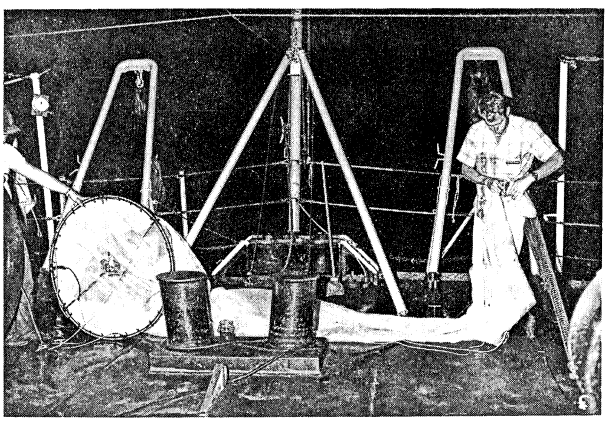

FIGURE 101.—Net used for plankton tows.

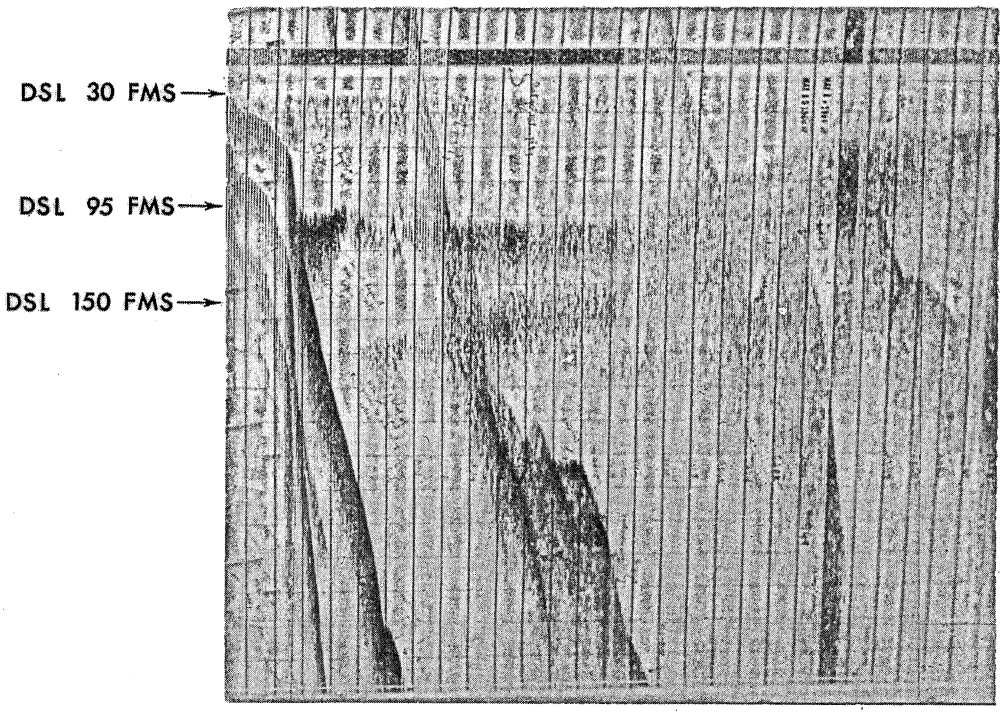


FIGURE 102.—PDR record showing deep scattering layer on morning of May 14, 1964, in Bay of Bengal. Top layer extends over outer shelf edge; middle layer intersects the steeply rising sea floor; and, bottom layer disappears as it descends to greater depth.

volved in each layer and an attempt to sample and photograph each layer at Great Basses Reef off southeast Ceylon on May 18. The deep-sea camera was used in this attempt together with closing plankton-net tows at depths of 120 to 220 fms. The photographs (camera lowering No. 7) did not show any recognizable organisms, but a few shrimp, copepods, and salps were obtained in the new tow. Although separate and distinct scattering layers were recorded on the PDR, the closing-net tows within and outside the layers showed no significant differences.

Corals collected at the Seahorse Shoal (fig. 103), by dredge hauls and SCUBA divers, were forwarded to Dr. Donald F. Squires, U.S. National Museum, Smithsonian Institution, Washington, D.C. Other biological samples from Seahorse Shoal, from Dredge No. 12 (Serial No. 710), and from plankton tows through the DSL on May 18 and June 16 were sent to Dr. I. E. Wallen of the Smithsonian Institution. Work aboard the *Pioneer* relating to the primary marine productivity studies is described in the paper (which follows) by Vicente B. Alvarez, chief of the biological party.

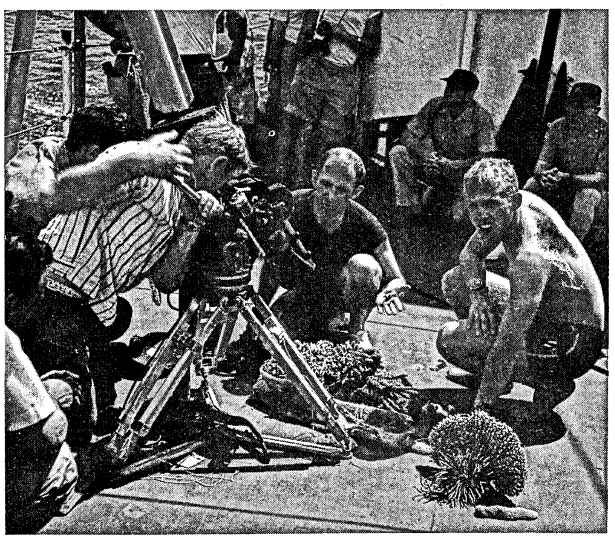

FIGURE 103.—Biological specimens obtained by SCUBA divers at Seahorse Shoal.

# Report on the University of Hawaii Primary Marine Productivity Sampling Program During USC&GS Ship "Pioneer" 1964 Indian Ocean Expedition*

VICENTE B. ALVAREZ †

A primary marine productivity sampling program by the Department of Botany, University of Hawaii was carried out aboard the USC&GS ship *Pioneer* in 1964 during the vessel's participation in the International Indian Ocean Expedition. The University of Hawaii program was conducted in the western Pacific and Indian Ocean during the period February 25 to July 30, 1964, and was supported by funds from the U.S. National Biological Program for the Indian Ocean Expedition, the U.S. Office of Naval Research, and the Graduate Research Committee of the University of Hawaii. The program was under the direction of Vicente B. Alvarez and Quintin Stephen-Hassard, biologists from the University of Hawaii, who also assisted in the overall biological program aboard the *Pioneer*, including the horizontal plankton-net tows for the U.S. Bureau of Commercial Fisheries and the vertical plankton-net tows for the Indian Ocean Biological Center of India.

The objectives of the marine productivity sampling program were: (1) To measure the relative rates of primary food production, that is, the rates at which inorganic materials are converted to organic materials in this part of the world's oceans; (2) to observe interrelationships between the physical, chemical, and biological factors that relate to primary productivity and their variation from place to place; and (3) to study results of different measuring techniques and their implications, such, as differences in observed conditions that could be attributed to the time of sampling.

In the ship's dry laboratory, two 1958-type incubators were placed beside the sink. A galvanized container was made for the incubators and a sea water pipeline was installed to provide discharge into the sink. The two 1962-type incubators were set up on the boat deck where they always were exposed to sunlight. Most of the biological sampling work was done from the fantail of the ship, using the winch on the starboard side. This winch had two drums. On one drum, 3/8-inch steel cable was used for the BCF horizontal net tows. On the other drum, hydrographic cable was used for both the productivity sampling and the vertical net tows. The oceanographic winch, on the starboard bow of the ship, was used for underway sampling to avoid contamination of the samples by the ship's discharges. However, during stormy weather, this sampling operation also had to be done from the fantail.

Primary productivity sampling was commenced on February 27 using twin, 6-liter, plastic samplers (fig. 104[1]). The morning stations were 30 minutes after sunrise. The local zone time was used for the biological records. Prior to sampling time, numbered plastic buckets were set up in the laboratory. Water samples were poured into the buckets from the opaque sea samplers, according to the assigned numbers. At the time samples were obtained, the 47-, 32-, 16-, and 1-percent light penetration, or light intensity, was determined on the sunlit side of the ship using either the Secchi disc or the submarine photometer. Two sets of samples from the morning vertical station were regularly processed; one set representing 47-, 32-, 16-, and 1-percent light depths was incubated in the 1958 incubator using neutral density filters representing each depth. The other set of samples was incubated in the sunlight incubators using the same set of neutral density filters. These sets of samples were incubated for 24 hours.

Underway stations were taken every two hours, processed, and incubated in the 1958 incubator for two to three hours. Both incubators were in constant use every day. For the first four in-situ stations, the ship stopped at about 11 o'clock to give time for sampling and processing of the samples. Later, the ship's stations were closer together and there were other operations to be considered. In-situ stations were then occupied

* Laboratory sample processing for the marine productivity program during the cruise was supported by ONR contract Nonr 4108(00).

† Department of Botany, University of Hawaii, Honolulu, Hawaii.

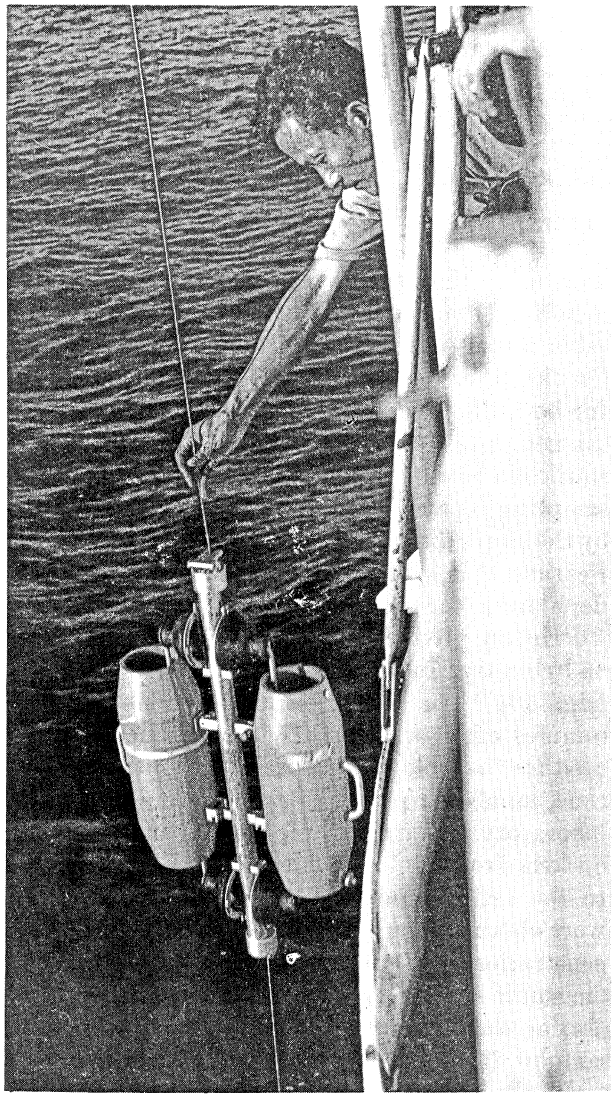

FIGURE 104[1].—Twin 6-liter plastic sampler used for marine productivity sampling program.

any time of the day as long as the samples could be set for at least two hours during daylight hours. Morning stations were usually omitted to give time for the preparation of the in-situ gear. Whenever possible, the party accomplished the morning stations as well as the in-situ stations. In-situ stations were usually taken simultaneously with a Nansen cast, a core, or a camera lowering.

Productivity samples were filtered in 25-millimeter membrane filters and washed with .001 normal hydrochloric acid and 35 parts per thousand sodium chloride solution. Samples were arranged consecutively in prenumbered planchet holders and stored in desiccators. Desiccants were redried as often as possible in the ships's oven to insure the samples being kept dry.

Electric incubators (1958) were checked regularly and changed with new lamps when they were found deteriorated. A hand light meter was used to check light intensity. Plastic tanks were regularly acid washed to insure maximum light for productivity samples. Utmost care was taken to prevent contamination of all equipment which came in contact with water samples, and all dark bottles were regularly checked for leaks.

Seston and pigment sampling was consistently done concurrently with the primary productivity work. Water samples with volumes ranging from 500 to 2,000 milliliters were taken from the volume of water obtained for primary productivity work and filtered through 25-mm Gelman type "H" filters. Two plastic buckets were set on a shelf directly above the filtering manifold and plastic tubing was used to siphon the sample into the filter manifold (fig. 105[2]). The flow was adjusted through a stopcock. This arrangement was found to be very useful, for while filtering the samples, other things could be accomplished. Three filter manifolds for productivity samples as

FIGURE 105[2].—Apparatus used for seston and pigment sample preparation in ship laboratory.

well as one set for the pigment and seston could run simultaneously. Pigment samples were treated with magnesium carbonate and allowed to dry in desiccators in the laboratory. Later, they were transferred to another desiccator in the freezer. Seston samples were stored in desiccators in the laboratory.

A separate PDR record was provided for each productivity sampling station. Other pertinent data were included in this record to make it more meaningful. Records were taken every 30 minutes before reaching the station and 30 minutes after. The horizontal net tows were made at regular intervals for the Bureau of Commercial Fisheries, although sometimes there were slight delays on the time for towing. All samples were preserved in 10-percent formalin with borax as a fixing agent.

Upon reaching the Indian Ocean, the standard International Indian Ocean net was lowered to the 200-meter depth whenever the occupied stations had depths of 200 m or greater. These vertical tows were taken regularly until the *Pioneer* reached the territorial waters of Indonesia. The method of preserving samples was similar to that used for the BCF samples. A comparative study of the 45-mm net and the International Indian Ocean standard net was made by using both nets during five vertical plankton tows.

Curiosity among the scientists on board about the organisms responsible for the deep scattering layer led to the conversion of one of the IIOE nets to a closing net. The tripping device of a Nansen bottle was utilized for this purpose, and a piece of one-inch circumference nylon rope was used to close and retrieve the net. The depth and the thickness of the deep scattering layer were determined by the PDR record (fig. 106[3]), and simultaneously, the net and the deep-sea camera were lowered to the desired depth. The net was lowered two times. The first time, the net was sent down to the lower layer of the deep scattering layer and was closed as it passed through the upper layer. The second time, the net was lowered to the lower portion of the deep scattering layer and was brought up without closing. Samples were preserved in formalin and properly labeled, but no significant differences were noted in a shipboard examination of these samples.

Five times during the expedition a light-shock experiment was conducted, and the data concerning this particular work were entered in the record book under indicator number "5." The covering for the sample bottles—to prevent light shock of

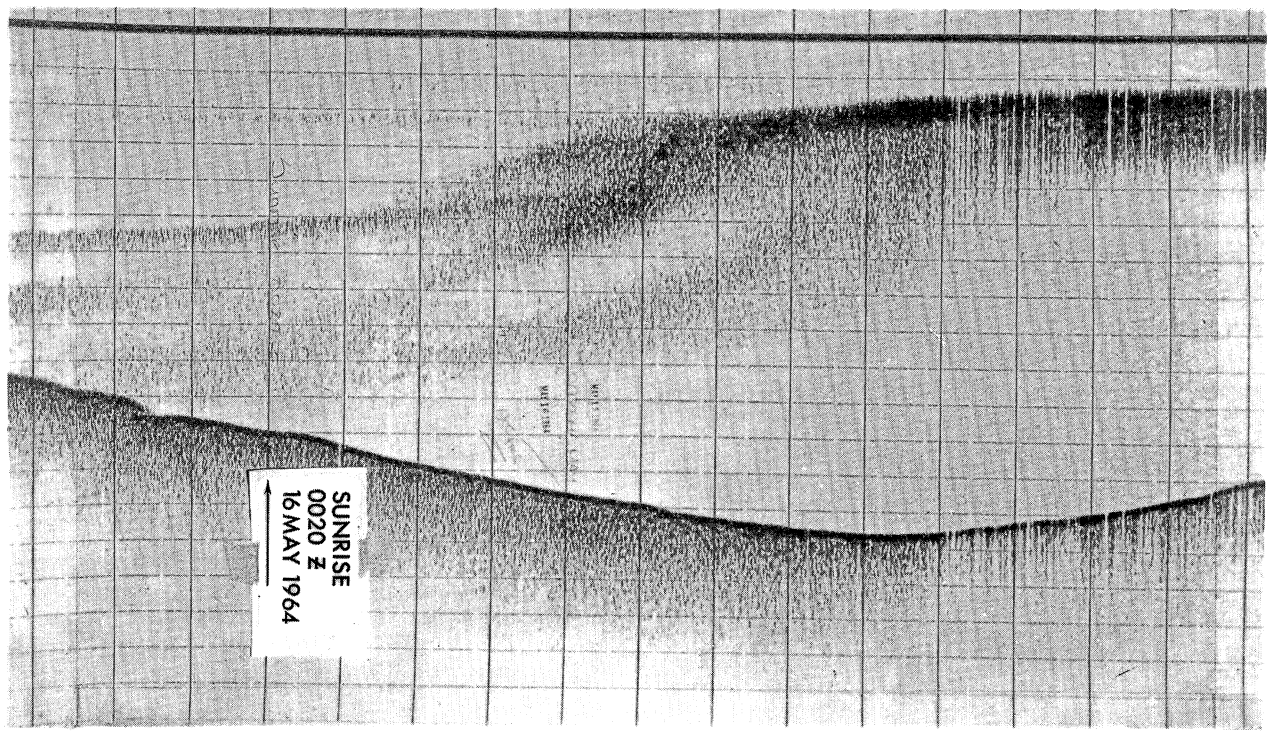


FIGURE 106[3].—PDR record showing deep scattering layer on May 15 and 16, 1964, in Bay of Bengal. Sunrise is indicated as 0020 GMT.

in-situ samples—posed many problems. Pairs of denim cloths with retrieving lines were used for this purpose. The technique appeared to work but twisting of the lines with the main line, to which the samples were attached, could not be avoided. A new method then was used to cover the sample bottles as they were being immersed in the water prior to incubation at in-situ stations. This method consisted of wrapping paper around the sample bottles before they were attached to the individual bottle holders. Upon touching the surface of the water, the papers automatically detached from the sample bottles without any delay in the operation.

The submarine photometer failed to function on the first day of sampling. A careful check by the electronics officer showed a leak in the housing of the submerged cell. A replacement for the damaged cell was not available on board ship so a message was transmitted to the University of Hawaii requesting a photoelectric cell. The message also included a request for two plankton nets to replace the two Bureau of Commercial Fisheries horizontal tow-ring nets which were lost during the towing operations. In the meantime, the party used a Secchi disc to determine light intensity at the various depths. The photocell replacement was delivered to the *Pioneer* on June 23 at Djakarta, Indonesia, and the submarine photometer was used by the party from Djakarta to Honolulu. The biological party chief, Mr. Vicente B. Alvarez, left the ship at Guam. On the way to Guam, Mr. Quintin Stephen-Hassard was briefed regarding the operation of the submarine photometer and the unfinished work to be done between Guam and Honolulu. All records, charts, samples, and equipment were checked by both biologists before the ship departed from Guam.

The biological party is grateful for the opportunity afforded them to conduct the marine productivity sampling program aboard the *Pioneer*. They also wish to express their thanks to the officers and men of the *Pioneer* for assisting in the biological sampling work and for the cooperation shown at all times.

# Meteorology

A major portion of the meteorological observations made during the *Pioneer*'s Indian Ocean Expedition were recorded by the automated shipboard meteorological station provided by the University of Michigan as a part of the IIOE program in meteorology. The system employed sensors for the measurement of: (1) Solar radiation, (2) air temperature, (3) water temperature, (4) humidity, (5) sea surface temperature, (6) wind speed and direction—two sensors, (7) atmospheric plus solar radiation, and (8) radiometer sensing-plate temperature. Eleven additional channels were available for information supplied by manual dial settings, that is, ship speed, ship direction, time, latitude, etc.

A detailed description of the automatic data recording system, including samples of meteorological data printouts, is given in the paper, entitled "Meteorological Data Logged by the University of Michigan Automatic Recording System During USC&GS Ship *Pioneer* 1964 Indian Ocean Expedition," by Dr. Donald J. Portman.

Twelve radiometersonde observations, measurements of incoming and reflected radiation aloft to approximately 100,000 feet at night, were made during the expedition (fig. 107). In addition, more than 300 radiosonde observations—upper-air soundings of temperature, humidity, and pressure—were recorded for the U.S. Weather Bureau program. Radiometersonde, radiosonde, and standard surface weather observations were furnished the U.S. Weather Bureau, San Francisco, Calif. Daily radio transmissions forwarded meteorological data to the United States.

Additional surface observations were recorded by personnel aboard the *Pioneer*. Surface observations were recorded on the bathythermograph log sheets for each BT lowering. The BT log sheets are reproduced in Volume 2 of this series of publications. More than 200 sea and swell observations were recorded on the Shipboard Wave Observation Log (PRNC–NHO–1192). The sea and swell data and meteorological data, observed as part of the bathythermograph observations, were forwarded to the National Oceanographic Data Center, Washington, D.C.

Meteorological observations made at oceanographic stations were recorded on the standard oceanographic-station log sheets and appear in the oceanographic data listings of Volume 2.

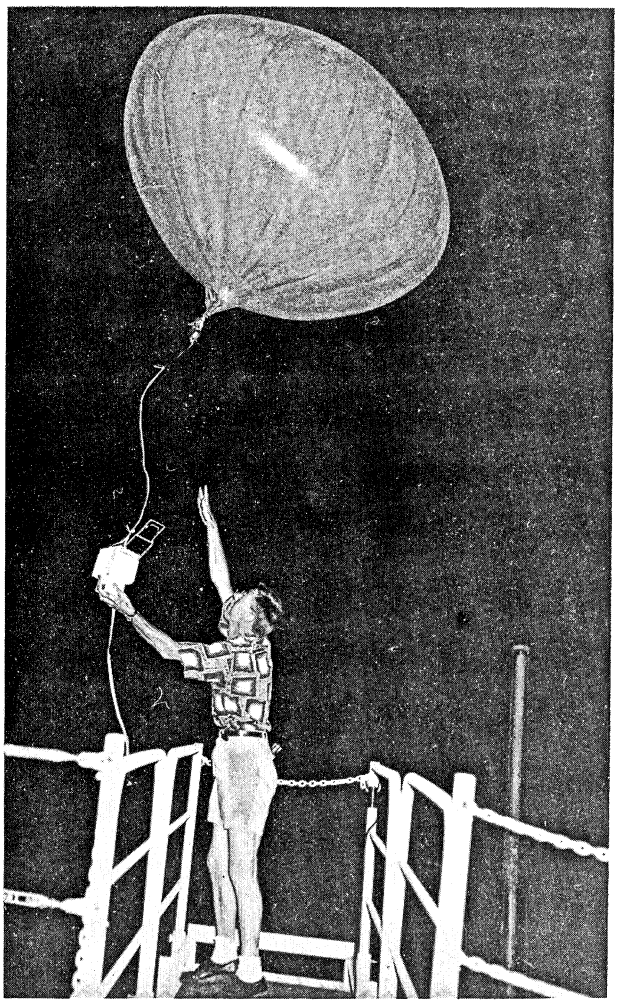

FIGURE 107.—Nighttime launching of weather balloon and attached radiometersonde.

# Meteorological Data Logged by the University of Michigan Automatic Recording System During USC&GS Ship "Pioneer" 1964 Indian Ocean Expedition

DONALD J. PORTMAN*

1. *Introduction.* An automatic recording system was placed aboard the USC&GS Ship *Pioneer* by University of Michigan personnel to obtain information with which to estimate the exchange of heat and water vapor at the air-sea interface. Similar systems were placed aboard five other research vessels participating in the International Indian Ocean Expedition. The data from the ships are to be combined with radiation data from island and coastal stations, with cloud cover and radiation data from satellites, and with other meteorological data to make analyses of the seasonal and latitudinal variations in energy exchange. This investigation was supported by the U.S. National Science Foundation and was designed to meet one of the major objectives of the meteorological phase of the International Indian Ocean Expedition as expressed by the Special Committee on Oceanic Research of the International Council of Scientific Unions.

2. *The Automatic Recording System.* Figure 108[1] is a block diagram of the automatic recording system with a list of the items recorded and the sensors used for automatic inputs. The latter required 9 channels, test signals required 4 channels, and the remaining 11 channels were for information supplied by manual dial settings. The coupling circuits convert the electrical response from each channel to a potential from 0 to 5 millivolts, linearly scaled for each source, and supply it to a Minneapolis-Honeywell multipoint potentiometer recorder. The switch of the multipoint recorder programs the channels in sequence at a rate of 6 minutes per cycle of 24 inputs.

At the same time the data are recorded on chart paper, a Daytex analogue-to-digital encoder, attached to the shaft of the recorder slide-wire drive mechanism, converts the 0- to 5-millivolt scale to one of 1,024 digits. The logic circuit receives the information and transfers it to the magnetic-tape recorder in the form of a two-part binary word. The tape recorder is a Honeywell Model 6151 Incremental Recorder using ½-inch-wide magnetic tape. Each half of the binary word uses 6 channels of the 7-channel tape in a 0.005-inch increment of tape. The seventh channel is reserved for a parity check. The program includes a ¾-inch record gap after each 32 complete cycles of the 24 data-channel inputs, so that a total of 8.48 inches of tape is required for 3 hours and 12 minutes of continuous recording. In this way, data are efficiently stored in a format compatible for data processing by automatic computer.

The entire recording system was housed in a standard metal cabinet, 2 by 2 by 5 feet, and was located in the ship's weather laboratory. The system was designed and built by K. J. Law Engineers, 26341 West Eight Mile Road, Detroit, Mich. A more complete description of the recording system may be obtained from that firm by request.

3. *Sensors.* A partial description of each sensor and its use during the cruise follows. Sources of additional information are cited.

(a) Solar radiation: Total incoming solar radiation was measured with a 10-junction Eppley (180°) pyrheliometer mounted on a gimbal support on the rail above the wheelhouse. It was equipped with a factory-built temperature compensation circuit for a 0 to 50°C range. The output was adjusted so that full scale on the recorder was 3.0 cal $cm^{-2}$ $min^{-1}$. Complete information on the pyrheliometer is available in Bulletin No. 2, August 1964, published by the Eppley Laboratory, Inc., Newport, R.I.

(b) Air temperature: A Victory Engineering Corp. 32A84, glass-enclosed, bead thermistor was mounted in a flat-plate thermal radiation shield to measure air temperature. The radiation shield was fastened to the yardarm on the main mast. It consisted of four parallel metal plates, one above the other, three-eighths of an inch apart, with the thermistor supported approximately in

*Department of Meteorology and Oceanography, University of Michigan, Ann Arbor, Mich.

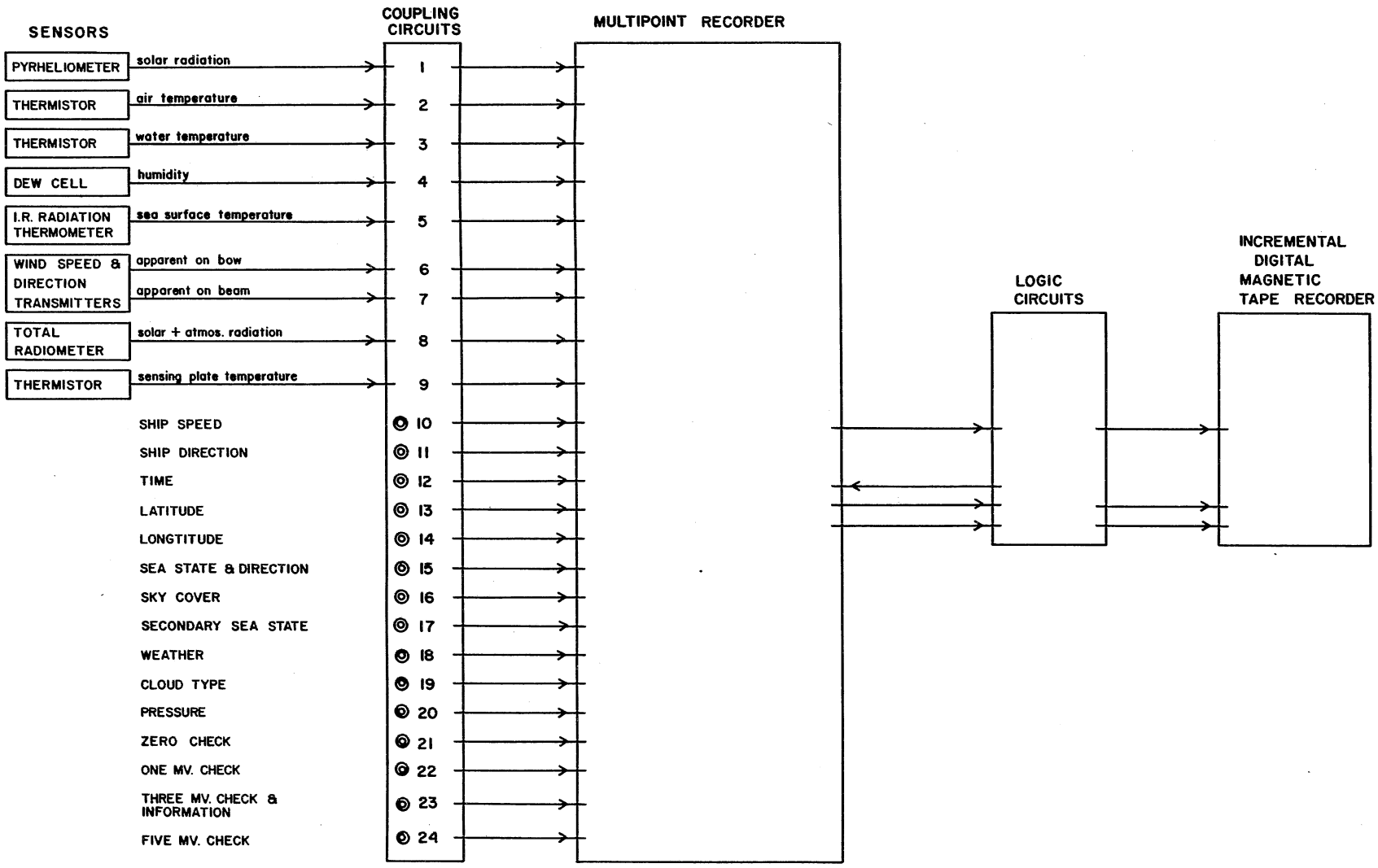


FIGURE 108[1].—Block diagram of the automatic meteorological data-recording system.

the center of the stack. The outward-facing surfaces of the plates were chrome plated and the inward-facing surfaces were blackened. The outer plates were 6 by 5 inches and the inner ones 3 by 5 inches. In this case the coupling circuit consisted of a Wheatstone bridge, of which the thermistor formed one arm. Full scale in the recording system corresponded originally to a temperature range of −10 to 40°C. It was changed while the ship was in port in Calcutta to a temperature range of −10 to 50°C.

(c) Water temperature: The temperature of the water used to cool the main engine was measured at the intake with a Victory Engineering Corp. 32A84 thermistor. The coupling circuit was similar to that used for the air temperature measurement, but the scale used throughout the cruise corresponded to a temperature range of 0 to 40°C.

(d) Humidity: The dewpoint temperature was measured with a Foxboro Dewcel enclosed in a Foxboro Model 2714 Weatherhood. It was mounted on the yardarm of the main mast, near the air temperature sensor. The temperature sensor in the element was a resistance thermometer which formed one arm of a conventional bridge circuit. The system was calibrated to give a full scale dewpoint temperature range of −12 to 43°C. Detailed description and specifications of the instrument may be obtained from the Foxboro Co., Foxboro, Mass.

A review of the dewpoint data obtained during the cruise showed that they were consistently higher than those reported by the weather observer who used a conventional sling psychrometer. At times, they were also higher than measured air temperatures. The calibration information and adjustments were carefully reviewed and it was not possible to account for the discrepancy. Therefore, the data have been omitted from the cruise data tabulation described in part 6.

(e) Sea surface temperature: A Barnes Infrared Thermometer, Model IT-2, was mounted on the rail above the wheelhouse. The field of view of the instrument was 3 degrees. It was mounted in a special housing to minimize vibration and weather effects, and was directed toward undisturbed water as normal to the surface as possible. The output was scaled by the coupling circuit to give a full scale range initially of −10 to 50°C. While the ship was in port in Calcutta, the range was changed to 0 to 50°C. A full description of the instrument may be obtained from Barnes Engineering Co., Stamford, Conn.

(f) Wind velocity (relative to the ship): The horizontal wind velocity vector components relative to the bow and to the beam were measured separately by wind-measuring equipment designed and manufactured by the Electric Speed Indicator Co. A standard three-cup anemometer, Type F420, was mounted on one end of the main mast yardarm and the wind vane on the other end. The anemometer generated a direct current which was supplied to the wind vane potentiometer. The latter was especially designed so that orthogonal wiper arms gave the desired wind components. Coupling circuits for the two inputs were arranged to give full scale values of 60 knots on either side of center scale (2.5 millivolts). A description of the standard equipment is given in "Instruction Book for Type F420–C and Type CAA–277 Wind Measuring Equipment," available from the Electric Speed Indicator Co., 12234 Triskett Road, Cleveland, Ohio, 44111.

(g) Atmospheric plus solar radiation: A Funk, or C.S.I.R.O., net radiometer was modified to function as a total hemispherical radiometer and was mounted on a gimbal support near the pyrheliometer on the rail above the wheelhouse. The modification consisted of replacing the lower hemispherical shell of polythene with a metal shell whose interior was blackened and fitted with a thermistor on the lower center surface. Analysis of the thermal balance of the sensing element, with reasonable assumptions relative to the radiative and convective transfers, shows that the total radiation incident upon the upper surface of the instrument is given in terms of the thermopile output and the temperature of the lower metal shell. Because of an error in construction and an oversight in testing, the coupling circuit for the thermopile did not provide for negative voltages that occur in the absence of solar radiation. The scaling provided for only an input of 0 to 2.5 cal $cm^{-2}$ $min^{-1}$, and consequently, total radiation data were not obtained at night. The imbedded thermistor formed the arm of a Wheatstone bridge similar to that used for thermistors to measure air and water temperature. The full scale range was −10 to 40°C.

Reliable data from this instrument were obtained only during the period of February 14 to March 18 because of failure of the thermopile due,

apparently, to moisture penetration. Complete information on the C.S.I.R.O. net radiometer and components for its modification may be obtained from the manufacturer, Middleton and Co., Pvt. Ltd., 317 Flinders Lane, Melbourne, Australia.

4. *Manual Inputs.* The series of manual inputs on channels 10 through 20, as listed in figure 108[1], were supplied to the recording system by setting a precision 10-turn potentiometer for each input in accordance with a simple scaling and coding system. The potentiometers were Beckman Instruments Co. Model A–FS Helipots. The ship's weather observer had the responsibility of making the settings once per hour, or more often if significant changes in any of the items occurred.

5. *Data Processing.* All cruise data recorded on magnetic tape were processed by an electronic computer. The processing was conducted in three steps: (1) Elimination of spurious data; (2) determination of hourly averages or most frequent values; and (3) computations and conversions. Criteria for eliminating spurious data were arbitrarily established on the basis of general knowledge of the environment, values of related variables, and reasonable ranges for time variations. After spurious data were removed from the record, hourly averages were computed for data having continuous scales. An exception was ship orientation data; for these and for coded manual data, the most frequent value was determined and tabulated as the value for the hour. The data were then converted to appropriate units for tabulation in accordance with calibration and scaling factors. True wind speed and direction were computed from the recorded (relative) wind vector data, ship speed, and orientation data. Finally, hourly values of total radiation (incoming solar plus atmospheric) were computed from the radiometer thermistor bridge and thermopile outputs.

6. *Data Tabulation.* The processed data were stored on magnetic tape in a format suitable for tabulation by line printer. A sample of the tabulation is shown in figures 109[2] and 110[3]. An explanation of the tabular headings, with units and code references, is given at the end of this paper. The data for a single hour require two printer lines which are on separate sheets for convenience. The extra space available on the second line was used to repeat several items for reference. In this way, the complete set of data for the cruise requires 138 pages. The sheets from the printer may be bound conveniently,

*Explanation of column headings for data sheet No. 1*

DATE = April 1, 2, 3, 1965
TIME = GMT
SRAD = Solar radiation (g cal $cm^{-2}$ $min^{-1}$)
TRAD = Total hemispherical radiation (g cal $cm^{-2}$ $min^{-1}$)
AIRT = Air temperature (°C)
SEAT = Water temperature at depth of cooling water intake (°C)
SFCT = Water surface temperature (°C)
CC = Total cloud amount*
LC = Type of low cloud*
MC = Type of middle cloud*
HC = Type of high cloud*
WX = Present weather*
V = Visibility*
PPP = Precipitation (inches)
WS = Wind speed (knots)
WD = Wind direction (degrees)
SS = Ship speed (knots)
SD = Ship direction (degrees)
LAT = Latitude (degrees)
LONG = Longitude (degrees)
Q = Quadrant of globe

*Coded data; for code see U.S. Department of Commerce, Weather Bureau Ship Code Card, TA631-0-2, January 1963.

| DATE | TIME | SRAD | TRAD | AIRT | SEAT | SFCT | CC | LC | MC | HC | WX | V | PPP | WS | WD | SS | SD | LAT | LONG | Q |
|---|---|---|---|---|---|---|---|---|---|---|---|---|---|---|---|---|---|---|---|---|
| 1 | 1 | .69 | XXXXX | 27.5 | 31.0 | 28.7 | 5 | 0 | 0 | 9 | 2 | 9 | .00 | 10.4 | 84 | 17.1 | 236 | 6.3 | 95.4 | NE |
| 1 | 2 | 1.07 | XXXXX | 27.8 | 30.8 | 28.8 | 5 | 0 | 0 | 9 | 2 | 9 | .00 | XXXXX | | .1 | 1 | 6.3 | 95.0 | NE |
| 1 | 3 | 1.31 | XXXXX | 27.9 | 30.6 | 28.7 | 5 | 0 | 0 | 9 | 2 | 9 | .00 | 3.4 | | .1 | 1 | 6.3 | 95.0 | NE |
| 1 | 4 | 1.39 | XXXXX | 28.0 | 31.1 | 29.4 | 5 | 0 | 0 | 9 | 2 | 9 | .00 | XXXXX | | XXXXX | 46 | 6.2 | 95.0 | NE |
| 1 | 5 | 1.40 | XXXXX | 27.8 | 31.2 | 29.4 | 5 | 0 | 0 | 9 | 2 | 9 | .00 | 9.6 | | 17.1 | 127 | 6.2 | 95.0 | NE |
| 1 | 6 | 1.27 | XXXXX | 28.0 | 31.7 | 29.7 | 5 | 0 | 0 | 9 | 2 | 9 | .00 | 7.6 | 331 | 17.1 | 131 | 6.1 | 94.8 | NE |
| 1 | 7 | 1.13 | XXXXX | 27.9 | 31.6 | 29.6 | 5 | 0 | 0 | 9 | 2 | 9 | .00 | 7.2 | 286 | 17.2 | 131 | 5.9 | 94.6 | NE |
| 1 | 8 | .59 | XXXXX | 28.0 | 31.5 | 29.5 | 5 | 0 | 0 | 9 | 2 | 9 | .00 | 7.3 | 68 | 17.1 | 272 | 5.8 | 94.2 | NE |
| 1 | 9 | .00 | XXXXX | 28.1 | 31.3 | 29.2 | 5 | 0 | 0 | 9 | 2 | 9 | .00 | XXXXX | | 17.1 | 272 | 5.8 | 93.7 | NE |
| 1 | 10 | .00 | XXXXX | 28.1 | 31.3 | 29.4 | 5 | 0 | 0 | 9 | 2 | 9 | .00 | XXXXX | | 17.1 | 272 | 5.8 | 93.7 | NE |
| 1 | 11 | .00 | XXXXX | 28.2 | 31.3 | 29.4 | 8 | 1 | 4 | 0 | 2 | 9 | .00 | 5.4 | 76 | 17.2 | 272 | 5.9 | 93.8 | NE |
| 1 | 12 | .00 | XXXXX | 28.2 | 31.3 | 29.1 | 8 | 1 | 3 | 9 | 2 | 9 | .00 | 1.7 | 19 | 4.1 | 272 | 5.9 | 93.1 | NE |
| 1 | 13 | .00 | XXXXX | 28.3 | 31.1 | 29.0 | 8 | 1 | 3 | 9 | 2 | 9 | .00 | 7.9 | 99 | 16.1 | 272 | 5.9 | 93.1 | NE |
| 1 | 14 | .00 | XXXXX | 28.4 | 31.1 | 29.1 | 8 | 1 | 3 | 9 | 2 | 9 | .00 | 6.9 | 101 | 16.1 | 272 | 5.8 | 93.5 | NE |
| 1 | 15 | .00 | XXXXX | 28.2 | 31.1 | 28.9 | 8 | 1 | 3 | 9 | 2 | 9 | .00 | 14.0 | 81 | 16.1 | 272 | 5.8 | 93.5 | NE |
| 1 | 16 | .00 | XXXXX | 28.2 | 31.1 | 28.7 | 8 | 1 | 3 | 9 | 2 | 9 | .00 | 3.6 | | .1 | 272 | 5.8 | 93.5 | NE |
| 1 | 17 | .00 | XXXXX | 28.1 | 31.1 | 28.8 | 5 | 0 | 0 | 9 | 2 | 9 | .00 | 2.2 | | .1 | 272 | 5.9 | 92.7 | NE |
| 1 | 18 | .00 | XXXXX | 27.9 | 31.0 | 28.8 | 5 | 0 | 0 | 9 | 2 | 9 | .00 | XXXXX | | .1 | 272 | 5.9 | 92.7 | NE |
| 1 | 19 | .00 | XXXXX | 27.8 | 31.0 | 28.7 | 5 | 0 | 0 | 9 | 2 | 9 | .00 | XXXXX | | .1 | 272 | 5.8 | 92.7 | NE |
| 1 | 20 | .00 | XXXXX | 27.6 | 31.0 | 28.8 | 5 | 0 | 0 | 9 | 2 | 9 | .00 | 3.6 | | .1 | 272 | 5.9 | 92.7 | NE |
| 1 | 21 | .00 | XXXXX | 27.6 | 31.0 | 28.8 | 5 | 0 | 0 | 9 | 2 | 9 | .00 | 3.1 | | .1 | 272 | 5.9 | 92.7 | NE |
| 1 | 22 | .00 | XXXXX | 27.9 | 31.0 | 28.8 | 5 | 0 | 0 | 9 | 2 | 9 | .00 | XXXXX | | .1 | 208 | 5.9 | 92.7 | NE |
| 1 | 23 | .00 | XXXXX | 29.1 | 31.0 | 28.8 | 6 | 2 | 3 | 8 | 2 | 9 | .00 | 2.6 | | .1 | 1 | 5.8 | 92.7 | NE |
| 1 | 24 | .46 | XXXXX | 28.2 | 30.9 | 29.0 | 6 | 2 | 3 | 9 | 2 | 9 | .00 | 3.1 | | .1 | 1 | 5.8 | 92.4 | NE |
| 2 | 1 | .96 | XXXXX | 28.1 | 31.0 | 29.0 | 6 | 2 | 3 | 9 | 2 | 9 | .00 | 3.4 | | .1 | 1 | 5.8 | 92.4 | NE |
| 2 | 2 | 1.25 | XXXXX | 28.4 | 31.0 | 28.0 | 6 | 2 | 3 | 9 | 2 | 9 | .00 | 2.4 | | .1 | 1 | 5.8 | 92.4 | NE |
| 2 | 3 | 1.40 | XXXXX | 28.0 | 31.3 | 29.5 | 6 | 2 | 3 | 9 | 2 | 9 | .00 | 4.6 | 85 | 16.6 | 269 | 6.0 | 92.3 | NE |
| 2 | 4 | 1.49 | XXXXX | 28.1 | 31.3 | 29.4 | 6 | 2 | 3 | 9 | 2 | 9 | .00 | 6.5 | | 16.6 | 269 | 5.9 | 92.0 | NE |
| 2 | 5 | 1.49 | XXXXX | 28.1 | 31.5 | 29.8 | 6 | 2 | 3 | 9 | 2 | 9 | .00 | 7.8 | 73 | 16.6 | 269 | 5.9 | 92.0 | NE |
| 2 | 6 | 1.33 | XXXXX | 28.2 | 31.5 | 29.8 | 3 | 2 | 0 | 1 | 2 | 9 | .00 | 7.7 | 81 | 16.6 | 269 | 5.9 | 91.6 | NE |
| 2 | 7 | 1.12 | XXXXX | 28.3 | 31.5 | 29.9 | 3 | 2 | 0 | 1 | 2 | 9 | .00 | 8.2 | 83 | 16.6 | 269 | 5.9 | 91.4 | NE |
| 2 | 8 | .59 | XXXXX | 28.3 | 31.4 | 30.0 | 3 | 2 | 0 | 1 | 2 | 9 | .00 | 1.0 | | 16.6 | 269 | 5.9 | 91.2 | NE |
| 2 | 9 | .00 | XXXXX | 28.3 | 31.3 | 29.8 | 3 | 2 | 0 | 1 | 2 | 9 | .00 | XXXXX | | 16.6 | 76 | 5.9 | 91.2 | NE |
| 2 | 10 | .00 | XXXXX | 28.3 | 31.4 | 29.7 | 3 | 2 | 0 | 1 | 2 | 9 | .00 | 2.9 | 31 | 17.1 | 71 | 5.9 | 91.3 | NE |
| 2 | 11 | .00 | XXXXX | 28.3 | 31.3 | 29.4 | 2 | 3 | 0 | 2 | 2 | 9 | .00 | 1.7 | | 17.2 | 71 | 6.0 | 91.6 | NE |
| 2 | 12 | .00 | XXXXX | 28.2 | 31.3 | 29.4 | 2 | 3 | 0 | 2 | 2 | 9 | .00 | 3.8 | | 16.1 | 76 | 5.7 | 91.9 | NE |
| 2 | 13 | .00 | XXXXX | 28.2 | 31.3 | 29.1 | 2 | 3 | 0 | 3 | 2 | 9 | .00 | 3.4 | | 16.2 | 76 | 5.7 | 92.2 | NE |
| 2 | 14 | .00 | XXXXX | 28.3 | 31.4 | 29.2 | 2 | 3 | 0 | 3 | 2 | 9 | .00 | 2.8 | 11 | 16.2 | 76 | 6.2 | 92.4 | NE |
| 2 | 15 | .00 | XXXXX | 28.3 | 31.5 | 29.4 | 2 | 3 | 0 | 3 | 2 | 9 | .00 | 1.6 | 165 | 16.2 | 76 | 6.2 | 92.3 | NE |
| 2 | 16 | .00 | XXXXX | 28.3 | 31.5 | 29.4 | 2 | 3 | 0 | 3 | 2 | 9 | .00 | XXXXX | | 16.2 | 76 | 6.2 | 92.3 | NE |
| 2 | 17 | .00 | XXXXX | 28.2 | 31.5 | 29.3 | 4 | 1 | 0 | 8 | 2 | 9 | .00 | 3.3 | 300 | 16.2 | 72 | 6.3 | 94.5 | NE |
| 2 | 18 | .00 | XXXXX | 27.7 | 31.4 | 29.2 | 4 | 1 | 0 | 8 | 2 | 9 | .00 | XXXXX | | 16.2 | 72 | 6.3 | 94.5 | NE |
| 2 | 19 | .00 | XXXXX | 27.5 | 31.1 | 29.1 | 4 | 1 | 0 | 8 | 2 | 9 | .00 | 7.6 | 291 | 16.2 | 72 | 6.3 | 94.5 | NE |
| 2 | 20 | .00 | XXXXX | 27.9 | 31.2 | 29.1 | 4 | 1 | 0 | 8 | 2 | 9 | .00 | 3.5 | 290 | 16.1 | 72 | 6.3 | 94.5 | NE |
| 2 | 21 | .00 | XXXXX | 27.7 | 31.3 | 29.1 | 4 | 1 | 0 | 8 | 2 | 9 | .00 | 3.5 | 0 | 16.1 | 72 | 6.6 | 97.0 | NE |
| 2 | 22 | .00 | XXXXX | 27.5 | 31.3 | 29.2 | 4 | 1 | 0 | 8 | 2 | 9 | .00 | XXXXX | | 16.9 | 77 | 6.8 | 94.5 | NE |
| 2 | 23 | .00 | XXXXX | 27.8 | 31.3 | 29.2 | 5 | 1 | 3 | 9 | 2 | 9 | .00 | XXXXX | | 16.9 | 77 | 6.9 | 94.4 | NE |
| 2 | 24 | .48 | XXXXX | 28.0 | 30.9 | 28.9 | 5 | 1 | 3 | 9 | 2 | 9 | .00 | 2.4 | 2 | 16.9 | 77 | 7.0 | 95.0 | NE |
| 3 | 1 | .51 | XXXXX | 28.0 | 30.8 | 28.9 | 5 | 9 | 1 | 0 | 15 | 9 | .00 | 5.3 | 351 | 16.9 | 77 | 7.0 | 95.4 | NE |
| 3 | 2 | 1.12 | XXXXX | 28.2 | 31.2 | 29.3 | 5 | 9 | 1 | 0 | 15 | 9 | .00 | 5.7 | 30 | 16.9 | 77 | 7.0 | 95.4 | NE |
| 3 | 3 | 1.35 | XXXXX | 28.4 | 31.3 | 29.8 | 5 | 9 | 0 | 9 | 14 | 9 | .00 | 7.3 | 3 | 16.9 | 77 | 7.1 | 95.9 | NE |
| 3 | 4 | 1.34 | XXXXX | 28.5 | 31.4 | 30.1 | 5 | 9 | 0 | 9 | 14 | 9 | .00 | XXXXX | | 16.9 | 77 | 7.1 | 95.9 | NE |
| 3 | 5 | 1.27 | XXXXX | 28.6 | 31.7 | 30.2 | 2 | 2 | 0 | 2 | 2 | 9 | .00 | 6.7 | 12 | 17.1 | 77 | 7.3 | 96.3 | NE |
| 3 | 6 | 1.17 | XXXXX | 28.7 | 31.9 | 30.1 | 2 | 2 | 0 | 1 | 2 | 9 | .00 | 4.8 | | 17.1 | 77 | 7.3 | 96.4 | NE |
| 3 | 7 | .95 | XXXXX | 28.9 | 31.7 | 30.9 | 2 | 2 | 0 | 2 | 2 | 9 | .00 | XXXXX | | 17.1 | 77 | 7.4 | 96.8 | NE |

FIGURE 109[2].—Sample of meteorological data sheet No. 1.

forming a book about ¾ by 11 by 15 inches. Complete tabulations are available at a nominal cost. These may be obtained from the author, Donald J. Portman, Department of Meteorology and Oceanography, University of Michigan, Ann Arbor, Mich., 48104.

7. *Summary.* A meteorological data logging system was operated during the entire cruise to obtain information to estimate heat and water vapor exchange between the atmosphere and ocean. The data were recorded continuously in a convenient way for machine processing and analysis. Although two sensors failed to function reliably much of the time, the accumulated data represent an important contribution to the large amount of information required to make a realistic analysis of space and time variations of air-sea interaction processes. Much of the success of the program is due Mr. Melvin L. Fields, U.S. Weather Bureau observer, who tended the system during the cruise. Acknowledgment also is made to many other individuals, both in the Coast and Geodetic Survey and at the University of Michigan, who were responsible for the system design, for its installation and operation aboard the *Pioneer*, and for data processing.

*Explanation of column headings for data sheet No. 2*

DATE=April 1, 2, 3, 1965
TIME=GMT
HT=Height of primary waves*
DIR=Direction of primary waves*
PER=Period of primary waves (special code given below)
HT=Height of secondary waves (swell)*
DIR=Direction secondary waves*
PER=Period of swell (special code given below)
CC=Total cloud amount*
WX=Present weather*
WS=Wind speed (knots)
WD=Wind direction (degrees)
PRESS=Sea level pressure (millibars)
LAT=Latitude (degrees)
LONG=Longitude (degrees)
Q=Quadrant of globe

Special code for sea period:
2=less than 5
4=5–10
6=10–15
8=over 15

*Coded data; for code see U.S. Department of Commerce, Weather Bureau Ship Code Card, TA631-0-2, January 1963.

| DATE | TIME | HT | DIR | PER | HT | DIR | PER | CC | WX | WS | WD | PRESS | LAT | LONG | Q |
|---|---|---|---|---|---|---|---|---|---|---|---|---|---|---|---|
| 1 | 1 | 1 | 36 | 3 | 2 | 24 | 5 | 5 | 2 | 10.4 | 84 | 1011.5 | 6.3 | 95.4 | NE |
| 1 | 2 | 1 | 36 | 3 | 2 | 25 | 5 | 5 | 2 | XXXXX | | 1012.1 | 6.3 | 95.0 | NE |
| 1 | 3 | 1 | 36 | 3 | 2 | 25 | 4 | 5 | 2 | 3.4 | | 1012.1 | 6.3 | 95.0 | NE |
| 1 | 4 | 1 | 36 | 3 | 2 | 25 | 4 | 5 | 2 | XXXXX | | 1011.8 | 6.2 | 95.0 | NE |
| 1 | 5 | 1 | 36 | 3 | 2 | 25 | 4 | 5 | 2 | 9.6 | | 1011.8 | 6.2 | 95.0 | NE |
| 1 | 6 | 1 | 36 | 3 | 2 | 25 | 4 | 5 | 2 | 7.6 | 331 | 1009.5 | 6.1 | 94.8 | NE |
| 1 | 7 | 1 | 36 | 3 | 2 | 25 | 4 | 5 | 2 | 7.2 | 286 | 1008.8 | 5.9 | 94.6 | NE |
| 1 | 8 | 1 | 36 | 3 | 2 | 25 | 4 | 5 | 2 | 7.3 | 68 | 1008.7 | 5.8 | 94.2 | NE |
| 1 | 9 | 1 | 36 | 3 | 2 | 25 | 4 | 5 | 2 | XXXXX | | 1008.7 | 5.8 | 93.7 | NE |
| 1 | 10 | 1 | 36 | 3 | 2 | 20 | 4 | 5 | 2 | XXXXX | | 1009.0 | 5.8 | 93.7 | NE |
| 1 | 11 | 1 | 5 | 6 | 3 | 19 | 5 | 8 | 2 | 5.4 | 76 | 1010.2 | 5.9 | 93.8 | NE |
| 1 | 12 | 1 | 4 | 5 | 3 | 18 | 5 | 8 | 2 | 1.7 | 19 | 1010.8 | 5.9 | 93.1 | NE |
| 1 | 13 | 1 | 4 | 5 | 3 | 18 | 5 | 8 | 2 | 7.9 | 99 | 1011.2 | 5.9 | 93.1 | NE |
| 1 | 14 | 1 | 4 | 7 | 3 | 19 | 4 | 8 | 2 | 6.9 | 101 | 1011.4 | 5.8 | 93.5 | NE |
| 1 | 15 | 1 | 4 | 7 | 3 | 19 | 4 | 8 | 2 | 14.0 | 81 | 1011.4 | 5.8 | 93.5 | NE |
| 1 | 16 | 1 | 4 | 7 | 3 | 19 | 4 | 8 | 2 | 3.6 | | 1011.4 | 5.8 | 93.5 | NE |
| 1 | 17 | 1 | 6 | 5 | 3 | 18 | 4 | 5 | 2 | 2.2 | | 1010.6 | 5.9 | 92.7 | NE |
| 1 | 18 | 1 | 6 | 5 | 3 | 18 | 4 | 5 | 2 | XXXXX | | 1009.0 | 5.9 | 92.7 | NE |
| 1 | 19 | 1 | 6 | 5 | 3 | 18 | 4 | 5 | 2 | XXXXX | | 1008.5 | 5.8 | 92.7 | NE |
| 1 | 20 | 1 | 6 | 5 | 3 | 18 | 4 | 5 | 2 | 3.6 | | 1008.5 | 5.9 | 92.7 | NE |
| 1 | 21 | 1 | 7 | 5 | 3 | 18 | 4 | 5 | 2 | 3.1 | | 1009.4 | 5.9 | 92.7 | NE |
| 1 | 22 | 1 | 6 | 5 | 3 | 18 | 4 | 5 | 2 | XXXXX | | 1009.6 | 5.9 | 92.7 | NE |
| 1 | 23 | 1 | 6 | 6 | 3 | 18 | 4 | 6 | 2 | 2.6 | | 1010.3 | 5.8 | 92.7 | NE |
| 1 | 24 | 1 | 7 | 4 | 3 | 18 | 4 | 6 | 2 | 3.1 | | 1011.4 | 5.8 | 92.4 | NE |
| 2 | 1 | 1 | 7 | 4 | 3 | 18 | 4 | 6 | 2 | 3.4 | | 1012.2 | 5.8 | 92.4 | NE |
| 2 | 2 | 1 | 7 | 4 | 3 | 18 | 5 | 6 | 2 | 2.4 | | 1012.2 | 5.8 | 92.4 | NE |
| 2 | 3 | 1 | 7 | 4 | 3 | 18 | 5 | 6 | 2 | 4.6 | 85 | 1011.8 | 6.0 | 92.3 | NE |
| 2 | 4 | 1 | 6 | 4 | 3 | 17 | 4 | 6 | 2 | 6.5 | | 1011.3 | 5.9 | 92.0 | NE |
| 2 | 5 | 1 | 6 | 4 | 3 | 18 | 5 | 6 | 2 | 7.8 | 73 | 1011.3 | 5.9 | 92.0 | NE |
| 2 | 6 | 1 | 7 | 4 | 3 | 17 | 5 | 3 | 2 | 7.7 | 81 | 1010.3 | 5.9 | 91.6 | NE |
| 2 | 7 | 1 | 7 | 4 | 3 | 18 | 5 | 3 | 2 | 8.2 | 83 | 1008.6 | 5.9 | 91.4 | NE |
| 2 | 8 | 1 | 6 | 4 | 3 | 18 | 5 | 3 | 2 | 1.0 | | 1008.0 | 5.9 | 91.2 | NE |
| 2 | 9 | 1 | 6 | 4 | 3 | 18 | 4 | 3 | 2 | XXXXX | | 1007.9 | 5.9 | 91.2 | NE |
| 2 | 10 | 1 | 6 | 4 | 3 | 17 | 4 | 3 | 2 | 2.9 | 31 | .0 | 5.9 | 91.3 | NE |
| 2 | 11 | 0 | 2 | 2 | 3 | 15 | 4 | 2 | 2 | 1.7 | | 1008.8 | 6.0 | 91.6 | NE |
| 2 | 12 | 0 | 2 | 2 | 3 | 15 | 4 | 2 | 2 | 3.8 | | 1009.2 | 5.7 | 91.9 | NE |
| 2 | 13 | 0 | 2 | 2 | 3 | 16 | 4 | 2 | 2 | 3.4 | | 1009.8 | 5.7 | 92.2 | NE |
| 2 | 14 | 0 | 2 | 1 | 3 | 15 | 4 | 2 | 2 | 2.8 | 11 | 1010.3 | 6.2 | 92.4 | NE |
| 2 | 15 | 0 | 2 | 1 | 3 | 15 | 4 | 2 | 2 | 1.6 | 165 | 1010.3 | 6.2 | 92.3 | NE |
| 2 | 16 | 0 | 2 | 1 | 3 | 15 | 4 | 2 | 2 | XXXXX | | 1010.3 | 6.2 | 92.3 | NE |
| 2 | 17 | 0 | 2 | 2 | 3 | 15 | 6 | 4 | 2 | 3.3 | 300 | 1009.9 | 6.3 | 94.5 | NE |
| 2 | 18 | 0 | 2 | 2 | 3 | 16 | 6 | 4 | 2 | XXXXX | | 1009.9 | 6.3 | 94.5 | NE |
| 2 | 19 | 0 | 2 | 3 | 3 | 15 | 6 | 4 | 2 | 7.6 | 291 | 1009.9 | 6.3 | 94.5 | NE |
| 2 | 20 | 0 | 2 | 2 | 3 | 16 | 6 | 4 | 2 | 3.5 | 290 | 1009.9 | 6.3 | 94.5 | NE |
| 2 | 21 | 0 | 2 | 3 | 3 | 16 | 6 | 4 | 2 | 3.5 | 0 | 1008.4 | 6.6 | 97.0 | NE |
| 2 | 22 | 0 | 2 | 3 | 3 | 16 | 6 | 4 | 2 | XXXXX | | 1008.7 | 6.8 | 94.5 | NE |
| 2 | 23 | 0 | 2 | 1 | 3 | 18 | 6 | 5 | 2 | XXXXX | | 1009.2 | 6.9 | 94.4 | NE |
| 2 | 24 | 0 | 2 | 2 | 3 | 18 | 6 | 5 | 2 | 2.4 | 2 | 1010.0 | 7.0 | 95.0 | NE |
| 3 | 1 | 0 | 2 | 1 | 3 | 18 | 5 | 5 | 15 | 5.3 | 351 | 1010.6 | 7.0 | 95.4 | NE |
| 3 | 2 | 0 | 2 | 2 | 3 | 18 | 5 | 5 | 15 | 5.7 | 30 | 1010.6 | 7.0 | 95.4 | NE |
| 3 | 3 | 0 | 2 | 1 | 0 | 2 | 1 | 5 | 14 | 7.3 | 3 | 1010.1 | 7.1 | 95.9 | NE |
| 3 | 4 | 0 | 2 | 1 | 0 | 2 | 0 | 5 | 14 | XXXXX | | 1010.1 | 7.1 | 95.9 | NE |
| 3 | 5 | 0 | 2 | 2 | 0 | 2 | 1 | 2 | 2 | 6.7 | 12 | 1009.2 | 7.3 | 96.3 | NE |
| 3 | 6 | 0 | 2 | 2 | 0 | 2 | 1 | 2 | 2 | 4.8 | | 1008.1 | 7.3 | 96.4 | NE |
| 3 | 7 | 0 | 2 | 2 | 0 | 2 | 1 | 2 | 2 | XXXXX | | 1007.6 | 7.4 | 96.8 | NE |

FIGURE 110[3].—Sample of meteorological data sheet No. 2.

# SCUBA-Diving Investigations

Self contained underwater breathing apparatus was used by Dr. Harris B. Stewart, Jr., Ens. Paul Larsen, and QMS Dick Rogers to investigate two locations during the *Pioneer*'s Indian Ocean Expedition—Seahorse Shoal in the South China Sea at 10°46.4′N, 117°44.6′E and Invisible Bank in the Andaman Sea at 11°11.3′N, 93°31.0′ E. A recompression chamber was carried abroad the *Pioneer* as part of the equipment for the diving program. A summary of events approaching Seahorse Shoal, as adapted from the daily log of Dr. Stewart follows:

"My pocket alarm went off a bit before 0600 (March 17, 1964). I was up in the chart room with the Precision Depth Recorder by about 0615. At 10 minutes past midnight (1610 GMT), we had crossed the crest of a seamount having a depth of 170 fathoms and rising from general depths of about 2,000 fms. The location was at approximately 12°45′N, 119°02′E—52 nautical miles due west of the NW tip of Busuanga Island in the Calamian group—but this feature was not shown on our chart. The PDR record showed a double peak along the trackline across it; and the towed-magnetometer record showed a marked magnetic anomaly coinciding with it.

"We were due at Seahorse Shoal about 0830, according to our dead-reckoning track as computed the night before. By 0930 (0130 GMT), we thought we had strayed west of the Shoal and turned left to 090° and reduced speed to one-third. Immediately the bottom was observed to shoal from 670 fms. Lookouts were posted to observe discolored water or any change in the texture of the sea surface that might indicate the Shoal. The Captain was in the crow's nest doing likewise. By 0945, the bottom had shoaled to 500 fms. Three minutes later it was 240 fms and we decided to pull in the magnetometer fish. In two more minutes the depth was 30 fms. Lcdr. Barbee raced to the bridge to signal "all stop" just as we heard someone shout "bottom in sight." I went to the starboard wing of the bridge and looked straight down. Alternating dark and light patches appeared to be sliding past the ship. By then the depth reading was 8 fms, less than 50 feet of water below keel depth. The bottom had risen like the front of the Empire State Building as we coasted along in dark shallow water, 66 nm from the nearest land—Piedras Point on Palawan Island, the westernmost tip of the Philippine Archipelago, bearing 120°.

"Since we were over the Shoal, we decided to dredge there first. The rock dredge was put over the side at 1000 local time. This dredge had been made aboard ship and had a somewhat lighter frame than the dredges generally used. The bottom depth was now 6 to 7 fms (36 to 40 ft), so we put out 60 ft of dredge line. We had a good pull almost immediately, and then a really good one that lifted the tension dial on the big winch console off the peg for the first time. Lcdr. Barbee ordered more cable out to release the tension and we put out a maximum of 325 ft. We then sneaked up on the dredge as we hauled in the cable. Nearly all hands were lining the rail as the dredge broke the surface at 1025. It looked empty and badly broken up. The pull had opened the seams of the frame and the inner wire mesh was badly torn, but a few pieces of coral were inside. Dredge No. 1 had been successful.

"As we started the dredge haul, Captain Brown asked if we would like to dive here. I answered 'yes' but said I would like to reserve judgment as to whether we should or not until I had some indication about the currents over the Shoal. By 1015 I could see there was little current, although the set the night before had been to the south and southeast at about 2 knots. Preparations were made for the diving operation as the first dredge haul was completed.

"I was equipped with the following items for the dive: Geology hammer, collecting bag, wrist compass, leg knife, watch, writing slate, inflatable life preserver, tanks, fins, and mask. The other two divers had similar equipment. Larsen and I stayed under and Rogers popped up to the surface to get his camera—a French Calypso with flash—from the tending boat. Then we all met at about 20 ft., checked our watches, and headed for the bottom so wonderfully visible in the warm clear water some 30 ft. below us. Once on the bottom, we could see the full 311 ft. of the *Pioneer*, and horizontally, the visibility was a good 200 ft. We saw no rock other than coral and algae, but there was lots of that. This was not the luxuriant reef type of Swan Island in the Caribbean, but more open, with more coral rubble and isolated patches of intense and varied growth (fig. 111). The topography was gently rolling with occasional NW–SE trending broad gentle swales. Flat and slightly meandering valleys between the swales might not have been noticed if it had not been for the deposits of white sands and gravels in these valleys (fig. 112). These deposits were made up of coral detritus, some *Halimeda* segments, and lots of the big coral reef foraminifera (marginulina?).

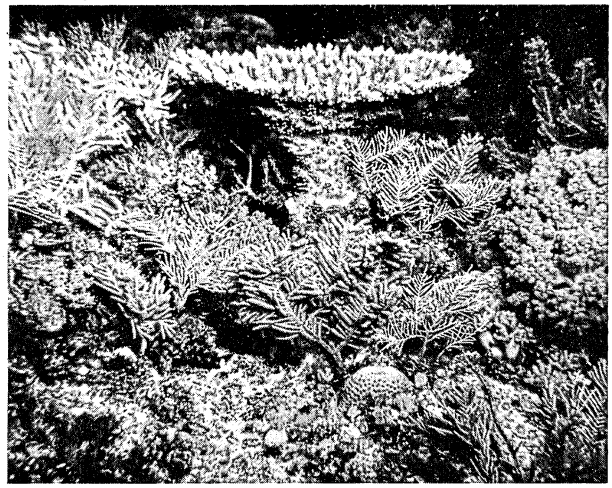

FIGURE 111.—Typical luxuriant growth on Seahorse Shoal.

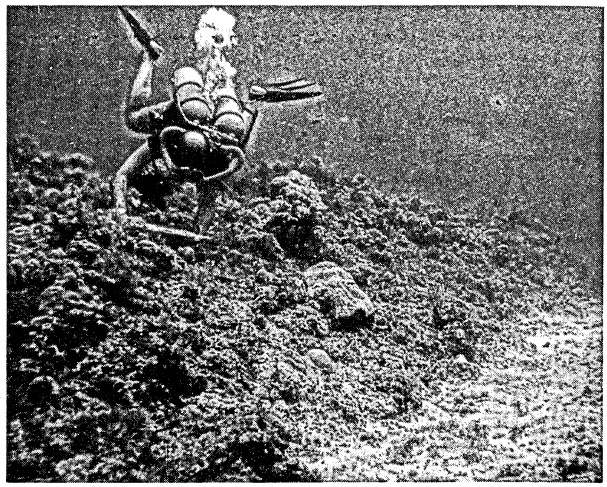

FIGURE 113.—Collecting biological specimens at Seahorse Shoal.

"After looking in vain for some sign of sedimentary or igneous rock, I resigned myself to being a biological specimen collector (fig. 113). The specimens were beautiful indeed. There were occasional crinoids. The two I collected for the sack were about 8 inches high and had perhaps 50 feathery arms each (fig. 114). One was a brilliant yellow, the other was black and white. One holothurian (Sticopus?) measured two ft. long and a good 5 inches in diameter. It was a brilliant red, but lost both its shape and color once it was aboard ship and placed in formalin. Several really fine corals were collected, some of which should end up in the museum back in Washington. By the time our dive was over, Rogers had shot some 24 of his 36 shots with the camera.

"After the planned 30 minutes, we started up with the three of us pulling on the bag which weighed about 100 pounds by then. My pockets were filled with sediment samples and we just could not get up. We unhooked our lifebelts, fastened them to the top of the bag, and inflated them. This provided just enough buoyancy, and we broke the surface just 34 minutes after we began the dive. The boat towed us to the ship where we used the diving ladder to bridge the gap between the bottom of the starboard Jacob's ladder and the water surface which now had 4- to 5-ft. waves. While we opened the sample bag for the photographers, the anchor was brought up. The ship changed course to 080° and moved into deeper water to prepare for a deeper dredge haul along the flank of the seamount.

"The second dredge haul (Dredge No. 2) from Seahorse Shoal was successful. Between 1550 and 1650, the ship had moved 1.15 nm on a course of 276°. As nearly as we could tell, the samples were obtained from depths of 250 to 400 fms on the flanks of the seamount. There were four chunks of black rock—not coral. One piece, about 6 by 4 by 2 inches, was yellowish brown, but one of the 2-inch sides was dense white. It was limestone, and contained circular fossils about ⅛-inch in diameter. One side had a borehole of some organism, possibly of a Pholad

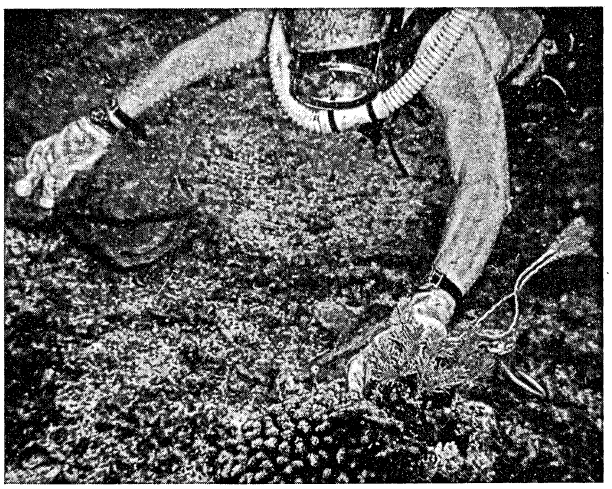

FIGURE 112.—Sand-covered channel on crest of Seahorse Shoal.

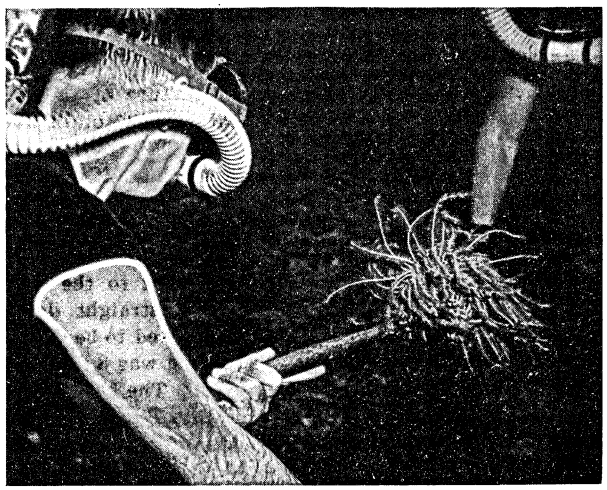

FIGURE 114.—Crinoid being recovered from Seahorse Shoal.

or Lithophaga of the boring mollusk type. A clear break along one side indicated that the rock had been in place until broken loose by the dredge. The largest of the other pieces was 11 by 5 by 3 inches, irregularly shaped, and covered with a heavy encrustation of manganese. Even an attached shell had a patina of manganese. The encrusting layer was as much as ¼-inch thick in places and followed the shape of the rock, even lining the numerous cavities. Where the sample had broken from the outcrop, the surface had the appearance of igneous rock, including what appeared to be fairly large phenocrysts. When broken, an exposed cavity appeared to be filled with sediment. The second dredge also was fabricated aboard ship from lightweight material and was damaged beyond repair."

The second SCUBA dive was made at Invisible Bank off the Andaman Islands on April 17, 1964. The ship arrived here about 1400 local time. A good swell was running and great white breakers formed, crested, and rolled off the rock awash. The *Pioneer* anchored in 9 to 10 fms of water and one of the launches was put over the side. This dive, when compared with that at Seahorse Shoal, was a disappointment. Although the water looked clear from the ship and was clear in the top 30 or 50 ft, it was quite turbid below a very sharp thermocline and very minute suspended material limited underwater visibility to approximately 40 to 50 ft. The coral growth consisted only of occasional solitary forms. The bottom was paved with golf- to baseball-sized algal balls and broken algal material. Samples of this material and the coarse calcareous sand underneath were obtained. A sample broken from the bottom appeared to be either a dark limestone or a highly calcareous siltstone. As the divers moved back nearer to the ship, there were schools of small yellow-fin tuna, red snapper, and many variously colored small tropical fish. One large barricuda was seen. As the group headed for the launch, it was joined by a 3- to 4-ft shark. The three divers climbed the Jacob's ladder in "one bunch" and the dive was completed.



U.S. GOVERNMENT PRINTING OFFICE: 1966 O—790–089

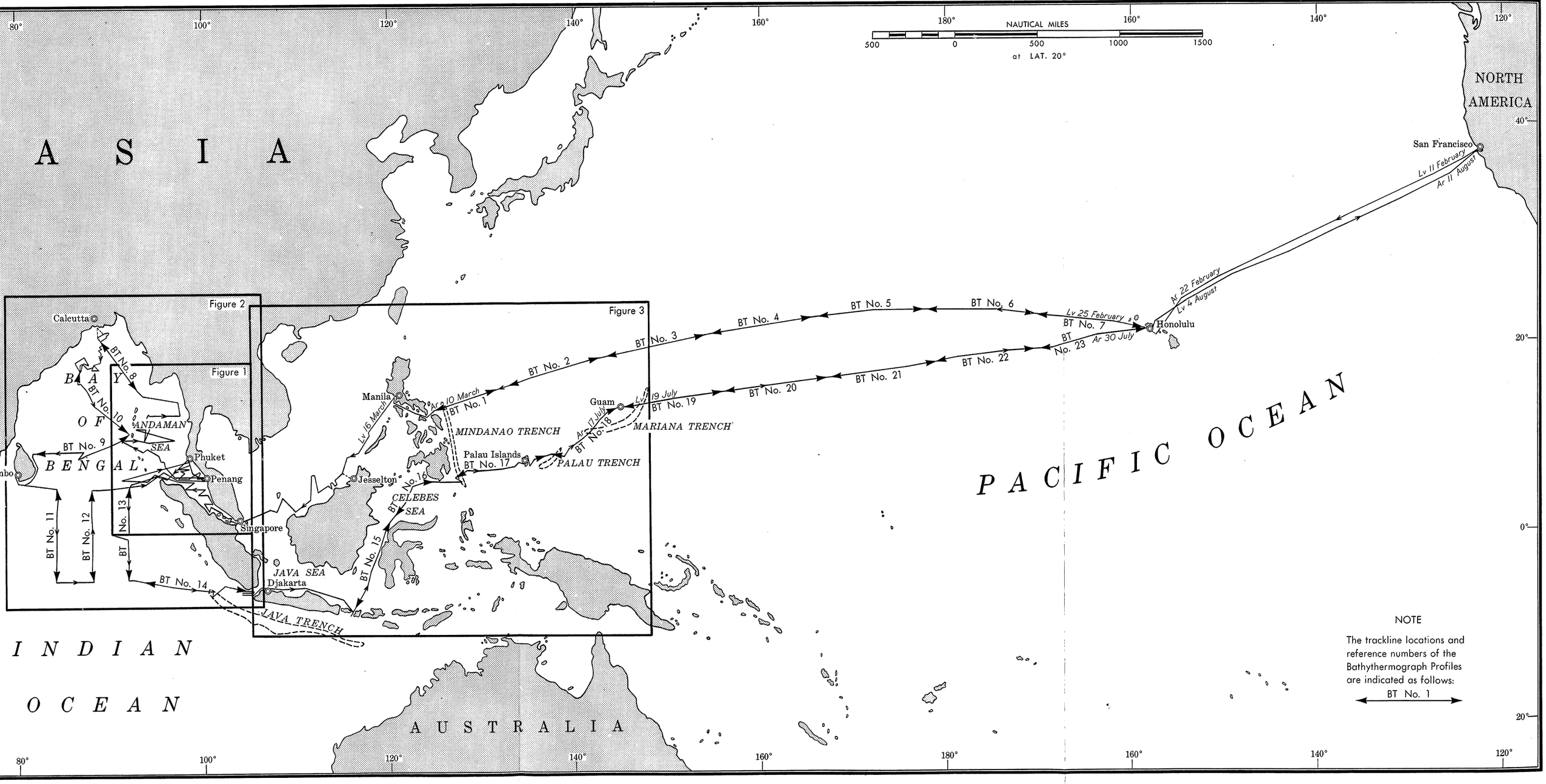


CHART 1.—USC&GS ship *Pioneer* trackline during 1964 Indian Ocean Expedition and locations of selected bathythermograph profiles.